rt No. FHWA-RD-78-95

EXTENSION AND REPLACEMENT OF ASPHALT CEMENT WITH SULFUR

March 1978
Final Report

Prepared for

FEDERAL HIGHWAY ADMINISTRATION
Offices of Research & Development
Washington, D.C. 20590

FOREWORD

This report presents the results of an investigation of the use of elemental sulfur as an extender of asphalt cement in highway paving mixtures. The findings will be of interest to research and operations personnel concerned with the design, construction, and evaluation of pavement utilizing sulfur extended asphalt binders.

Physical properties of numerous blends of sulfur and asphalt were determined. Laboratory screening and characterization tests were performed on selected combinations of aggregate, asphalt and sulfur produced by three different mixing methods. The resulting relationships between response characteristics, mixture compositions, and design variables were programmed into the Texas FPS-BISTRO and VESYS IIM design programs. The report concludes that sulfur extended asphalt binders have the potential to produce pavements which are more economical with performance characteristics equal or superior to conventional asphaltic concrete pavements.

This report is being distributed to selected Federal and State research and operations personnel. Additional copies of the report for the public are available from the National Technical Information Service (NTIS), Department of Commerce, 5285 Port Royal Road, Springfield, Virginia 22161.

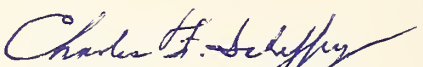

Charles F. Scheffey

NOTICE

Technical Report Documentation Page

1. Report No.	2. Government Accession No.	3. Recipient's Cotolog No.
FHWA-RD-78-95		

4. Title and Subtitle	5. Report Date
Extension and Replacement of Asphalt Cement With Sulfur	March, 1978
	6. Performing Orgonizotion Code
	8. Performing Orgonizotion Report No.
7. Author(s) D. E. Pickett, D. Saylak, R. L. Lytton W. E. Conger, D. Newcomb, and R. A. Schapery	
9. Performing Orgonizotion Nome and Address Texas Transportation Institute Texas A&M University College Station, Texas 77843	10. Work Unit No. (TRAIS) FCP No. 34G1-023
	11. Contract or Grant No. DOT-FH-11-8799
12. Sponsoring Agency Nome and Address Offices of Research and Development Federal Highway Administration U. S. Department of Transportation Washington, D. C. 20590	13. Type of Report and Period Covered Final Report
	14. Sponsoring Agency Code M-05-44

15. Supplementary Notes

FHWA Contract Manager: Edward Harrigan

16. Abstract

The potential shortage of asphalt cement and over supply of sulfur make it advantageous to reduce the dependence of the paving industry upon asphalt cement while utilizing readily available sulfur. This report presents the results of an investigation of the use of elemental sulfur as a partial replacement and/or extender of asphalt cement in highway paving mixtures.

Physical properties of numerous combinations of sulfur-asphalt emulsions were determined. Various aggregates, asphalt cements, and sulfur were tested in a series of laboratory screening tests utilizing nine independent design variables. Characterization tests were performed on selected combinations of aggregate, asphalt and sulfur utilizing three different mixing methods.

The resulting relationships between response characteristics, mixture compositions, and design variables were programmed into the Texas FPS-BISTRO and VESYS IIM design programs. Texas FPS-BISTRO screened a number of design combinations to find the optimum combinations. VESYS IIM was used to evaluate performance of selected optimum pavements.

The studies indicate that the addition of sulfur to asphaltic concrete can produce pavements which are more economical with performance characteristics equal or superior to conventional asphaltic concrete pavements.

17. Key Wards	18. Distribution Statement
sulfur, asphalt, emulsions, aggregates, characterization, Texas FPS-BISTRO, VESYS IIM, fatigue, ruttin, service-ability index, slope variance, mix design, performance prediction, pavement systems design.	No restriction. This document is available to the public through the National Technical Information Service, Springfield, Virginia 22161

19. Security Classif. (of this report)	20. Security Classif. (of this page)	21. No. of Pages	22. Price
Unclassified	Unclassified	310	

TABLE OF CONTENTS

LIST OF TABLES

LIST OF FIGURES

CHAPTER I

INTRODUCTION

Background

Asphalt is an extremely important construction material, particularly with respect to roadways. Asphalt type materials have been used to construct more than 90 percent of the total hard-surfaced road system of the United States (1). About 25 million tons of asphalt are used annually in construction of new roadways, whereas about 7 million tons are used for maintenance and rehabilitation of the existing road system (2).

Asphalt is obtained by refining crude petroleum. As the development of our current energy shortage has developed, it has increasingly become more profitable for refiners to use the asphalt residue in blending of heavy fuel oil rather than marketing the asphalt as an individual product. This has caused a reduction in the amount of asphalt materials available for roadway construction with a resultant increase in the price of asphalt during the last few years. Big prices for asphalt cement have tripled in some regions of the country during the last four years (2). This situation is not expected to improve in the immediate future.

With the apparent shortage of asphalt materials, researchers, material suppliers, design engineers, and the construction industry are exploring ways to use available materials, such as local aggregates, waste materials and substitute binders, more efficiently for roadway construction. It is highly desirable that a substitute or supplement for asphalt cement be developed. Elemental sulphur has played a major role in this search for methods to reduce the dependence of our nation upon the use of asphalt cement as a highway paving material. Existing world stockpiles of sulphur are estimated to be 26 million metric tons due primarily to pollution abatement processes which are recovering sulphur from various sources (18). Sulphur is one of few materials which is expected to be in vast oversupply in the future. In 1975, world production of sulphur totaled 52 million metric tons while consumption amounted to 45.7 million metric tons. The oversupply of sulphur has significantly lowered its commercial price (23). The combination of the shortage of asphalt cement and the overabundance of sulphur has set the stage for researching the practicality of substituting the latter product for the former.

Utilization of recovered sulphur as a substitute or supplement for asphalt cement would serve a twofold purpose: an outlet would be provided for the current oversupply of sulphur, and the dependence of the paving industry upon the use of asphalt cement would be reduced. Another potential benefit is the possibility of improved performance of pavements incorporating sulphur as an extender of the asphalt cement binder.

Purpose

The general purpose of this study was to investigate the use of elemental sulphur as a partial replacement and/or extender of asphalt cement in highway paving mixtures.

Specific Objectives

The specific major objectives of this study are as follows:

1. To investigate the effect of the addition of elemental sulphur on the physical properties of sulphur-asphalt emulsions.
2. To investigate the solubility and settling characteristics of sulphur in various asphalt cements.
3. To develop statistically based relationships between mixture response characteristics and mixture composition and design variables.
4. To evaluate and demonstrate the influence of partial substitution of sulphur for asphalt cement in asphalt paving mixtures.
5. To determine suitable mix design alternatives which will result in a reduction of the quantities of asphalt cement normally specified, but which will still yield a comparable level of performance as provided by conventional asphalt mixtures in flexible pavements.
6. To make comparative analyses of pavement systems utilizing conventional asphaltic concrete and sulphur-asphalt concrete.

Scope of the Investigation

The purpose and objectives of this study were accomplished by means of five major tasks listed below.

Task A - Selection of Design Systems and Materials Characterization Tests.
Task B - Development of Sulphur Extended Asphalt Systems.
Task C - Development of Statistically Based Relationships from Laboratory Tests for Use in Pavement Design Systems.
Task D - Incorporate Statistical Relationships into Pavement Design Systems.
Task E - Sensitivity Analyses.

A series of screening tests were performed in order to develop statistically based relationships between materials response characteristics, mixture composition and design variables. These relationships were incorporated into a pavement design system for a sensitivity analysis of the effect of these variables on pavement performance. Further details of these tasks are discussed subsequently.

Study of the available literature indicates that two different methods have been used by researchers to introduce the sulphur into the paving mixture. In order to determine the differences and advantages of

the systems, three alternative approaches were investigated for this project. These three systems are a) Aggregate-Asphalt-Sulphur (AAS), b) Aggregate-Emulsion (AE), and c) Aggregate-Emulsion-Sulphur (AES). The letters designate the order in which the components are added to the mixture. In the AAS system, the aggregate is first mixed with the liquid asphalt cement and then the molten sulphur is added. In the AE system, the sulphur and asphalt cement are first mixed to form an emulsion which is then mixed with the aggregate. In the AES system, a sulphur-asphalt emulsion is mixed with the aggregate and molten sulphur is then mixed with this combination.

Task A consisted of a literature review, selection of the pavement design system and structural design subsystem to be used in application of the test results and analysis thereof, and determination of the characterization tests necessary for input data to the selected design system and subsystem.

Task B consisted of selection of the experimental design variables and mixture combinations, and determination of the physical properties of sulphur-asphalt emulsions (SAE) using various grades of asphalt cements and quantities of sulphur. An experimental design was developed in order to determine what combinations of variables should be tested in order to examine the relative influence of various factors and their first order interactions on the behavior of the compacted mixture combinations. In addition, numerous combinations of aggregate, asphalt and sulphur were prepared using the three sulphur-asphalt systems for subsequent testing. Laboratory tests were performed on the SAE binders to determine the specific gravity, ring and ball softening point, viscosity, penetration, sulphur settling rate, and amount of dissolved sulphur for each combination of sulphur and asphalt.

Task C included an extensive laboratory testing program from which statistically-based relationships between mixtures, design variables and response characteristics were developed for subsequent incorporation into the selected pavement structural design subsystem. A series of preliminary screening tests in this task included determination of unit weight, percent air voids, percent voids in mineral aggregate, Marshall stability and flow, and Hveem stability. Based upon results of the screening tests, the dominant variables were determined. Further qualification tests included resilient modulus, flexure fatigue properties, thermal expansion, creep properties, and permanent deformation properties. The screening and qualification test data were analyzed, and the relationships and parameters necessary for evaluation of pavement systems were developed.

Task D required programming of the developed statistical relations into the selected structural design subsystem and pavement design system. Specific distress mechanisms treated within the subsystems included fatigue cracking, rutting, and roughness.

Task E was used to find optimum combinations of material properties and layer thicknesses which will be cost effective in different climates,

on different subgrades and base courses, and under different loading conditions. A selected pavement design system (FPS-BISTRO) was used to screen a large number of possible design combinations to determine the most cost effective designs for cold, moderate and warm climates. Using a structural design subsystem (VESYS IIM), the optimum pavements were studied to determine their resistance to various forms of distress.

CHAPTER II

REVIEW OF THE LITERATURE

Asphalt

Asphalt exists in solution as a natural constituent of most petroleums. In the refining of crude petroleum, asphalt materials are the residue remaining after fractionating the crude. Deposits of asphalt also exist in nature. In such deposits, the asphalt is often mixed with variable amounts of impurities such as minerals, water, and other substances. Natural deposits in which asphalt exists within the voids of a porous rock structure are known as rock asphalts.

Asphalt is a very versatile product for use in the construction industry because it is a strong cement which is highly waterproof and durable. It also has the ability to readily adhere to many substances. It is estimated that over 60 million tons (54 billion kg) of asphalt are used each year with more than half of this amount going into road construction (85). Asphalt is a viscoelastic material which imparts controllable flexibility to the mixture when combined with mineral aggregates. It is a solid or semisolid at normal atmospheric temperatures, but is readily liquefied by the application of heat. These characteristics and properties of asphalt make it a highly important material in construction of roadways.

Asphalt pavements consist of combinations of mineral aggregates and asphaltic material constructed in various thicknesses and types. The asphalt serves as a cementing agent to bind the aggregate in proper position in order to transmit the applied wheel loads to the underlying layers (20). To function properly, the asphaltic material should completely coat each aggregate particle with an adhesive film which should, in turn, provide a bond between adjacent particles and the underlying layer. There are many different types of asphalt pavements and types of asphaltic materials used in these pavements. When properly compacted, the ideal asphalt-aggregate mixture should offer resistance to all disruptive forces, including climatic conditions; and should possess sufficient mechanical stability, resilience and flexibility to withstand the shocks and stresses caused by heavy high-speed traffic without experiencing permanent distortion (21). With respect to mechanical stability, the asphaltic material serves two somewhat conflicting purposes in its role as a binder. It exhibits a cohesive action which makes the aggregate particles adhere to each other and tends to increase the stability. However, the asphalt binder also has a lubricating property which tends to decrease the mechanical stability. This lubricating capability is important in facilitating compaction of the mixture. Obviously, it is important to use the correct type and amount of asphalt binder for a particular desired mixture.

The viscosity of the asphaltic material binder is related to the lubrication properties. Neppe emphasizes that viscosity is the most important single physical property of the binder which determines resistance to deformation of an asphalt aggregate mixture subjected to stress (21). The viscosity of asphaltic materials varies with temperature. This viscosity variation is an important factor when considering the behavior of asphalt binder in a mixture during variable climatic conditions. The viscosity of asphaltic material is controlled by the refining process, by blending of various asphaltic materials and by air blowing. In this latter process, air is blown through asphaltic material while it is maintained at a relatively high temperature. Air blown asphalts are generally the stiffest asphalts produced and possess the ability to retain a firm consistency at the temperatures which will be reached when exposed to climatic conditions. Although widely used in roofing materials, battery boxes, crack and joint fillers for concrete pavements, and waterproof paints, air blown asphalts are not commonly used in paving mixtures.

Sulphur

Sulphur is a non-metallic element with an atomic number of 16 (22). As found in nature, it has a mean atomic weight of 32.066. Natural deposits of sulphur are found throughout the world. The occurrence of these deposits is often associated with the formation of salt domes. Ordinary commercial sulphur produced in the United States by the Frasch process from salt dome deposits is one of the purest raw materials known. Increasingly important sources of sulphur are pollution-abatement processes and processing of sour gas (23). With the current emphasis on protection of the environment, it is estimated that tremendous quantities of sulphur will be recovered from power plant stack gas emissions, coal liquefaction, and processing of shale oil and synthetic natural gas (18). Existing sulphur markets cannot currently absorb the large quantities of sulphur which will result from desulphurization of fossil fuels and smelter gases (85).

Sulphur is a yellow solid at normal temperatures, but becomes progressively lighter in color as the temperature is lowered. At the melting point, sulphur is a light yellow, transparent, relatively inviscid liquid. As the temperature of the liquid is raised, the color darkens to a deep orange hue. Sulphur crystallizes in at least two distinct forms, the rhombic and monoclinic, and has a specific gravity of about 2.0. In solid form, sulphur has a unit weight of about 125 pcf (2000 kg/m^3) while commercial crushed bulk sulphur has a unit weight ranging between 85 and 90 pcf (1360 and 1400 kg/m^3)(60).

The melting point of sulphur depends upon the crystalline form at the time of melting and on the temperature history immediately prior to melting (22). A temperature of about 246°F (119°C) is normally considered to be the melting temperature of most sulphur. The liquid sulphur has a unit weight of about 112 pcf (1792 kg/m^3) at the melting point. The ignition temperature is reported to range between 478 and 511°F (248 and 266°C)(22).

The viscosity of liquid sulphur changes dramatically with temperature. Up to about 320°F (160°C), the viscosity decreases gradually with increasing temperature. However, the viscosity undergoes a very large and abrupt increase with temperature above 320°F (160°C). At 370°F (187.8°C) the viscosity reaches a tremendously high maximum which practically prevents it from flowing, and the liquid is almost opaque. Above 370°F (187.8°C) it again acts in a more normal fashion and the viscosity decreases at a relatively moderate rate with increasing temperature. This temperature-viscosity relationship for the temperature ranges discussed above is presented in Figure 1. Upon cooling, the sulfur passes through these described phases in reverse order.

The tensile strength of bulk elemental sulphur is reported to range between 180 and 280 psi (1240 and 1930 kPa) whereas the tensile strength of sulphur threads is much higher (24). The compressive strength of bulk elemental sulphur is about 1800 psi (12,407 kPa) and the modulus of elasticity of plastic-elastic sulphur threads reportedly ranges between 28 and 8500 psi (193 and 58,590 kPa) (25).

The properties of sulphur can be altered by the use of plasticizers. A plasticizing agent may be either a low melting point solid or high boiling point liquid which imparts flexibility to a rigid material when added in relatively small amounts (25).

Sulphur-Asphalt Mixtures

An excellent source of information about sulphur-asphalt applications is an annotated bibliography prepared by Gallaway and Saylak (36).

The use of sulphur in the production of asphaltic materials was initiated many years ago. Sulphur was used in the late 1800's and early 1900's to modify the properties of asphalts before air blowing became the major method of changing asphalt characteristics (4). In 1866 and 1892, patents were issued to Day and Dubbs, respectively, for modifying asphalt with sulphur (33, 34). In their processes, bituminous materials were heated with about 25 percent sulphur until the evolution of gas ceased and a plasticized sulphur resulted. This material was somewhat susceptible to thermal fracture and was lacking in ductility (35). These processes were abandoned subsequently when air blowing was introduced. In 1921, Bacon reported results of his experiments in preparing mixtures of sulphur and sand in an effort to produce an acid resistant material (87).

A composition of asphalt and Thiokol plasticized sulphur was used in 1936 by the Ohio Department of Highways for construction of an experimental road in which bricks were joined with the sulphur-asphalt material (37, 82). It showed such promise that specifications for the material were adopted by the Ohio Department of Highways.

In 1938, Bencowitz and Boe reported results of their laboratory tests on tne properties of sulphur-asphalt mixtures (38). They found that sulphur-asphalt aggregate mixtures possess much higher stabilities at

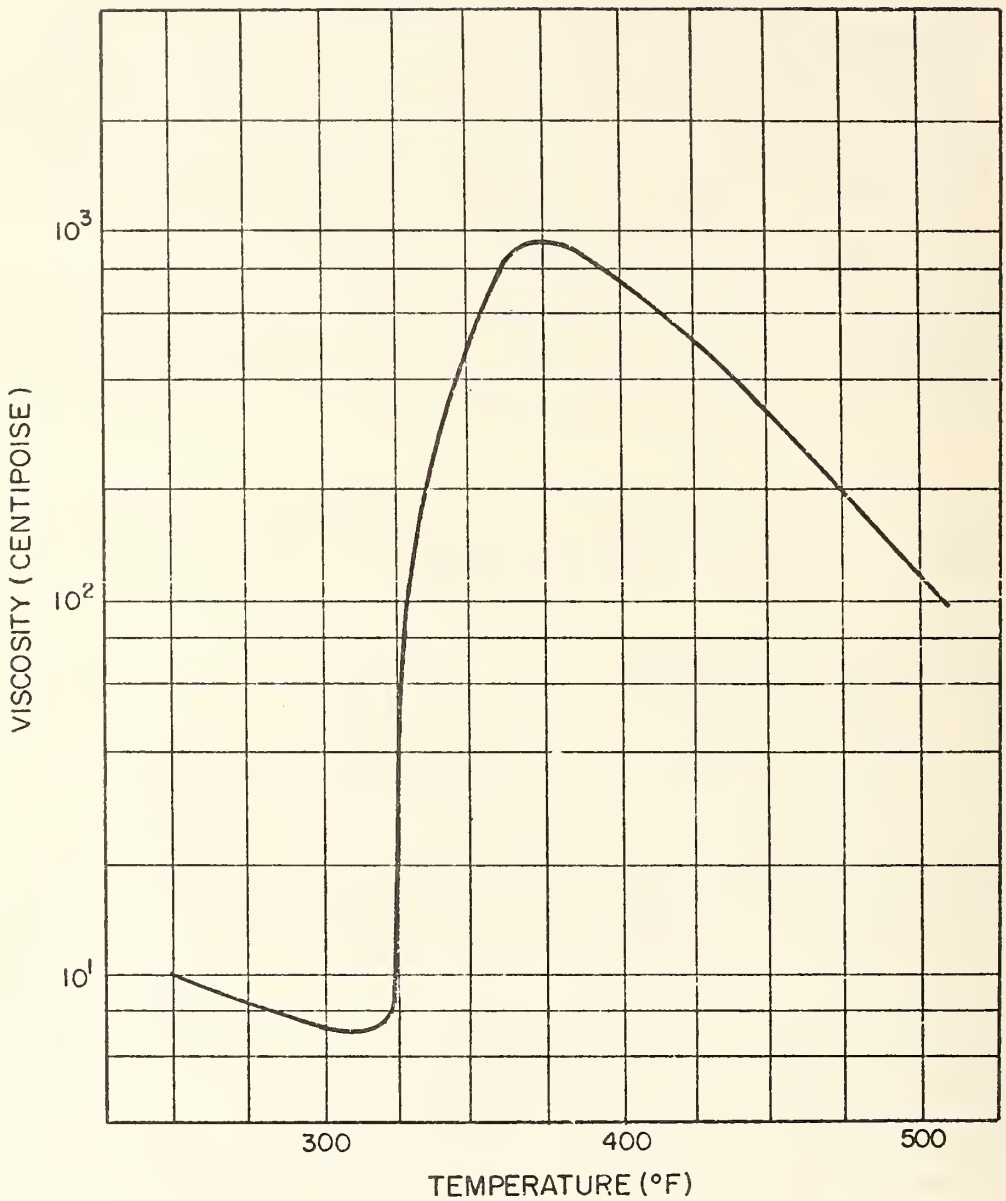

FIG. 1--Viscosity-temperature curve for liquid sulphur.

$^{o}C = (^{o}F - 32) \times 5/9$

140°F (60°C) than conventional asphaltic concrete mixtures, with very little change in brittleness at temperatures near freezing. They also pointed out that mixtures with sulphur absorb appreciably less water than similar mixtures without sulphur (38).

Williford performed x-ray studies of paving asphalts in 1943 and reported that the best paving asphalts were found to have the highest sulphur content. He concluded that sulphur was a contributing factor to the formation of superior asphaltic bodies (39). In 1958, Welborn and Babashak reported that the addition of small amounts of sulphur greatly increased the effectiveness of rubber on asphalt in a rubberized asphalt for roads (40).

In 1963, Shell Canada Limited began a laboratory study to investigate the use of sulphur in flexible pavements (4, 6). This program eventually led to the development of a sand-asphalt-sulphur paving material called "Thermopave". The results of the study, including actual field trials in 1964 in Oakville, Ontario, and St. Boniface, Manitoba, demonstrated that good pavements could be constructed by properly mixing and placing certain combinations of sand, sulphur and asphalt cement (6). It was also shown that conventional pavement compaction procedures were detrimental to such a pavement during construction. The sands employed in the process were relatively uniformly graded locally available materials not normally considered acceptable for use in pavement construction. The techniques developed and results of laboratory and field tests are reported in a series of technical papers by I. Deme, et al. (4 - 7). This concept was also investigated by Shell Oil Company and Shell Development Company (3).

In 1964, field test sections of sand-asphalt-sulphur materials were placed by Shell in Oakville, Ontario and St. Boniface, Manitoba using conventional hot mix asphaltic concrete paving equipment and procedures. It was found that rolling procedures normally employed for asphaltic concrete were not acceptable for the mixtures with sulphur, whereas an unrolled test section was found to perform satisfactorily. It was shown that rolling of the mixture containing sulphur caused a breakdown of the bond between the materials as the mixture cooled (3). In 1970, another field trial was conducted in Richmond, British Columbia in which the "Thermopave" system was used to place the material between wooden forms without the use of compaction or densification. The reported results indicated that such uncompacted sand-asphalt-sulphur mixes possessed adequate potential for use as a pavement surfacing material and as a pavement base over a weak subgrade (4). This project demonstrated that a liquid sulphur supply and distribution system could be readily adapted to a batch hot mix plant to permit large volume production of sand-asphalt-sulfur mixes. Hauling truck insulation and safety precautions for handling sulphur are discussed in the referenced report.

In 1970, Medcalf reported the development of an improved road surfacing material containing bitumen, sulphur, and mineral matter such as sand, rock, road metal and clinker (41). He recommended preparing the

mixture in hot mix plants and completely filling the voids between aggregate particles with sulphur-asphalt binder. Increased Marshall stabilities resulted from this mix. Nicolau reported results of laboratory tests performed by Society Nationale des Petroles d'Aquitaine in France on the use of sulphur-asphalt binders in preparation of road surfacing material (42). This mixture, containing gravel as the aggregate phase, exhibited higher stabilities than similar mixes without sulphur.

Lee reported on his research of the properties of sulphur-asphalt systems at Iowa State University (43). His work indicated that treating aggregates with sulphur could improve adhesion, water resistance, stability and tensile strength; as well as reducing the required asphalt content and making unsuitable absorptive aggregates satisfactory for highway use. In 1973, a U. S. patent was issued to Kopvillem and Maclean (assignors to Shell Oil Company) for "casting sulphur-asphalt-aggregate mixes in forms without the application of conventional densification procedures" (8). Prior to that time, a U. S. patent was issued to Sadtler for preparation of road paving material using sulphur, asphalt, and aggregate in which it was claimed that powdered sulphur enhanced certain useful properties of asphaltic materials (44). A U. S. patent was also issued to Bacon and Bencowitz for a method of paving which utilized sulphur and asphalt in the mixture (45). In 1973, Gatarz reported that the addition of sulphur to the asphalt resulted in improved performance of pavements (46).

Gulf Oil Canada Limited developed and field tested a process to incorporate elemental sulphur in conventional paving mixtures (9). Kennepohl reports that the key advantage of this process is that a significant portion of the asphalt cement can be replaced by sulphur while maintaining a total binder content of the paving mixture similar to that for conventional asphaltic concrete mixtures (9). In the Gulf process, the liquid sulphur and asphalt are first mixed together in a colloid mill to form an emulsion which is then mixed with the aggregate (10). Gulf's first industrial scale mix production was made in a batch operated plant in Port Colborne, Ontario. The success of this first field trial prompted Gulf's decision to proceed with a full-scale field test at Blue Ridge, Alberta, during the fall of 1974. Field performance of the test sections is currently being monitored. Gulf also used sulphur-asphalt-aggregate mixtures to overlay a one mile section of Alberta Highway 43 near Windfall in 1974, in order to evaluate the field performance of sulphur-asphalt-aggregate as pavement maintenance and rehabilitative material (9). Gulf is currently evaluating the engineering properties of sulphur-asphalt mixtures (17).

A similar process of combining the sulphur and asphalt cement into an emulsion prior to mixing with the aggregate was developed by Societe Nationale des Petroles D'Aquitaine (SNPA), a French company (11). SNPA obtained a British patent for their process of preparing sulphur-asphalt binders (47). SNPA participated in the Lufkin, Texas, field trial to be

discussed subsequently. In addition, SNPA has conducted successful field applications of the process in France (12, 84).

In 1974, Ahmad reported on his extensive laboratory study of sand-asphalt-sulphur mixtures (35). He concluded that such mixtures possessed properties equivalent to or better than conventional asphaltic concrete, and that pavements made with sand-asphalt-sulphur could cost as much as 57 percent less than conventional asphaltic concrete.

The U. S. Department of the Interior-Bureau of Mines investigated sulphur-asphalt road mixtures in 1972, the results of which were reported by Sullivan (48). It was found that the use of sulphur-asphalt binder with poorly graded aggregates such as blow sand and mine tailings resulted in significant improvements of the engineering properties of the mixtures. In 1973, the Bureau of Mines and the Sulphur Institute initiated efforts to introduce pavement materials to researchers and the paving industry of the United States the techniques then under development in Canada to utilize sulphur in paving mixtures (3). In conjunction with this effort, a laboratory study was performed by Texas Transportation Institute and reported by Gallaway (3). Further study of sulphur-asphalt-aggregate systems by Saylak culminated in construction, during August, 1975, of a field test section incorporating various thicknesses and types of sulphur-asphalt concrete mixtures on U. S. Highway 69 near Lufkin, Texas (13, 49). Participating agencies were the Federal Highway Administration, Texas State Deparment of Highways and Public Transportation, Moore Brothers Construction Company, SNPA, Texas Transportation Institute, U. S. Bureau of Mines, Texasgulf Inc., Robertson Tank Lines, Inc., and The Sulphur Institute. The binder for the mixture consisted of sulphur-asphalt emulsion prepared in a turbine mill. The field performance is periodically monitored in order to evaluate the long term performance. The Bureau of Mines placed some sulphur-asphalt-sand patches on roadways in Boulder City, Nevada, during 1974 and 1975 (2). Fine blow sand and medium construction sand containing 6 weight percent asphalt and 17 and 13.5 weight percent sulphur, respectively, were used as a patching material. A hand tamp was used for compaction prior to screening the surface with a 2" by 4" board. In January 1977, the Bureau of Mines constructed a roadway test section using sulphur-asphalt concrete near Las Vegas, Nevada (2). The aggregate was dense graded crushed volcanic material to which was added directly the molten sulphur and liquid asphalt cement. It is significant to note that the sulphur and asphalt cement were added directly rather than first being mixed as an emulsion. This test section is being observed for subsequent evaluation. Sand-asphalt-sulphur can be mixed by any of the three methods (AAS, AE, or AES) but the particular mixture used in the characterization tests was the AAS system.

Glascock reports that the Louisiana Department of Highways conducted a research program to familiarize department personnel with sulphur-asphalt paving mixtures and to verify results obtained by others (86). He indicated that mixtures of sand, asphalt and sulphur exhibited somewhat higher Marshall stabilities, with a slightly greater water sensitivity, than conventional asphaltic concrete mixtures.

As discussed previously, Texas Transportation Institute (TTI) is involved in the post construction evaluation of the Lufkin, Texas field test section. TTI is also performing various laboratory tests on specimens of sulphur-asphalt aggregate mixtures for the Bureau of Mines. In April, 1977, a field test section using the Shell concept was constructed in Kenedy County, Texas (15). The paving mixture consisted of sulphur, asphalt, locally available blow sand, and concrete sand. TTI and the Texas State Department of Highways and Public Transportation are participating in the project. TTI is currently evaluating the basic physical properties of some mixtures prepared with broken bituminous pavement sections (recycling) obtained from resurfacing activities (2).

Although significant progress has been made recently in evaluation of certain sulphur-asphalt aggregate mixtures, the literature is somewhat lacking in the parameters and procedures needed for design of pavements of such mixtures using varied aggregates in various climatic conditions. This is the basis for this research project.

The role of sulphur in sulphur-asphalt paving mixtures is twofold. It increases the workability of the mix and provides a mechanical interlocking effect (3, 7, 61). The sulphur serves as a filler of the voids between the aggregate particles. As the molten sulphur cools below the melting point of about 245°F (118°C) it solidifies and creates the interlocking effect which is sometimes referred to as "structuring" (62). In conventional asphaltic concrete paving mixtures, the optimum asphalt content dictated by stability and voids requirements is insufficient to provide the adequate workability of the hot mix which would permit mix densification in the field without considerable compaction effort. The addition of sulphur increases the fluid content of the mixture and thus reduces or eliminates the compactive energy requirements for consolidating the mix, without adversely affecting its ultimate stability (80).

Hydrogen Sulfide Emissions

Commercially pure sulphur in the powder or solid form is non-toxic. Although sulphur dust may cause eye irritation and rarely skin irritation, there is no evidence to indicate inhalation of the dust will cause poisoning. However, when sulphur and asphalt cement are mixed at temperatures in excess of about 305°F (151.7°C), gaseous hydrogen sulfide (H_2S) is formed. This evolved hydrogen sulfide is a potential danger to human beings as well as a pollution hazard to the atmosphere. Hydrogen sulfide exhibits an odor similar to rotten eggs which can be detected by humans at concentrations as low as 0.02 ppm (26). Odor is not an effective indicator of hydrogen sulfide concentration level, because the gas paralyzes the sense of smell with the result that high concentrations can go undetected (27, 28).

Sienko considers hydrogen sulfide to be as toxic as hydrogen cyanide and four times as toxic as carbon monoxide (29). At concentrations above

200 ppm, hydrogen sulfide acts as an asphyxiant by paralyzing the respiratory center (28). It can be fatal to humans at concentrations in excess of 400 ppm by paralyzing the respiratory center, or by producing systemic poisoning if absorbed into the blood (27, 28).

At concentrations below 200 ppm, hydrogen sulfide is primarily an irritant to the eyes and the respiratory tract, similar in behavior to chlorine, but with less intensity (30). Exposure to hydrogen sulfide concentrations of 20 ppm results only in eye irritation.

The American Conference of Governmental Industrial Hygienists has set a maximum allowable concentration (MAC) of hydrogen sulfide at 20 ppm with respect to exposure without injury to health (28). Since this level of concentration causes eye irritation, a maximum allowable concentration of 5-10 ppm has been suggested (28). The Texas State Department of Health has set a maximum allowable concentration of 10 ppm whereas the Occupational Safety and Health Administration enforces a maximum allowable concentration of 20 ppm (31). Selected hydrogen sulfide levels and their associated environmental effects are shown in Table 1.

Since a potential health hazard exists when mixing asphalt and sulphur, precautions must be taken to insure the safety of personnel in the vicinity of hot sulphur and asphalt mixtures. The Texas Transportation Institute has published a short, illustrated pamphlet for distribution to engineers, contractors, and other parties interested in construction of sulphur-asphalt pavements (32). This pamphlet contains information concerning possible emission of hydrogen sulfide during mixing and placing of sulphur-asphalt pavements. It recommends that safety precautions include wearing of safety goggles and simple respirators.

TABLE 1

TOXICITY OF HYDROGEN SULFIDE GAS (3)

H_2S Concentration (ppm)	Environmental Impact
.02	Odor Threshold Value
10	Texas State Dept. of Health Maximum Allowable Concentration
20	OSHA Maximum Allowable Concentration
70-150	Slight symptoms after exposure of several hours
170-300	Maximum concentration that can be inhaled for one hour without serious consequences
400-700	Dangerous after continuous exposure of 30 min - 1 hr
600	Fatal with exposure greater than 30 minutes

CHAPTER III

TASK A: SELECTION OF DESIGN SYSTEMS AND MATERIALS CHARACTERIZATION TESTS

This task is broken into three individual subtasks: obtaining users manuals and descriptive information, selection of the analysis methods, and selection of materials characterization tests.

User's Manuals and Descriptive Information

This project requires utilization of a pavement design system and structural design subsystem. A pavement design system is a computer program that is capable of investigating a large variety of pavement design strategies and determining the economically optimum combination of materials and layer thicknesses which will provide an acceptable level of riding quality over a specified analysis period. The structural design subsystem forms a part of this overall design system; it has the capability of predicting the performance (as measured by some criterion such as serviceability index) of a specified pavement. The former system is used to perform economic analysis whereas the latter system is used to perform stress and distress analysis of a given pavement section.

A magnetic tape copy of the VESYS IIM structural design subsystem program was obtained from the Federal Highway Administration (FHWA). A draft of the VESYS IIM User's Manual was also obtained (51). In order to verify the operation of the program, an example problem was run on the Texas A&M University AMDAHL 470 V/6 computer. The output results were identical with those computed by the FHWA using their IBM 360/65 computer. A copy of the VESYS IIM sensitivity analysis prepared by Austin Research Engineers for the FHWA was obtained and studied for this project (52). The VESYS IIM program used for this project is capable of analyzing a three-layer flexible pavement. The University of Utah has a contract with the FHWA to expand the capability of the program to handle a five-layer pavement.

VESYS IIM is a comprehensive and complex computer program used for analysis of flexible pavements. The program requires approximately 67 input values, about 27 of which are program control variables while the remainder are independent variables (52). A flow diagram of the VESYS IIM pavement analysis and design system is presented in Figure 2. Detailed descriptions of the program are contained in the literature (41, 52, 53). The program utilizes the appropriate viscoelastic and distress properties of the materials to predict stress, strain, fatigue cracking, rut depth, slope variance, Present Serviceability Index, and service life with time. The VESYS IIM program is capable of analyzing element response altered by temperature and loading rate fluctuations.

A variety of pavement design systems has been programmed recently

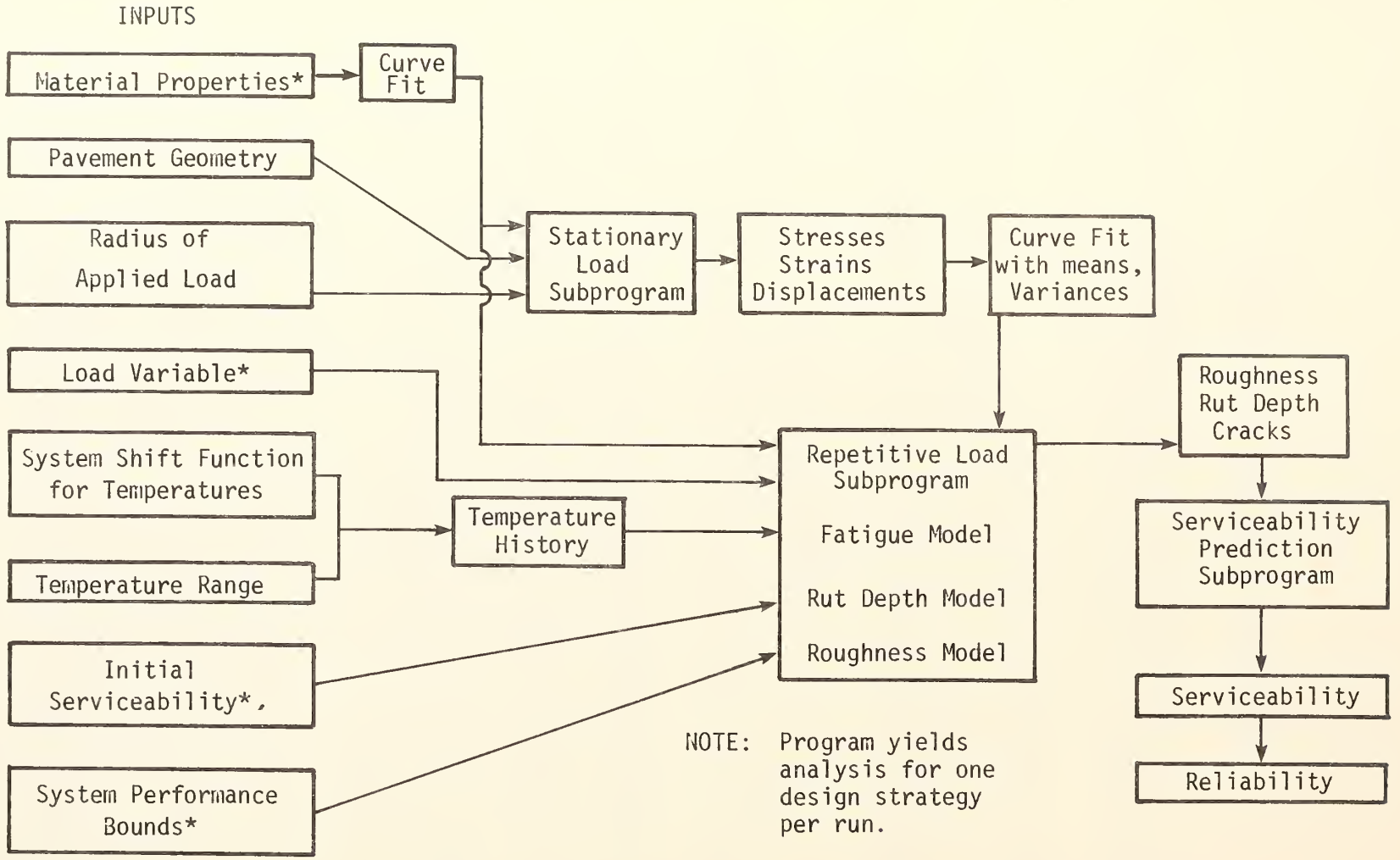

*Stochastic input

FIG. 2--VESYS IIM pavement analysis and design system (52).

and many of them are an outgrowth of the Texas Flexible Pavement Design System (FPS) (54, 55). Subsequent developments include the Texas Rigid Pavement Design System (RPS) (56), the SAMP 6 flexible pavement design system using the AASHTO Interim Guide structural subsystem (57), and the Texas FPS-BISTRO, an updated version of the Texas FPS which uses elastic theory as a basis for stress and strain calculations within the structural subsystem (58, 59). Input data to this latter program include material stiffness, Poisson's ratio, layer thickness, and position and magnitude of load.

Selection of Analysis Methods

On the basis of the review of the existing flexible pavement systems analysis computer programs, it was decided that a modification of the FPS-BISTRO would best serve the purposes of this project for the required screening analyses. The modification of this program includes the following:

1. Calculation of primary response.
   a. Stress and strain at the bottom of the surface course.
   b. Confining stress and difference in major and minor principal stresses at the center of the base course.
   c. Stress and strain at the bottom of the base course.
   d. Vertical strain at the top of the subgrade.

2. Incorporation of failure criteria.
   a. Fatigue law for surface course.
   b. Barksdale, Duncan and Chang's permanent deformation criterion for granular base course.
   c. Fatigue law for cement stabilized base course.
   d. Fatigue law for asphalt stabilized base course.
   e. Permanent deformation criterion for subgrade.

The changes were made and FPS-BISTRO was run successfully with them included. The program compares the calculated primary response with the failure criteria for each layer, and the design is rejected as infeasible if any of the criteria are not met. Using the Texas FPS-BISTRO program, screening analyses were performed to determine optimum pavement designs.

The VESYS IIM program was selected for use as the structural design subsystem. The optimum pavements found in the Texas FPS-BISTRO screening analyses were further analyzed for stress, distress, and performance using the VESYS IIM program.

Selection of Materials Characterization Tests

The use of the selected computer programs requires pavement material properties as input data. The Texas FPS-BISTRO program uses the elastic modulus and Poisson's ratio of all layers, flexural fatigue parameters

K_1 and K_2 of the surface and stabilized base course layers, initial tangent modulus for the base, and cohesion and angle of shearing resistance of the base course. Material properties required for the VESYS IIM program include fatigue parameters K_1 and K_2, time-temperature shift function, creep compliance, permanent deformation, and the temperature dependence of fatigue and permanent deformation. The laboratory tests performed to obtain these material properties are discussed subsequently in this report.

CHAPTER IV

TASK B: DEVELOPMENT OF SULPHUR EXTENDED ASPHALT SYSTEMS

This task included five subtasks as listed previously in the Scope of the Investigation. The first item of consideration under this task was selection of the experimental design variables and mixture combinations. Included in this task were development of the techniques and processes for dispersing and increasing the solubility of sulphur in asphalt cement. A major portion of this task was devoted to processing and preparation of specimens of sulphur asphalt emulsions (SAE), and preparation of specimens of numerous combinations of aggregate, asphalt and sulphur for use in subsequent testing. The three approaches (AAS, AE, and AES system mixtures) were used in preparation of these test specimens.

Selection of Mixture Composition and Experimental Design Variables

Since this project required evaluation of numerous combinations of aggregate, asphalt, and sulphur, it was necessary to select the type and quantity of these constituents to be used in laboratory testing. It was also necessary to select values for specimen preparation variables such as moisture condition and compaction effort. The basis for making these selections is included in the following sub-sections of this report.

Sulphur Selection

Elemental sulphur (sulphur in the free state) used in this project was a commercial grade of about 99.8 percent purity. It should be noted that this purity is not essential and should not be a factor dictating the use of commercial grade sulphur. The sulphur was purchased in the solid (powder) form and shipped in 50 lb (23kg) waterproof plastic bags which were also used for storage of the sulphur.

Review of available literature indicated that preparation of paving mixture specimens in which sulphur is included should be accomplished within a temperature range of 245°F to 305°F (118°C to 152°C) (60). This range is comparable with that normally encountered in preparation of conventional asphaltic concrete specimens. The lower temperature limit was established for two primary reasons. A temperature of 245°F (118°C) is about the melting point of sulphur, and processing of mixtures below this temperature destroys the structuring effects of sulphur. The upper temperature limit was established for two important reasons also. Above a temperature of about 305°F (152°C), hydrogen sulfide gas is emitted, and the viscosity of the sulphur begins to rise abruptly. The actual mixing temperature was 290°F (143°C) for specimens of aggregate, asphalt and sulphur used in this project.

TABLE 2

ASPHALT CEMENT SELECTION

ASPHALT DESIGNATION	GRADE	REFINING PROCESS	PRODUCER	LOCATION PRODUCED
ET AC-5	AC-5	Vacuum-Steam	American Petrofina Co. of Texas	Mt. Pleasant, Texas
ET AC-10	AC-10	Vacuum-Steam	American Petrofina Co. of Texas	Mt. Pleasant, Texas
ET AC-20	AC-20	Vacuum-Steam	American Petrofina Co. of Texas	Mt. Pleasant, Texas
WT AC-10	AC-10	Solvent De-asphalting (Slightly Waxy)	American Petrofina Co. of Texas	Big Spring, Texas
DS AC-10	AC-10	Solvent/Air Blown	Diamond Shamrock Co.	Sheerin, Texas
DS AC-20	AC-20	Solvent/Air Blown	Diamond Shamrock Co.	Sheerin, Texas
DENV AC-10	AC-10	Vacuum-Steam	Continental Oil Co.	Denver, Colorado
SM AC-10	AC-10	Vacuum-Steam (High Age Rate)	Continental Oil Co.	Santa Maria, Calif.
ME AC-10	AC-10	Vacuum-Steam	Gulf Oil Canada	Middle East
WC AC-10	AC-10	Vacuum-Steam (Waxy)	Gulf Oil Canada	Western Canada

TABLE 3

PHYSICAL PROPERTIES OF ASPHALT CEMENTS

ASPHALT	PENETRATION		VISCOSITY			RING & BALL SOFTENING POINT (^{o}F)	SPECIFIC GRAVITY @ 60^{o}F
	@ 39.2^{o}F	@ 77^{o}F	@ 77^{o}F (x 10^{4} POISES)	@ 140^{o}F (POISES)	@ 275^{o}F (STOKES)		
ET AC-5	16	178	200	512	2.64	100	1.02
ET AC-10	8	108	78	909	3.28	117	1.03
ET AC-20	3	66	200	2084	2.97	120	1.04
WT AC-10	5	85	109	1013	2.57	112	1.03
DS AC-10	7	123	62	1030	5.27	115	0.98
DS AC-20	5	75	2	2408	5.07	124	0.98
DENV AC-10	6	93	82	1249	3.02	112	1.01
SM AC-10	10	135	55	1172	2.94	105	1.03
ME AC-10	10	73	—	1377	3.12	114	1.02
WC AC-10	18	99	140	1364	3.65	110	1.02

^{o}C = (F - 32) x 5/9
1 poise = 0.1 Pa·s
1 stoke = 0.0001 m^{2}/s

Asphalt Cement Selection

Ten asphalt cements were selected for use in the project and were tested and graded in accordance with AASHTO Specification M266-73 (63). This selection includes asphalt cements manufactured by the vacuum-steam and the solvent (propane) de-asphalting processes. Two of the asphalt cements are waxy, two are air blown and one has a high aging rate. The selected grades (AC-5 to AC-20) of asphalt cements are within the range normally utilized in flexible pavement construction in the United States. Grades softer than AC-5 were not selected because asphalt refiners have expressed an interest in producing only the harder asphalts since the occurrence of the fuel crisis (50). Asphalt grades in excess of AC-20 are not presently available in large quantities, nor are they expected to be for the near future.

Information regarding the refining process, producer and location produced for each asphalt cement used in this study is shown in Table 2.

The two asphalt cements obtained from Diamond Shamrock Gas and Oil Co., Sunray, Texas, were produced from West Texas crude oil using a mixture of 10 parts of solvent refined materials and 1 part of oil residium to obtain a 130-150 penetration grade asphalt cement. This asphalt was then air blown until the penetration was about 85 and graded as an AC-20. The Diamond Shamrock AC-10 was obtained by combining the air blown AC-20 and an AC-3 which is not air blown in the proportions required to produce the desired viscosity. The selection of asphalt cements was varied in order to evaluate the effects of grade, source, presence of wax and manufacturing process on solubility and settling rate of sulphur in the asphalt cements.

Each of the asphalt cements was subjected to a series of standard laboratory tests to determine their physical properties. These tests, with applicable standard specifications, were as follows:

Penetration	AASHTO T49	(64)
Viscosity @ 77°F (25°C)	ASTM Tentative	(65)
Viscosity @ 140°F (60°C)	AASHTO T202	(66)
Viscosity @ 275°F(135°C)	AASHTO T201	(67)
Ring & Ball Softening	AASHTO T53	(68)
Specific Gravity	ASTM D 70	(69)

Results of these tests are presented in Table 3.

Asphalt viscosity was included as a variable in the experimental design of the screening tests which are discussed subsequently in this report. The ET AC-5 and ET AC-20 asphalt cements were selected for use in the screening tests where the experimental design required low and high levels, respectively, of asphalt viscosity.

Aggregate Selection

Approximately fifteen aggregates were studied for use in the laboratory testing portion of this project. Final selection of the aggregates to be used in the screening tests was based upon the combination of aggregate physical properties which most nearly satisfy the requirements established by the experimental design as explained subsequently in this report. Efforts were made to obtain aggregates which are available for use in the construction of pavements. Materials such as glass beads and flat metal plates, while possessing some of the extreme ideal physical properties, were not used because it was judged that the results would be of questionable practical significance.

The experimental design for this project required that roundness, sphericity, roughness, size and gradation of the aggregates be considered as variables. These physical characteristics of the aggregates were determined in accordance with standard test procedures.

Benson's literature survey indicated that shape of the aggregate has appreciable effect on the physical properties of the mixture, on the proper asphalt content, and on the voids relationship (114). Hargett's study showed that shape of the aggregate particles affects the interlocking resistance that is developed in bituminous mixtures, and may also affect voids and workability (113). Research by Livneh and Greenstein indicates that flaky aggregates produce bituminous mixtures which possess weakness planes, low densities, high optimal bitumen contents, and high breakage values (115). Two measures of aggregate shape are roundness and sphericity.

Aggregate roundness is a measure of the sharpness (angularity) of the corners and edges of the particles. Qualitative expressions such as angular, subangular, subrounded and rounded are somewhat vague with reference to roundness. These descriptive terms can be defined more usefully by expressing numerically the roundness of the grains. It is also required that a numerical expression of roundness be used in the experimental design. The roundness of a particle can be determined by $(r/R)/N$, where r is the radius of a corner, R is the radius of the maximum circle inscribed by the particle, and N is the number of corners in the particle. Krumbein developed a comparison chart in which grains under study could be compared with silhouettes of grains of specific roundness values (70). A Krumbein Number Chart is included as Figure 3 of this report. Aggregate roundness can range between 0.1 and 1.0. The roundnesses of the aggregates examined for this project were determined as follows: Photomicrographs of the fine grained aggregates were made. In accordance with the previously noted definition of roundness, actual measurements of the images of selected particles were made on the photomicrographs. Values for roundness were then calculated using the proper equation. The roundnesses of the larger sized particles were determined in a similar manner except that images of selected particles were transferred directly to paper and measurements were made thereon. These calculated values of roundness were then evaluated with respect to values

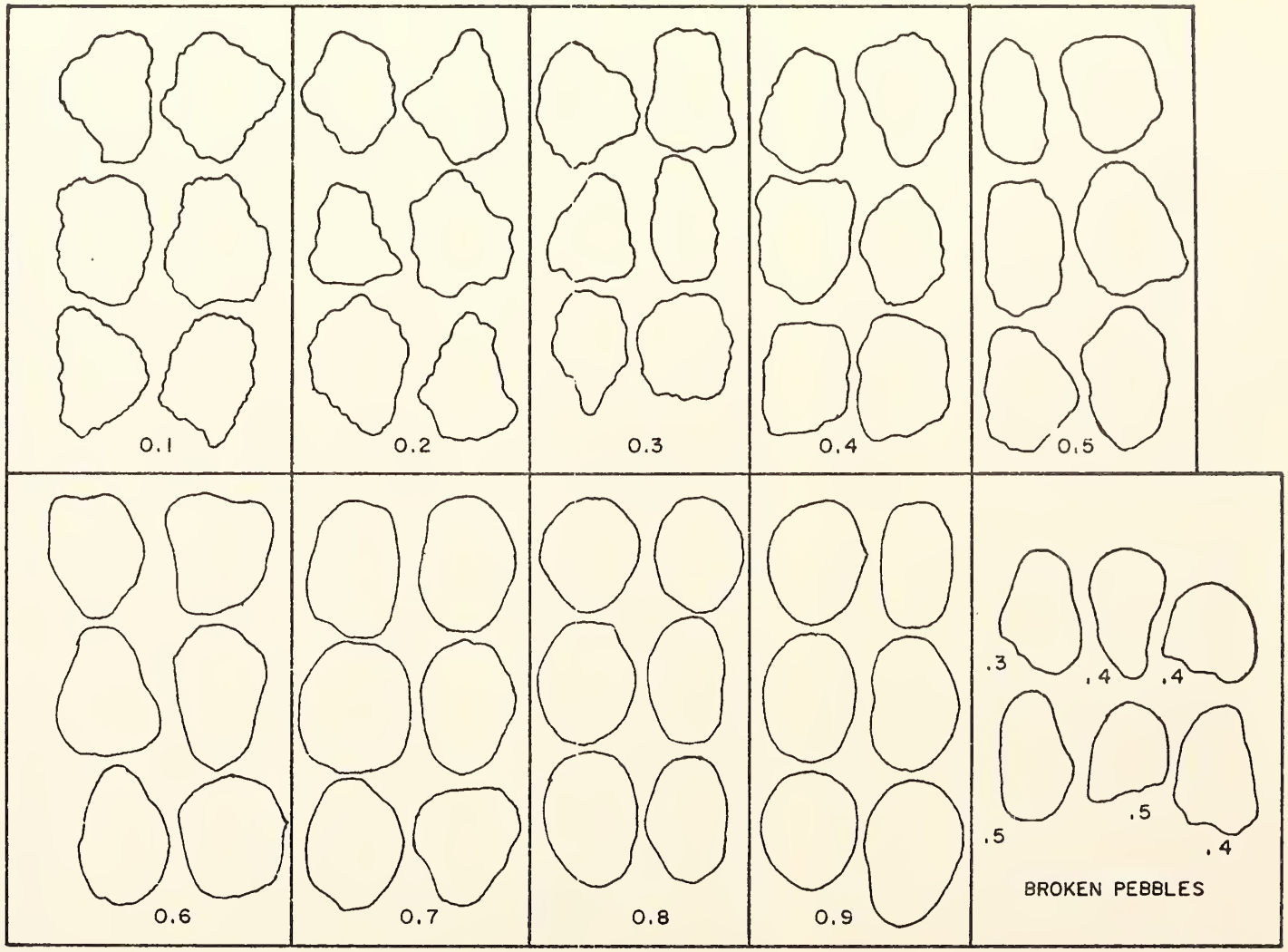

FIG. 3--Krumbein number aggregate roundness chart (70).

obtained by visual comparison of the particles (or photomicrographs thereof) with the Krumbin Chart. The final selection of values of roundness for each particle was based upon both the visual comparison and the calculated values.

Sphericity of an aggregate is an index of how closely a particle represents a sphere. Sphericity can be calculated as D_d/D_c, where D_d is the diameter of a circle with an area equal to that of the particle projection as it rests on its flat side, and D_c is the diameter of the smallest circumscribing circle of the particle. The required measurements were made on photomicrographs of the smaller particles and projected images of the larger particles. G. Rittenhouse prepared a chart for visual comparison of sphericity of aggregate particles (71). The practical range of aggregate sphericity if 0.45 to 0.97. Figure #4 presents sphericity numbers for typical aggregate shapes within the range used in this project. Figure 5 shows photomicrographs of two of the aggregates used in this project. The Rockdale slag has a roundness of 0.10 and a sphericity of 0.70, whereas the Gifford Hill fines have a roundness of 0.70 and a sphericity of 0.75.

Roughness is a measure of surface texture of the aggregate particles. This property is dependent upon the degree to which particle surfaces are polished or dull, smooth or rough and the type of surface texture. Roughness or surface texture is usually described in terms such as very rough, rough, smooth, and polished. Monismith indicates that surface texture has little influence on stiffness provided that mixtures are compared at their design asphalt contents (111). However, his findings show that for certain circumstances, mixtures containing rough textured aggregate would exhibit longer fatigue life. Griffin found that increased roughness of surface texture of the fine aggregate increased the minimum percentage of voids in the mineral aggregate and increased the optimum asphalt content (112). Hargett's study indicates that surface texture has a profound effect on the stability of a bituminous mixture (113). It has been suggested by Mather that roughness of aggregate particles should probably be expressed in terms of arithmetic average deviation of the actual surface from the mean surface (72). This method would probably be rather expensive for determination of roughness of a large number of aggregates. However, since a numerical value of roughness was required for use in the experimental design for this project, numbers were arbitrarily assigned to the terms listed previously. Table 4 presents the roughness classification system used for this project. Roughness values were determined either by visual examination of the larger particles or photomicrographs of the smaller particles.

The grading of the aggregate in a bituminous mixture is generally considered to be important. Monismith indicates that longer service lives are exhibited by dense-graded mixtures than by open-graded mixtures (111). Benson's study of the literature showed that aggregate gradation and size range influence the strength and stiffness characteristics of the mixture, permeability, asphalt content, economy, workability and skid resistance (114). Hargett's research also showed that bituminous

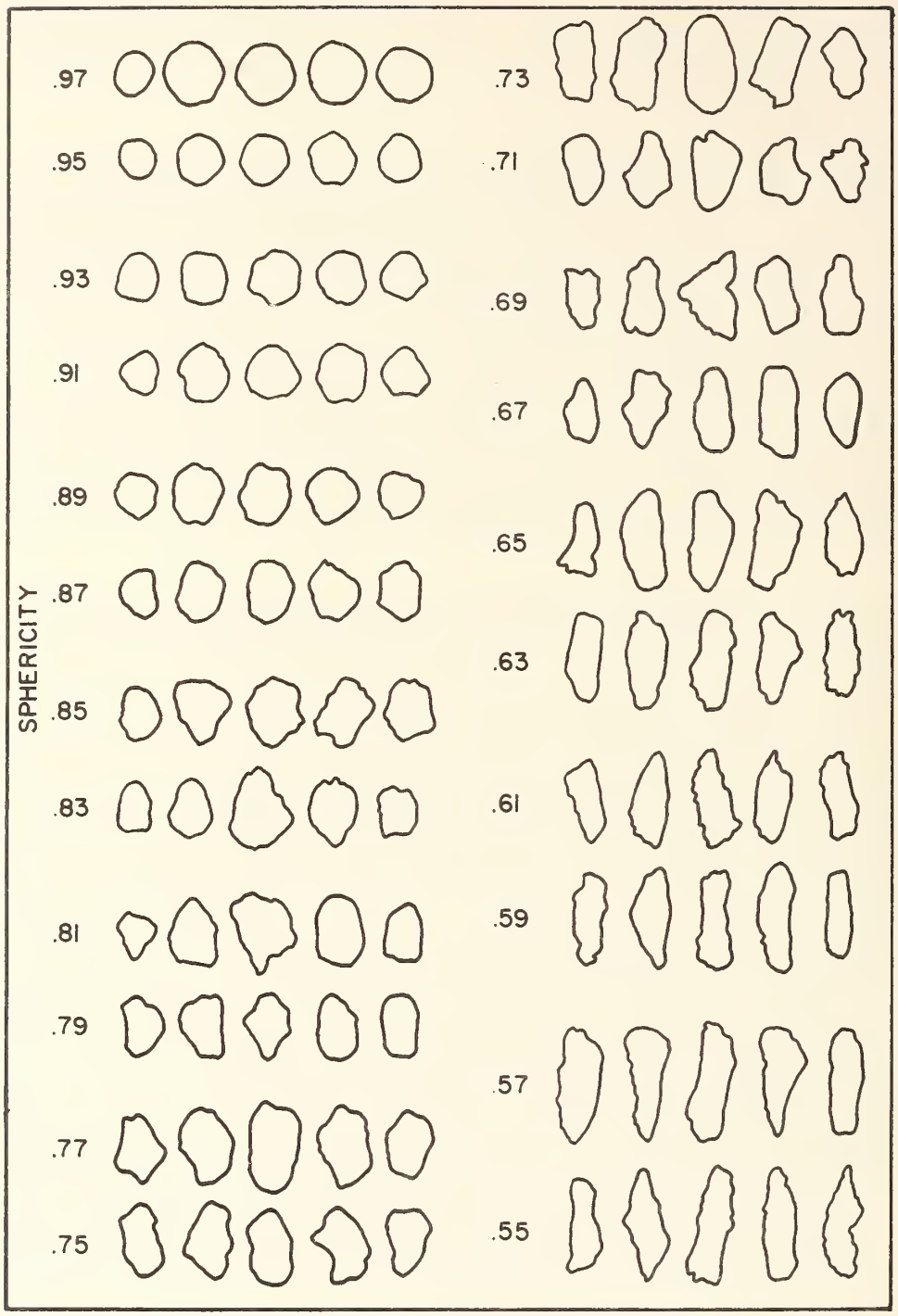

FIG. 4--Aggregate sphericity number chart (71).

ROCKDALE SLAG

GIFFORD HILL FINES

FIG. 5--Photomicrograph of two aggregates used in screening tests.

TABLE 4

ROUGHNESS (SURFACE TEXTURE) OF AGGREGATE

VISUAL CLASSIFICATION	ROUGHNESS NUMBER
Very Rough	1
Rough	2
Smooth	3
Polished	4

mixtures are affected by the maximum and minimum size of particles, and the gradation of the particle sizes within the size limits (113). Gradations (grain size distributions) of the various aggregates were determined in accordance with the procedures of ASTM C 136 (73) and ASTM C 117 (74). Since development of the experimental design required a numerical expression of the aggregate variables, it was necessary to devise a system which described both the size and gradation of a particular aggregate. It was also desirable that a relationship exist between this system and the performance of the aggregates within a sulphur asphaltic concrete. Numerous different combinations and ratios of particle sizes were tried. The most appropriate appears to be:

$$SGN = \frac{D_{85} - D_{50}}{(D_{20})^2}$$

where SGN is defined as the size and gradation number,

D_{85} is the grain size in inches, at which 85% of the sample is finer,
D_{50} is the grain size in in., at which 50% of the sample is finer, and
D_{20} is the grain size in inches, at which 20% of the sample is finer.

Generally, a large value of SGN indicates an aggregate which is well-graded with particle sizes ranging between large and very small. A small value of SGN indicates a relatively large, uniformly graded aggregate. A typical beach sand would have an intermediate SGN, even though it may be uniformly graded. Normally, a uniformly graded fine aggregate will perform better in a sulphur asphaltic concrete than will a uniformly graded coarse aggregate. The performance of sulphur asphaltic concrete usually improves with increasing SGN of the total aggregate system used in the mixture. The SGN is influenced by the maximum and minimum particle sizes, and gradation of the particle sizes within these limits. Although the SGN may be useful in evaluating a potential aggregate for use in sulphur asphaltic concrete, it should not be the only basis for acceptance of gradation of the aggregate. Typical aggregate gradings and respective values of SGN are shown in Figure 6. Gradation curves for the individual aggregates studied in this project are included in Appendix A. A summary of the

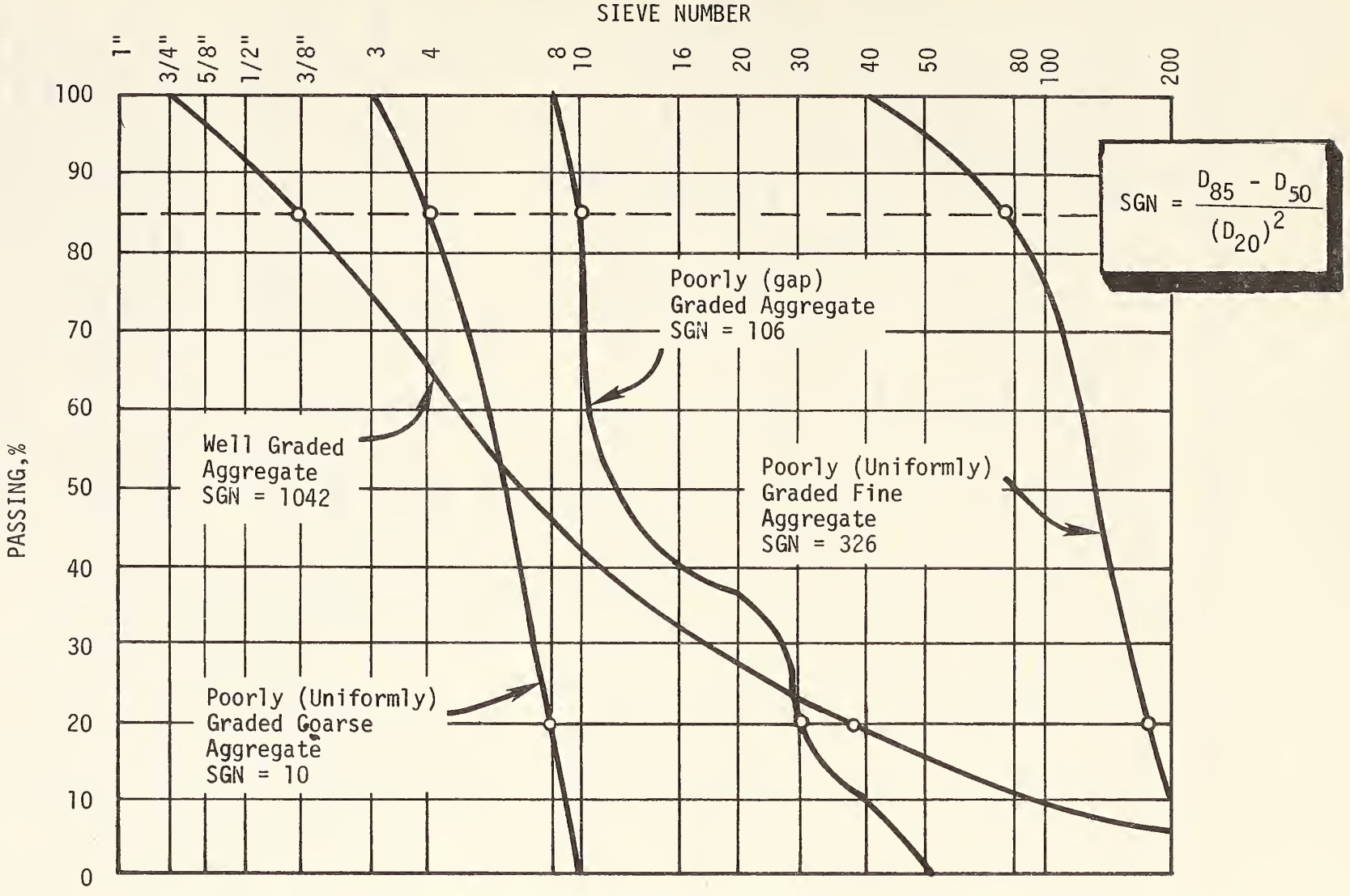

FIG. 6--Typical aggregate gradings showing size and gradation numbers (SGN).

physical properties of the aggregates selected for use in the screening tests is presented in Table 5.

The crushed limestone used in the screening tests was obtained from Texas Crushed Stone Company, Georgetown, Texas. The limestone material was separated into individual sizes, by sieving, and then combined in the amounts required to produce a gradation which complied with Asphalt Institute Type IVb mix (88). The fluvial gravel was obtained from Gifford-Hill Company, Bryan, Texas, and was sized in a manner similar to that of the crushed limestone. It was necessary to add rock flour fines to the gravel in order to comply with the gradation requirements. Kenedy County sand is a dune sand obtained from Kenedy County, Texas. The beach sand was obtained from the Texas Gulf Coast near Corpus Christi, Texas. It is the sand used by Dr. H. Admad in his research of sand-asphalt-sulphur for his Ph.D. Dissertation (35). The concrete sand is a typical sand which meets the requirements of ASTM C33-71 (89), and was obtained from Gifford-Hill Company, Bryan, Texas. The crushed granite was obtained from Texas Crushed Stone Company, Georgetown, Texas. Gifford-Hill Company, Eagle Lake, Texas, supplied the crushed Eagle Lake gravel. The Superrock material was a synthetic expanded clay lightweight aggregate manufactured by Superrock Incorporated in Streetman, Texas. The Superrock fines were obtained from the same manufacturer. The Rockdale slag is a waste product of the burning of lignite at the Aluminum Company of America power plant near Rockdale, Texas. Gifford-Hill fines were obtained by selecting certain size fractions of the concrete sand supplied by Gifford-Hill Company.

Selection of Asphalt Cement and Sulphur Contents

The experimental design requires that high and low levels of asphalt cement and sulphur contents be used in the screening tests. For the Aggregate-Asphalt-Sulphur (AAS) system mixtures, asphalt cement contents of 2 and 6 percent by weight of total mix were used as low and high levels, respectively; whereas sulphur contents of 12 and 18 percent by weight of total mix were used as low and high sulphur levels, respectively. These low and high levels of asphalt cement and sulphur, based on a percentage by weight of total mix, were used regardless of the type aggregate used in the mixture.

Prior to selection of high and low levels of asphalt cement and sulphur contents for the Aggregate-Emulsion (AE) system mixtures, results of the AAS system mixtures were evaluated. It was apparent that values for high sulphur and/or asphalt cement content may have been high for some of the aggregates used, but low for other aggregates used, depending upon the voids in the compacted mixture. A similar situation existed for the low value used. Thus, it was obvious that a revised method of establishing low and high levels for asphalt cement and sulphur contents was needed. In order to adapt these two variables to each individual aggregate, rather than use the same percentages by weight of asphalt

TABLE 5

PHYSICAL PROPERTIES OF AGGREGATES

AGGREGATE	VARIABLE LISTED IN EXPERIMENTAL DESIGN			
	ROUNDNESS	SPHERICITY	ROUGHNESS	SGN [a/]
Crushed Limestone (Grade IV b)	0.20	0.70	1.5	977
Kenedy County Sand A	0.35	0.71	2.0	78
Ahmad's Beach Sand	0.40	0.80	2.2	64
Concrete Sand	0.58	0.83	2.7	680
Fluvial Gravel (Grade IV b)	0.73	0.77	3.3	977
Crushed Granite	0.15	0.75	1.2	8
Crushed Eagle Lake Gravel	0.30	0.75	3.0	2
Superrock	0.78	0.87	1.8	56
Rockdale Slag	0.10	0.70	3.5	87
Gifford-Hill Fines (No. 8 - No. 50)	0.70	0.75	3.1	64
Superrock Fines	0.60	0.80	2.0	86

[a/] SGN = SIZE & GRADATION NO. = $\frac{D_{85} - D_{50}}{(D_{20})^2}$

1 cm. = 0.394 in.

cement and sulphur for all aggregates, the following criteria were established. The asphalt cement content variable was changed to binder (asphalt cement plus sulphur) content variable. When a high binder content (formerly asphalt cement content) was specified by the experimental design, approximately 75 percent of the voids in mineral aggregate (VMA) was filled with binder whereas about 40 percent of the VMA was filled with binder for a specified low binder content. For the required high and low sulphur contents, 70 percent and 30 percent of the volume of binder, respectively, were filled with sulphur. Use of these criteria required estimation of the VMA for each aggregate used. The results obtained from the screening tests performed on samples prepared for the AAS system were useful when estimating VMA for the various aggregate mixtures of the AE system.

For the Aggregate-Emulsion-Sulphur (AES) system mixtures, the low and high levels of asphalt cement and sulphur contents were identical to those used for the AE system with the exception that 10 percent (by weight of total mix) sulphur was added after the previously noted amounts of asphalt cement and sulphur were introduced. The method of adding the components of this system is discussed subsequently.

The selected values for low and high asphalt cement, binder and sulphur contents are summarized in Table 6.

Selection of Moisture Condition and Compaction Effort

The final independent variables used in the experimental design were moisture condition and compactive effort. Where a low level of

TABLE 6

SELECTED ASPHALT, BINDER AND SULPHUR CONTENTS FOR SCREENING TESTS

System	Asphalt Cement (w/o of mix)		SAE Binder (v/o of VMA)		Sulphur (v/o of SAE)		Sulphur (w/o of mix)	
	Low	High	Low	High	Low	High	Low	High
AAS	2	6	---	---	---	---	12	18
AE	---	---	40	75	30	70	---	---
AES	---	---	40	75	30	70	10 Additional	
Note:	SAE is sulphur-asphalt emulsion v/o is volume percent w/o is weight percent							

moisture condition was specified, the specimens were tested in a dry condition at the temperatures required for the particular test in progress. Where a high level of moisture condition was specified, the compacted specimens were vacuum saturated at room temperature (about 72°F, 22°C) for a period of 45 minutes and then soaked in water for a period of two days prior to testing. The vacuum saturation was accomplished by placing the specimens in a chamber, covering them with water and applying a partial vacuum of about 27.5 inches (698.5 mm) of mercury.

The low and high levels of compactive effort used in the experimental design were 2 and 75 blows per face, respectively, of the specimen utilizing the standard Marshall method of compaction (75). The level of compaction affects the air void content. The former was used as a variable because it is much easier to control than is air void content, although air voids would have been the more desirable independent variable to control.

Processing of Sulphur-Asphalt Emulsion (SAE) Binders

This portion of the project required preparation and laboratory testing of the SAE binders. The purposes were to determine the effects upon the blend stability created by varying mixing temperature, storage temperature, source of asphalt cement, viscosity of asphalt cement and sulphur content of the emulsion. The blend stability of the emulsion is the ability of the blend to prevent settlement of the sulphur during a period of 24 hours when stored at a temperature of 250°F (121.1°C). The physical properties of SAE binders were determined, relative solubilities of sulphur in the various asphalt cements were determined.

Preparation of Sulphur-Asphalt Emulsions

The emulsions were prepared in the laboratory by use of an Epinbach Laboratory Homogenizer. This is a portable stainless steel colloid mill which has a single shear speed of 1750 rpm and a flow capacity of 50 gal/hr. (0.2 m^3/hr). It has a recycling capability and the spacing between rotor and stator is adjustable. The procedure used for emulsion preparation was to preheat the asphalt cement and sulphur separately, pour them into the steam heated homogenizer, mix and recycle for 2 minutes with the rotor/stator opening set at 12.5 microns, and then mix and recycle for 5 minutes with the opening set at 5 microns.

Each asphalt cement listed in Table 2 was mixed with sulphur in the amounts of 20, 30, 40 and 50 percent by weight emulsion. In this report, weight percent is shown as w/o whereas volume percent is shown as v/o. It was anticipated originally that mixing temperatures of 250°F, 275°F and 300°F (121°C, 135°C and 149°C) would be used for each combination. However, poor dispersion of the sulphur and asphalt was obtained at temperatures below about 275°F (135°C) because the components did not

emulsify easily. Experience has shown that sulphur-asphalt emulsions mixed at temperatures above approximately 305°F (152°C) produce hydrogen sulfide gas (H_2S). Therefore, mixing temperatures of 285°F (141°C) and 300°F (149°C) were used for preparation of the emulsions. The amounts of sulphur and asphalt cements and the mixing temperatures are summarized in Table 7. The weight percents and corresponding volume percents of each fraction are listed.

TABLE 7

SULPHUR AND ASPHALT CONTENTS USED IN EMULSIONS

Sulphur Content		Asphalt Content	
w/o	v/o	w/o	v/o
20	11	80	89
30	18	70	82
40	25	60	75
50	33	50	67
Mixing Temperatures: 285°F and 300°F (141°C and 149°C)			

Determination of Physical Properties of Emulsions

For each emulsion, the physical properties determined in the laboratory included specific gravity, ring and ball softening point, penetration at 77°F (25°C) and viscosity at 140°F and 275°F (60°C and 135°C). Tests were performed in accordance with the appropriate ASTM procedures as listed previously for the asphalt cement. When it was necessary to reheat a sample of sulphur-asphalt emulsion in order to perform a test, efforts were made to assure that the sulphur was well dispersed in the asphalt.

Results of the laboratory tests are presented in Table 8. The general trend of the data is shown in Figure 7 where specific gravity, penetration, softening point and viscosities are plotted versus the sulphur/asphalt content. Similar curves for each emulsion tested are included in Appendix B. The individual test results which appear suspect are believed to be the result of non-homogeneous samples of the SAE binder.

TABLE 8

PHYSICAL PROPERTIES OF SULPHUR-ASPHALT EMULSIONS

Asphalt Cement	Mixing Temp. (^{o}F)	Sulphur Content of SAE (w/o)	Specific Gravity	Penetration @ 77^{o}F	Ring and Ball Softening Point (^{o}F)	Viscosity @ 140^{o}F (Poises)	Viscosity @ 275^{o}F (Stokes)
ET AC-5	285	0	1.02	178	100	512	2.64
		20	1.10	175	103	293	1.21
		30	1.21	145	103	409	1.88
		40	1.29	134	105	722	1.16
		50	1.46	138	106	479	1.23
	300	20	1.21	171	104	318	1.25
		30	1.23	160	104	294	1.35
		40	1.33	123	100	363	1.15
		50	1.52	170	106	331	1.25
ET AC-10	285	0	1.03	108	117	909	3.28
		20	1.15	120	110	621	1.46
		30	1.24	130	114	625	1.49
		40	1.31	121	122	708	1.53
		50	1.45	98	113	668	1.63
	300	20	1.14	103	125	739	1.61
		30	1.24	123	121	837	1.62
		40	1.32	109	116	853	1.62
		50	1.48	65	116	770	1.66

$^{o}C = (^{o}F - 32) \times 5/9$

TABLE 8 (CONTINUED)

Asphalt Cement	Mixing Temp. (^{o}F)	Sulphur Content of SAE (w/o)	Specific Gravity	Penetration @ 77^{o}F	Ring and Ball Softening Point (^{o}F)	Viscosity @ 140^{o}F (Poises)	Viscosity @ 275^{o}F (Stokes)
ET AC-20	285	0	1.04	66	120	2084	2.98
		20	1.16	50	114	830	1.67
		30	1.20	97	122	907	1.66
		40	1.29	78	120	1632	1.63
		50	1.41	42	119	1341	1.91
	300	20	1.12	60	126	1023	1.80
		30	1.21	65	140	1056	1.91
		40	1.29	58	124	1762	2.27
		50	1.39	98	128	1159	1.64
WT AC-10	285	0	1.03	85	112	1013	2.58
		20	1.15	112	130	581	1.14
		30	1.26	107	118	512	1.13
		40	1.35	110	109	770	1.25
		50	1.50	63	120	588	1.26
	300	20	1.15	130	114	652	1.10
		30	1.24	110	125	547	1.23
		40	1.42	108	118	588	1.21
		50	1.50	53	114	675	1.36

$^{o}C = (^{o}F - 32) \times 5/9$

TABLE 8 (CONTINUED)

Asphalt Cement	Mixing Temp. (^{o}F)	Sulphur Content of SAE (w/o)	Specific Gravity	Penetration @ 77^{o}F	Ring and Ball Softening Point (^{o}F)	Viscosity @ 140^{o}F (Poises)	Viscosity @ 275^{o}F (Stokes)
DS AC-10	285	0	0.98	123	115	1030	5.28
		20	1.08	110	115	800	3.05
		30	1.16	97	119	827	1.15
		40	1.23	71	129	921	4.25
		50	1.36	79	115	1532	3.69
	300	20	1.09	101	116	910	3.15
		30	1.15	105	121	975	3.78
		40	1.23	62	131	1135	3.85
		50	1.33	65	128	1016	4.57
DS AC-20	285	0	0.98	75	124	2408	5.07
		20	1.10	113	123	1839	3.97
		30	1.16	110	129	1480	4.21
		40	1.25	52	145	1617	4.52
		50	1.33	34	135	651	5.00
	300	20	1.10	102	122	1812	4.49
		30	1.16	100	131	1767	4.64
		40	1.19	51	127	1297	5.48
		50	1.32	36	141	1448	5.33

$^{o}C = (^{o}F - 32) \times 5/9$

TABLE 8 (CONTINUED)

Asphalt Cement	Mixing Temp. (^{o}F)	Sulphur Content of SAE (w/o)	Specific Gravity	Penetration @ 77^{o}F	Ring and Ball Softening Point (^{o}F)	Viscosity @ 140^{o}F (Poises)	Viscosity @ 275^{o}F (Stokes)
DENV AC-10	285	0	1.01	93	112	1249	3.02
		20	1.13	125	116	842	1.40
		30	1.21	120	113	784	1.48
		40	1.32	120	114	729	1.45
		50	1.48	96	110	620	1.50
	300	20	1.13	139	130	681	1.34
		30	1.21	129	116	807	1.36
		40	1.30	100	114	759	1.41
		50	1.48	106	114	890	1.57
SM AC-10	285	0	1.03	135	105	1172	2.95
		20	1.14	115	111	769	1.52
		30	1.21	114	106	748	1.37
		40	1.25	130	112	691	1.45
		50	1.41	103	111	769	1.52
	300	20	1.16	166	121	657	1.71
		30	1.22	168	106	639	1.57
		40	1.31	135	123	718	1.88
		50	1.49	89	121	657	1.71

$^{o}C = (^{o}F - 32) \times 5/9$

TABLE 8 (CONTINUED)

Asphalt Cement	Mixing Temp. (^{o}F)	Sulphur Content of SAE (w/o)	Specific Gravity	Penetration @ 77^{o}F	Ring and Ball Softening Point (^{o}F)	Viscosity @ 140^{o}F (Poises)	Viscosity @ 275^{o}F (Stokes)
ME AC-10	285	0		73	114	1377	3.12
		20	1.15	123	114	627	1.38
		30	1.22	125	113	587	1.29
		40	1.29	109	112	624	1.45
		50	1.39	114	116	778	1.39
	300	20	1.14	117	114	616	1.30
		30	1.18	123	114	609	1.30
		40	1.29	114	115	696	1.32
		50	1.39	104	116	703	1.64
WC AC-10	285	0		99	110	1364	3.65
		20	1.16	137	112	641	1.39
		30	1.23	160	110	603	1.42
		40	1.31	98	114	630	1.62
		50	1.40	105	109	575	1.53
	300	20	1.15	141	112	685	1.49
		30	1.22	153	112	577	1.50
		40	1.31	132	112	624	1.56
		50	1.41	66	111	622	1.60

$^{o}C = (^{o}F - 32) \times 5/9$

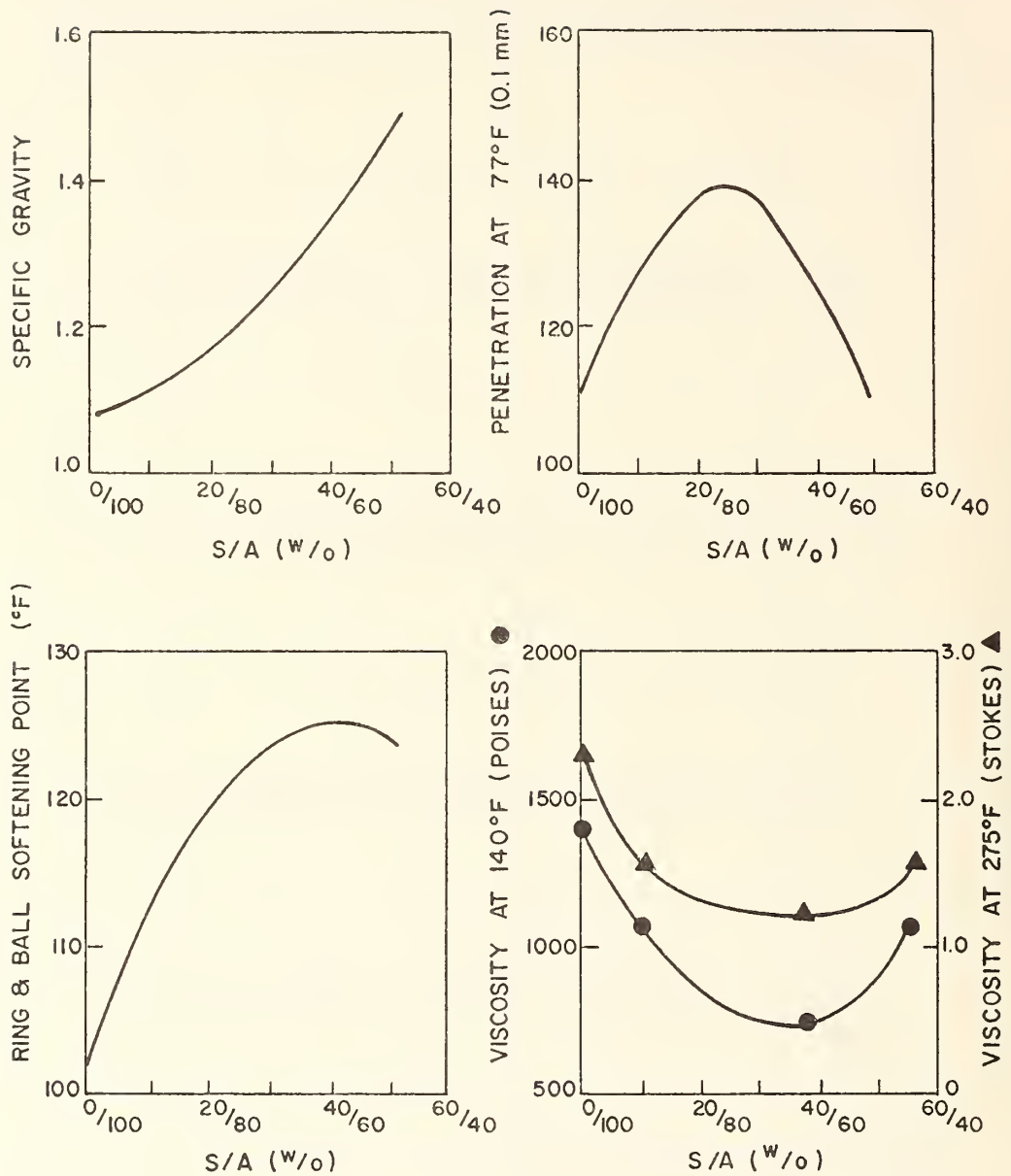

FIG. 7--General trend of physical properties of sulphur-asphalt emulsions.

$^{o}C = (^{o}F - 32) \times 5/9$

Since sulphur has a specific gravity about twice that of asphalt cement, the specific gravity of the composite SAE blend increases with increasing sulphur content. The general shape of the curve for specific gravity vs. sulphur-asphalt content is slightly concave upward with increasing sulphur content. The specific gravity was found to increase less than expected, considering the specific gravity of the two components, up to 20% sulphur content. This was similar to the trend reported by Garrigues (12 and Gallaway (81).

The general trend of the penetration test data indicates that penetration increased with sulphur content up to about 20 or 30 w/o sulphur, and then decreased as the sulphur content continued to increase. The penetration at 50 w/o sulphur was generally less than that of the asphalt cement. These observations are similar to trends published by Kennepohl, Garrigues, and Bencowitz (9, 12, 38). Some exceptions to this general trend are the SAE made with ET AC-5 and DS AC-10 asphalt cements prepared at temperatures of 285°F (140.6°C) and 300°F (148.9°C) and SM AC-10 asphalt cement mixed at a temperature of 285°F (140.6°C). The DS AC-10 asphalt cement was produced by the air blowing process. Each of these asphalt cements possessed a penetration in excess of 120 which was relatively high in comparison with the other asphalt cements tested. The penetration of the SAE binders made with the three noted asphalt cements generally decreased as sulphur content increased, rather than exhibiting an initial increase in penetration. It has been reported that the repeatability of penetration test results is influenced by the maturing of the test specimens of SAE (10, 11). Garrigues believes that this maturing process results from additional dissolving of dispersed sulphur which occurs during the first 30 hours after preparation of the SAE binder (12).

Results of the ring and ball softening point tests were quite erratic, although the general trend was gradually increasing softening point with sulphur increase. In many instances, the softening point began to decrease at sulphur contents in excess of 30 or 40 w/o. Similar erratic trends are reported by Gallaway for SAE binders tested in connection with the Lufkin, Texas field trials (81).

Significant changes in viscosity of SAE binders occur with changes in sulphur content. Generally, the addition of 10 to 20 w/o sulphur to the asphalt cement decreased the viscosity measured at 140°F (60°C) by as much as fifty percent for all asphalt cement grades tested. At sulphur contents in excess of about 20 to 30 w/o, the viscosity began to rise abruptly. A similar trend existed for the viscosities measured at 275°F (135°C), although the rise of viscosity of SAE binders at sulphur contents in excess of about 30 w/o was more gradual than that measured at 140°F (60°C). Results of laboratory tests by Gallaway (81) and Kennepohl (9) indicate a similar trend of viscosity-temperature characteristics for sulphur-asphalt blends. As shown on the individual curves in Appendix B, there were some exceptions to the general trend discussed above. Many of the tests indicated that the viscosity measured at 140°F (60°C) of the SAE binder with 50 w/o sulphur was somewhat lower than that

of SAE binder with 40 w/o sulphur. Kennepohl indicates that a viscosity range of 200 to 600 centistokes is considered the appropriate region of good work-ability with respect to aggregate coating during mixing, spreading, and compaction of asphaltic paving mixtures (9). The Asphalt Institute recommends that asphaltic cement be within a viscosity range of 150 to 300 centistokes for mixing of asphalt paving mixtures (78). Except for the SAE binders made with the DS AC-10 and DS AC-20 air blown asphalt cements, the viscosities measured at 275°F (135°C) ranged between 100 and 200 centistokes which was lower than for the asphalt cements alone. This indicates that for most of the asphalt cements tested, the addition of sulphur should permit mixing, placing, and compaction of paving mixtures at temperatures below those which would be effective for the asphalt cements alone.

Sulphur Settling Rate Measurements

Since the specific gravity of sulphur is approximately twice that of asphalt cement, it was necessary to investigate the possibility that the sulphur might settle out of the SAE blends. Sulphur settling rates were determined by placing five glass test tubes of each emulsion into an oven at a temperature identical to the mixing temperature. Each test tube was filled to an identical height of six inches (152.4 mm). One test tube of emulsion was removed from the oven after storage times of 0.5, 1.0, 2.5, 4.0, and 6.0 hours each. Upon removal from the oven, the test tubes of emulsion were brought to room temperature and then chilled in a refrigerator. Initially, measurements were made of the height of sulphur which settled to the bottom of the test tubes by sawing the lower ends of the test tubes lengthwise to expose the settled sulphur. Due to difficulties encountered with breaking of the test tubes during sawing, this measurement procedure was modified subsequently as follows: After the test tubes were removed from the oven, they were maintained at room temperature for a period of at least 24 hours and then they were placed in an oven at 140°F (60°C) for about one hour. A one-eighth inch diameter steel rod was pushed through the emulsion until the settled sulphur, if any, prevented further penetration of the rod. The height of the settled sulphur was then determined from the depth to which the rod penetrated. Figure 8 shows a photograph of test tubes which were sawed to expose the settled sulphur.

The sulphur settlement rate measurements are presented as plots of height of settled sulphur vs. elapsed storage time. Graphs for each asphalt tested are included in Appendix C. Figures 9 and 10 present graphs for sulphur settling heights for ET AC-5 and DS AC-20 asphalt cements, respectively. These two graphs represent the approximate maximum and minimum limits of settling heights encountered in the project.

Generally, greater amounts of sulphur settled from SAE blends prepared with more fluid asphalt cements from the same source, i.e., more settlement occurred in the AC-5 blends than in the AC-10 blends. Examination of the sulphur settling height graphs indicates that very little

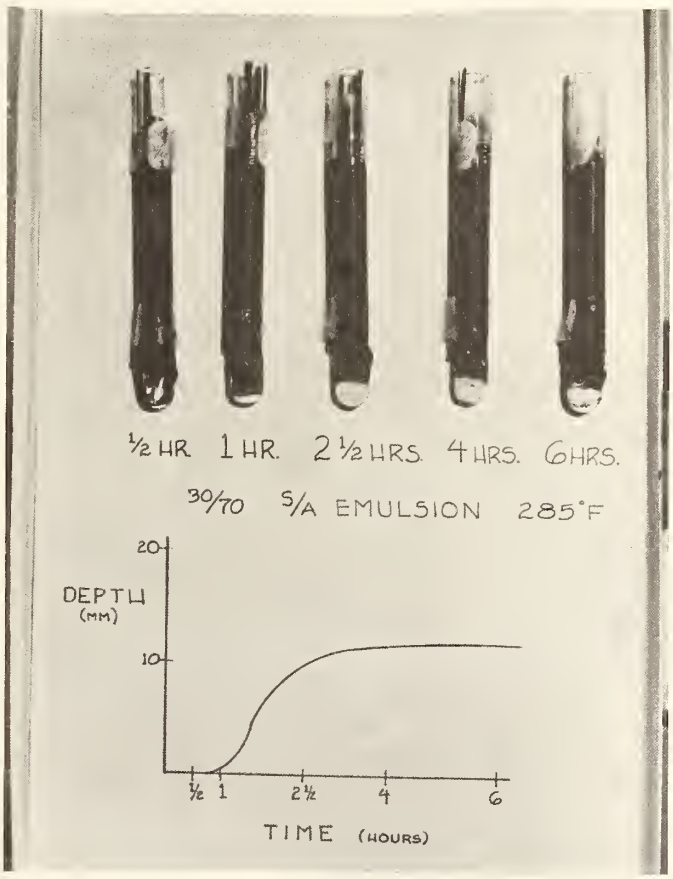

FIG. 8--Typical settling of sulphur from sulphur-asphalt emulsion.

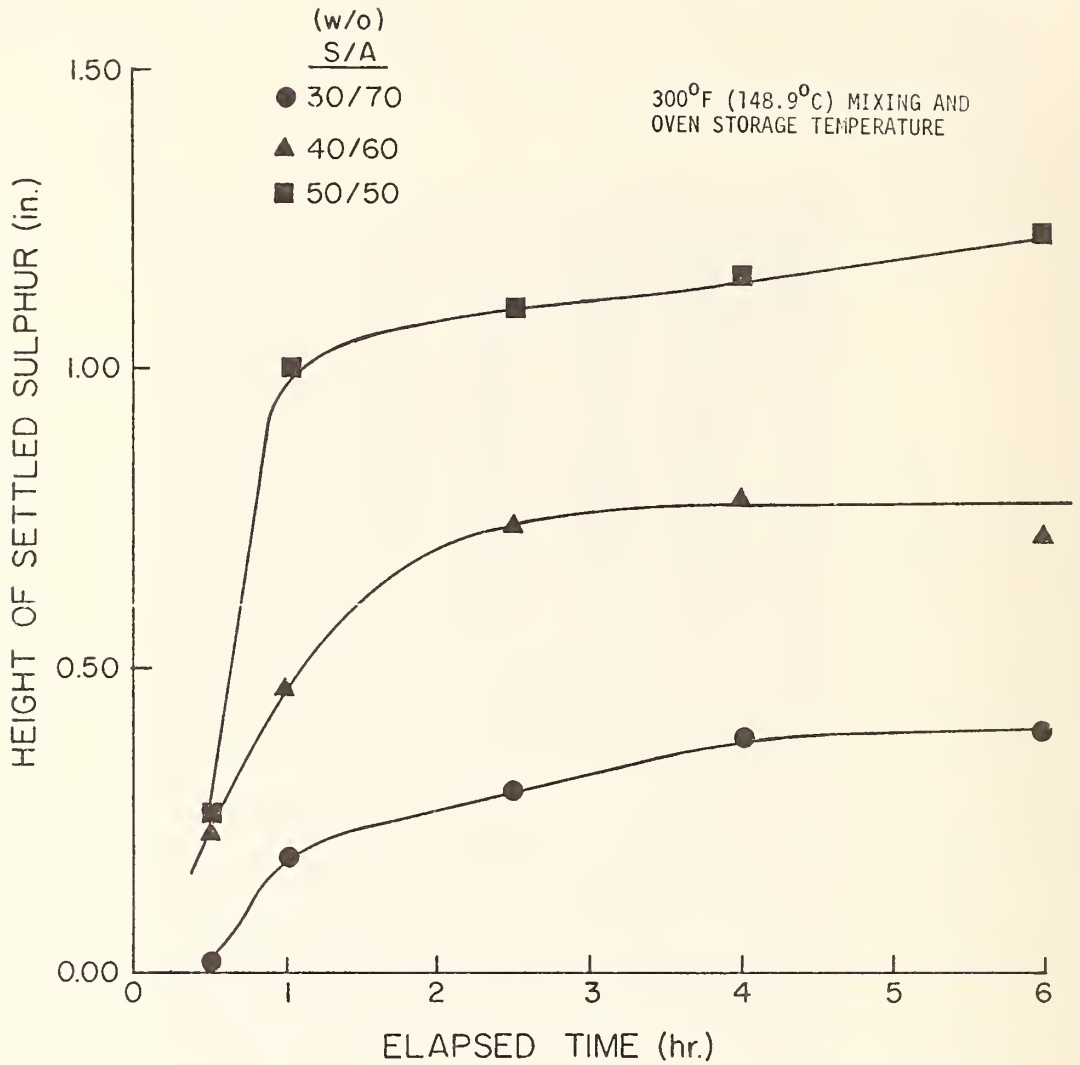

FIG. 9--Sulphur settling height of sulphur-asphalt emulsion made with ET AC-5 asphalt cement.

1 cm. = 0.394 in.

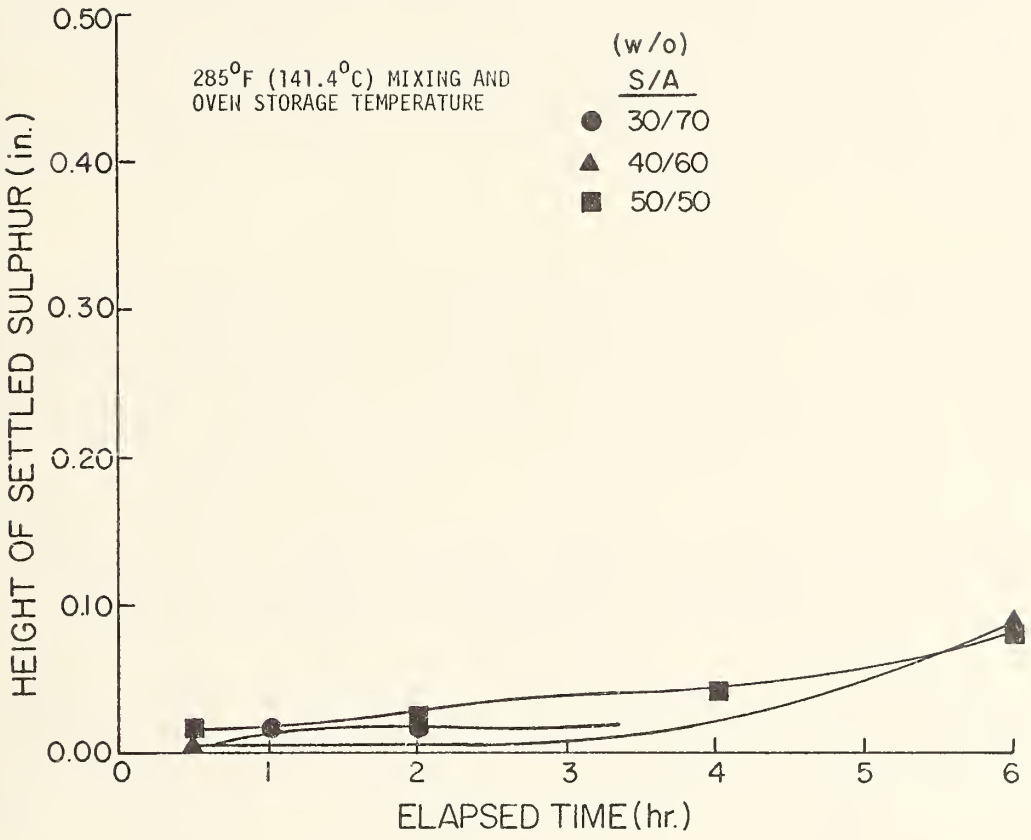

FIG. 10--Sulphur settling height of sulphur-asphalt emulsion made with DS AC-20 asphalt cement.

1 cm. = 0.394 in.

sulphur settled from any of the SAE blends containing 20 w/o sulphur. As the sulphur content of the blends increased, the amount of sulphur which settled increased. Generally, a slightly greater amount of sulphur settled from the blends prepared and stored at 300°F (148.9°C) than from those blends prepared and stored at 285°F (140.6°C). No significant differences were observed in the amount of sulphur which settled from the various asphalt cements with the same grade, except for the two Diamond Shamrock Company asphalt cements designated as DS AC-10 and DS AC-20. Very little sulphur settled out of the SAE blends prepared with these two asphalt cements which were manufactured by the air blowing process. Apparently, the air blowing process gives the asphalt cement the capability of maintaining sulphur particles in suspension for long periods of time. Large amounts of sulphur, e.g. 50 w/o, in a SAE blend can impart a dark-brown color to the mixture.

The capability of the asphalt cement to maintain the sulphur in suspension is referred to as blend stability (9). The stability of a SAE blend is of practical significance when the SAE is used as a binder in paving mixture. One concept for the use of sulphur in paving mixtures involves preparation of a SAE binder and then mixing the binder with the aggregate (12). In the event that it became necessary or desirable, with respect to operational requirements, that the SAE binder be stored in a tank prior to mixing with the aggregate, it would be particular important that the sulphur not settle from the SAE. Otherwise, the binder would not be a homogeneous mixture. In such a case, settlement of the sulphur could probably be prevented by circulating the heated SAE. One important factor which would probably preclude long-term storage of SAE binder is the formation of dangerous hydrogen sulfide gas in the storage tank.

The length of time before observable settlement of sulphur occurs in SAE blends varies with the grade and source of asphalt cement and with the amount of sulphur in the blend. It is probable that settlement of the sulphur begins immediately upon termination of mixing or circulation. Settlement of sulphur was judged to be significant at a time of 0.5 hour for most SAE blends made with sulphur quantities in excess of 30 w/o. It can be concluded that most SAE blends with sulphur quantities greater than 30 w/o are of limited stability for times in excess of about 0.5 hour. It can also be concluded that air blowing of the asphalt cement significantly improves the blend stability of the SAE blend.

Relative Solubility of Sulphur in Asphalt Cements

When sulphur and asphalt are heated and combined in an emulsion, three distinct types of reactions can occur: a) the sulphur can react chemically with the asphalt and result in dehydrogenation, b) the sulphur can be dissolved in the asphalt, and c) sulphur in the crystalline form can remain in suspension in the asphalt. The mode of reaction which results in the dissolved sulphur is generally considered to be sulphurization through attack of the double bonds in the asphalt cement (9). Sulphur can be dissolved in asphalt at temperatures below 300°F (148.9°C). The

dissolving mechanism is believed to be separate from the chemical dehydrogenation reactions, and Garrigues reports that it is a function of time (12). At temperatures above about 305°F (151.7°C), dehydrogenation occurs and hydrogen sulfide gas is formed. Finely dispersed crystalline sulphur as well as dissolved sulphur affect the physical properties of sulphur-asphalt emulsion binders (50). Relative amounts of dissolved sulphur in the emulsions were determined for this project by use of the differential thermal analysis (DTA) equipment, Model KA2H, as manufactured by Robert L. Stone Co., Austin, Texas. The DTA equipment actually measures the crystalline sulphur in the samples. DTA equipment operates on the principle that thermal energy is absorbed (endothermic reaction) or evolved (exothermic reaction) during a physical or chemical change as a sample of material is heated. The equipment is capable of tracing a thermogram as the test progresses.

For this project, the DTA tests were performed on emulsion samples which were chilled in a refrigerator immediately after completion of mixing. In an effort to establish a consistent test procedure with respect to preparation of the specimens, a comparison was made of emulsion cooled in the refrigerator with emulsion cooled at room temperature. This comparison indicated that some minor settlement of the sulphur occurred in the room-cooled emulsion, even though such settlement was not visually apparent.

It was also necessary to obtain separately, thermograms of 100 percent sulphur and 100 percent asphalt cement to use as controls. The relative amounts of crystalline sulphur were then determined by comparing the area under the thermogram for the test specimen to that for the control specimens. The dissolved sulphur was assumed to be the difference between the total sulphur placed in the emulsion and the crystalline sulphur determined by DTA. A composite typical data trace is shown in Figure 11. Data collected from determination of sulphur solubility by DTA are presented in Table 9. The repeatability of the results are believed to be within $\pm$ 10 percent.

With reference to Figure 11, the endothermic reaction at a temperature of about 204°F (96°C) occurs when the sulphur undergoes a transition from the orthorhombic to the monoclinic state, whereas the endothermic reaction at a temperature of about 246.1°F (118.9°C) indicates the melting of the sulphur. The magnitude of the peak at the transition of orthorhombic to monoclinic sulphur depends upon the amount of time which has elapsed between obtaining the sulphur sample in the molten state and performing the DTA. The monoclinic sulphur will revert to orthorhombic sulphur, but at least 20 hours is required for this reaction to occur completely. The area under the portion of the thermogram at the melting point was used in calculating the amount of crystaline sulphur.

Evaluation of the dissolved sulphur data indicates considerable minor scatter in the results. Individual dissolved sulphur contents ranged between a low of 10.0 percent and a high of 23.4 percent by weight. No particular trend, other than erratic, could be interpreted from the

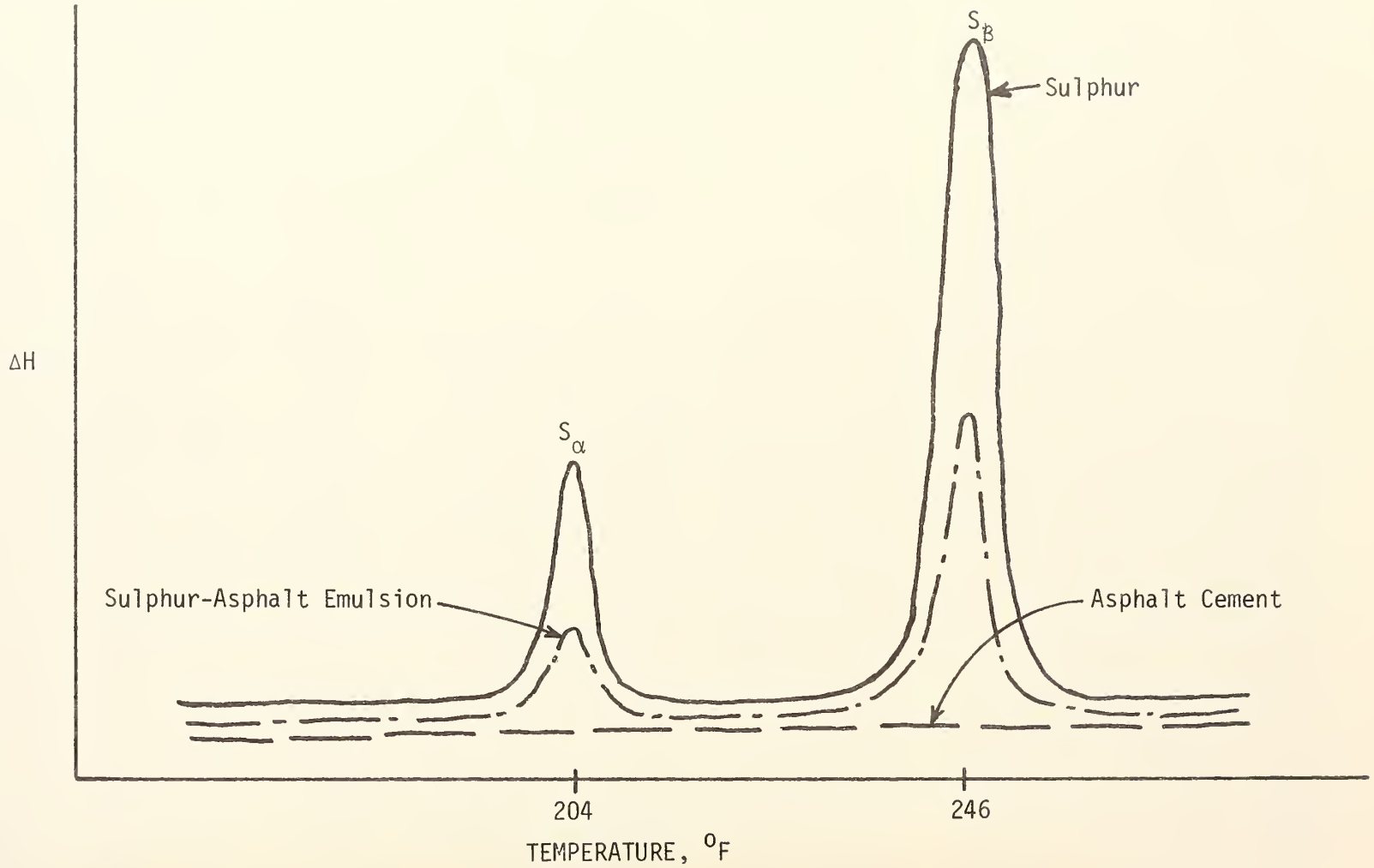

FIG. 11--Typical composite DTA trace to determine solubility of sulphur in sulphur-asphalt emulsions. $^{o}C = (F - 32) \times 5/9$

TABLE 9

DISSOLVED SULPHUR IN SULPHUR-ASPHALT EMULSIONS (SAE)

Asphalt Cement	Mixing Temp. (^{o}F)	Total Sulphur Content (w/o of SAE)	Dissolved Sulphur (w/o of SAE)
ET AC-5	285	20	18.8
		30	16.1
		40	23.4
		50	18.4
	300	20	18.9
		30	22.9
		40	20.5
		50	17.9
ET AC-10	285	20	18.9
		30	23.7
		40	16.5
		50	16.6
	300	20	19.1
		30	22.0
		40	19.1
		50	19.2
ET AC-20	285	20	18.8
		30	19.1
		40	20.4
		50	20.3
	300	20	19.4
		30	18.3
		40	20.4
		50	19.5

$^{o}C = (^{o}F - 32) \times 5/9$

TABLE 9 (CONTINUED

Asphalt Cement	Mixing Temp. (^{o}F)	Total Sulphur Content (w/o of SAE)	Dissolved Sulphur (w/o of SAE)
WT AC-10	285	20	20.0
		30	20.2
		40	19.9
		50	18.3
	300	20	17.8
		30	17.7
		40	20.0
		50	15.6
DS AC-10	285	20	16.9
		30	16.2
		40	15.0
		50	20.0
	300	20	17.9
		30	16.9
		40	21.6
		50	17.3
DS AC-20	285	20	16.6
		30	16.4
		40	16.0
		50	16.2
	300	20	18.3
		30	17.7
		40	16.0
		50	15.2

$^{o}C = (^{o}F - 32) \times 5/9$

TABLE 9 (CONTINUED)

Asphalt Cement	Mixing Temp. (^{o}F)	Total Sulphur Content (w/o of SAE)	Dissolved Sulphur (w/o of SAE)
DENV AC-10	285	20	18.8
		30	19.0
		40	17.4
		50	19.2
	300	20	18.8
		30	22.4
		40	20.3
		50	18.7
SM AC-10	285	20	18.7
		30	23.4
		40	21.5
		50	17.0
	300	20	17.5
		30	21.2
		40	16.8
		50	18.6
ME AC-10	285	20	14.9
		30	13.6
		40	15.0
		50	15.0
	300	20	16.6
		30	15.8
		40	12.1
		50	15.0

$^{o}C = (^{o}F - 32) \times 5/9$

TABLE 9 (CONTINUED)

Asphalt Cement	Mixing Temp. (^{o}F)	Total Sulphur Content (w/o of SAE)	Dissolved Sulphur (w/o of SAE)
WC AC-10	285	20	15.7
		30	17.8
		40	10.0
		50	15.1
	300	20	13.9
		30	13.7
		40	16.4
		50	15.0

$^{o}C = (^{o}F - 32) \times 5/9$

amounts of dissolved sulphur as total sulphur content increased for a particular asphalt cement at a particular mixing temperature. The variability of the tabulated results is attributed primarily to the method used for obtaining the test specimens. It is possible that settlement of the sulphur may have occurred in some of the samples prior to the time at which the DTA specimens were obtained. If so, the sample would not have been homogeneous and a small specimen obtained therefrom may not have been representative of the entire sample. The measured amount of crystalline sulphur would then depend upon the position within a non-homogeneous sample at which the specimen was obtained. Thus, the calculated amount of dissolved sulphur would have been in error for such a nonhomogeneous sample since the DTA measures crystalline sulphur rather than dissolved sulphur.

The overall average dissolved sulphur content for all the asphalt cements tested is about 18 percent by weight. The threshold of dissolved sulphur appears to vary slightly depending upon the mixing temperature and the grade and source of the asphalt cement, but it is independent of the total amount of sulphur added to the emulsion. Evaluation of the data indicates that the average amount of dissolved sulphur for a particular asphalt cement is slightly greater for the 300°F (148.9°C) mixing temperature than for the 285°F (140.6°C) temperature. The amount of sulphur dissolved in the Mideast and western Canada asphalt cements (ME AC-10 and WC AC-10) is somewhat less than the amount dissolved in the other asphalt cements. The functioning of the DTA equipment was questionable during testing of emulsions made with these two asphalt cements. The relative amount of dissolved and crystalline sulphur for typical SAE blends is presented graphically in Figure 12.

The dissolved sulphur results reported herein are consistent with those found in the literature. Garrigues tests indicate that solubilities were 14 and 18 percent by weight at emulsification temperatures of 150°C and 180°C, respectively, for an 80/100 penetration asphalt cement (12). Kennepohl reports that up to 19 percent by weight elemental sulphur can be dissolved in asphalt cement (9).

Experimental Design

The purpose of this experimental design was to examine the relative influence of various factors and their first order interactions on the behavior of the mixture compositions. The nine independent variables considered included materials and mixture variables as listed in Table 10, each variable being represented symbolically. Combinations of these variables, as specified by the experimental design, were used in preparation of mixture specimens for each system to be studied. As detailed subsequently in this thesis, laboratory tests were performed on specimens made in accordance with the specified variable combinations in order to determine the dominant variables for each alternative mixture system.

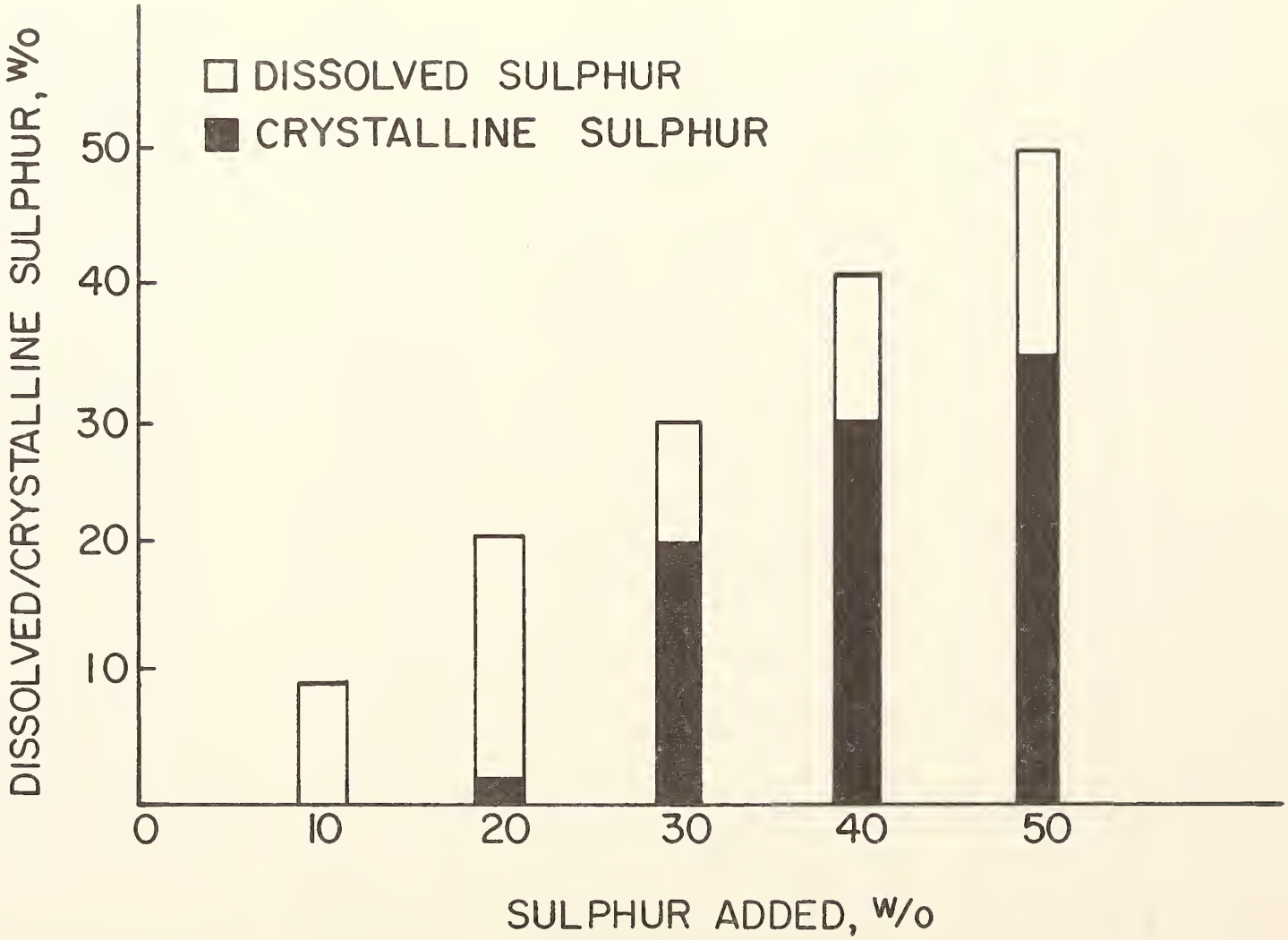

FIG. 12--Dissolved and crystalline sulphur determined by DTA.

TABLE 10

EXPERIMENTAL DESIGN VARIABLES

Variable	Symbol
Aggregate Roundness	A
Aggregate Sphericity	B
Aggregate Surface Roughness	C
Aggregate Size & Gradation	D
Asphalt Viscosity	E
Binder (Asphalt & Sulphur) Content	F
Sulphur Content	G
Moisture Condition	H
Degree of Compaction	I

In the design of the experiment, there are nine different factors (variables), and each factor was to be considered at two levels (high and low). This a 2^9 factorial experiment, which means that 512 treatment combinations need to be considered. Since this number of treatments is impractical, an alternative is to use a fractional replication of the factorial experiment in order to reduce the number of treatment combinations.

It was decided that any variable whose effects on mixture properties were already known from literature or previous experience could be omitted from the factorial. It was further decided that a one-eighth (1/8) replication of the factorial would be used such that 64 treatment combinations were identified to be tested. In selecting the 64 treatment combinations, second and higher order interactions and a few of the first order interactions were confounded with the main and the other first order interaction effects because they were known to be insignificant from theoretical or practical considerations. Seven interactions with suitable orders are confounded. Using techniques suggested by Kempthorne (77), the interactions to be confounded are CDEFH, ABFHI, ABCDEI, CDEGI, ABG, and ABCDEFGH where the letters represent the corresponding variables listed in Table 10.

Using the one-eight factorial, the variable combinations determined by the experimental design are listed in Table 11. The presence of a

TABLE 11

EXPERIMENTAL DESIGN VARIABLE COMBINATIONS
FOR SCREENING TESTS

AB	ABCD	ABCFI	ABCDFH
CD	ABCE	ABCHI	ABCEFH
CE	ABDE	ABDFI	ABDEFH
DE	ABFH	ABDHI	ACDEFH
FH	ACFG	ABEFI	ACDEGH
AGI	ACGH	ABEHI	BCDEFG
BGI	ADFG	ACDGI	BCDEGH
CFI	ADGH	ACEGI	*
CHI	AEFH	ADEGI	ABCDEFI
DFI	AEGH	AFGHI	ABCDEHI
DHI	BCFH	BCDGI	ACDFGHI
EFI	BCGH	BCEGI	ACEFGHI
EHI	BDFH	BDEGI	BCDFGHI
	BDGH	BFGHI	BCEFGHI
	BEFG	CDEFI	BDEFGHI
	BEGH	CDEHI	
	CDFH		
	CEFH		
	DEFH		

*Indicates all variables at a low level

symbol in the treatment combinations indicates the corresponding variable was considered at a high level whereas the absence of a symbol indicates the variable was considered at a low level. The selection of values used as high and low levels of the variables was discussed previously.

Processing of Sulphur-Asphalt Pavement Mixtures

This portion of the project involved preparation of specimens of sulphur-asphaltic concrete for subsequent testing. As noted previously, at least two different mixing sequences have been used by researchers to prepare laboratory mixtures of sulphur, asphalt and aggregates (7, 61). Comments made during a presentation made by Kennedy (17) indicate that the method utilizing sulphur-asphalt emulsion binder produce the best results; whereas some laboratory tests by Deme (7) indicated that mixes prepared by precoating sand with asphalt, prior to adding sulphur, produced slightly better mechanical properties.

In order to evaluate the differences of mixing sequences, three alternate approaches were investigated for this project. These were the AAS, AE, and AES systems in which the sequence of letters corresponds to the order in which the components are introduced into the mixture. The first "A" in each term represents aggregate, the second "A" in the AAS system represents asphalt, the "S" represents sulphur, and the "E" represents sulphur-asphalt emulsion.

Mixtures for each system were prepared in a well ventilated laboratory beneath a Kem Metal Co. vented hood. Sulphur was heated in an automatic electric heater manufactured by Sta-Warm Electric Company. Aggregate and asphalt cement were heated in an oven manufactured by Precision Scientific Co. Mixing was accomplished in a preheated mixing bowl with preheated utensils by use of a Hobart Model A-200 bench mixer. A Bunsen burner was used to apply heat periodically to the exterior of the metal mixing bowl during the mixing process. Mixing times and temperature are discussed subsequently.

Specimens of each mixture were molded immediately after the last mixing cycle was complete. The specimens were 4 inches (100 mm) in diameter and about 2.5 inches (65 mm) in height. Compaction was accomplished by use of the Marshall compaction hammer which has a weight of 10 pounds (4.5 kg) and fall of 18 inches (460 mm) in accordance with ASTM D 1559-73 requirements (75). The number of blows per face of specimen varied in accordance with the values listed previously. Three replicate specimens were molded for each mixture tested.

Upon completion of the compaction operation, the specimens were allowed to cool to room temperature and were then extruded from the molds by use of a hydraulic jack apparatus. The specimens were then placed in a 72°F (22.2°C) room for a period of at least 24 hours before performing any preconditioning or laboratory tests thereon.

For mixtures containing sulphur in the binder, it is extremely important that compaction be accomplished at temperatures in excess of 240°F (115.6°C) which is the solidification point of the sulphur. Paving mixtures containing sulphur in excess of the amount that will remain dissolved in the asphalt (about 20 percent by weight of binder) will develop a crystalline structure within the excess sulphur as the mixture cools below the solidification point of the sulphur. Such paving mixtures must be compacted at temperatures in excess of the solidification point or the structuring effect will be destroyed and a less stable mix will result. Previous work shows that sand-asphalt-sulphur specimens mixed at 300°F (148.9°C) but compacted at 200°F (93.3°C) had Marshall stabilities below 100 lb (45.5 kg), whereas the same mixture compacted at 300°F (148.9°C) possessed stabilities of about 3,500 lbs (1587.6 kg) (61). Compaction at temperatures below the solidification point destroys the structuring effect of the sulphur. Field tests by Shell Canada Limited indicated that conventional rolling of a sand-asphalt-sulphur mixture caused damage to the sulphur crystal structure which was forming as the mix cooled (6).

Aggregate-Asphalt-Sulphur (AAS) System

Mixtures were prepared and samples compacted for this system. The aggregates were combined with asphalt cements and sulphur in accordance with the requirements of the experimental design. As discussed previously, asphalt cement contents of 2 and 6 percent by weight of total mix and sulphur contents of 12 and 18 percent were used as low and high levels, respectively.

For this system, mixtures were prepared in the laboratory using two separate wet mix cycles. In the first cycle, aggregate and asphalt cement were preheated to 300°F (148.9°C) and then mixed for a period of about 2 minutes with a bench mixer. This operation put a coating of asphalt cement on the aggregate particles. Depending upon the amount of asphalt cement added and the type aggregate being used, certain mixtures contained more asphalt than needed to coat the particles. Next, sulphur which had been preheated to 300°F (148.9°C) was added to the hot aggregate-asphalt and mixed for a period of about 2 minutes. Portions of the mixture were then placed in preheated molds and compacted by use of the Marshall procedure ASTM D 1559 (75), to form specimens on which the screening tests could be performed. A schematic diagram of the procedure is presented in Figure 13.

It is important that the mixing and sample preparation of these mixtures be accomplished at temperatures ranging between 260°F (126.7°C) and 320°F (160.0°C). The former temperature was specified because it is somewhat higher than the melting (or solidification) point of the sulphur. As discussed previously, the latter is the temperature above which the sulphur experiences an abrupt and very large increase in viscosity and significant amounts of hydrogen sulfide gas are emitted.

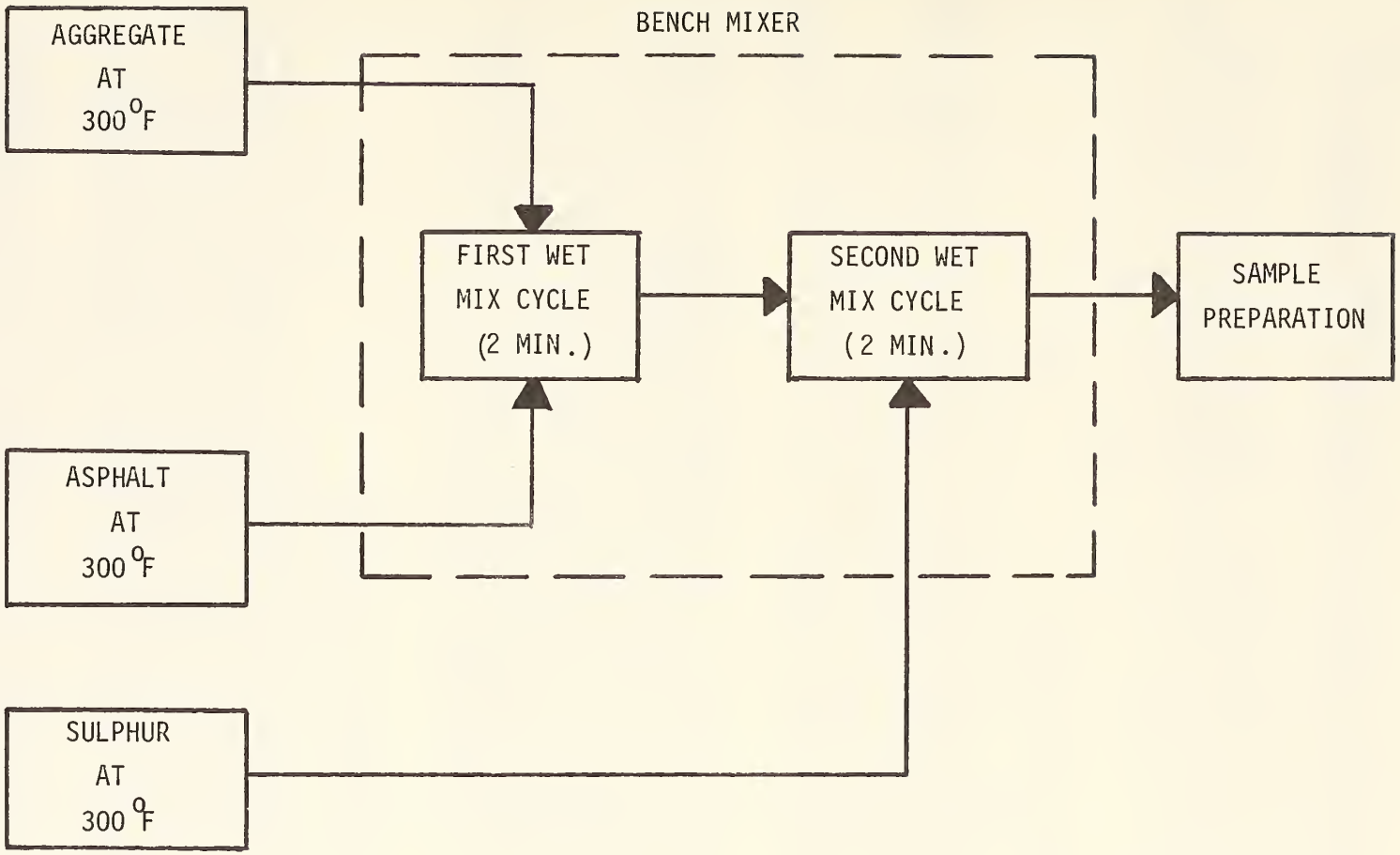

FIG. 13--Schematic of AAS mixture preparation.

$^{o}C = (^{o}F - 32) \times 5/9$

Although these viscosity changes are reversible (76), they do produce an adverse effect on the workability of the mix at temperatures in excess of about 325°F (162.8°C).

Prior to this research project, it was believed that the sulphur in the AAS system served primarily as a filler which provided mechanical interlock but did not permit any significant reduction in asphalt cement per unit volume of pavement (50, 79). An altered view is described subsequently.

Aggregate-Emulsion (AE) System

For this system, the aggregates were combined with the asphalt cement and sulphur, and specimens were molded in accordance with the requirements of the experimental design. Sulphur-asphalt emulsion (SAE) binder contents of about 40 and 75 percent by volume of the voids in mineral aggregate (VMA) were used as low and high values, respectively as required by the experimental design. For the required low and high values of sulphur, 30 and 70 percent of the volume of binder was composed of sulphur.

Mixtures were prepared in the laboratory using one wet mix cycle for this system. Sulphur and asphalt were first mixed at a temperature of 285°F (140.6°C) in an Epinbach Laboratory Homogenizer to form the sulphur-asphalt emulsion (SAE) binder. This hot SAE binder was then mixed with aggregate which had been preheated to 300°F (148.9°C). A bench mixer was used for a wet mix cycle time of about two minutes. Portions of the mixture were then placed in preheated molds and compacted by use of the Marshall procedure, ASTM D 1559 (75), to form specimens for subsequent screening tests. The procedure for preparation of AE system specimens is presented schematically in Figure 14.

Aggregate-Emulsion-Sulphur (AES) System

This approach was established initially in an effort to incorporate the beneficial features of both the AAS and AE systems. The specimens for this system were prepared by combining the aggregates, asphalt cements and sulphur in accordance with the requirements of the experimental design. The low and high levels of asphalt cement and sulphur used for this system were the same as used for the AE system except that 10 percent sulphur, by weight of total mix, was added after the noted amounts of sulphur-asphalt emulsions were mixed with the aggregate.

This system was prepared in the laboratory by use of two separate wet mix cycles. In the first cycle, aggregate which had been preheated to 300°F (148.0°C) was mixed for two minutes with sulphur-asphalt emulsion which had been prepared at a temperature of 285°F (140.6°C). Next, sulphur which had been preheated at 300°F (148.9°C) was added to

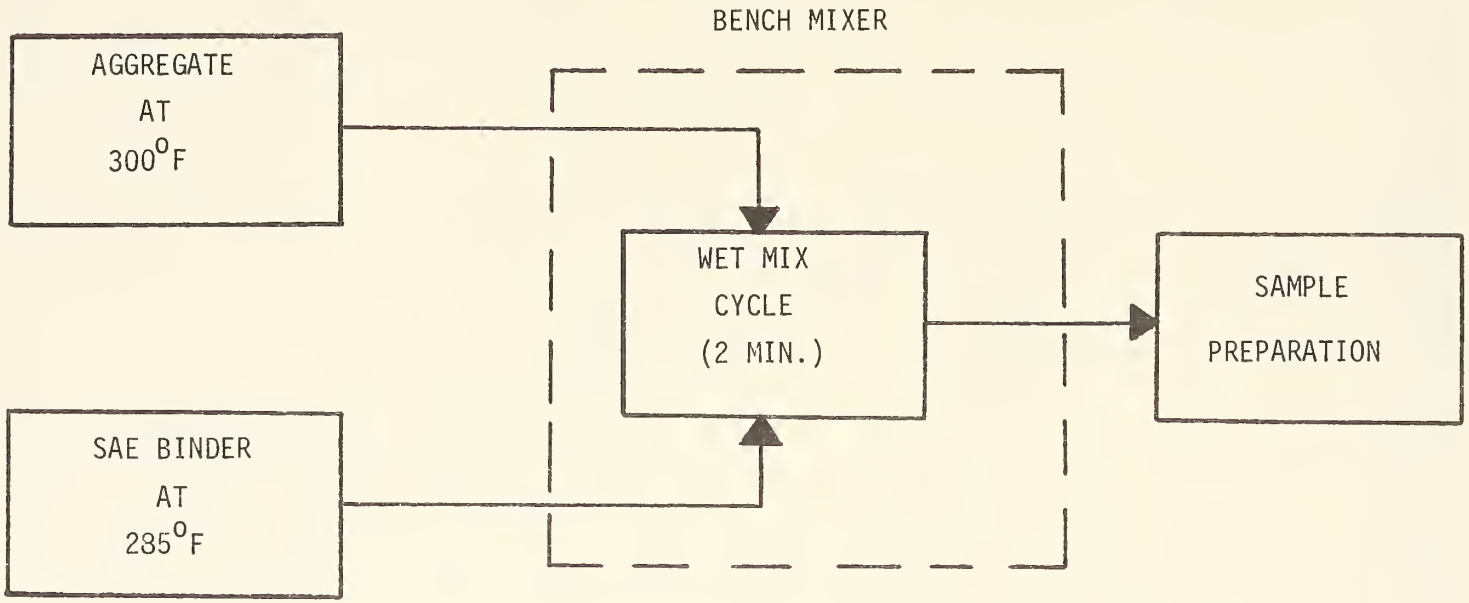

FIG. 14--Schematic of AE mixture preparation.

$^{o}C = (^{o}F - 32) \times 5/9$

the hot aggregate - SAE binder combination and mixed for about two minutes. Portions of the mixture were then placed in preheated molds and compacted for subsequent screening tests. A schematic diagram of the processing of the AES system is presented in Figure 15.

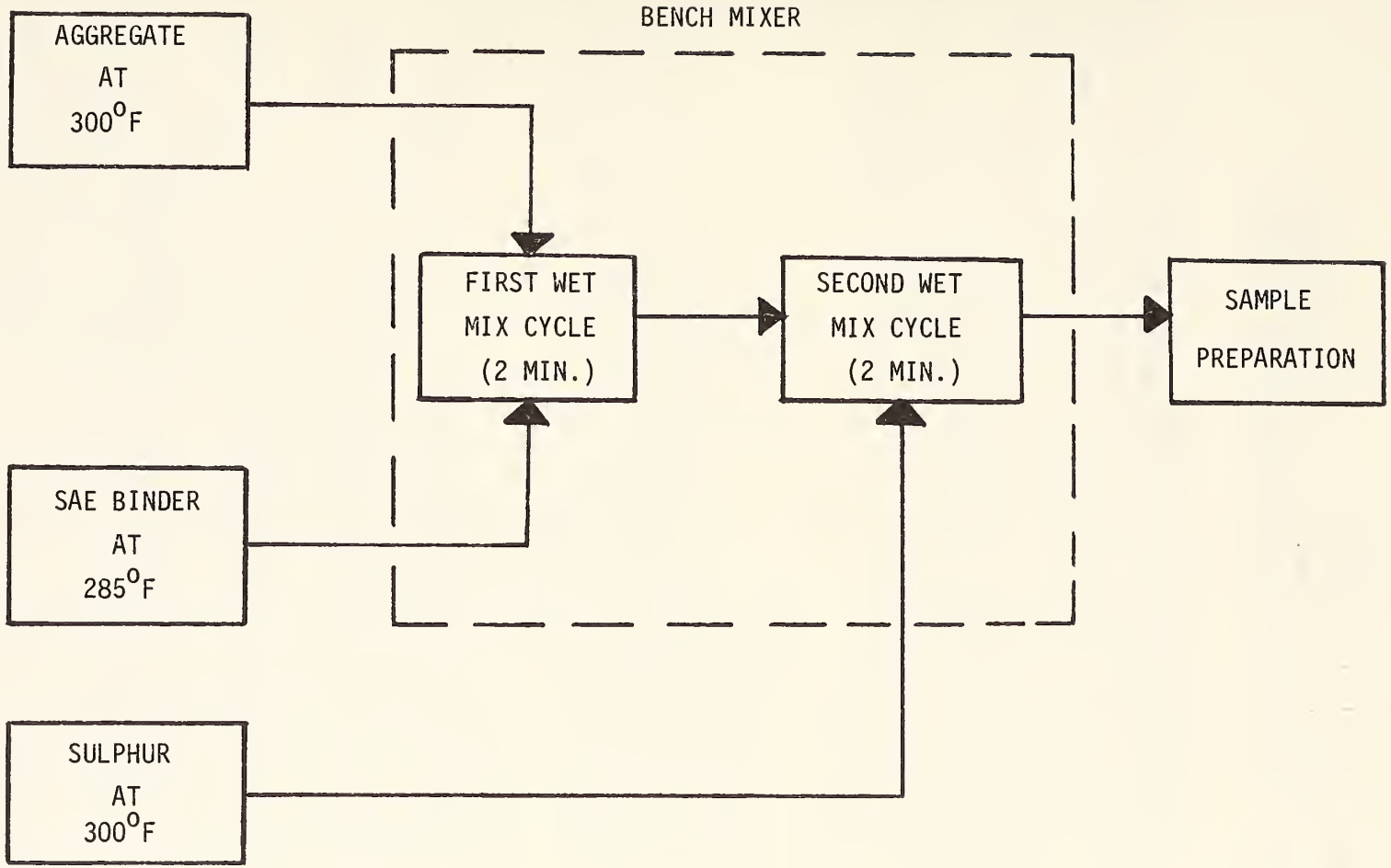

FIG. 15--Schematic of AES mixture preparation.

$^{o}C = (^{o}F - 32) \times 5/9$

CHAPTER V

TASK C: DEVELOPMENT OF STATISTICALLY BASED RELATIONSHIPS FOR PAVEMENT DESIGN SYSTEMS

This task included an extensive laboratory testing program from which statistically-based relationships between mixtures, design variables and material response characteristics were developed for subsequent incorporation in the selected pavement structural design subsystem and pavement system design. The laboratory testing effort was divided into two major subtasks: a) screening tests for the identification of influential mix design variables, and b) characterization and qualification tests. Advanced statistical experimental design analyses were utilized to minimize testing time by eliminating insignificant and irrelevant parameters. Materials and process variables discussed previously were incorporated into the screening tests, and the most promising mixture designs were subjected to the characterization tests for subsequent analysis in Tasks D and E.

Preliminary Screening Tests

All of the specimens prepared in Task B for the three sulphur-asphalt pavement mixture systems (AAS, AE and AES) were subjected to a series of preliminary screening tests. These tests were used to determine the influence of the nine variables on the mixtures, and to determine the mixtures which exhibited desirable characteristics for use in highway pavements.

A flow chart presenting the various testing activities involved in this phase of the project is included as Figure 16. As discussed previously, the mixtures prepared under Task B were compacted by the Marshall procedure. Bulk densities of compacted specimens and maximum specific gravities of paving mixtures were determined for each mixture. These relationships were used in calculation of voids in mineral aggregate (VMA) and air voids content for each compacted specimen. As discussed previously, one of the test variables was moisture condition, and the samples were moisture conditioned by vacuum saturation and soaking, when required by the experimental design. The compacted specimens were then tested to determine the resilient modulus, Hveem stability and Marshall stability. Each test consisted of three replications in accordance with the requirements of the respective ASTM or other cited test method. The geometry of the test specimens was such that each of the aforementioned tests could be performed on them. Since the Marshall stability test was the only destructive test procedure, it was the final test performed on each specimen. Thus, the entire series of screening tests could be performed on a single specimen.

A summary of each test method follows:

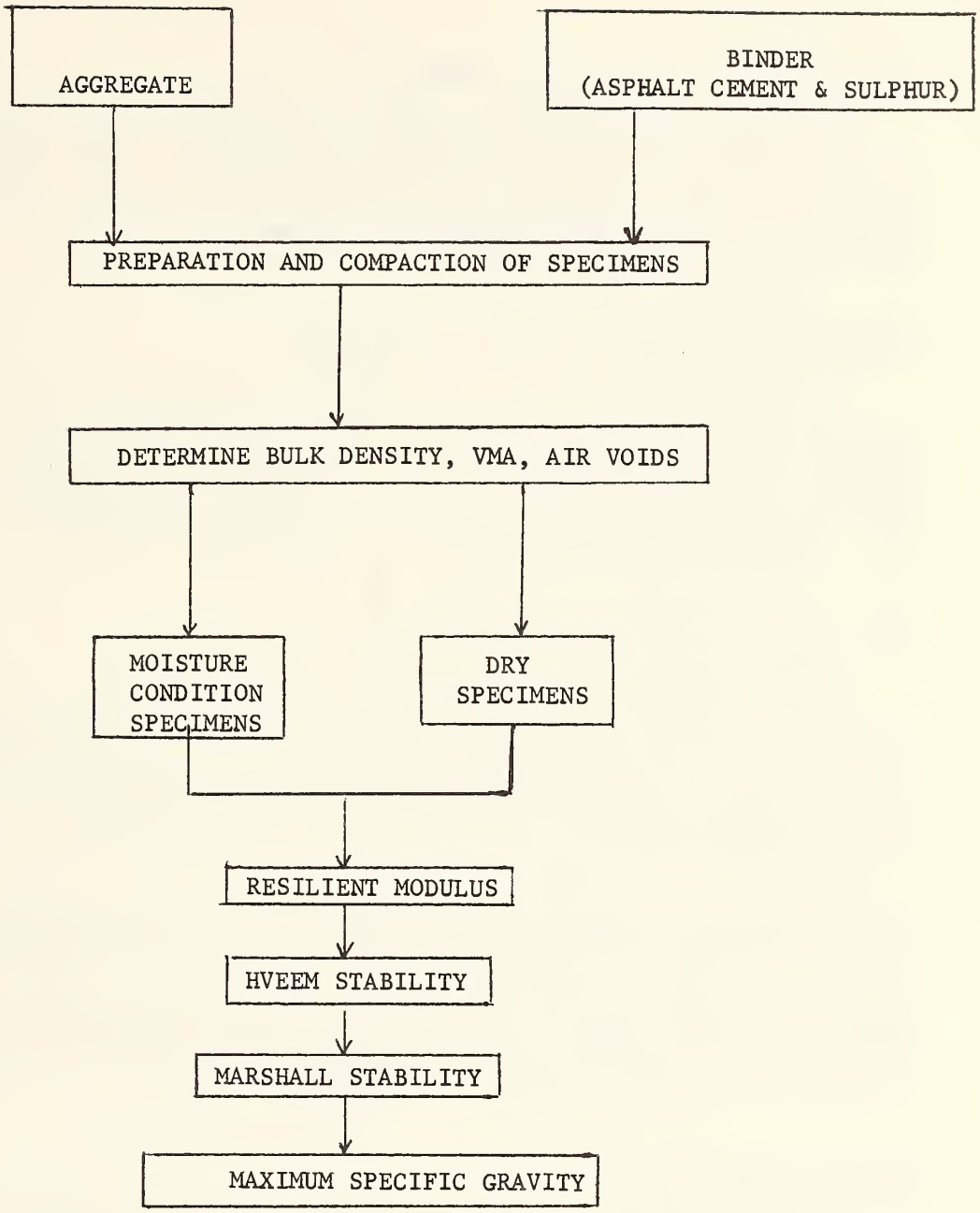

FIG. 16--Flow chart for preliminary screening tests of sulphur-asphalt pavement mixtures.

Bulk Density of Compacted Specimens

Bulk densities of the compacted specimens were determined in accordance with the procedures contained in ASTM D 2726-73 (90). The weights of the dry specimens in air, specimens immersed in water, and specimens in a saturated surface-dry condition were measured. Bulk densities were calculated therefrom.

Maximum Specific Gravity of Paving Mixtures

ASTM D 2041-71 was used to determine the maximum specific gravity of each paving mixture (91) after the destructive Marshall test. In this method, the particles of the sample are separated, placed in a flask, covered with water and then de-aired. Weights of the dry sample in air, flask filled with water, and flask filled with sample plus water are used to calculate the maximum specific gravity of the mixture.

Air Voids and VMA of Compacted Specimens

The air voids in a compacted paving mixture consist of the air spaces between the binder-coated aggregate particles. Air voids were calculated in accordance with the procedure recommended by the Asphalt Institute (92). The bulk specific gravity of the compacted mixture and the maximum specific gravity of the mixture are used in calculation of the percent air voids.

The voids in the mineral aggregate, VMA, are defined as the void space between the aggregate particles in a compacted paving mixture. The VMA, expressed as a percent of the total volume, includes the air voids and the effective binder content. The VMA were determined as recommended by the Asphalt Institute (92). The bulk specific gravity of the mineral aggregate, and percentage of aggregate by total weight of mixture are used to calculate the VMA.

Resilient Modulus

For an elastic material, the elastic modulus, E, is the ratio of stress to strain. Although the same relationship applies to visco-elastic materials, the test conditions under which the modulus is determined must be defined because the elastic modulus is dependent upon the duration of the applied load. Short term loadings result in much higher elastic moduli for viscoelastic materials than long term loadings because the material creeps with time.

Under short-duration dynamic loads on a viscoelastic material, the apparent Young's modulus, or stiffness, E, is frequently defined as the resilient modulus, M_R (93). The complex (dynamic) modulus, denoted

by E*, is a complex number which defined the relationship between stress and strain for a linear viscoelastic material subjected to sinusoidal loading stress (96). The real part of the complex modulus is a measure of the material elasticity whereas the imaginary part is a measure of its viscosity. Review of the literature and discussion with pavement design research engineers indicate that the terms resilient and dynamic moduli are often used interchangeably by pavement designers (97). These parameters are used in conjunction with layered-elastic and finite element methods for structural design of pavements. The dynamic modulus is often determined from triaxial compression tests of specimens, a method that is somewhat complicated and expensive. Schmidt developed his equipment in an effort to provide a method which would require relatively little effort and expense, but would provide sufficiently accurate resilient moduli (93). The test equipment and procedures used for determination of resilient moduli of specimens for this project are similar to those developed by Schmidt (93, 94, 95). A typical test setup is shown in Figure 17. Specimens of 4 inches (101.6 mm) diameter and about 2.5 inches (63.5 mm) height were used for this project. Using two pairs of clamping screws, the specimen is positioned and mounted in a yoke and then placed in the resilient modulus device. A load is applied across the vertical diameter of the cylindrical test specimen and the resulting elastic deformation across the horizontal diameter is measured by use of a pair of compensating, highly sensitive Schaevitz transducers. The loading procedure consists of applying a light load of 0.1 second duration every three seconds through a load cell. To apply the load, air pulses are supplied to a Bellofram pneumatic cylinder from an Automatic Switch Company electrically activated solenoid valve. The time of the load (pulse width) is controlled by a Raytheon integrated circuit timer and the load magnitude is controlled by a Kendall Model 10 pressure regulator. A typical loading pattern is shown in Figure 18.

Using the previously discussed procedure, the resilient modulus is computed from the following formula (93);

$$M_R = \frac{P(\mu + 0.2734)}{\Delta t}$$

where μ is Poisson's ratio,

P is dynamic load in pounds,
t is sample thickness (height) in inches and
Δ is total deformation in inches.

Schmidt suggested using a value of 0.35 for asphaltic concrete because it gave reasonable agreement with stiffness measured in direct tension at a temperature of 73°F (22.8°C)(93). Gallaway and Saylak suggest a Poisson's ratio of 0.30 for all mixtures. The resilient modulus calculated by this formula varies by $\pm$ 24 % as Poisson's ratio varies from 0.2 to 0.5, i.e. by 0.15 on either side of 0.35. Resilient moduli in the screening tests were measured at temperatures of 68°F (20.0°C). Since

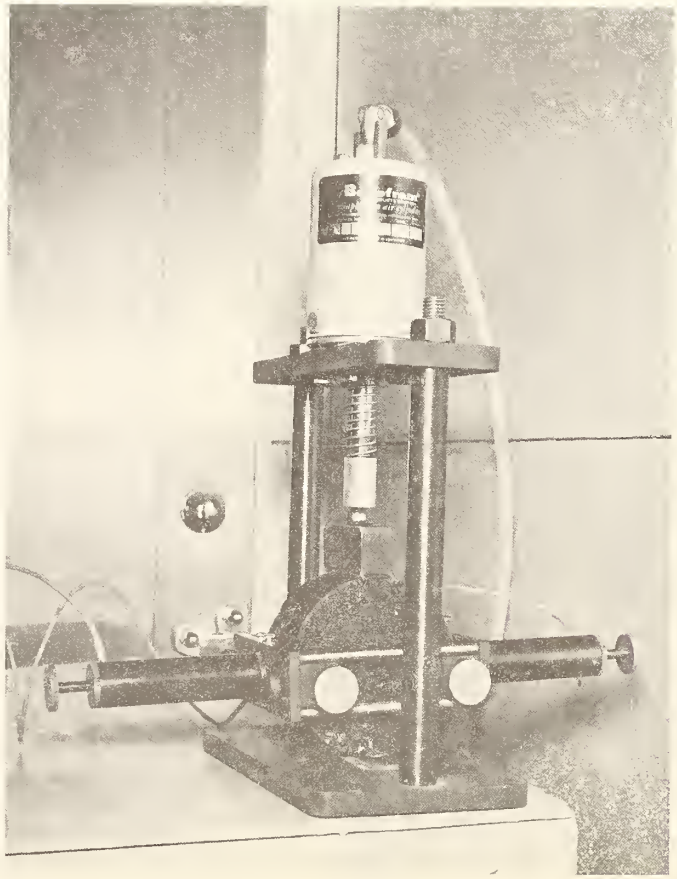

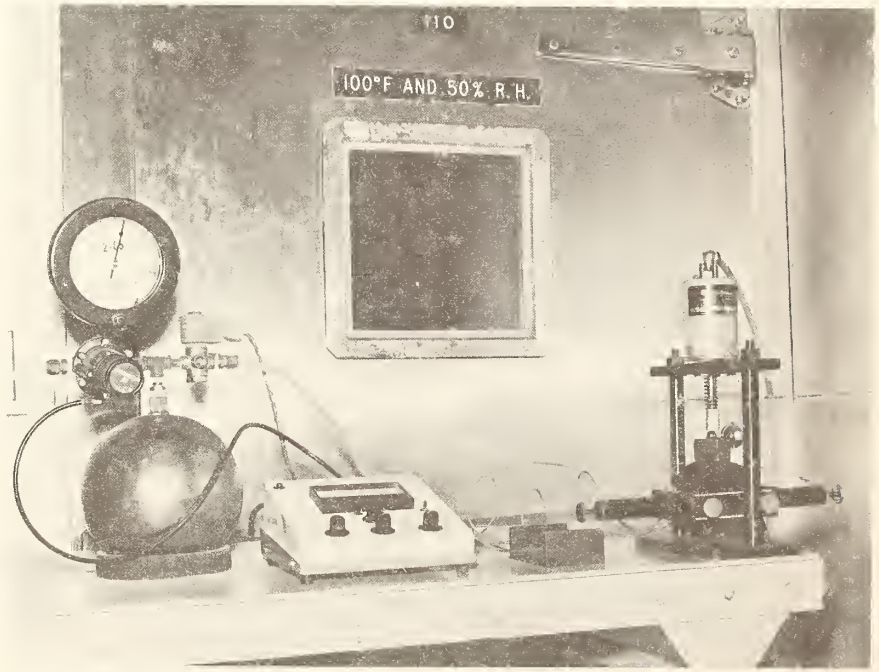

FIG. 17--Schmidt type diametral resilient modulus (M_R) device.

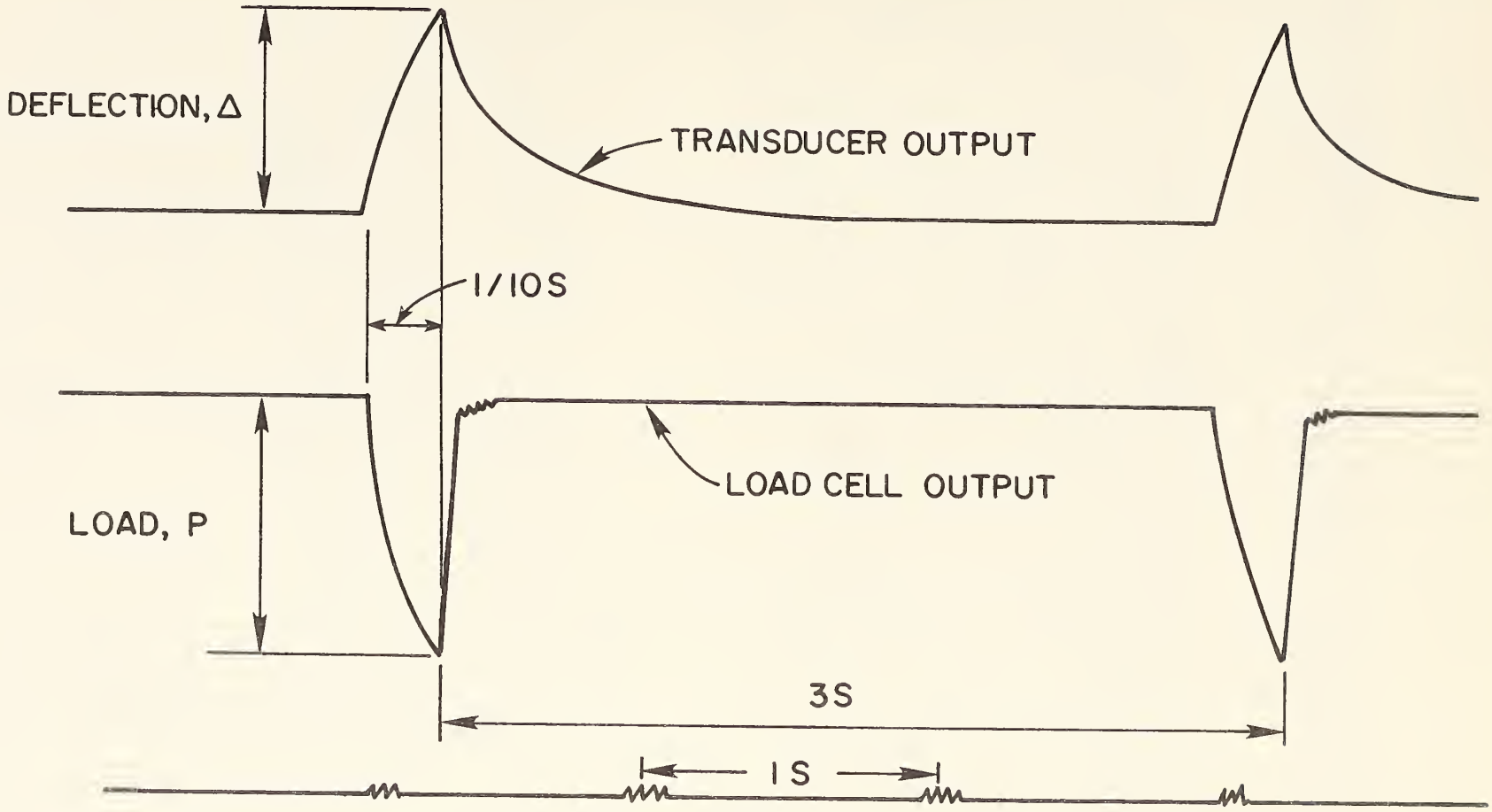

FIG. 18--Loading pattern for resilient modulus test.

the resilient modulus test is non-destructive, the specimens were stored for subsequent testing after completion of the resilient modulus tests.

Hveem Stability

Some state and municipal agencies (e.g. Texas State Department of Highways and Public Transportation, and California Divison of Highways) utilize the Hveem method of mix design and control for asphalt paving materials rather than the commonly used Marshall method. The concepts of the Hveem test were advanced and developed by F.N. Hveem, formerly Materials and Research Engineer for the California Division of Highways (92). This test has since been standardized as ASTM D 1560, Resistance to Deformation and Cohesion of Bituminous Mixtures by Means of Hveem Apparatus (99). Specimens of 4 inches (101.6 mm) diameter by about 2.5 inches (63.5 mm) height are placed in the Hveem stabilometer and subjected to a gradually increasing vertical load. As the vertical load increases, the specimen attempts to deform laterally. This results in generation of pressures within an annular oil cell which is separated from the test specimen by use of a flexible rubber diaphragm. The lateral pressures are read from a hydraulic pressure gage at selected vertical loads. The Hveem stability is calculated by an established formula and is a measure of the resistance to lateral deformation due to vertical load.

Marshall Stability and Flow

The concepts of the Marshall method of designing paving mixtures were formulated by Bruce Marshall, formerly Bituminous Engineer with the Mississippi State Highway Department (92). The U.S. Army Corps of Engineers, through extensive research and correlation studies, improved and added certain features to Marshall's test procedure, and ultimately developed mix design criteria. The procedure has been standardized as ASTM D 1559 (75). The test procedure is currently used by a major segment of the paving industry to establish proportions and performance characteristics of hot mixed asphaltic concrete. This method is used for both laboratory design and field control of paving mixtures. Specimens of 4 inches (101.6 mm) diameter by about 2.5 inches (63.5 mm) height are heated to 140°F (60°C), placed in the testing head, and a testing load is applied at a constant rate of deformation. The total load required to produce failure (defined as the maximum load reading obtained) is recorded as the Marshall stability value. The formation of the specimen at failure, expressed in units of 1/100 inch (0.25 mm), is recorded as the Marshall flow value. The Marshall test is destructive and was therefore the final test performed in the series of a screening tests. Marshall stabilities and flow numbers are qualitative measures of a pavement's ability to withstand traffic loads and permanent deformation, respectively.

Evaluation and Statistical Analyses of Screening Test Results

As stated previously, the screening tests were performed in order to evaluate the influence of the nine mixture and materials variables. Originally, the fractional factorial experiment was designed on the basis of the nine variables being at either a high or low value. However, after design of the experiment and beginning of the screening tests it was obvious that it would not be practical to consider the nine variables at two levels only. Since the materials used in the screening tests did not possess ideal characteristics, the actual number of levels of the nine factors varied between 2 and 15 for the different variables. Even if it was known beforehand that the levels of the nine factors could exhibit such large variation, it would have been impractical to consider all treatment combinations. To further complicate the situation, all of the 64 treatment combinations indicated by the experimental design could not be considered because of practical limitations. For example, certain combinations of aggregate properties could not be obtained. Since all of the design treatment combinations could not be tested, the designed fractional factorial experiment was of little use when attempting to analyze the results of the screening tests.

The independent variables for this analysis are the design or decision variables (materials and mixture variables), whereas the dependent variables are the response or test variables. A tabulation of the values of design variables and resultant response variable for the various treatment combinations for each of the three sulphur-asphalt mixture systems is included in Appendix D. As would be expected, a tremendous range of test values resulted since the design variable were so highly variable. Table 12 presents the upper and lower bounds of the nine design variables and the seven response variables determined from the screening tests for each of the three sulphur-asphalt mixture systems.

Although the originally proposed method of analysis of the fractional factorial experiment could not be accomplished because of the multitude of variable levels, the best alternative was to fit a second order response surface to the different response variables individually. This could be accomplished since the levels at which the experiments were actually conducted were known. The second order response surface considered was of the form:

$$y = \beta_o + \sum_{i=1}^{9} \beta_i x_i + \sum_{i,j=1}^{9} \beta_{ij} x_i x_j + \varepsilon$$

for each response variable

where

β_o, β_i, β_{ij} are the regression coefficients,

TABLE 12

UPPER AND LOWER BOUNDS OF THE DESIGN AND RESPONSE VARIABLES FOR THE SCREENING TESTS FOR AAS, AE AND AES SYSTEM MIXTURES

Variable	Symbol	Upper Bound			Lower Bound		
		AAS	AE	AES	AAS	AE	AES
Decision (design) Variables:							
Roundness	A	0.78	0.78	0.78	0.10	0.10	0.10
Sphericity	B	0.87	0.87	0.87	0.70	0.70	0.70
Roughness	C	3.5	3.5	3.5	1.2	1.5	1.5
Size and Gradation	D	977	977	977	2	2	2
Type of Asphalt	E	1	1	1	0.1	0.1	0.1
Vol. Binder (% VMA)	F	99.9	94.0	98.3	1.0	15.5	48.6
Vol. Sulphur (% Binder)	G	81.8	70.0	83.4	50.0	30.0	44.7
Moisture Condition	H	1	1	1	0.1	0.1	0.1
Compaction Effort	I	1	1	1	0.1	0.1	0.1
Response (test) Variables:							
Bulk Sp. Gravity	J	2.46	2.46	2.44	1.13	0.87	1.10
VMA (%)	K	49.0	49.3	49.9	16.0	12.7	22.0
Air Voids (%)	L	34.3	39.9	25.4	0.0	1.0	0.4
Resilient Modulus ($X10^6$ psi)	M	4.73	1.58	2.76	0.06	0.01	0.08
Hveem Stability	N	88	75	93	1	2	22
Marshall Stability (lb)	O	29512	8300	27310	0	36	250
Marshall Flow (1/100 in.)	P	25	32	35	4	6	5

1 KP_a = 0.1451 psi; 1 K_g = 2.205 lbs.; 1 cm = 0.394 in.

x_i are the test variables (A,B,C, ..., I),

$x_i\ x_j$ are the first order interactions,

ε is the experimental error and

y is the response variable.

This type of response surface was fitted for each of the seven response variables. The regression coefficients for these factors and the first order interactions for each response variable are presented in Appendix E. The first order interactions AB, AG, and BG are intentionally omitted in the analysis because they are known to be insignificant from previous experience before the experiment was conducted. Table 13 presents standard measures of the response surface fitting for each of the three sulphur asphalt system mixtures analyzed. It is observed that the coefficient of determination (R^2) is high in all the cases and the F-statistic is significant at the 1 percent level, thus exhibiting that the curve fit is very good. The design variables, or their first order interactions, for which the F-statistic is insignificant can be considered to have little or no effect on the response variable.

The purpose of this exercise in statistical evaluation of the screening test results was to establish a mathematical method for designing a sulphur-asphaltic concrete mixture based upon the expected contribution of the individual variables to the mixture. This would enable estimation of response variables (test results) such as stability and resilient modulus by use of known design variables such as compaction effort, aggregate properties, and percent sulphur in the binder. What often makes mix design as much an art as a science is that there are important interactions among the variables, the effects of which are usually considered on the basis of experience or intuition.

Significantly different regression equations were developed for the AAS, the AE and the AES processes of combining the sulphur-asphalt binder with the aggregate. The task of designing the mix for each of these systems then became a search for the best combinations of design variables. It is this search that is normally done by trial and error and intuition, but may be accelerated by the use of non-linear programming techniques such as the Davidson-Fletcher-Powell Method (100). In such a design system, the objective function is to maximize (or minimize) the value of a particular indicator test that is considered to be most important. The constraints which must be satisfied are either the minimum or maximum specified values of the other indicator tests that are required for standard asphalt mixes, or the normal ranges of the independent variables that are encountered in realistic mix designs.

For purposes of illustration, one individual case was considered for each of the three mixture systems studied in this project. This case was a determination of the optimum levels of the nine design variables which would maximize the resilient modulus if all variables were allowed to float

TABLE 13

MEASURES OF RESPONSE SURFACE FITTING FOR AAS, AE AND AES SYSTEM MIXTURES

Response Variable	R^2	F	Mean Square Error	Level of Significance (%)
AAS System Mixtures				
Bulk Sp. Gr.	.990	234	0.002	0.01
VMA	.876	17	8.8	0.01
Air Voids	.985	165	1.9	0.01
Resilient Modulus	.926	31	0.06	0.01
Hveem Stability	.932	34	62.9	0.01
Marshall Stability	.903	23	2378865	0.01
Marshall Flow	.738	7	7.5	0.01
AE System Mixtures				
Bulk Sp. Gr.	.999	1376	0.0004	0.01
VMA	.982	109	2.3	0.01
Air Voids	.996	533	0.4	0.01
Resilient Modulus	.872	13	0.02	0.01
Hveem Stability	.937	29	35.4	0.01
Marshall Stability	.955	41	214567	0.01
Marshall Flow	.764	6	6.0	0.01
AES System Mixtures				
Bulk Sp. Gr.	.999	1234	0.0003	0.01
VMA	.988	135	1.1	0.01
Air Voids	.998	783	0.09	0.01
Resilient Modulus	.939	25	0.02	0.01
Hveem Stability	.925	20	36.9	0.01
Marshall Stability	.981	85	1023482	0.01
Marshall Flow	.853	10	5.6	0.01

free, but were subject to the constraints given in Table 14. It has been found in the course of these screening tests and the associated analysis with FPS-BISTRO and VESYS IIM that the resilient modulus is one of the most reliable indicators of the in-service performance of a pavement. A high resilient modulus is associated with low rutting and roughness, a higher serviceability index. However, it does not necessarily indicate a higher incidence of fatigue cracking. The previously noted non-linear search technique was used to find the optimum levels of the design variables. The optimum levels thus obtained for the three mixture systems are presented in the appropriate columns of Table 15. The trend of values for the design variables was about as expected for the three systems, although exceptions to the trend did exist. The AE and AES systems indicated that low roundness and sphericity numbers, high size and gradation numbers (SGN), and relatively high volumes of binder and sulphur were required to produce a maximum resilient modulus. However, the roundness number for the AAS system was higher than anticipated, whereas the volume of binder was lower than for the two other systems. The AAS and AES systems required a low degree of compaction, whereas the AE system required a relatively high compactive effort. It is possible that a high compactive effort destroyed the structuring effect created by the sulphur. The inconsistencies in the comparison of the three systems cannot be explained at this time except as a result of a failure of the regression equations to correctly model the actual response surface.

There are several advantages to this method of mix design using these regression equations in a non-linear programming scheme. An example of one major advantage is the case where only poor aggregate is available for construction. Since sulphur-asphalt pavement mix design is a rather recent innovation, the literature does not abound with design data for mixtures containing various types of aggregates. Using the regression equations generated by this process, it is possible to determine the resilient modulus, or other mix parameters such as Hveem or Marshall stability, which could be anticipated for given aggregates and asphalts. In addition, the equation could be used to determine the best combination of design variables to meet a particular mix criterion without having to run an extensive series of laboratory tests.

The results of the evaluation are reported exactly as determined by the analysis method used. Although critical, detailed examination and comparison of individual values indicates discrepancies, a broad view of the results shows a trend of increasing resilient modulus with increasing aggregate size and gradation number. This statistical approach to mixture design is worthy of further analysis because it could result in a considerable reduction of laboratory testing efforts when attempting to determine the best mixture from an evaluation of mixtures with a wide range of values of the design variables.

Determination of Dominant Variables

Using the screening test data, a determination of the dominant variables, with respect to the resilient modulus and Marshall stability,

TABLE 14

RESPONSE VARIABLE CONSTRAINTS USED IN
OPTIMUM DESIGN TO MAXIMIZE RESILIENT MODULUS

Response Variable	Variable Symbol	Constraint Value	
		Minimum	Maximum
Bulk Specific Gravity	J	None	None
VMA (%)	K	14	None
Air Voids (%)	L	2	15
Resilient Modulus ($X10^6$psi)	M	.5	None
Hveem Stability	N	30	None
Marshall Stability (lb)	O	750	None
Marshall Flow (1/100 in.)	P	6	18

1 kPa_a = 0.1451 psi

1 kg = 2.205 lbs.

1 cm = 0.394 in.

TABLE 15

SUMMARY OF OPTIMUM DESIGN VARIABLES TO MAXIMIZE RESILIENT MODULUS

DESIGN VARIABLES	SYMBOL	SULPHUR-ASPHALT SYSTEM MIXTURE		
		AAS	AE	AES
Roundness	A	0.59	0.15	0.18
Sphericity	B	0.75	0.70	0.70
Surface Roughness	C	2.80	1.50	1.50
Size & Gradation Number	D	977	977	977
Asphalt Viscosity	E	0.1	0.1	0.99
Binder Content (v/o VMA)	F	65.7	94.0	89.5
Sulfur Content (v/o BIND)	G	80.8	70.0	83.9
Moisture Condition	H	0.1	0.1	0.1
Compactive Effort	I	0.17	0.73	0.1
Resilient Modulus ($\times 10^6$ psi)		2.65	2.53	2.53

1 KPa = 0.1451 psi

was made for each of the three sulphur-asphalt systems. This was accomplished by multiplying the range of each design variable by the partial derivative of the respective regression equations for the test variables. Mean values of the design variables were used in the equations. A comparison of the absolute values of the numbers thus obtained was used as the basis for determination of variable domination. Therefore, the interactions of the variables were considered in the evaluation of the dominant variables.

The dominant variables from the screening tests are presented in Table 16 in the order of rank for each system. Interpretation of the reported dominant variables is somewhat difficult. It appears that asphalt viscosity and degree of compaction, which in turn influences air voids, are dominant variables in the AE and AES systems, whereas aggregate properties such as roundness, roughness and SNG are dominant in the AAS system. Sulphur and binder contents do not dominate to the extent anticipated. This sensitivity analysis indicated the design variables that the selected test variables (resilient modulus and Marshall stability) are more sensitive to, and does not necessarily indicate the design variables that should be used in the characterization tests. In fact, the best aggregate, an intermediate viscosity asphalt and good compaction effort were selected for preparation of the characterization test specimens. The sulphur content was varied primarily because that is the subject of this research.

Characterization Tests

The laboratory tests performed in this portion of the project were designed to provide a further screening of the mixture designs and to classify them with respect to their mechanical, creep, and thermal behavior. These laboratory tests generated data which reflected realistic pavement material behavior and failure properties. The test results were directly applicable to the development of the statistically based relationships for the various pavement design subsystems discussed previously.

Existing experimental techniques appear to be adequate for characterizing most pavement materials for the various environmental and traffic conditions to be analyzed (51, 101). The laboratory tests for this portion of the experimental program included creep tests to determine creep compliance, flexural fatigue tests, and repeated load triaxial tests for evaluation of permanent deformation. In addition, the type laboratory tests (air voids, Marshall Stability, etc.) used in the screening test phase were also performed on specimens of the mixtures used in this characterization test phase. These characterization tests are based on the assumption that the mixtures being tested are linearly viscoelastic and thermorheologically simple. A comparison of samples made by the three sulphur-asphalt pavement mixture systems (AAS, AE, and AES was made).

TABLE 16

DOMINANT VARIABLES IN SCREENING TESTS

System	Rank Order of Variables	
	With Respect to Resilient Modulus	With Respect to Marshall Stability
AAS	Agg. Roundness	Agg. Roughness
	Agg. Roughness	Agg. Roundness
	Size & Grad. No.	Agg. Sphericity
	Sulphur Content	Sulphur Content
	Degree of Compaction	Degree of Compaction
	Binder Content	Size & Grad. No.
	Agg. Sphericity	Binder Content
	Moisture Condition	Asphalt Viscosity
	Asphalt Viscosity	Moisture Condition
AE	Degree of Compaction	Degree of Compaction
	Asphalt Viscosity	Asphalt Viscosity
	Agg. Roundness	Agg. Roundness
	Size & Grad. No.	Size & Grad. No.
	Sulphur Content	Sulphur Content
	Agg. Sphericity	Agg. Roughness
	Agg. Roughness	Agg. Sphericity
	Moisture Condition	Binder Content
	Binder Content	Moisture Condition
AES	Degree of Compaction	Asphalt Viscosity
	Agg. Roundness	Degree of Compaction
	Asphalt Viscosity	Agg. Sphericity
	Agg. Sphericity	Agg. Roundness
	Size & Grad. No.	Size & Grad. No.
	Agg. Roughness	Agg. Roughness
	Moisture Condition	Moisture Condition
	Sulphur Content	Sulphur Content
	Binder Content	Binder Content

Selection of Asphalt Cement and Aggregate

As discussed previously, it was difficult to conclude that asphalt cement viscosity was a dominant variable for all systems. Therefore, the ET AC-10 asphalt cement was selected for use in all the characterization tests. This grade of asphalt cement is probably the most frequently used grade for producing hot mixed asphaltic concrete in the United States. The source and properties of this asphalt cement were listed previously in this report.

It was decided that all characterization tests would be performed on mixtures utilizing a standard crushed limestone aggregate. For comparative purposes, certain characterization tests were performed on mixtures made with beach sand for use in subsequent analyses. In addition, selected characterization tests were performed on specimens made from crushed volcanic aggregate and from recycled asphaltic concrete pavement, although the properties of these two materials were not used in the system design and structural design analyses.

The standard limestone was a very hard crushed limestone obtained from White's Mines at a quarry near Brownwood, Texas. U.S. Standard sieves meeting the requirements of ASTM E 11-70 were used to separate the aggregates into individual fractions sized from 3/4 inch (1.905 cm) to minus No. 200 sieve size (102). The individual fractions were then combined as required to produce a grading which complied with the Asphalt Institute Type IVb specificiations (78). The crushed limestone grading and the Type IVb specification limits are shown on Figure 19. The bulk specific gravity and absorption of the limestone, as determined by ASTM C 127 and ASTM C 128, was 2.589 and 1.56 percent, respectively (103, 104).

Before the arrival of the standard crushed limestone aggregate, it was necessary to perform some of the characterization tests on specimens made with crushed limestone from the U.S. Bureau of Mines, Boulder City, Nevada, and with crushed limestone from Georgetown, Texas, meeting approximately the same gradation requirements as noted previously.

The beach sand was a uniformly graded fine sand obtained from the Texas Gulf Coast near Corpus Christi, Texas. The grading is presented on Figure 19. The bulk specific gravity was determined by ASTM C 128 to be 2.65 (104).

The U. S. Bureau of Mines prepared specimens incorporating volcanic aggregate for resilient modulus and flexure fatigue tests. The aggregate was obtained near Boulder City, Nevada, and the grading approximates that of the crushed limestone reported previously.

The recycled asphaltic concrete mix was obtained from Boulder City, Nevada. This mixture was broken up and removed from an existing pavement. The original asphalt cement binder content of the mixture was 5.5

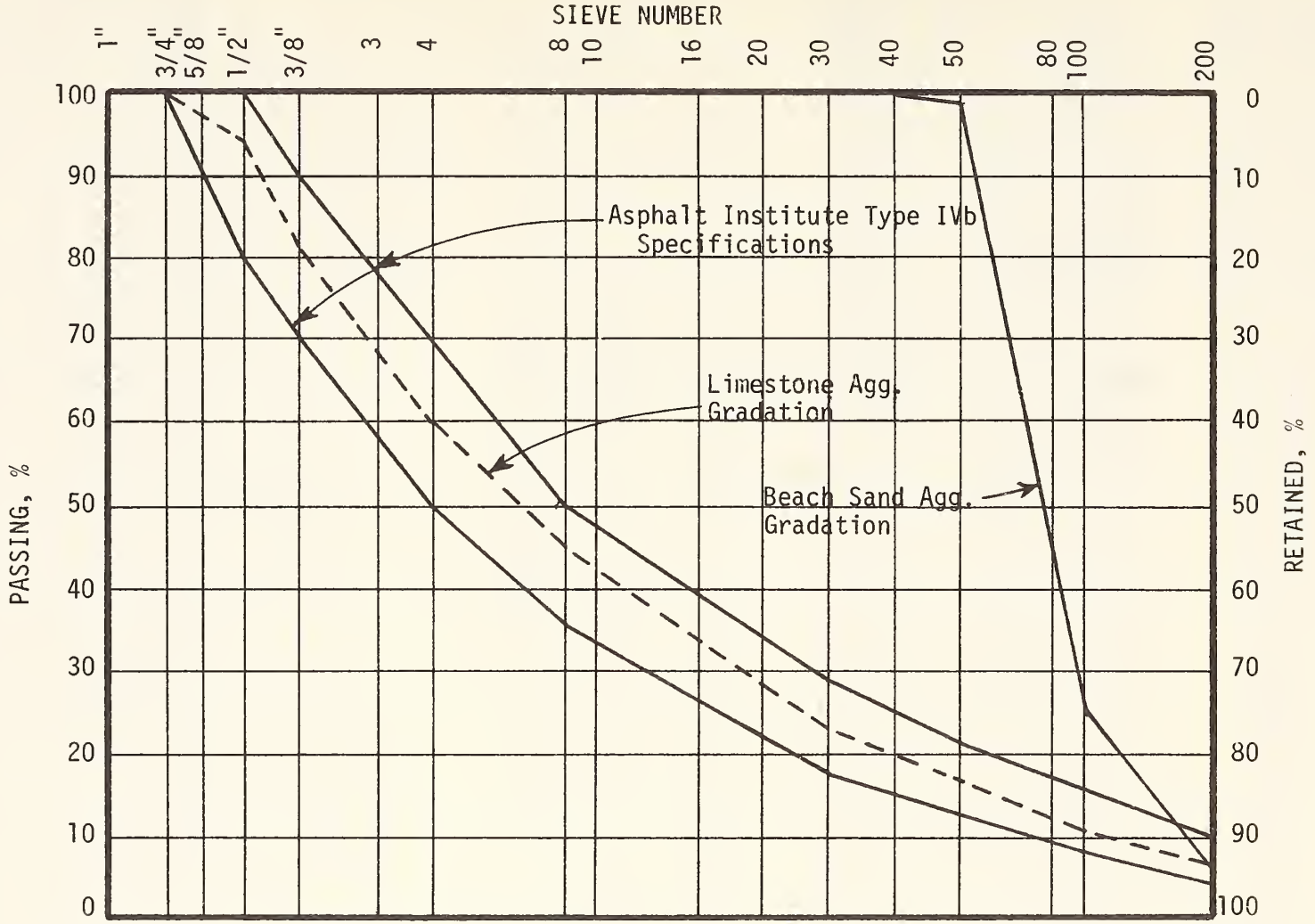

FIG. 19--Aggregate gradation of mixtures used for characterization tests.

1 cm = 0.394 in.

percent, and the aggregate gradation was similar to that of the previously reported crushed limestone.

Sample Preparation

Mixtures for the characterization tests were prepared in a manner similar to that used in preparation of mixtures for the screening tests. Details are included under Task C in this report. The three sulphur-asphalt pavement mixture systems (AAS, AE, and AES) were employed as needed. It should be recalled that these systems refer only to the sequence in which the ingredients were introduced into the mixture.

Specimens of each mixture were molded immediately after the last mixing cycle for the particular system being utilized. The dimensions and compaction effort used for the specimens depended upon the type tests to be performed thereon. This information is presented in the following subsections which detail the characterization tests.

Bulk Density, Air Void, VMA, Resilient Modulus, Hveem Stability, and Marshall Stability and Flow

The bulk density, air voids, VMA, resilient modulus, Hveem stability, and Marshall stability and flow of the mixtures used in the characterization test series were determined in accordance with the appropriate procedures outlined in the preliminary screening tests portion of this report. Specimens for the above tests were prepared in accordance with the Marshall procedure using 50 blows per face of the standard Marshall hammer (75).

Flexure Fatigue Tests

The procedure for the flexure fatigue test is described in detail in the VESYS II Users Manual and Transportation Research Board Special report 162 (51, 105). Epps and Monismith report that repeated loading fracture is one of the three most significant distress mechanisms which affect serviceability of asphaltic concrete pavements (106). They further indicate that a controlled stress mode of loading is encountered in relatively stiff pavements with thicknesses in excess of about 6 inches, whereas a controlled strain mode of loading is approached in thin pavement sections of about 2 inches thickness or less.

Specimens for the flexure fatigue tests were beams molded to dimensions of 3 by 3 by 15.25 inches (7.6 by 7.6 by 38.7 cm). The beams were molded by placing the mixture in two layers in a metal mold and compacting with a Soiltest Model CN-425A electro-hydraulic kneading compactor. The first and second layers received 26 and 56 blows, respectively, of the compaction foot at a contact pressure of 450 psi (3102 kPa). A static

load of 100 psi (689 kPa) was then applied to the top surface of the beam and maintained for a period of one minute, after which the beam was carefully removed from the mold. After cooling overnight, the bulk density of the beams were obtained in accordance with the procedures of ASTM D 2726-73 (90).

The beam specimens were tested in a constant stress mode and the number of load applications to failure was measured. Half-wave sine loads were applied in the third-point manner of loading from beneath the specimen at a temperature of 68°F (20°C) and a frequency of 100 cycles per minute (1.67 Hz). A pneumatically operated upward loading fatigue testing apparatus similar to the device used by Epps (121) was used for the flexure fatigue tests. The flexure fatigue tester is shown in Figure 20.

Moment, M, stress, σ, stiffness, E, and strain, ε, based on the deflection at midspan of a beam in third-point loading, as shown in Figure 21, can be calculated by means of the following relationships:

$$M_{max} = PL/6 \qquad (a)$$

$$\sigma_{max} = PL/bh^2 \qquad (b)$$

$$E = \frac{23PL^3}{108wbh^3}\left[1 + \frac{216(1+\mu)h^2}{115L^2}\right] \qquad (c)$$

$$\varepsilon_{max} = \frac{\sigma_{max}}{E} = \frac{4.69wh}{L^2 + 1.88(1+\mu)h^2} \qquad (d)$$

where P = load,
L = length of beam,
w = deflection at midspan,
b = width of beam,
h = height of beam,
I = moment of inertia = $\frac{bh^3}{12}$ and
μ = Poisson's ratio.

The term outside the bracket in Equation (c) is the customary strength of materials solution for a third-point loaded beam, as shown in Figure 21, in which shear deformation is neglected. The term inside the bracket represents a correction to account for shear deformation (107). Irwin and Gallaway indicate that the stiffness values can be found to be as much as 16 percent greater than those computed using only the bending deformation when the correction is used to reduce the test data.

Since strain continually increases throughout the duration of these tests, the strain reported herein is the initial bending strain obtained by the following equation in accordance with the procedure in the VESYS II M Users Manual:

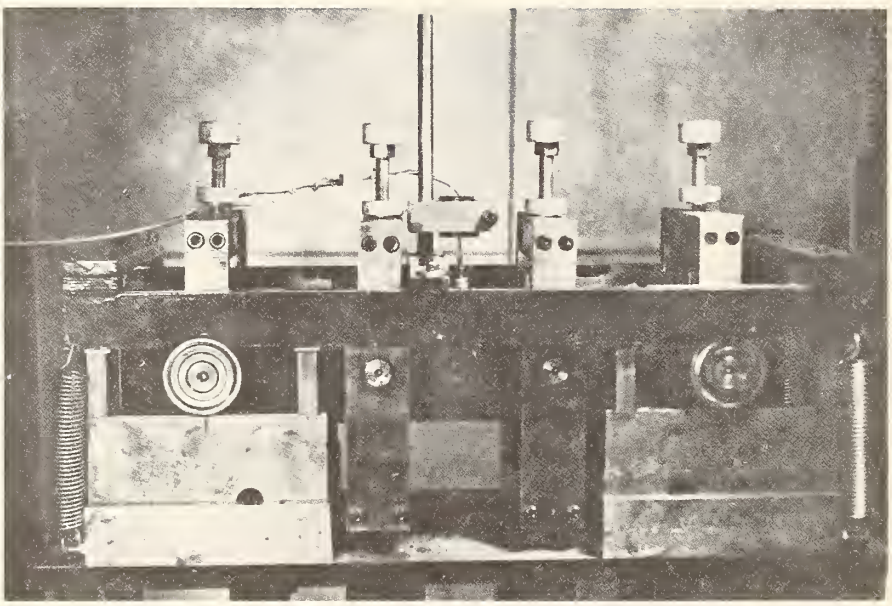

FIG. 20--Third-point flexure fatigue tester.

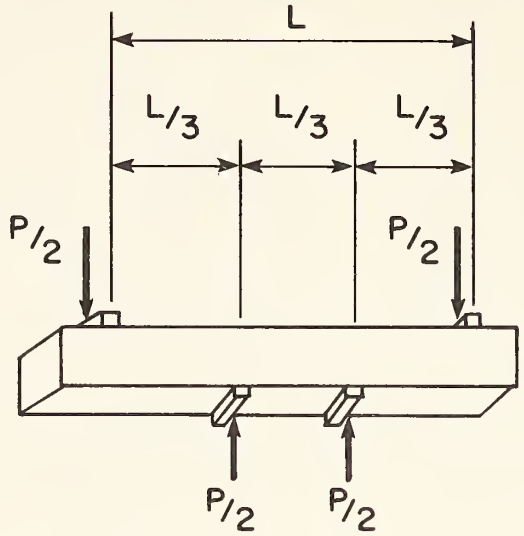

a) THIRD-POINT LOADED BEAM.

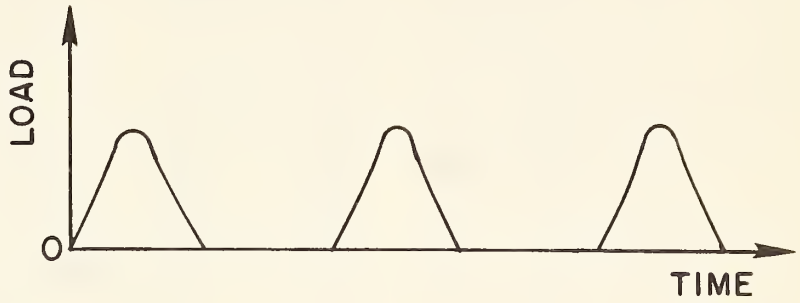

b) LOADING CONDITIONS.

FIG. 21--Flexure fatigue support and loading conditions.

$$e = \frac{12\ hd}{(3L^2 - 4a^2)}$$

where e = extreme fiber strain at 200 repetitions
L = reaction span length (L in Fig. 21a), inches
a = $(\frac{L}{2} - 2)$, inches
d = dynamic deflection of beam center at 200 repetitions, inches
h = specimen depth, inches

The equation used in VESYS II M structural design program to relate initial bending strain and number of cycles to failure is:

$$N_f = K_1 \ (\frac{1}{\varepsilon})^{K_2}$$

where N_f is the number of repetitions to failure,
ε is initial strain and
K_1 and K_2 are fatigue parameters.

The fatigue parameters K_1 and K_2 with the composition of the mixture.

Uniaxial Creep Tests

All creep tests were run in accordance with the procedure described in the Federal Highway Administration VESYS IIM Users Manual (51). The tests were performed on cylindrical samples four inches (10 cm) in diameter and eight inches (20 cm) high. Efforts were made to obtain densities of these uniaxial specimens similar to the densities of the Marshall stability and flexural test specimens. Numerous variations of sample preparation were tried in order to develop a method which would produce desired densities in the compacted specimens. The procedure finally selected for preparation of uniaxial test specimens consisted of placing the mixture in the mold in three layers of approximately equal thickness, spading each layer of material vigorously with a heated spatula 15 times around the perimeter and 10 times in the interior, applying 75 blows per lift with the Marshall hammer falling 18 inches (45.7 cm) and then applying vertically a staic load of 411 psi (2833 kPa) for a period of one minute. The compacted specimen was permitted to air cool overnight and was then extruded by use of a hydraulic ram. After determination of air voids, VMA, and bulk specific gravity of the compacted specimens, the ends were either sawed or capped with a sulphur based capping compound to insure parallel planes of loading for the creep tests. A Gilmore closed-loop, feedback control, electro-hydraulic tester was used for the creep tests. An Instron Model 74 Environmental Chamber was used to provide the desired temperature conditions during the tests. Temperatures higher than ambient were maintained by the heating unit of the chamber, whereas the colder temperatures were maintained by using a Sargent Water Bath Cooler to cool ethylene glycol and circulate the fluid through copper tubing coiled inside the chamber. Compressed carbon dioxide was used to lower the

temperature in the chamber immediately after setting up the previously cooled specimen and associated testing apparatus. After each specimen setup was complete, a period of several hours was allowed to elapse prior to the start of the creep test in order to permit stabilization of temperatures. The axial deformation was measured with a pair of linear variable differential transformers (LVDT). Load and deformation were recorded simultaneously on strip chart by a model 3006 Oscillograph manufactured by B & F Instruments, Inc. The testing apparatus used for the creep tests is shown in Figure 22.

The type loads applied to the specimen in the creep test were of the square-wave type as presented in Figure 23. For conditioning of the specimen, three loads were applied and held for 10 minutes duration each at the peak vertical load to be used in the creep tests. Minimal unload time was permitted between the first two loads, whereas an unload time of 10 minutes duration was allowed after the third conditioning load. This initial conditioning is necessary to bring the specimen to a state that is representative of the state in which the material is likely to exist in-situ in a pavement structure (10). If the conditioning loads are not applied, the test results will result in predicted values of pavement distress that are much larger than those which would actually be encountered in pavements (52). After the sample conditioning phase was complete, the LVDTs were rezeroed and the incremental static (creep) loads were applied. This was accomplished by applying incremental loads with durations of 0.1, 1, 10, 100 and 1000 seconds to the sample. These loads were followed by unload periods of 2, 2, 2, 4 and 8 minutes, respectively. The permanent deformation was measured at the ends of the unload periods or when rebound became negligible. The creep load pattern is presented in Figure 23. During the 1000 second load, the magnitude of the creep deformation is measured at times of 0.03, 0.1, 1.0, 3.0, 10.0, 30.0, 100.0, 500.0, and 1000.0 seconds.

The creep compliance, as required for use in the VESYS IIM program, was computed from the recorded data as follows:

$$D_t = \frac{\varepsilon_t}{\sigma_o}$$

where D_t is creep compliance at time, t,

ε_t is axial strain at time, t, and

σ_o is applied vertical stress in psi.

There are a variety of ways of representing the creep compliance as a function of time, but perhaps one of the most useful is the power law form:

$$D_t = D_o + D_1 \, t^n$$

where D_o is the glassy compliance,

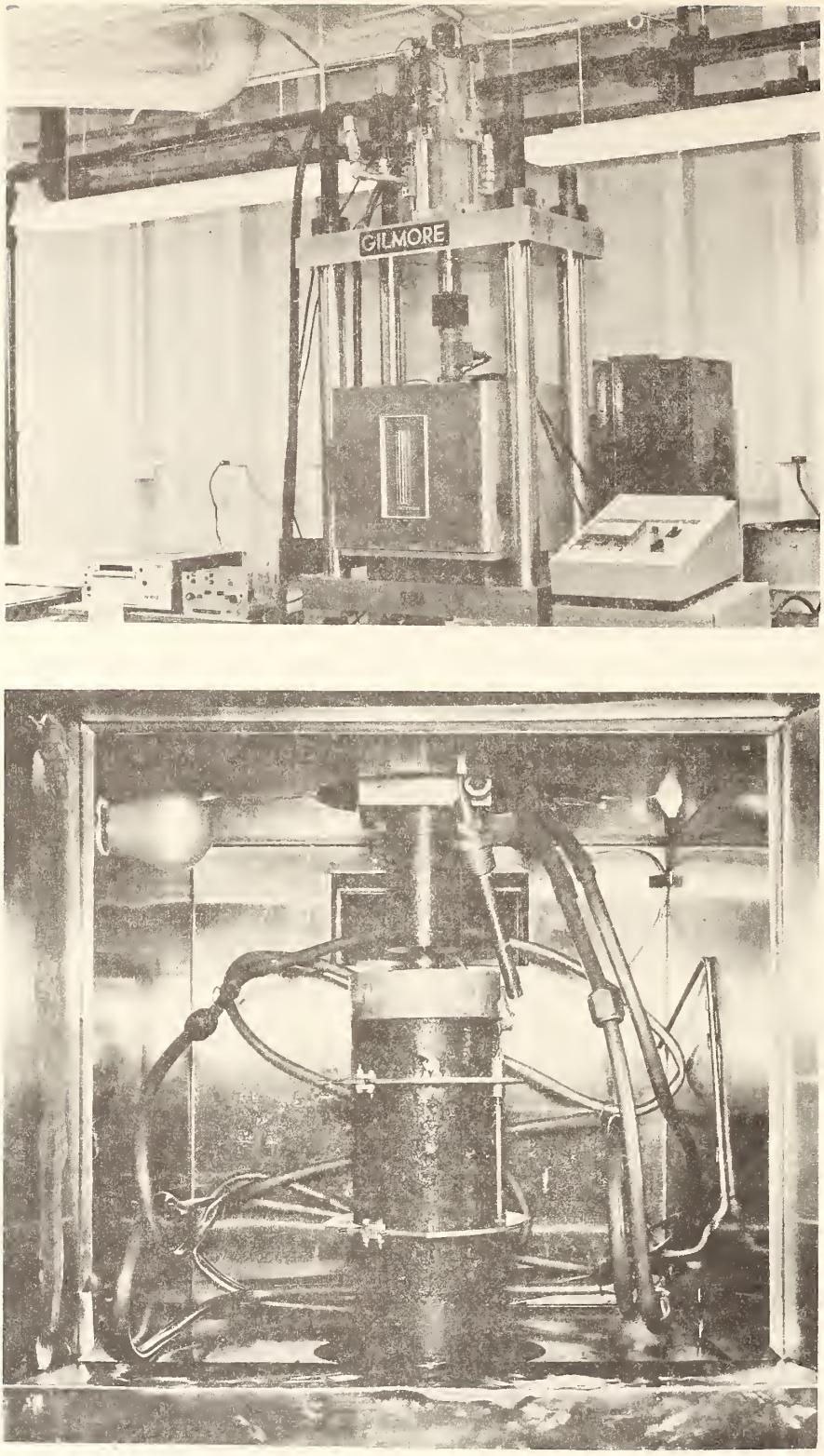

FIG. 22--Uniaxial creep test equipment.

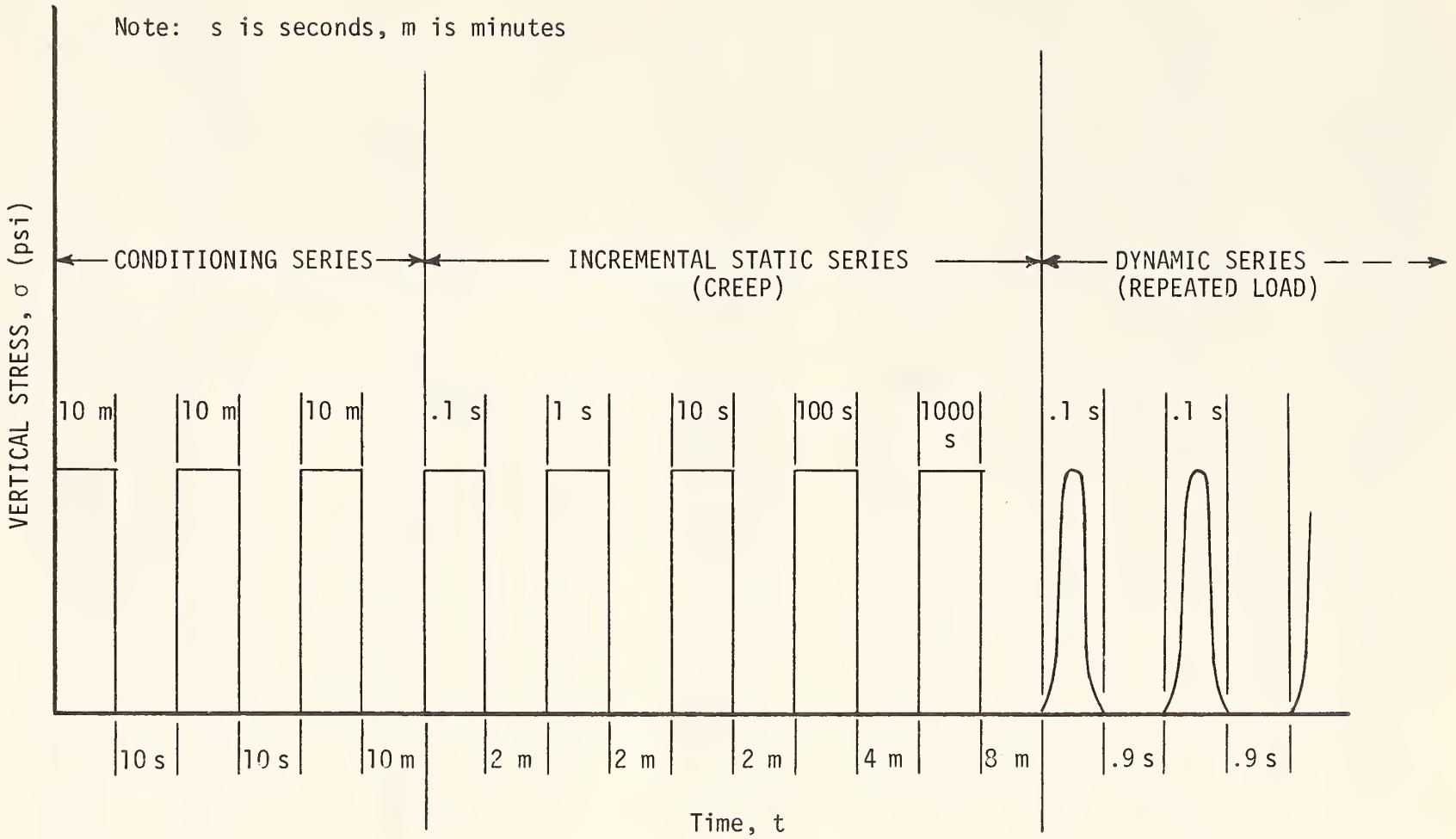

FIG. 23--Load history used in creep and repeated load uniaxial tests.

1 KPa = 0.1451 psi

D_1 is the intercept of the straight line portion of the creep curve on log-log paper with the one second time line, and
n is the slope of the logarithmic creep compliance curve.

Time-Temperature Superposition

Since asphaltic concrete pavement mixtures are viscoelastic materials, certain response characteristics such as modulus and creep compliance are functions of time and temperature. It is not practical to measure directly the complete behavior of the compliance as a function of time at constant temperatures using normal methods because extremely long periods of time would be required for each test (108). Instead, master creep curves which can be developed by use of the time-temperature relationships were established for this project by performing creep tests for relatively short periods of time at various temperatures. Superposition techniques were then used to determine shift factors for the creep compliance curves. Literature indicates that asphaltic concrete closely resembles a thermorheologically simple material (116). Thermorheological simplicity is the ability to generate a master creep compliance curve by shifting the individual isothermal creep curves at each temperature along the log-time axis.

Temperature is a major environmental influence on viscoelastic pavement response. The VESYS IIM program has the capability of handling material properties as a function of temperature variations. The computer input variable BETA relates the time-temperature shift factor, a_t, to the temperature variable for the pavement materials. This relationship is given by:

$$\text{Log } a_t = \beta(T_o - T)$$

where β is the value input for BETA,
T_o is the reference temperature for the master creep curve,
T is the temperature variable, and
a_t is the time-temperature shift factor for a temperature T.

The time-temperature shift factor is determined by:

$$a_t = \frac{t_T}{t_{T_o}}$$

where t_T is the time to obtain a given value of a material property at temperature T, and
t_{T_o} is the time to obtain the same value of the material property at the reference temperature, T_o.

The values of BETA were determined from the creep tests performed at various temperatures for this project.

Repeated Load Uniaxial Compression Tests

In accordance with the procedure in the VESYS IIM Users Manual, the same cylindrical specimens used in the creep tests were also used in measuring permanent strain, an important indicator of the rutting potential of pavement. The equipment discussed previously for the creep tests was used for these repetitive load tests. The repeated loads were started after the unload period at the end of the creep tests. A minimum time of 8 minutes was allowed for this final unload period, although certain specimens required more time for the rebound to become negligible. Haversine type loads were applied to the specimen such that each load application had a magnitude equal to the applied vertical stress used in the creep test. As shown in Figure 23, the load duration was 0.1 second followed by a rest period of 0.9 second. A minimum of 100,000 load applications was applied and the accumulated permanent deformation was measured at 1, 10, 100, 200, 1000, 10,000 and 100,000 repetitions.

Data from the repeated load triaxial tests were used to calculate permanent strain which was plotted vs. load repetitions on log-log scale. Each curve has its own intercept, I, and slope, S, which were used in calculating input data for the VESYS IIM permanent deformations subprogram. The equation of the curves is:

$$\varepsilon_a = IN^S \qquad (a)$$

where ε_a is accumulated permanent strain,
I is intercept of the curve with the vertical axis at one repetition,
N is number of repetitions, and
S is the slope of the curve.

The incremental amount by which the strain increases with each load repetition is:

$$\frac{d\,\varepsilon_a(N)}{dN} = ISN^{S-1} = \Delta\,\varepsilon_a \qquad (b)$$

The fractional increase of the total strain, F (N), that is permanent with each load repetition is:

$$F\,(N) = \frac{\Delta\,\varepsilon_a}{\varepsilon_r + \Delta\,\varepsilon_a} \qquad (c)$$

If it is assumed that the resilient strain, ε_r, is large in comparison to the increase of the permanent strain with each load repetition, then the following approximation can be made.

$$F\,(N) = \frac{\Delta\,\varepsilon_a}{\varepsilon_r} = \frac{IS}{\varepsilon_r}\,N^{S-1} \qquad (d)$$

Equation (d) may be shown as follows:

$$F(N) = \mu N^{-\alpha} \qquad (e)$$

where $\mu = IS/\varepsilon_r$

$\alpha = 1 - S$

The resilient strain was determined from the repeated load uniaxial compression tests. The constants α and μ are input data for the VESYS IIM program. When the power α equals 0, this means that the percent of incremental permanent strain increase with each load remains constant at a value of μ. When the power α is positive, this means that the fraction F (N) gets smaller with each load application. A negative α means that there is a progressive increase in permanent strain with each additional loading.

Thermal Expansion Tests

Thermal expansion coefficients were measured using a quartz tube dilatometer similar to that described by ASTM D 696 (110). The change in length of the specimen was monitored by a linear variable differential transformer (LVDT) and recorded by a Hewlett-Packard Digital Recorder. Temperature changes were accomplished by lowering the temperature of the entire testing apparatus to about -45°F (-43°C), and then allowing the system to gradually return to ambient temperature. Liquid nitrogen was used to cool the system. The heating rate, as controlled by insulation, was about 3^{o}C per hour so that a total time of about 24 hours was required to perform the test. The apparatus was set up such that two specimens could be run simultaneously. A photograph of the test apparatus is presented in Figure 24.

Evaluation of Characterization Test Results

As noted previously, the characterization tests were performed in order to determine the mechanical, creep, and thermal behavior of sulphur-asphalt pavement materials. Results of the characterization tests are discussed herein.

Bulk Density, Air Voids, VMA

No significant changes in bulk density were evident within the range of sulphur and binder contents used in the characterization tests. Generally, as the amount of sulphur within the binder increased, the bulk density increased slightly for relatively constant binder (asphalt and sulphur) contents in the mixtures. Bulk densities of typical mixtures used in the characterization tests are shown in Table 17.

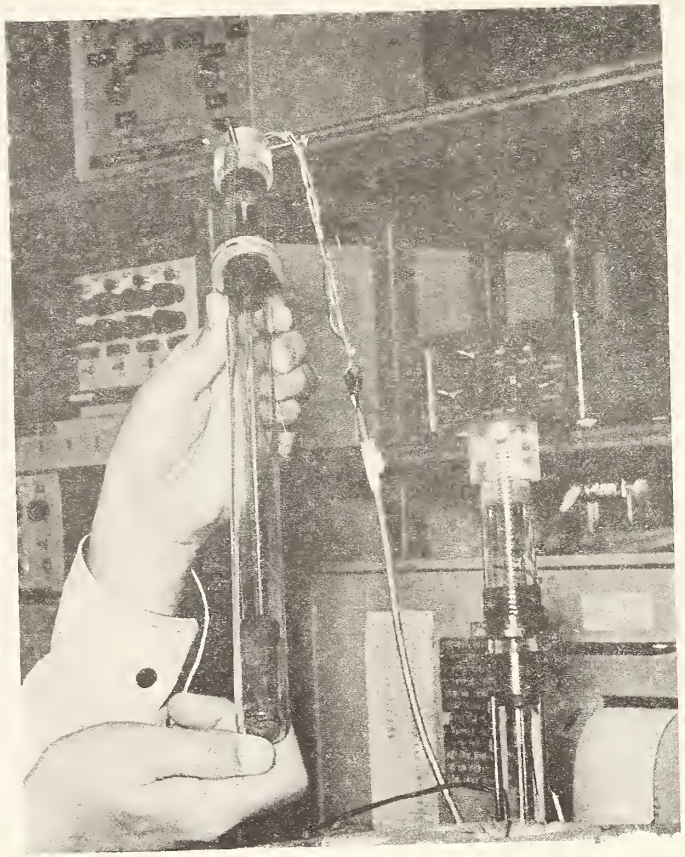

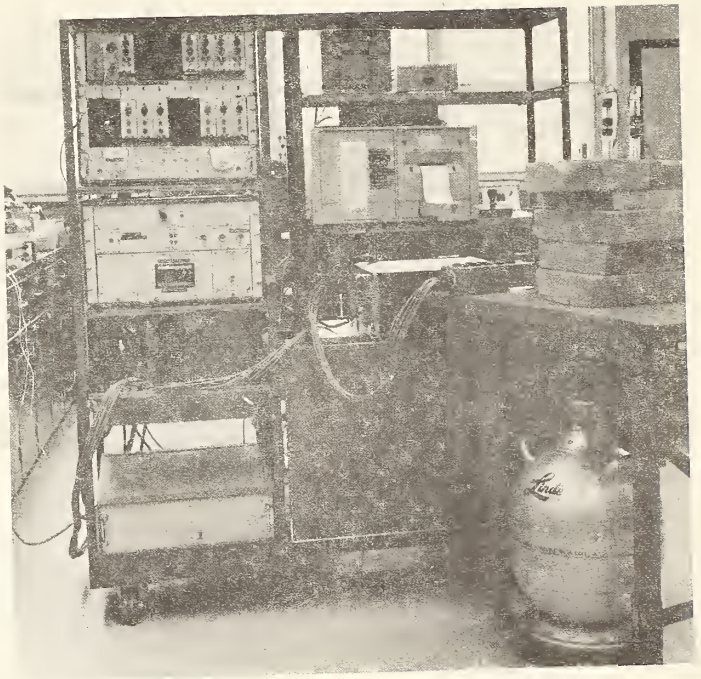

FIG. 24--Thermal expansion test apparatus.

TABLE 17

PHYSICAL PROPERTIES OF TYPICAL CHARACTERIZATION TEST MIXTURES AT 72°F

Aggregate	Sulphur Content (w/o)	Asphalt Content (w/o)	Bulk Sp. Gr.	Air Voids (%)	VMA (%)	Hveem Stability	Marshall Stability (lb.)	Marshall Flow (1/100 in.)	Resilient Modulus @ 68°F (x 10^6 psi)
Limestone	0	6.0	–	–	–	–	–	–	.301
Limestone	1.8	5.1	2.440	1.80	12.64	47	2364	12	.263
Limestone	4.1	3.9	2.453	1.59	12.83	53	3185	11	.321
Limestone	0	4.5	2.367	4.72	12.70	65	2419	10	.379
Limestone	1.2	4.3	–	–	–	–	–	–	–
Limestone	3.0	2.5	–	–	–	–	–	–	–
Beach Sand	0	8.0	–	–	–	–	–	–	.028
Beach Sand	13.5	6.0	2.046	11.06	37.86	53*	3300*	–	.320
Recycled Boulder Mix	1.25	5.5	2.294	5.83	–	85	11520	9	1.950

*(Ref. 35)

°C = (°F - 32) x 5/9
1 kg = 2.205 lbs.
1 cm = 0.394 in.
1 kPa = 0.1451 psi

Hveem and Marshall Stability

The data in Table 17 show that Hveem and Marshall stabilities increased with sulphur content. In all cases where the total binder content was held approximately constant, mixtures containing sulphur exhibited higher stabilities than the mixtures without suplphur. This trend is consistent with that reported in the literature (7, 61). The Marshall flow values generally decreased with increasing sulphur content.

Resilient Modulus

Typical resilient moduli, as determined by use of the Schmidt testing apparatus, are presented in Table 17 for mixtures used in the characterization tests. In addition, Figure 25 graphically shows results of resilient modulus tests on mixtures made with the Nevada crushed limestone and volcanic aggregate. Resilient modulus increases with sulphur content for mixtures where the total binder content remains approximately constant. At a sulphur content of about 4 w/o, the resilient modulus is approximately three times that of ordinary asphaltic concrete for the materials tested. Obviously, the values of resilient moduli will vary with materials and mixture variables, but the trend of increasing resilient modulus with sulphur content would remain unchanged. Both Table 17 and Fig. 25 show typical values of the properties of sulphur-asphalt mixes, but the figure is not meant to be a plot of the tabulated values. For example, the table gives test results using a standard TTI crushed limestone whereas the figure shows results of tests using a Nevada limestone. The differences that can be noted between the resilient moduli in the table and in the figure represent the degree of variation that was found in the testing program.

Flexural Fatigue

Figure 26 presents typical plots of initial bending strain versus the number of stress repetitions to failure for Nevada limestone and recycled Boulder mixtures resulting from the characterization test phase of the project. For comparative purposes, graphs for other mixtures obtained from the literature are also presented. The fatigue curves for all specimens tested for this project are included in Appendix F. Data for each curve were obtained by performing flexural fatigue tests on a series of specimens at various levels of initial bending strain.

It can be seen from Figure 26 that the fatigue results for the Nevada limestone differ significantly from the other results presented on the graph. Flexural fatigue curves for the volcanic aggregate contained in Appendix F are similar to the Nevada limestone curves. It is believed that the technique used in testing the Nevada limestone and volcanic aggregate beams was primarily responsible for the noted difference in results. In the original testing procedure, the beams were loaded down-

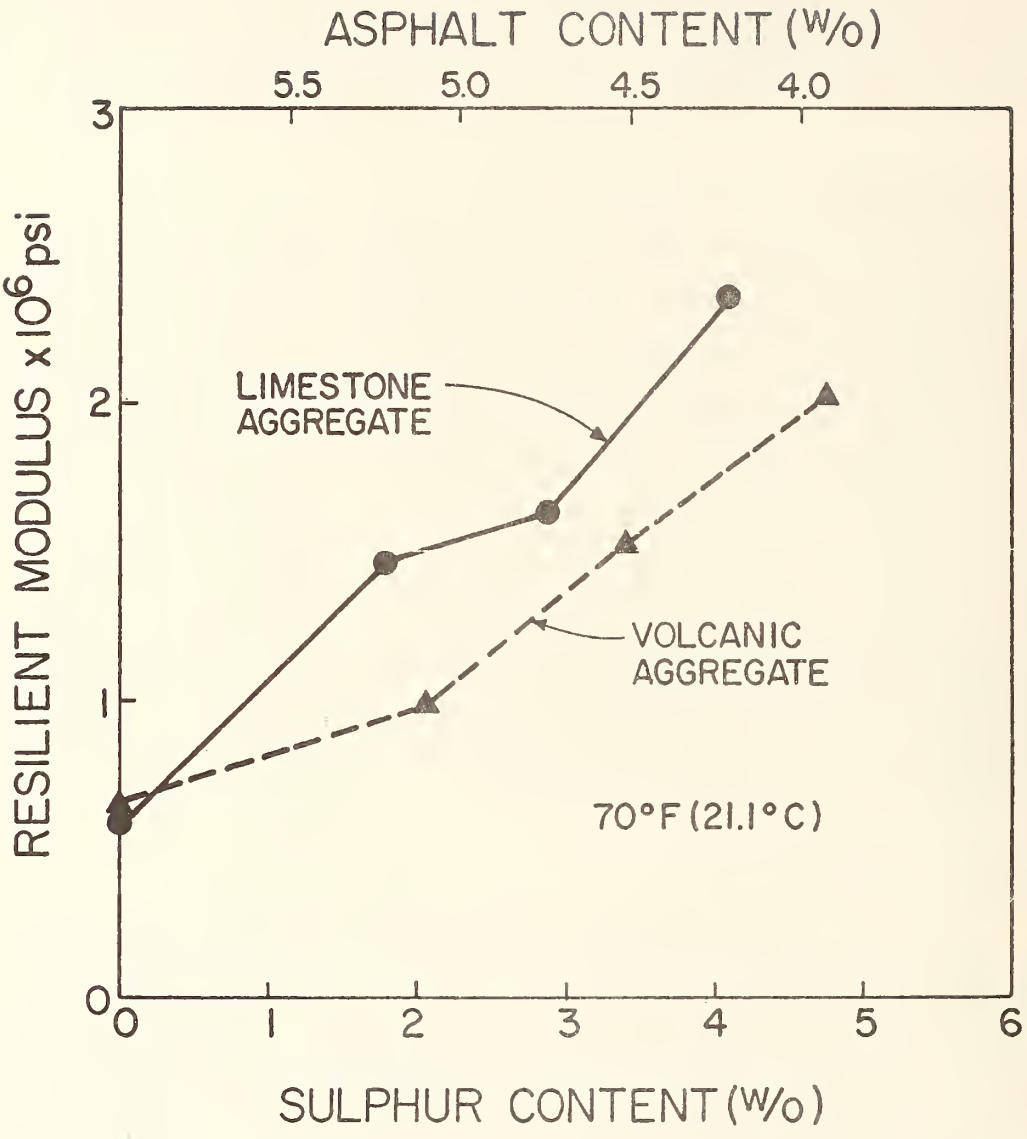

FIG. 25--Variation of resilient modulus with sulphur and asphalt content.

1 KPa = 0.1451 psi

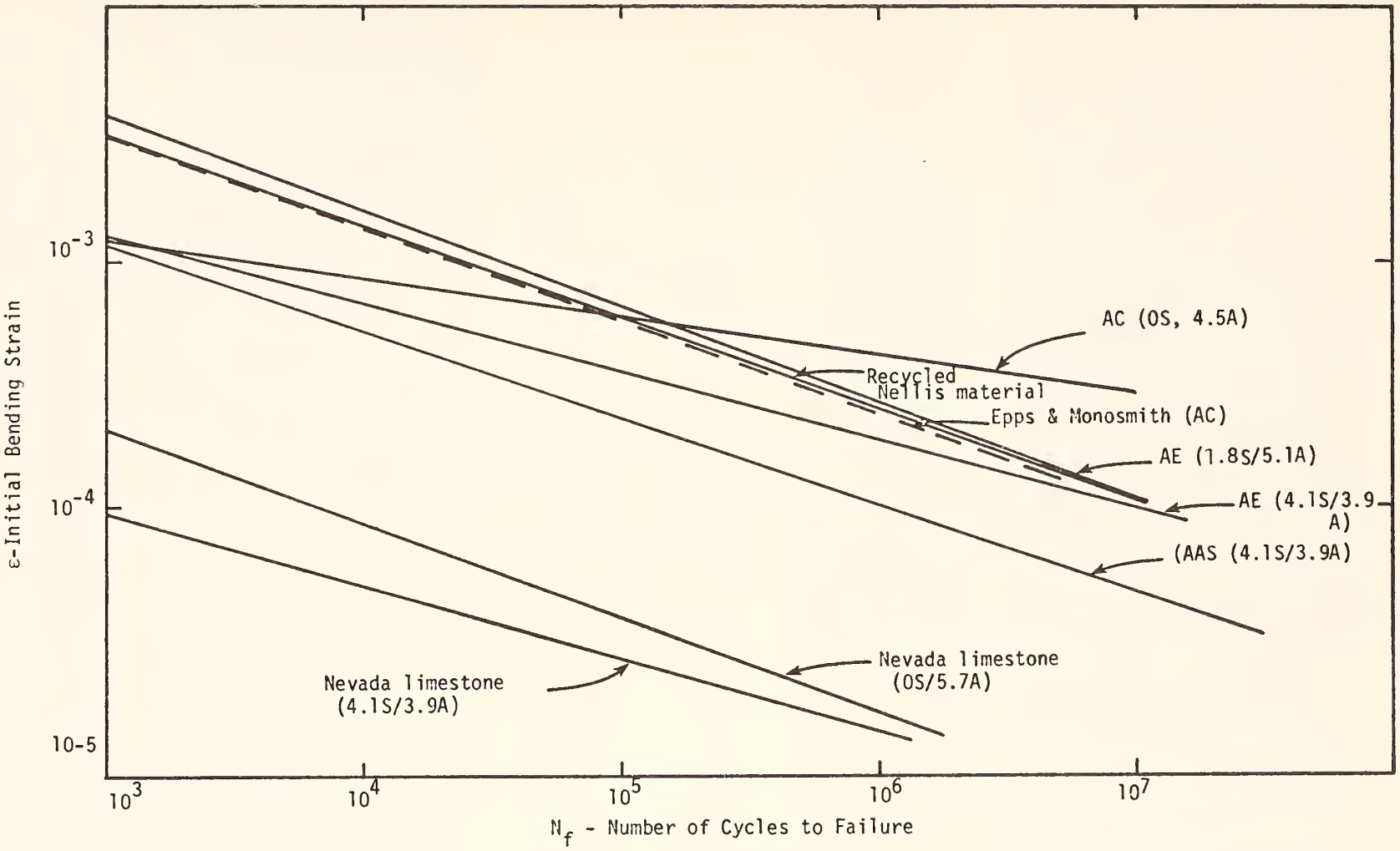

1 cm = 0.394 in.

FIG. 26.- Flexural Fatigue Curves for Sulphur-Asphalt Pavement Mixtures.

ward and were not forced to return to the at-rest position after each load repetition. Thus, permanent deformation was accumulated with each applied load, which resulted in premature failure of the Nevada limestone and volcanic aggregate beam specimens. These results indicate that mixtures containing the Nevada limestone and volcanic aggregate, both with and without sulphur, have shorter fatigue lives than the other mixtures presented on Figure 26. It is believed that the results shown on Figure 26 and in Appendix F for the Nevada limestone and volcanic aggregate are not accurate indications of the fatigue behavior of these materials. The flexural fatigue testing procedure was changed subsequently to incorporate a method for loading a beam specimen upward and returning it to its original at-rest position after each load repetition. This latter testing procedure is believed to more closely represent the actual mode of loading of a pavement in the field (106).

As discussed previously, the fatigue parameters K_1 and K_2 which are obtained from flexural fatigue curves vary with the mixture components. The value of K_2 is the inverse of the absolute value of the slope of the straight line. The value of the strain at the intersection of the straight line with the vertical axis at one repetition is denoted as I, and K_1 may be calculated from:

$$K_1 = (I)^{K_2}$$

Alternatively, K_1 may be calculated from the fatigue law:

$$N_f = K_1 \left(\frac{1}{\varepsilon}\right)^{K_2}$$

where N_f is number of load repetitions to failure,

ε is strain at N_f, and K_1 and K_2 are fatigue parameters.

As shown in Figure 27, the value of K_1 gets larger at a decreasing rate as the percent sulphur increases. The plots of K_2 versus sulphur content shown in Figure 28 are mirror images of the logarithmic plots of K_1. The flatter slopes of fatigue curves produce larger values of K_2. If two materials had equal values of K_1, then a larger value of K_2 for one material would indicate the potential for a longer fatigue life. As listed in Table 18, the values of K_1 ranged between 1.9×10^{-2} and 1.0×10^{-26}, whereas the values for K_2 ranged between 1.36 and 9.02 for the various materials tested in this project. These are within the ranges of values for K_1 and K_2 reported in the literature. Table 19 duplicates a table in reference (52) which shows typical values of K_1 and K_2. Figure 29 shows the relationship between K_2 and log K_1 found in this study and compares these results with previously reported data (52).

The regression equation relating $|\log K_1|$ to K_2 for the data from reference (52) was found to be:

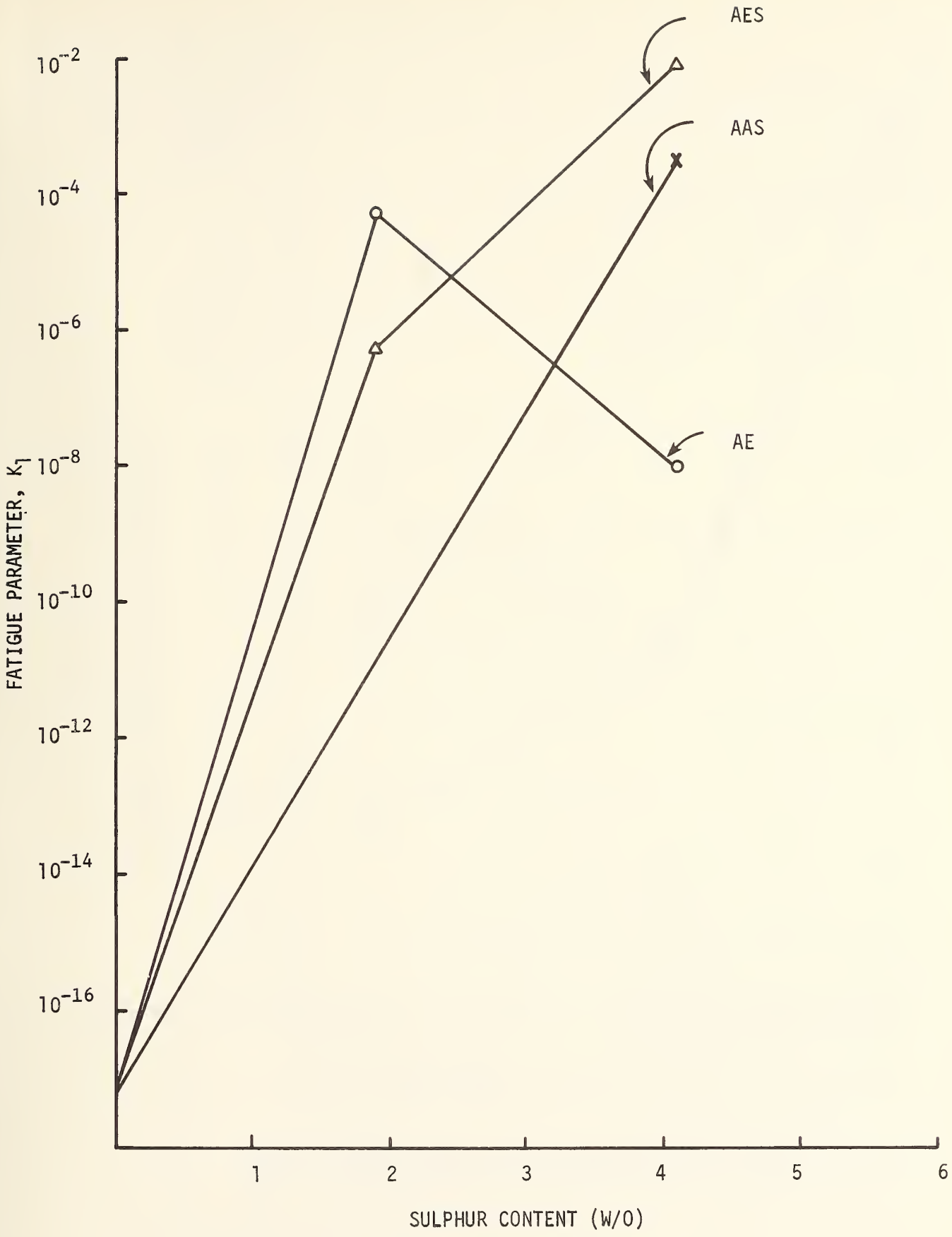

FIG. 27 -- Variation of K_1 with sulphur content.

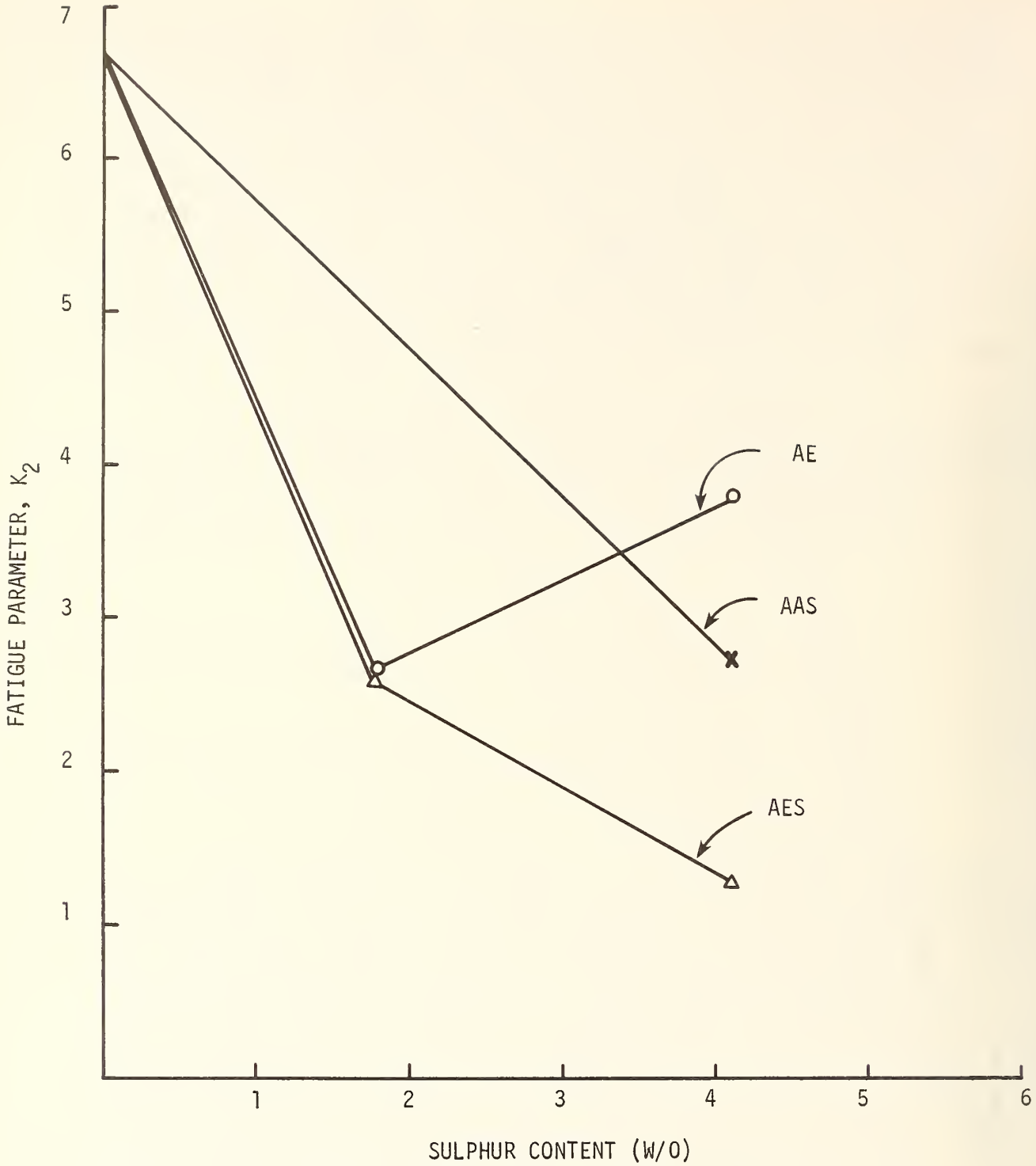

Fig. 28 -- Variation of K_2 with sulphur content.

TABLE 18

FATIGUE AND PERMANENT DEFORMATION PROPERTIES
OBTAINED FROM CHARACTERIZATION TESTS

Aggregate	Asphalt Content (w/o)	Sulphur Content (w/o)	Text Temp. (°F)	Fatigue Parameters		Permanent Def. Parameters		Dynamic Modulus
				K_1	K_2	ALPHA, α	GNU, μ	(x 10^6 psi)
AAS System Mixtures								
* Nevada Limestone	5.7	0.0	68	2.09×10^{-7}	2.65	-	-	-
* Nevada Limestone	5.1	1.8	68	3.39×10^{-11}	3.26	-	-	-
* Nevada Limestone	4.5	2.9	68	2.51×10^{-12}	3.87	-	-	-
* Nevada Limestone	3.9	4.1	68	2.45×10^{-11}	3.42	-	-	-
* Volcanic	7.0	0.0	68	1.41×10^{-7}	2.76	-	-	-
* Volcanic	5.9	2.1	68	7.94×10^{-9}	2.96	-	-	-
* Volcanic	5.2	3.4	68	9.12×10^{-12}	3.60	-	-	-
* Volcanic	4.4	4.7	68	2.09×10^{-11}	3.50	-	-	-
Georgetown Limestone	5.7	0.0	68	-	-	.666	.106	.352
Georgetown Limestone	3.9	4.1	68	-	-	.832	.080	1.689
Georgetown Limestone	3.9	4.1	140	-	-	.650	.022	.805
Standard Limestone	4.5	0.0	35	1.06×10^{-26}	4.02	-	-	-
Standard Limestone	4.5	0.0	68	1.81×10^{-17}	6.76	.687	.319	.268
Standard Limestone	4.5	0.0	110	7.45×10^{-6}	3.12	.299	.075	.073
Standard Limestone	5.1	1.8	68		-	.745	.147	.272
Standard Limestone	3.9	4.1	35	3.02×10^{-14}	5.00	.542	.045	7.147

$^{o}C = (^{o}F - 32) \times 5/9$
1 kPa = 0.1451 psi

*These samples were prepared by the U.S. Bureau of Mines.

TABLE 18 (CONTINUED)

Aggregate	Asphalt Content (w/o)	Sulphur Content (w/o)	Test Temp. (°F)	Fatigue Parameters		Permanent Def. Parameters		Dynamic Modulus
				K_1	K_2	ALPHA, α	GNU, μ	(x 10^6 psi)
AAS System Mixtures								
Standard Limestone	3.9	4.1	68	1.57×10^{-5}	2.74	-	-	-
Standard Limestone	3.9	4.1	110	4.26×10^{-3}	2.22	-	-	-
Standard Limestone	3.9	4.1	140	-	-	.053	.592	.139
Beach Sand	6.0	13.5	68	5.36×10^{-14}	4.17	.674	.078	.583
Beach Sand	6.0	13.5	110	-	-	.814	.176	.158
Recycled Boulder	(org)5.0 (new)1.25	1.5	72	2.51×10^{-20}	5.67	.562	.023	4.065
AE System Mixtures								
Standard Limestone	5.1	1.8	68	2.94×10^{-4}	2.67	.760	.50	.156
Standard Limestone	5.1	1.8	110	-	-	.600	.158	.066
Standard Limestone	3.9	4.1	68	1.01×10^{-8}	3.79	.777	.232	.214
Standard Limestone	3.9	4.1	110	-	-	.813	.54	.279
AES System Mixtures								
Standard Limestone	5.1	1.8	68	2.70×10^{-5}	2.58	-	-	-
Standard Limestone	3.9	4.1	68	1.86×10^{-2}	1.36	-	-	-

°C = (°F - 32) x 5/9
1 kPa = 0.1451 psi

TABLE 19. K_1 and K_2 as found by previous studies [52].

Source	Type Material	(^oF)	K_1	K_2
Kingham and Kallas	A. C. Surface	40	$5.45(10^{-11})$	4.32
		60	$6.31(10^{-11})$	4.32
		80	$3.12(10^{-9})$	4.14
Pell and Taylor	Asphalt treated Base Mix G. Base Course 6% Asphalt Gap graded	32	$4.55(10^{-16})$	5.29
		50	$4.50(10^{-14})$	4.83
		68	$3.90(10^{-13})$	4.52
		86	$2.63(10^{-9})$	3.80
Kirk	A. C. Surface, Crushed granite and limestone filler	32	$1.87(10^{-18})$	6.43
		50-59 (same curve)	$2.58(10^{-17})$	6.24
		77	$6.72(10^{-16})$	6.16
Kingham Relation based on AASHO Road Test Data	Developed from AASHO data	5	$2.60(10^{-17})$	5.00
		25	$1.48(10^{-16})$	5.00
		45	$2.53(10^{-15})$	5.00
		65	$9.50(10^{-14})$	5.00
		70	$2.81(10^{-13})$	5.00
		85	$4.63(10^{-12})$	5.00
		105	$4.03(10^{-10})$	5.00
Penn State Data	A.C.Surface	55	6.28×10^{-9}	3.92
		70	4.66×10^{-7}	3.61
		85	2.90×10^{-6}	3.51

$^oC = (^oF - 32) \times 5/9$

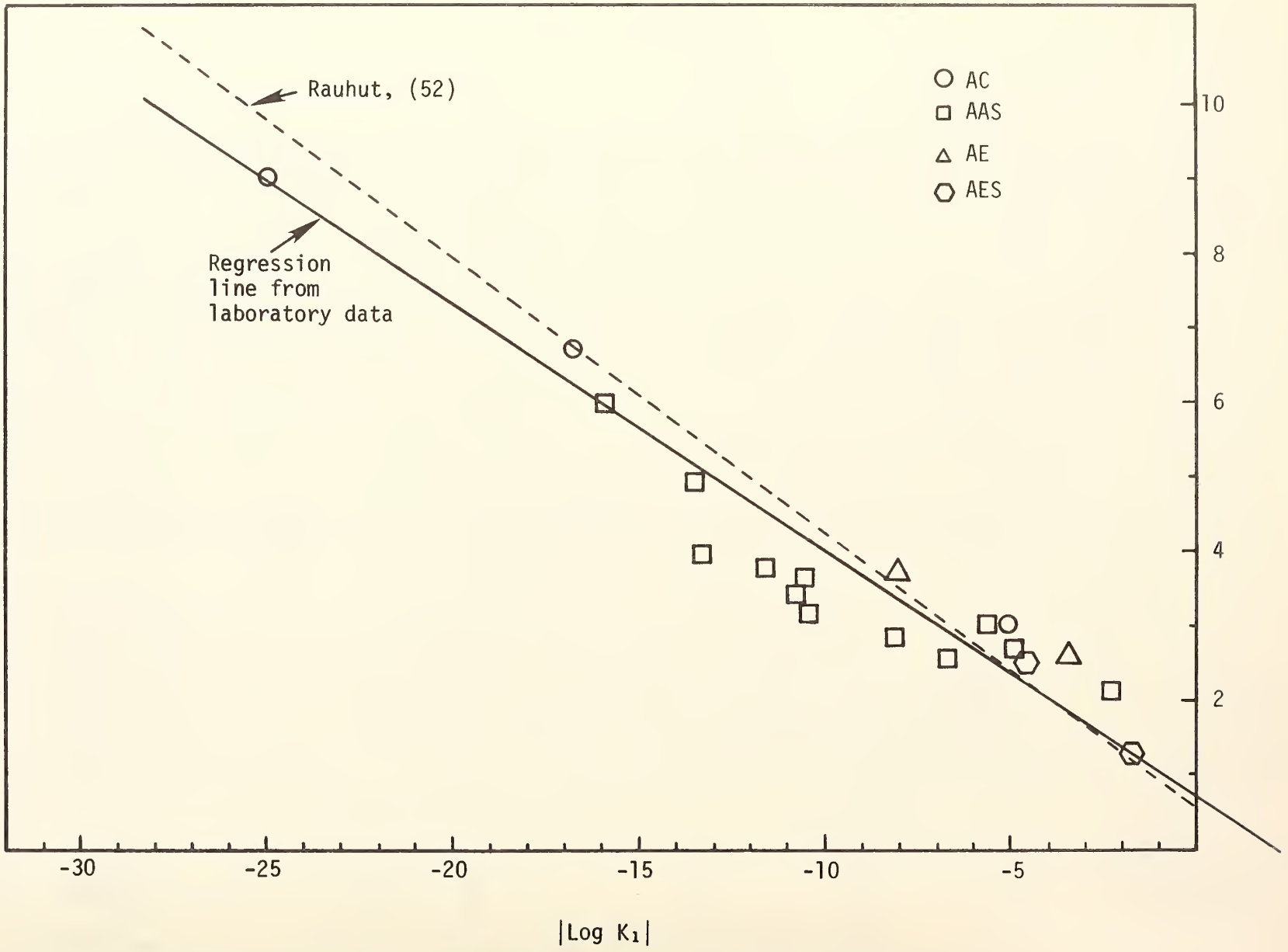

Fig. 29 - Relation Between K_2 and |Log K_1| for All Fatigue Tests.

$$| \log K_1 | = 3.012\ K_2 - 2.133$$

The R^2 for this equation was 0.956 for 45 observations. The high degree of correlation is significant considering the variety of sources and procedures represented in that table. A similar regression equation for all of the fatigue test data in the testing program reported here was found to be:

$$| \log K_1 | = 2.702\ K_2 - 1.552$$

This equation has an R^2 value of 0.7786 for 21 observations. This equation has been found to be very useful in verifying the K_1 and K_2 results of a series of fatigue tests. If the two values depart significantly from this relation, and especially if they plot substantially below the line, then the test data can be considered erroneous. Even values of K_1 and K_2 measured at temperatures other than 68°F (20°C) were found to plot closely to this line.

Since these fatigue parameters vary with temperature the AC and AAS materials were tested at several temperatures in order to determine the temperature dependency of K_1 and K_2 These results are shown along with the published results in Figures 30 and 31. The VESYS IIM program for structural design was modified to incorporate equations which characterize the temperature variations of the materials studied in this project. These equations developed for this program are shown in Table 20.

Creep Compliance

A typical creep compliance curve for one of the sulphur-asphalt concrete mixtures made with the standard limestone aggregate is presented in Figure 32. This curve is based upon measurements made during the 1000 seconds creep test. Similar curves which were obtained for each of the pavement mixtures evaluated in the characterization test phase are presented in Appendix G. Each creep compliance curve in the appendix is a mean curve which represents two or more replicate creep tests on specimens of the same mixture.

As discussed previously, the creep compliance is the ratio of creep strain to the constant applied stress. The creep compliance values reported herein are within the range of those reported in the literature (52).

For an asphaltic concrete to be linearly viscoelastic, the creep compliance should be essentially constant for given time and temperature values over a relatively wide range of applied stress levels. Research by Sharma and Kim indicate that asphaltic concrete materials display linear viscoelastic response only for short times, low stresses, and low temperatures (117). They further show that air void ratio significantly

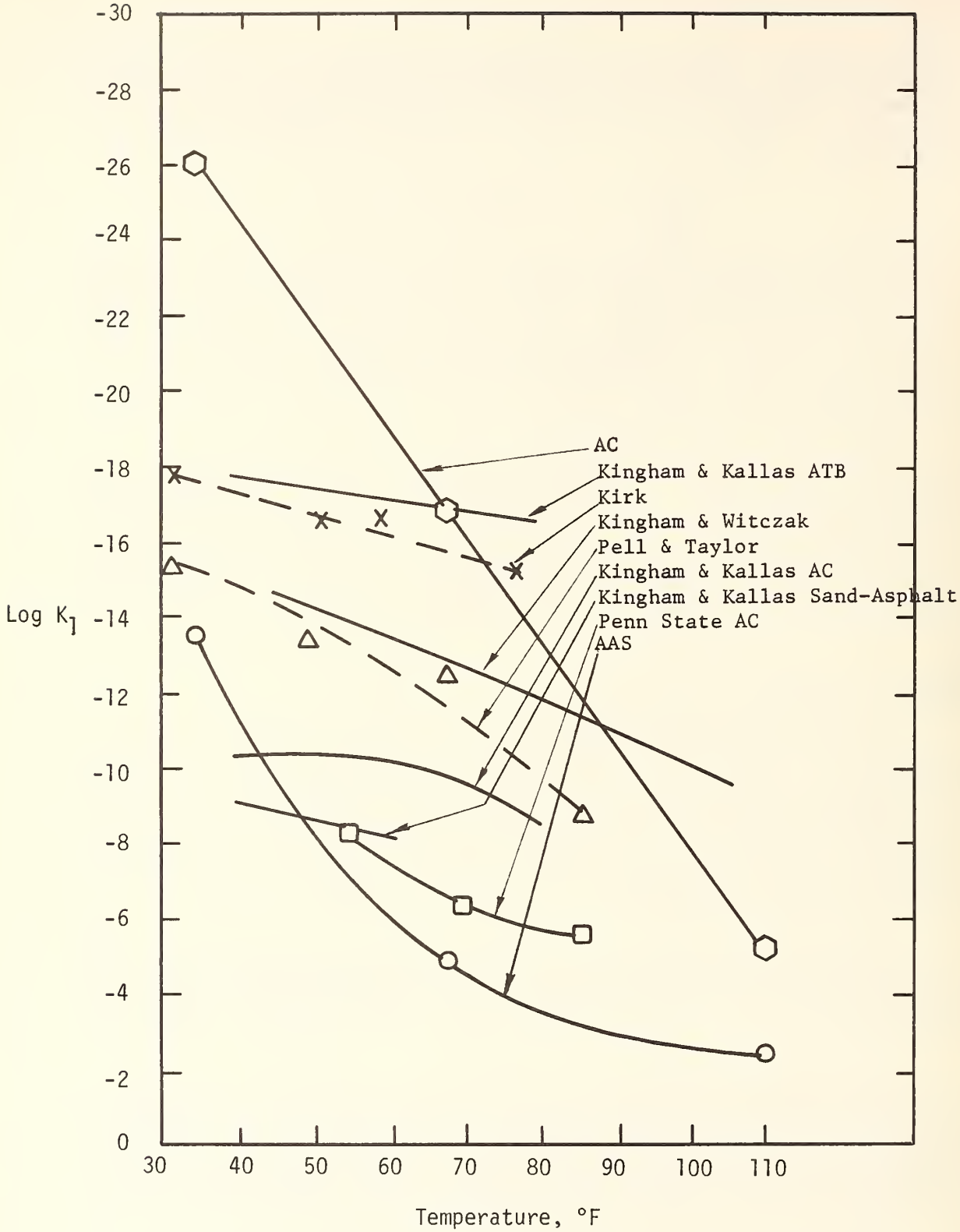

Fig. 30 - Relation of Log K_1 to Temperature for Various Asphalt Mixes.

$^{o}C = (^{o}F - 32) \times 5/9$

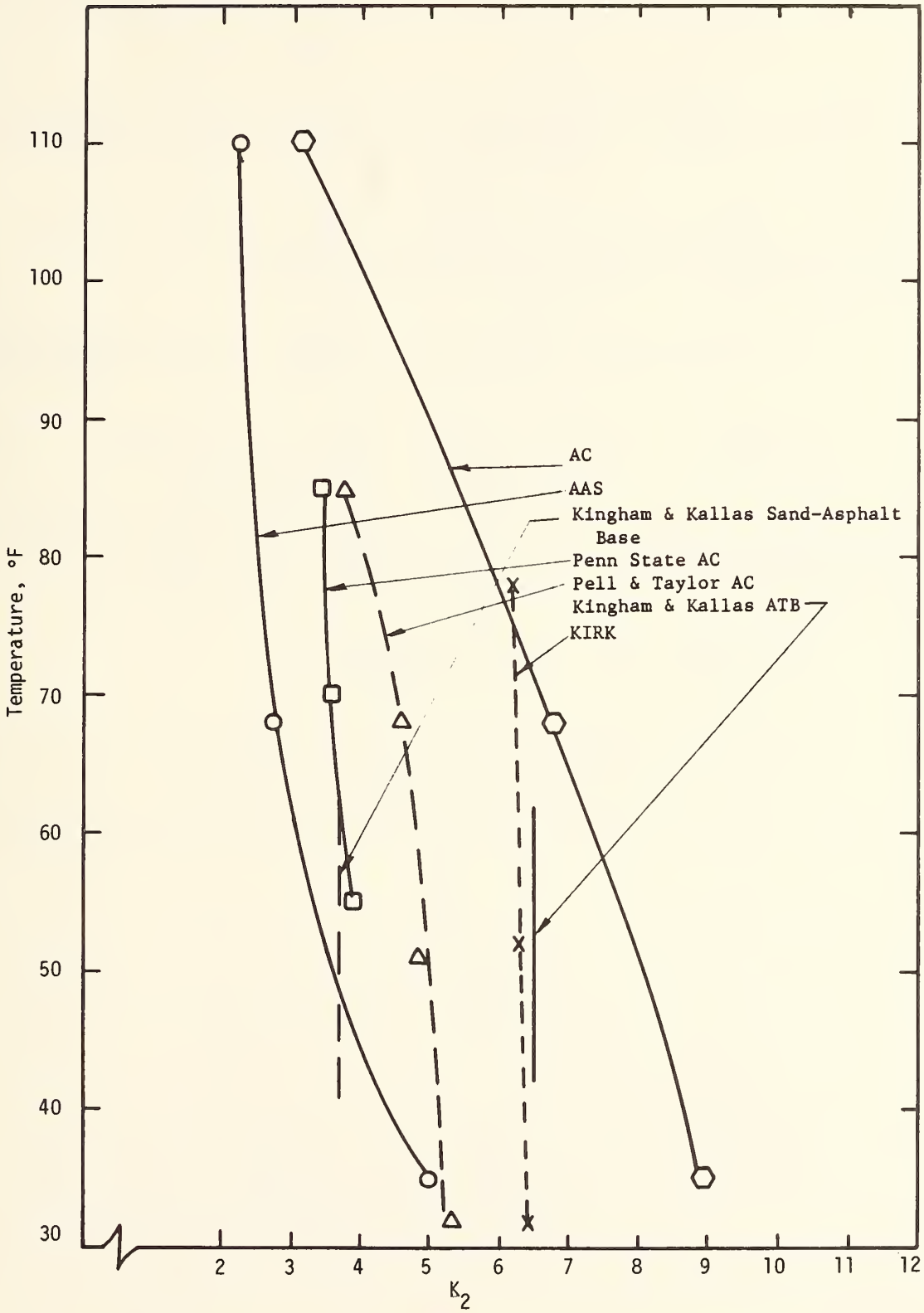

Fig. 31 - Relation of K_2 to Temperature for Various Asphalt Mixes.

$^{o}C = (^{o}F - 32) \times 5/9$

Table 20 - Temperature Dependency of K_1 and K_2 for AC and AAS Materials

ASPHALTIC CONCRETE (0 $^{W}/_{o}$ Sulphur, 4.5 $^{W}/_{o}$ Asphalt)
$\log \left\| \log K_1 \right\| = -0.375 \log T + 1.9936 - 5.4577 (\log \frac{T}{35})^{3.3707}$
$\log K_2 = -0.25 \log T + 1.3411 - 3.616 (\log \frac{T}{35})^{3.396}$
AGGREGATE-ASPHALT-SULPHUR (4.1 $^{W}/_{o}$ Sulphur, 3.9 $^{W}/_{o}$ Asphalt)
$\log \left\| \log K_1 \right\| = 3.503 - 1.536 \log T$
$\log K_2 = 4.596 - 3.893 \log T + 0.8875 (\log T)^2$

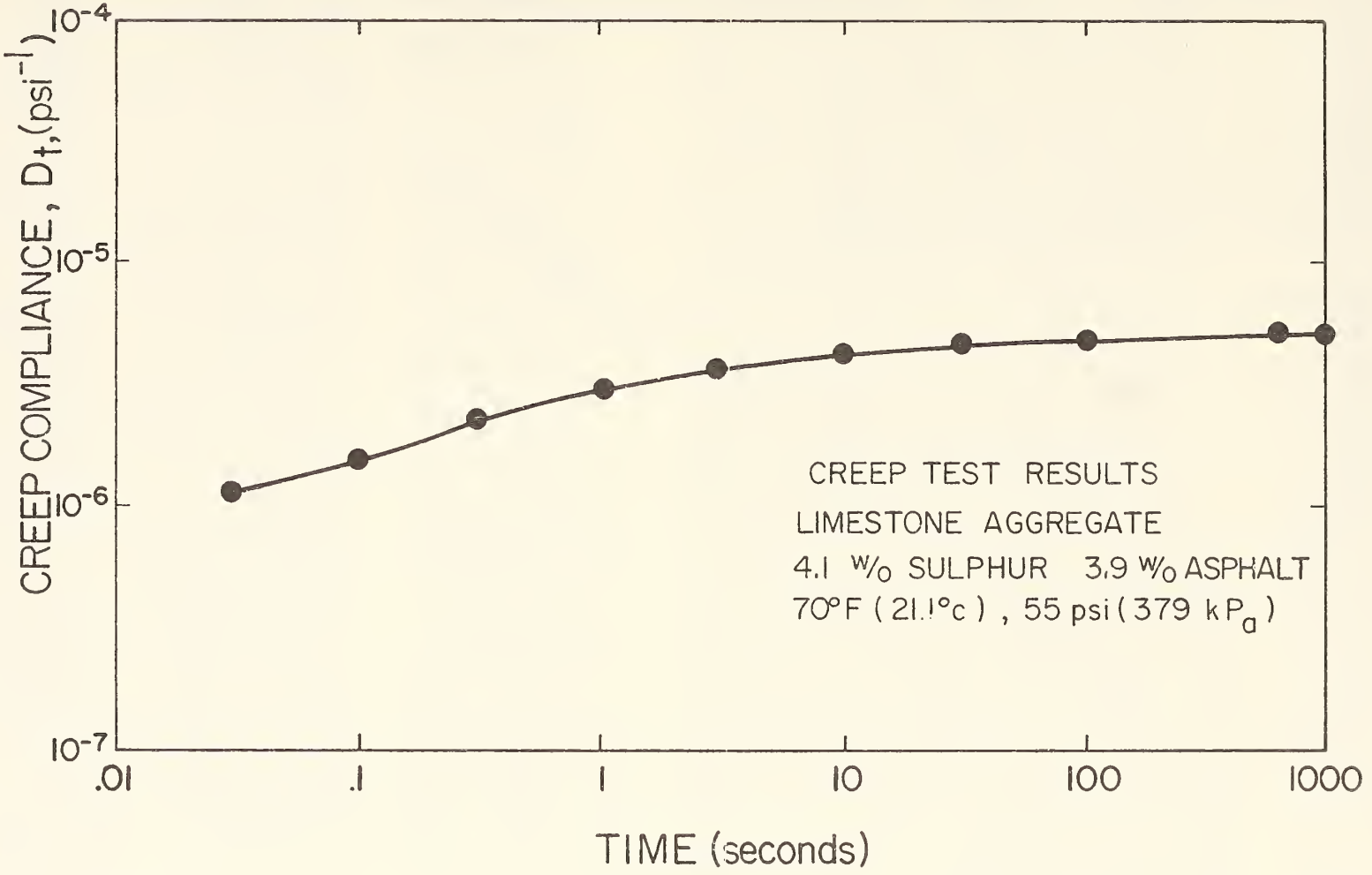

FIG. 32--Constant load creep test results.

1KPa = 0.1451 psi

influences the creep response of asphaltic concretes. Although creep tests were performed at various temperatures for the sulphur-asphalt mixtures studied in this project, the range of stress levels was not adequate to establish non-linearity of the mixtures. However, since durations of the repeated tire loadings considered in the VESYS IIM program are very short, it is sufficiently accurate to assume that the materials are linearly viscoelastic.

Time-Temperature Superposition

As discussed previously, asphaltic concrete materials are considered to be thermorheologically simple. For each mixture studied, the shift factors, a_T, were determined by shifting the creep compliance curves along the log-time abscissa as required to form master creep curves. Figures 32 and 34 present graphs of log a_T versus temperature for the mixtures studied in this project. Very little difference was evident between curves obtained for mixtures containing the same amounts of constituents, but prepared by the different systems. Also shown on the figure is a typical example of the calculations necessary to obtain BETA, and the calculated values of BETA for the mixtures. As can be seen in standard references on viscosity and viscoelasticity (e.g., 128), BETA can be expected to vary directly as the logarithm of the ratio of viscosity. As noted earlier in this report, the viscosity of the sulphur-asphalt binder decreases until the sulphur content is about 20 w/o and then begins to increase again. A similar variation of BETA is thus to be expected. The values of BETA contained in Table 21 indicate that such a response was observed in the materials tested in this program.

Permanent Strain

Permanent strain parameters were obtained from the repeated load uniaxial compression tests. The results are presented as graphs in the form of permanent (accumulated) strain versus load repetitions contained in Appendix H. Each graph shown in this appendix is a mean curve which represents two or more replicate repeated load uniaxial tests on specimens of the same mixture. A typical permanent strain curve is shown in Figure 35.

As discussed previously, the slope, S, and intercept, I, were determined for each curve. These values were used in calculating the permanent deformation parameters ALPHA and GNU used in the VESYS IIM program. A tabulation of these parameters is shown in Table 18. Also shown are values for the dynamic moduli as determined from the repeated load uniaxial compression test.

Thermal Expansion

The linear coefficients of thermal expansion determined experimentally for the mixtures used in the characterization tests are presented in Table 22.

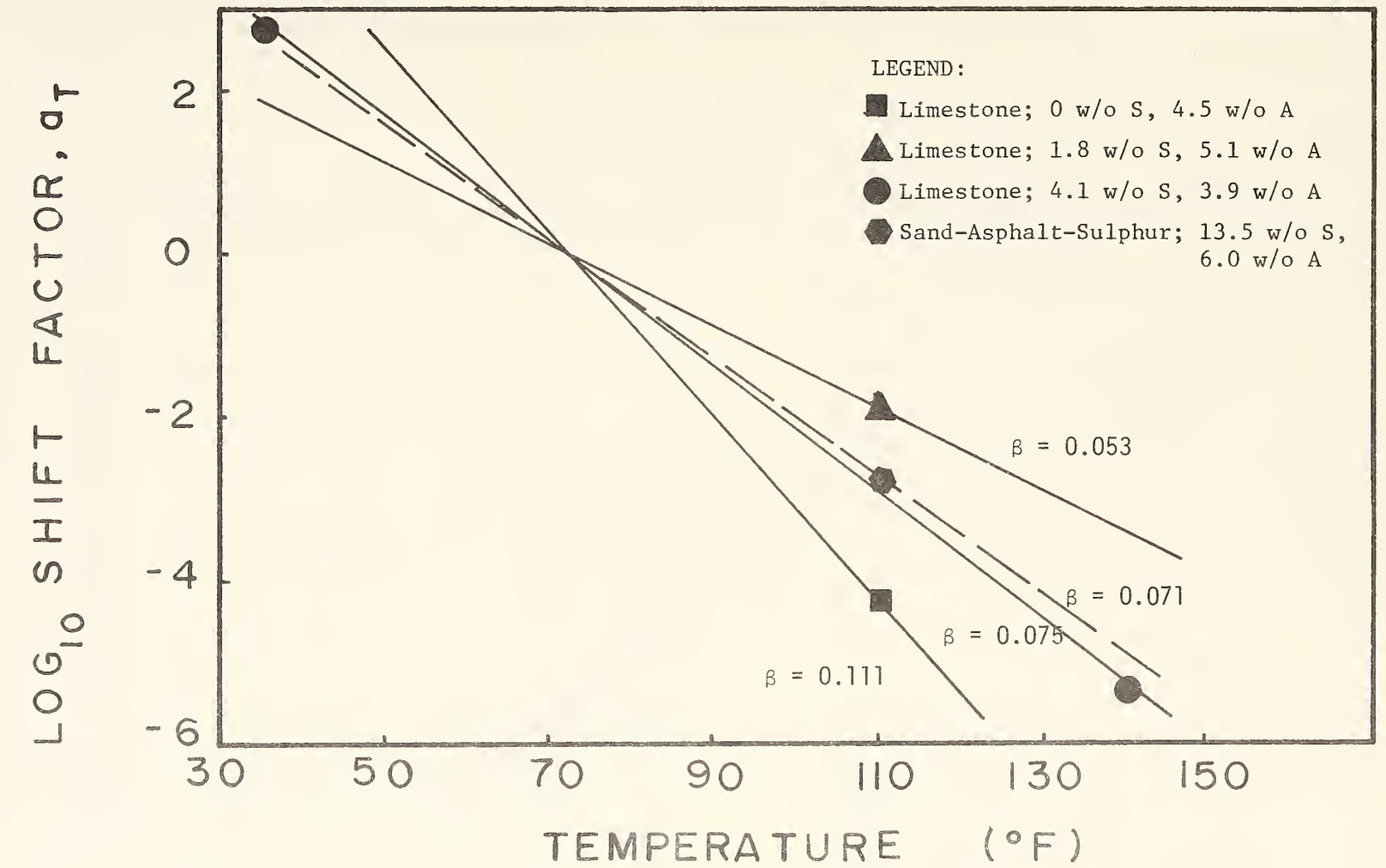

FIG. 33--Shift factor as a function of temperature for AAS system mixtures.
$^{o}C = (^{o}F - 32) \times 5/9$

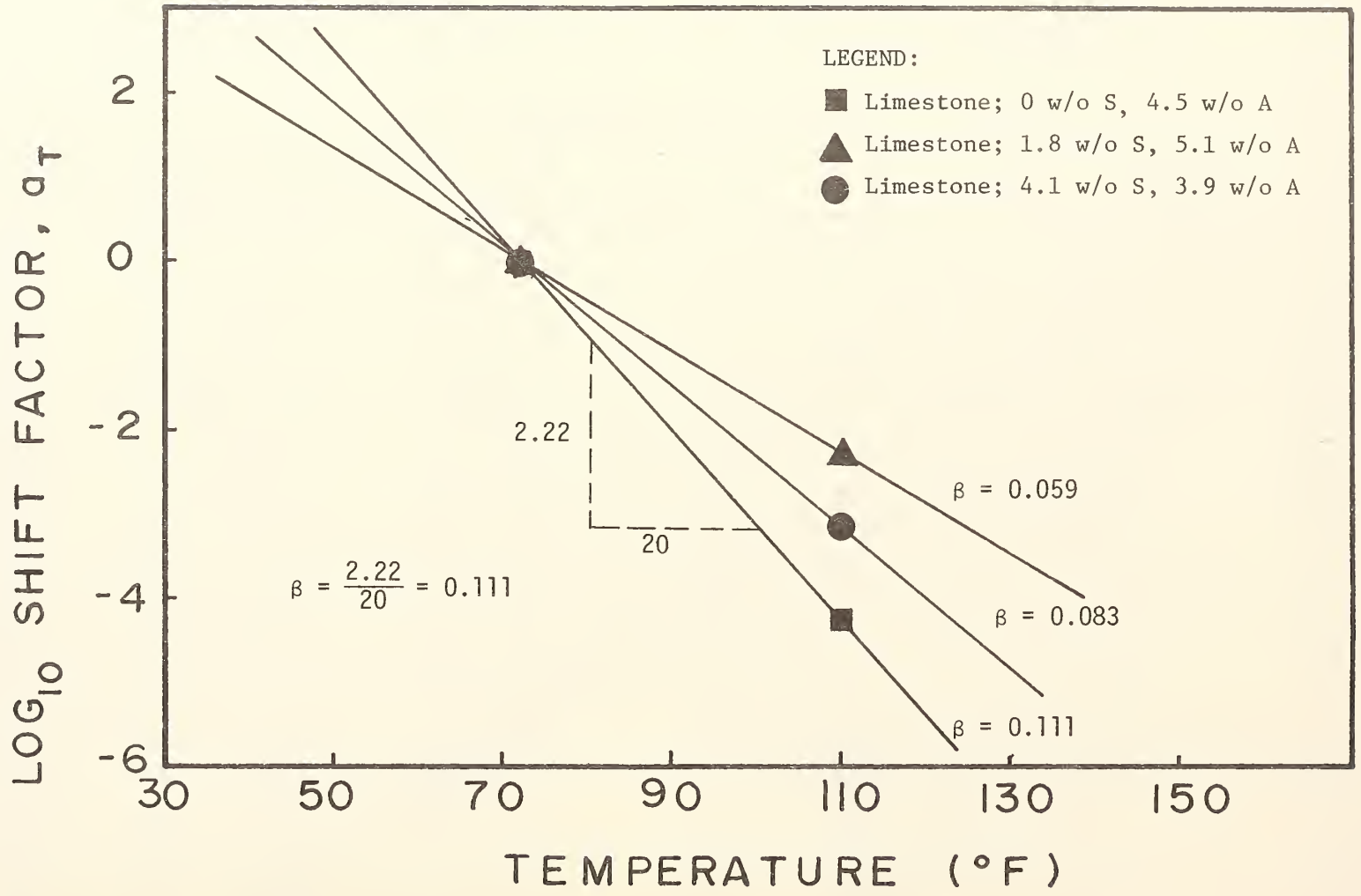

FIG. 34--Shift factor as a function of temperature for AE system mixtures.

$^{\circ}C = (^{\circ}F - 32) \times 5/9$

TABLE 21

BETA VALUES FOR CHARACTERIZATION
TEST MIXTURES

Type Aggregate	Sulphur (w/o)	Asphalt Cement (w/o)	Mixture System	BETA Value
Crushed Limestone	0.0	4.5	-	0.111
Crushed Limestone	1.8	5.1	AAS	0.053
Crushed Limestone	4.1	3.9	AAS	0.075
Crushed Limestone	1.8	5.1	AE	0.059
Crushed Limestone	4.1	3.9	AE	0.083
Beach Sand	13.5	6.0	AAS	0.071

TABLE 22

LINEAR COEFFICIENT OF THERMAL EXPANSION FOR
CHARACTERIZATION TEST MIXTURES OF SULPHUR-ASPHALT CONCRETE

Type Aggregate	Sulphur (w/o)	Asphalt Cement (w/o)	Mixture System	Linear Coeff. of Thermal Expansion ($\times 10^{-6}$ in./in. per ^{o}C)
Limestone	0.0	4.5	-	18.8
Limestone	1.8	5.1	AAS	22.0
Limestone	1.8	5.1	AE	20.8
Limestone	1.8	5.1	AES	22.6
Limestone	4.1	3.9	AAS	20.9
Limestone	4.1	3.9	AE	20.5
Limestone	4.1	3.9	AES	25.3
Beach Sand	13.5	6.0	AAS	29.3
Published Values (35):				
Asphalt Cement				200
Asphaltic Concrete				21 - 25
Sulphur				64.1
Sand				5.9 - 12.5
Limestone				10.8 - 85.0

1 cm. = 0.394 in.

$^{o}F = (^{o}C \times 9/5) + 32$

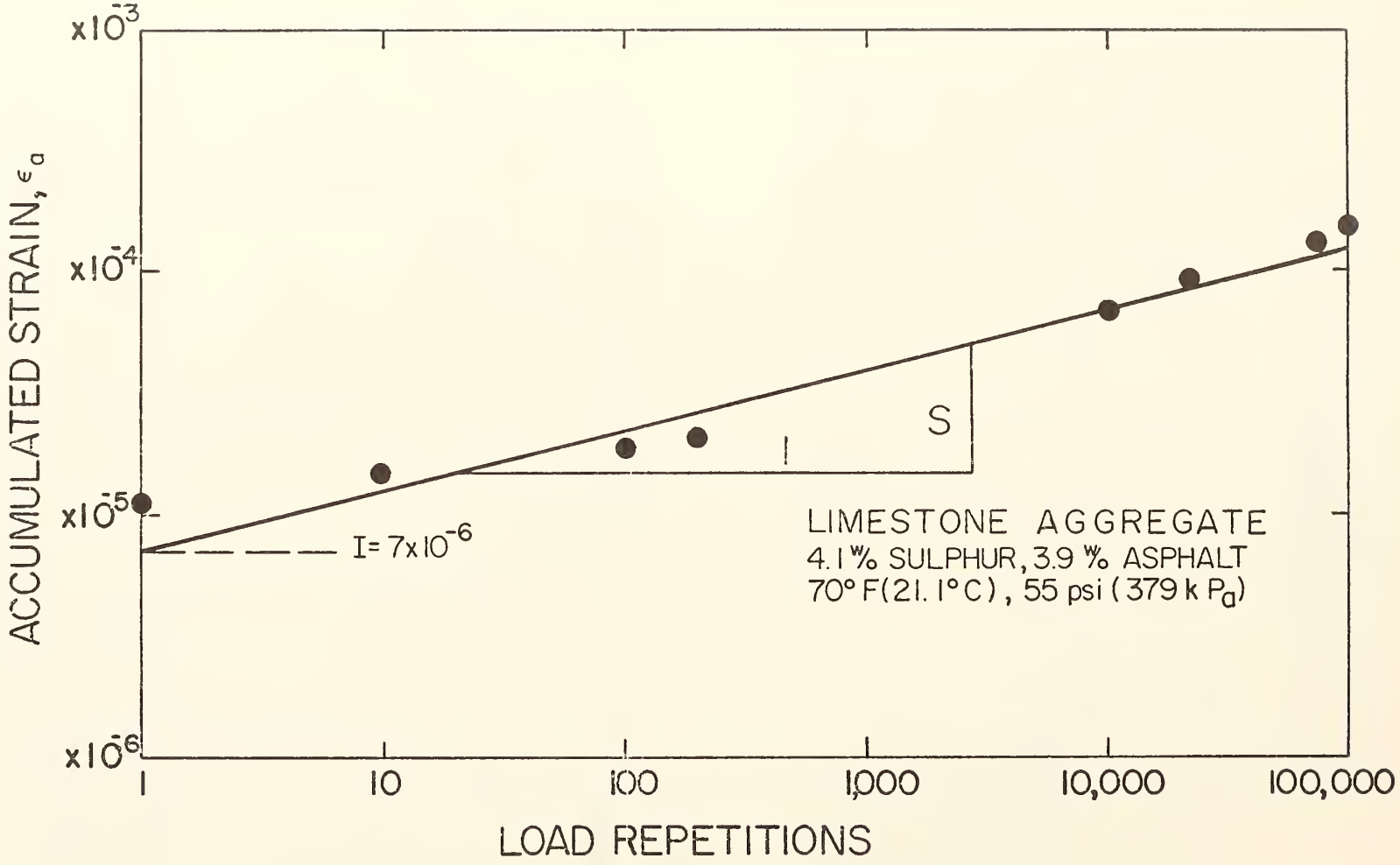

FIG. 35--Permanent strain from uniaxial compression test.
1 cm. = 0.394 in.

Also included in the table are published values for linear coefficients of thermal expansion for the various constituents used in the composite mixture.

The thermal expansion coefficient of the composite mixture results from the combined effects of the individual constituents and the amount of air voids within the compacted mixture. Thermal expansion coefficients decrease with increasing air void content of mixtures. Interpretation of the data indicates that the thermal expansion coefficients decrease slightly with increasing sulphur content for mixtures in which the total binder content remains approximately constant. There appears to be no significant difference between the coefficient of thermal expansion of conventional asphaltic concrete and sulphur-asphalt concrete made with the limestone aggregate. However, the coefficient of thermal expansion of the sulphur-asphalt concrete made with beach sand is significantly larger (about 56%) than that of the conventional asphaltic concrete. This difference is a potential source of detrimental stresses at the interface of adjacent layers of asphaltic concrete and sulphur-asphalt concrete made with beach sand (35).

Introduction to Micromechanics

The stresses, deflections, and temperature distributions in particulate composites, such as pavement materials, are dependent on the so-called "effective" mechanical and thermal properties. These properties (e.g. Young's modulus, Poisson's ratio, and thermal expansion coefficient) are defined in the same way properties are defined for bodies made of monolithic materials. With composites, however, it is necessary to introduce the restriction that the sizes of the aggregate particles and their spacings are small compared to the overall dimensions of the relevant specimen or pavement structure.

The subject of micromechanics deals with the prediction of effective properties in terms of the properties of each respective phase and phase geometry. Many equations exist for predicting properties of isotropic and anistropic composites (129). These equations are very useful for estimating the influence of changes in constituent (phase) properties and their volume fractions on the effective properties. Such studies aid in understanding the influence of constituents on the behavior of composites and in designing a pavement material which will achieve desirable or preselected values of effective mechanical and thermal properties. In addition to these theoretical studies, some experimental work is normally required in the design of composites in order to estimate the in-situ constituent properties and possible effects of phase geometry. However, the amount of experimental work needed is usually considerably less than would be the case if micromechanics theory were not employed.

This section will apply micromechanics equations to isotropic pavement materials consisting of limestone aggregate, sulphur, and asphalt.

Also, the effect of voids will be considered. The objectives of this work are to (i) illustrate the use of the relatively simple theory given in (129), and (ii) determine the accuracy of this theory by comparing the results with experimental data on Young's modulus of the composite, and (iii) improve the understanding of the influence of sulphur on the overall mechanical behavior of the pavement material.

Discussion of the Theory

In order to simplify the discussion of this theory, a composite consisting of only two phases or constituents will be considered first. The effective bulk modulus, K, and shear modulus, G, of the composite depend on the volume fractions and the moduli of the two phases. In addition, the geometry of the phases (e.g. size distribution and shape of particles) influence the overall or effective moduli.

In order to estimate the possible influence of phase geometry, it is helpful to calculate upper and lower bounds on K and G, where these bounds are valid regardless of the geometry. Specifically:

$$K_L \leq K \leq K_U \tag{1}$$

and

$$G_L \leq G \leq G_U \tag{2}$$

where the subscripts L and U denote the lower and upper bounds, respectively, on bulk modulus, K, and shear modulus, G. From (129), the lower bounds are:

$$K_L = K_1 + \frac{v_2}{\frac{1}{K_2-K_1} + \frac{3v_1}{3K_1+4G_1}} \tag{3}$$

and

$$G_L = G_1 + \frac{v_2}{\frac{1}{G_2-G_1} + \frac{6(K_1+2G_1)v_1}{5G_1(3K_1+4G_1)}} \tag{4}$$

where the subscripts (1) and (2) identify the moduli, K and G, and volume fraction, v, for each of the two phases. Also it is assumed that:

$$K_2 \geq K_1 \text{ and } G_2 \geq G_1 \tag{5}$$

Namely, the subscript (1) is used for the softest of the two phases. The upper bounds, K_u and G_u, are obtained from Eqs. (3) and (4) by interchanging the subscripts (1) and (2) throughout these expressions.

In deriving these bounds, it was assumed that the composite is (i) linearly elastic, (ii) continuous (i.e. no voids or cracks), and (iii) statistically homogeneous (129).

The Young's modulus, E, and Poison's ratio, ν, may be calculated using standard elasticity relations (130):

$$E = \left[\frac{1}{3G} + \frac{1}{9K}\right]^{-1} \tag{6}$$

and

$$= \frac{3K-2G}{2(3k+G)} \tag{7}$$

The inverse relationships are:

$$K = \frac{E}{3(1-2\nu)} \tag{8}$$

and

$$G = \frac{E}{2(1+\nu)} \tag{9}$$

It is to be noted the substitution of lower bounds, K_L and G_L, in Eg. (6) yield the lower bound to Young's yield the upper bound Eu.

The use of these equations for a two phase system consisting of sulphur and limestone will be illustrated. The individual mechanical properties are given in Table 23. The mid-range values of E and ν in Table 23 were used in Eq. (8) and (9) to calculate K and G, respectively. Thus, for sulphur:

$$\begin{aligned} &E = 3.55 \times 10^6 \text{ PSI}, \ \nu = 0.23 \\ &K = 2.19 \times 10^6 \text{ PSI}, \ G = 1.44 \times 10^6 \text{ PSI} \end{aligned} \tag{10}$$

and for limestone:

$$\begin{aligned} &E = 14.1 \times 10^6 \text{ PSI}, \ \nu = 0.285 \\ &K = 10.9 \times 10^6 \text{ PSI}, \ G = 5.49 \times 10^6 \text{ PSI} \end{aligned} \tag{11}$$

In as much as sulphur is the softer of the two materials, the lower bounds are given by Eq. (3) and (4), in which sulphur is taken as phase number 1. The upper bounds follow from Eq. (3) and (4) by taking limestone as phase number 1. In turn, the bounds on Young's modulus then follow from Eq. (6); these are shown in Figure 36 as a function of limestone volume fraction, c.

TABLE 23

PHASE MECHANICAL PROPERTIES

Material and Source of Data	Young's Modulus $E \times 10^{+6}$ (PSI)	Poisson's Ratio	Bulk Modulus $K \times 10^{6}$ (PSI)	Shear Modulus $G \times 10^{6}$ (PSI)
Sulphur (J)	2.34 - 4.75	0.18 - 0.28	1.77 - 2.43	0.92 - 2.02
Limestone (K)	12.6 - 15.6	0.27 - 0.30	9.13 - 13.0	4.85 - 6.14

1 kPa = 0.1451 psi

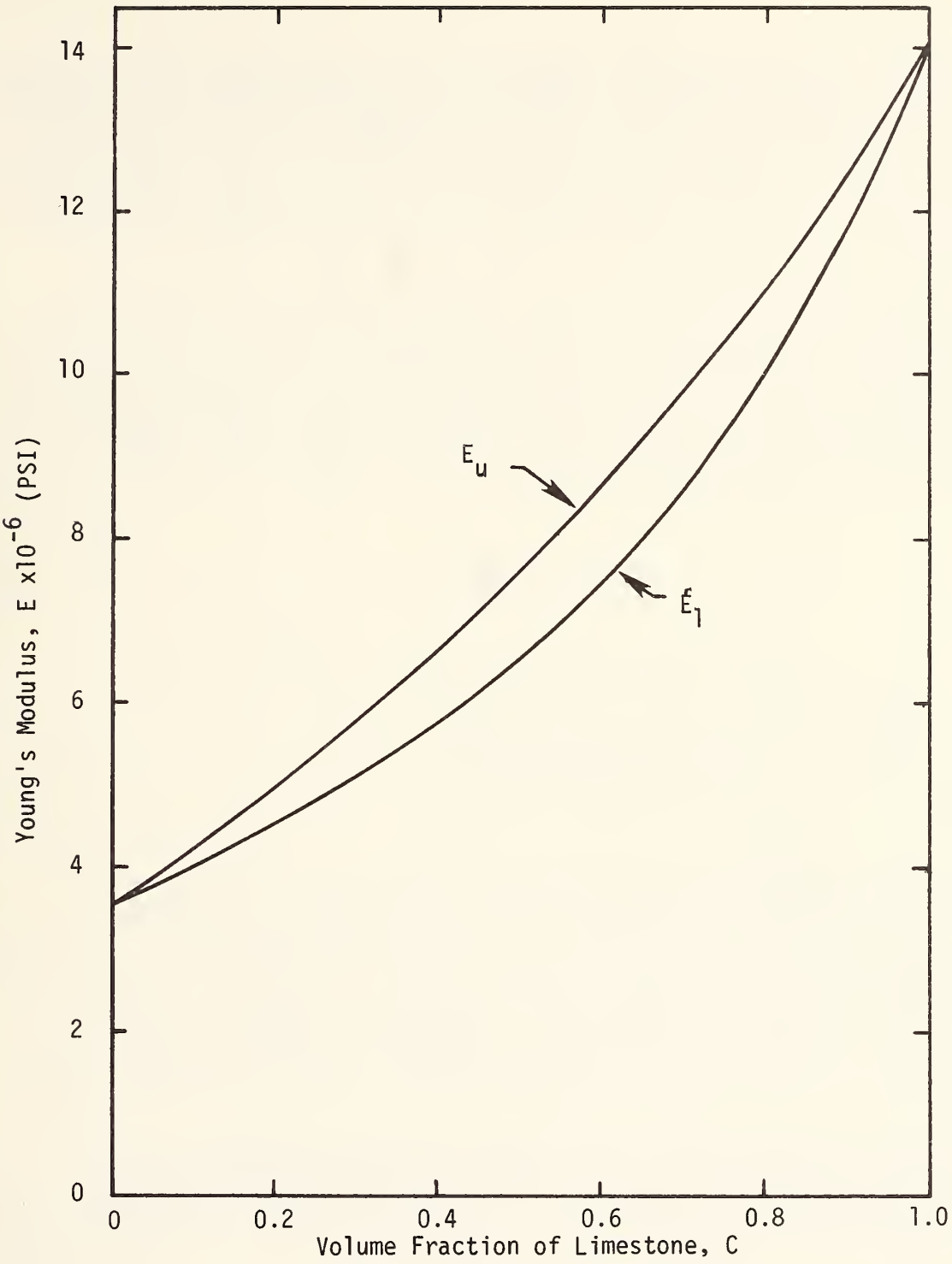

Fig. 36 - Bounds for Young's Modulus of Limestone-Sulphur Composite

1 kPa = 0.1451 psi

The spread in these moduli is due entirely to phase geometry. Namely, regardless of particle size distribution and which material is the matrix, the actual effective moduli will not fall outside these bounds. Considering the relatively small spread in these bounds (cf. Fig. 35), the results show that the phase geometry has little effect on the composite properties. It should be recognized, however, that the spread in bounds may be large whenever there is a very large difference in phase properties, such as for a limestone-asphalt composite.

It is important to point out that for a certain type of particulate composite, the equations for K_L and G_L are approximations to the actual effective moduli. Specifically if a particulate composite is considered in which the particles are approximately spherical in shape, the size distribution is very broad, and/or the particle volume fraction is small; then, on the basis of the analysis in (135) and letting phase number 2 correspond to the particles, the effective moduli are:

$$K = K_m + \frac{C}{\frac{1}{K_p - K_m} + \frac{3(1-C)}{2K_m + 4G_m}} \tag{12}$$

and

$$G = G_m + \frac{C}{\frac{1}{G_p - G_m} + \frac{6(K_m + 2G_m)(1-C)}{5G_m(3K_m + 4G_m)}} \tag{13}$$

where $c \equiv v_2$ is the volume fraction of particles and the indices (m) and (p) designate matrix and particle values, respectively. It should be noted that these equations are written in a different form than those in (135); but, it can be shown that Eq (12) is equivalent to Eq (38) in (135) and Eq (13) is equivalent to Eq (54) in (135). Thus, for the special phase geometry described above, the lower bounds in Eq (3) and (4) can be interpreted as estimations of the actual effective values. As one further point, the analysis in (135) reveals that the formula for shear modulus, Eq (13), may not be as accurate as that for bulk modulus.

Equations (6), (7), (12) and (13) can be used to estimate the effect of voids on effective moduli. For example, if sulphur contains a 10% void fraction, the void properties are $C = 0.1$, $K_p = G_p = 0$, and the sulphur properties in Eq (10) are used for K_m and G_m. It is found for this porous sulphur that:

$$K = 1.77 \times 10^6 \text{ PSI and } G = 1.18 \times 10^6 \text{ PSI}$$
$$E = 2.90 \times 10^6 \text{ PSI and } \nu = 0.23 \tag{14}$$

Consider next the composite consisting of a $C = 0.80$ volume fraction of limestone aggregate in the porous sulphur matrix. The effective

moduli of this composite are found by substituting the limestone properties in Eq (11) for the particle moduli and the porous sulphur properties in Eq (14) for the matrix moduli into Eq (12) and (13). Additionally, with the use of Eq (6) and (7), the following properties are found:

$$K=6.49\times10^{6}\text{PSI}(4.47\times10^{10}\text{Pa}) \text{ and } G= 3.71\times10^{6}\text{PSI}(2.56\times10^{10}\text{Pa})$$

$$E = 9.36 \times 10^{6} \text{ PSI } (6.45\times10^{10}\text{Pa}) \text{ and } \nu = 0.26 \qquad (15)$$

It should be noted that the two-phase Eq. (12) and (13) have been used successively in order to predict the effective moduli of the three-phase composite consisting of sulphur, limestone, and voids. This same technique will be employed later to predict the effective moduli of actual composite specimens containing asphalt, sulphur, limestone, and voids. An assessment of the theory will then be made by comparing the predicted moduli with measured values. First, however, the experimental work will be described.

Description of the Aggregate-Asphalt-Sulphur Mix

The aggregate-asphalt-sulphur mix was prepared using two wet mix cycles. In the first, aggregate and asphalt, both preheated to 300°F (149°C), were mixed for about 30 seconds in a 2 gal.(.008m^3) Beacon mixer. This operation put an asphalt coating on the surface of the aggregate particle. Sulphur, also at 300°F (149°C), was then added to the hot aggregate-asphalt mixture and mixed for an additional 30 seconds. This additional time was necessary to achieve a uniform dispersion of the sulphur throughout the final mixture.

As mentioned in Chapter II, the molten sulphur, in addition to increasing the workability of the mixture, normally fills the voids between the asphalt coated aggregate particles. As the mixture cools below approximately 245°F (118°C), the sulphur solidifies, creating a mechanical interlock between the aggregate particles from which the mix derives a relatively high degree of stability. This interlocking effect is shown in Figure 37, which is a photomicrograph of a representative mixture design. Note how the sulphur conforms to the geometry of the voids.

Cylindrical test specimens (4 in.(102mm) diameter by 2.5 in.(64mm) thick were prepared by compacting the mix according to the Marshall procedure at 75 blows per face (ASTM D1559-72). After at least 48 hours at room temperature (73°F, 22.8°C), the sample was assumed to be at thermal equilibrium with the room environment. It was then tested using the Mark III Resilient Modulus device,as described earlier in this chapter.

Linear elastic analysis, under the assumption of plane stress, yields the following expression for Young's modulus (94):

$$E = \frac{(\nu + 0.2734)}{t\Delta}_{p}$$

where ν = Poisson's ratio of the sample (assumed to be 0.35)
P = amplitude of the applied vertical load
t = specimen thickness
Δ = amplitude of the change in horizontal diameter due to P.

For short-duration loading on viscoelastic materials, such as asphaltic pavement, the Young's modulus is often called the resilient modulus, and denoted by M_R. In order to remain consistent with the previous discussion the resilient modulus will be denoted by the symbol E. Even though elasticity theory was used to derive Eq (16), it can be applied to viscoelastic materials as long as it is recognized that the value of E will be different for other rates of loading. Similarly, with this understanding the micromechanics equations given in the previous section can be used to predict resilient modulus and Poisson's ratio (136).

Discussion of Experimental and Theoretical Results

Experimental values of Young's modulus, as found from Eq. (16), are recorded in Table 24 for eight different composite materials. Each value shown is an average of the moduli obtained from three specimens made from the same mix.

The theoretical results for Young's modulus and Poisson's ratio were calculated in the following manner. The effective bulk and shear moduli of a composite consisting of limestone particles and asphalt matrix were first derived from Eq (12) and (13). Then, these effective properties were assigned to particles (asphalt coated limestone) in a sulphur matrix, and Eq (12) and (13) were again employed. Finally, voids were introduced in this composite by treating voids as the particles with moduli $K_p = G_p = 0$ in Eq (12) and (13) and using as matrix moduli the effective values found for the three-phase composite (limestone + asphalt + sulphur). For each stage of this analysis, the Young's modulus and Poisson's ratio were derived from Eq (6) and (7) after finding the bulk and shear moduli.

The sulphur and limestone moduli given in Eq (10) and (11) were used in these calculations. The bulk modulus for the asphalt was assumed to be 0.5×10^6 PSI, which is a typical value for soft polymeric materials (137). The shear modulus of the asphalt depends strongly on the rate of loading and temperature. Also, it can be expected to depend on whether or not there is any significant amount of mechanical mixing and chemical interactions with the sulphur. Therefore, rather than guessing some value for asphalt shear modulus, an "in-situ" or "effective" value was calculated from the micromechanics equations. Specifically, by trial and error, the shear modulus was found such that the theoretical Young's modulus would agree with the experimental value for experiment No. 132. This approach yielded a shear modulus of $G = 0.02 \times 10^6$ PSI for the asphalt. This particular mix was used because

TABLE 24

EXPERIMENTAL AND THEORETICAL RESULTS

Result Number	Experiment Number and Volume Fractions	Experimental Results for Pavement	Theory		
			Asphalt + Limestone	Asphalt + Limestone + Sulphur	Asphalt + Limestone + Sulphur + Voids
1	No. 132 Limestone - 0.672 Asphalt - 0.125 Sulphur - 0.127 Voids - 0.076	$E=0.91 \times 10^6$ PSI	$E=0.78 \times 10^6$ $\nu = 0.45$	$E=1.06 \times 10^6$ $\nu = 0.43$	$E=0.91 \times 10^6$ $\nu = 0.41$
2	No. 210 Limestone - 0.793 Asphalt - 0.124 Sulphur - 0.051 Voids - 0.032	$E=1.36 \times 10^6$	$E=0.91 \times 10^6$ $\nu = 0.45$	$E=1.43 \times 10^6$ $\nu = 0.41$	$E=1.34 \times 10^6$ $\nu = 0.40$
3	No. 403 Limestone - 0.654 Asphalt - 0.042 Sulphur - 0.129 Voids - 0.175	$E=1.45 \times 10^6$	$E=1.96 \times 10^6$ $\nu = 0.43$	$E=2.18 \times 10^6$ $\nu = 0.42$	$E=1.54 \times 10^6$ $\nu = 0.37$
4	No. 104 Limestone - 0.719 Asphalt - 0.043 Sulphur - 0.130 Voids - 0.108	$E=2.59 \times 10^6$	$E=2.08 \times 10^6$ $\nu = 0.43$	$E=2.28 \times 10^6$ $\nu = 0.42$	$E=1.84 \times 10^6$ $\nu = 0.39$
5	No. 111 Limestone - 0.770 Asphalt - 0.047 Sulphur - 0.139 Voids - 0.044	$E=4.42 \times 10^6$	$E=2.04 \times 10^6$ $\nu = 0.43$	$E=2.25 \times 10^6$ $\nu = 0.42$	$E=2.06 \times 10^6$ $\nu = 0.40$
6	No. 311 Limestone - 0.743 Asphalt - 0.070 Sulphur - 0.144 Voids - 0.043	$E=2.45 \times 10^6$	$E=1.41 \times 10^6$ $\nu = 0.44$	$E=1.68 \times 10^6$ $\nu = 0.42$	$E=1.54 \times 10^6$ $\nu = 0.41$
7	No. 110 Limestone - 0.722 Asphalt - 0.137 Sulphur - 0.137 Voids - 0.004	$E=0.809 \times 10^6$	$E=0.76 \times 10^6$ $\nu = 0.45$	$E=1.05 \times 10^6$ $\nu = 0.43$	$E=1.04 \times 10^6$ $\nu = 0.43$
8	No. 310 Limestone - 0.672 Asphalt - 0.144 Sulphur - 0.150 Voids - 0.034	$E=0.523 \times 10^6$	$E=0.69 \times 10^6$ $\nu = 0.45$	$E=1.01 \times 10^6$ $\nu = 0.43$	$E=0.95 \times 10^6$ $\nu = 0.42$

1 KPa = 0.1451 psi

it contains an intermediate amount of asphalt compared to the other mixes employed. All other theoretical predictions shown in Table 24 were made using this value of shear modulus.

The predicted moduli for the complete pavement material (the last column in Table 24 and the experimental values may now be compared. Using the numbers in the first column as a reference, it may be observed that theory and experiment agree well for result numbers 1-3, the theory is low for result numbers 4-6, and the theory is somewhat high for result numbers 7 and 8. At this time it is not clear why these discrepancies exist. Certainly, the assumption of spherical particles will lead to some error. Perhaps, however, a significant source of error is the mixing of asphalt and sulphur, which was not taken into account. Indeed, it should be noted that when the amount of asphalt is small (result numbers 3-6) the prediction is low, and for largest amount of asphalt (result numbers 7 and 8) the prediction is high. Such behavior would occur if the relative amount of asphalt that mixes with the sulphur is greatest for result numbers 3-6 and least for result numbers 7 and 8. However, further studies are needed in order to determine the accuracy of this explanation.

Conclusions

Micromechanics theory has been used to predict the effective moduli of asphalt-limestone-sulphur composites. The agreement between theory and experiment is reasonably good in most cases studied. However, there is a systematic discrepancy which is believed to indicate that the effective shear modulus of the asphalt is dependent on the amount of asphalt present. Indeed for samples with the smallest amount of asphalt, the asphalt shear modulus appears to be greatest, possibly as a result of reinforcement due to mixing with the sulphur. It is believed that further experimental and theoretical studies, employing a greater variation of mixes than used here, would help in understanding the effect of the sulphur. The studies should include two-phase mixes consisting of only sulphur and aggregate, sulphur and asphalt, and asphalt and aggregate.

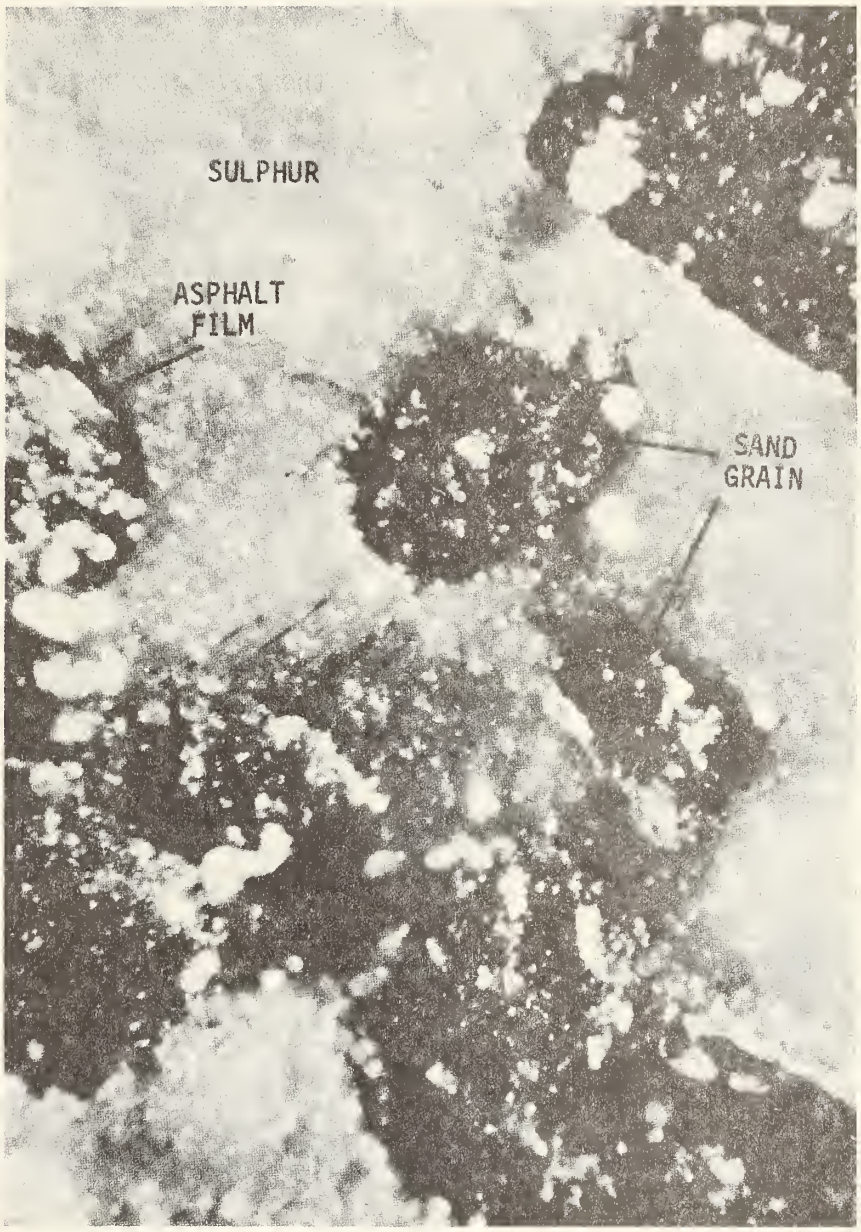

FIG. 37 - Photomicrograph of sand-asphalt-sulphur matrix showing the mechanical interlock of sand particles provided by the sulphur (Mag: 120X).

CHAPTER VI

TASK D: INCORPORATE STATISTICAL RELATIONSHIPS INTO PAVEMENT DESIGN SYSTEMS

The purpose of this task was to make the pavement design system and structural design subsystem computer programs operational, and to incorporate the characterization test results and other input data into the program for subsequent analysis.

Obtain Computer Programs

As discussed under Task A, the Texas FPS-BISTRO program was selected for analysis of the pavement system whereas the VESYS IIM program was selected as the structural design subsystem. Texas Transportation Institute has available the Texas FPS-BISTRO program in the form of a deck of computer cards. A magnetic tape copy of the VESYS IIM program was obtained from the Federal Highway Administration.

Make Computer Programs Operational

The modifications to the FPS-BISTRO program listed under Task A were incorporated into the program and trial runs were made to verify the operation of the program. An example problem was analyzed by use of the VESYS IIM program in order to verify its operation on the Texas A&M University AMDAHL 470 V/6 computer. The output was identical with that furnished by the Federal Highway Administration.

Assemble Input Data for Texas FPS-BISTRO Program

It was necessary to assemble and program certain input data for the pavement design system computer program. Items required for the FPS-BISTRO program include climatic data, material costs, user costs maintenance costs, traffic data, construction data, and material properties. Each of these input items is discussed herein, with the exception of material properties which are discussed in the following subsection of this report.

Tables 25 and 26 contain a listing of the input data used for the Texas FPS-BISTRO analysis for this report. A length of analysis period of 20 years sets a time boundary on the analysis and was selected because this is the period often recommended for design of Interstate funded pavements in the United States (120). The minimum time to the first overlay and the minimum time between overlays was selected as 3 years. Obviously, this specifies the minimum time the initial design must last. Choice of this time should consider availability of initial

TABLE 25

SUMMARY OF TEXAS FPS-BISTRO INPUT DATA

BASIC DESIGN CRITERIA	
Length of the Analysis Period (Years)	20.0
Minimum Time to First Overlay (Years)	3.0
Minimum Time Between Overlays (Years)	3.0
Minimum Serviceability Index P2	2.5
Design Confidence Level	B
Interest Rate or Time Value of Money (Percent)	6.0
PROGRAM CONSTRAINTS	
Max Funds Available Per Sq. Yd. for Initial Design (Dollars)	15.00
Maximum Allowed Thickness of Initial Construction (Inches)	34.0
Accumulated Max Depth of all Overlays (Inches) (Excluding Level-Up)	5.0
TRAFFIC DATA	
ADT at Beginning of Analysis Period (Vehicles/Day)	8000.
ADT at End of Twenty Years (Vehicles/Day)	16000.
One-Direction 20 -Year Accumulated No. of Equivalent 18-KSA	5000000.
Average Approach Speed to the Overlay Zone (MPH)	55.0
Average Speed Through Overlay Zone in Overlay Direction (MPH)	30.0
Average Speed Through Overlay Zone in Non-Overlay Direction (MPH)	55.0
Proportion of ADT Arriving Each Hour of Construction (Percent)	7.0
Percent Trucks in ADT	15.0
ENVIRONMENT AND SUBGRADE	
District Temperature Constant	22.0

1 cm = 0.394 in.
1 KPa = 0.1451 psi
1 mph = 1.6 km/h

TABLE 25 (CONTINUED)

Swelling Probability	0.0
Potential Vertical Rise (Inches)	0.0
Swelling Rate Constant	0.0

CONSTRUCTION AND MAINTENANCE DATA

Serviceability Index of the Initial Structure	4.2
Serviceability Index After an Overlay	4.2
Minimum Overlay Thickness (Inches)	2.0
Overlay Construction Time (Hours/Day)	10.0
Asphaltic Concrete Compacted Density (Tons/C.Y.)	1.95
Asphaltic Concrete Production Rate (Tons/Hour)	200.0
Width of Each Lane (Feet)	12.0
First Year Cost of Routine Maintenance (Dollars/Lane-Mile)	50.00
Annual Incremental Increase in Maintenance Cost (Dollars/Lane-Mile)	20.00

DETOUR DESIGN FOR OVERLAYS

Traffic Model Used During Overlaying	3
Total Number of Lanes of the Facility	4
Number of Open Lanes in Restricted Zone (Overlay Direction)	1
Number of Open Lanes in Restricted Zone (Non-Overlay Direction)	2
Distance Traffic is Slowed in Overlay Direction (Miles)	0.50
Distance Traffic is Slowed in Non-Overlay Direction (Miles)	0.50
Detour Distance Around the Overlay Zone (Miles)	0.0

MATERIALS INFORMATION

Layer		Unit Cost	Thickness Min.	Thickness Max.	Salvage %
1	Asphaltic Concrete	38.00	1.00	10.00	25.00
2	Crushed Limestone	16.00	4.00	10.00	70.00
3	Sand Asphalt Sulphur Base	28.00	4.00	10.00	25.00

TABLE 26

MATERIAL PROPERTIES USED IN TEXAS FPS-BISTRO PROGRAM

Temperature (°F)	120	72	40
Stiffness (psi):			
Asphaltic Concrete Surface	20,000	500,000	2,200,000
Sulphur-Asphalt Surface	350,000	750,000	5,000,000
Sand-Asphalt-Sulphur Base	60,000	400,000	2,000,000
Limestone Base	20,000	40,000	60,000
Clay Subgrade	5,000	10,000	15,000
Poisson's Ratio:			
Asphaltic Concrete Surface	0.47	0.35	0.28
Sulphur-Asphalt Surface	0.42	0.35	0.30
Sand-Asphalt-Sulphur Base	0.40	0.30	0.25
Limestone Base	0.39	0.39	0.39
Clay Subgrade	0.40	0.40	0.40
Fatigue Parameter K_1:			
Asphaltic Concrete Surface	2.80×10^{-4}	3.83×10^{-16}	2.06×10^{-25}
AAS (4.1S/3.9A) Surface	2.74×10^{-2}	1.04×10^{-7}	2.93×10^{-18}
AE (4.1S/3.9A) Surface	1.36×10^{-0}	2.80×10^{-3}	1.72×10^{-8}
AE (1.8S/5.1A) Surface	1.00×10^{-0}	3.44×10^{-1}	2.10×10^{-4}
AES (4.1S/3.9A) Surface	5.66×10^{-1}	1.53×10^{-4}	2.46×10^{-11}
AES (1.8S/5.1A) Surface	3.69×10^{-0}	3.86×10^{-5}	9.53×10^{-9}
Sulphur Recycled Surface	1.86×10^{-5}	3.46×10^{-12}	8.35×10^{-30}
Sand-Asphalt-Sulphur Base	$8.42 \times 10^{-}$	$4.03 \times 10^{-}$	$1.96 \times 10^{-}$
Fatigue Parameter K_2:			
Asphaltic Concrete Surface	2.45	6.41	8.72
AAS (4.1S/3.9A) Surface	2.18	2.67	4.34
AE (4.1S/3.9A) Surface	2.99	3.66	5.93
AE (1.8S/5.1A) Surface	2.10	2.58	4.18
AES (4.1S/3.9A) Surface	1.07	1.31	2.13
AES (1.8S/5.1A) Surface	2.03	2.49	4.04
Sulphur Recyled Surface	1.15	3.00	4.09
Sand-Asphalt Sulphur Base	3.28	4.02	6.52

Base Course Material Properties:
Initial Tangent Modulus - 1/3 x Resilient Modulus
Cohesive Shear Strength - 25 psi
Angle of Internal Friction - 50°
Allowable Permanent Deformation in Base Course - 0.5 in.

$^{o}C = (F - 32) \times 5/9$

1 psi = 6895 Pa

1 cm = 0.394 in.

and future funds, public reaction to overlaying a recently constructed pavement, and expansive soils which could result in relatively short-lived initial designs. A minimum serviceability index of 2.5 was selected because it represents the terminal serviceability index often considered for interstate highways. A design confidence level of 80 percent was chosen for this analysis. This variable controls the reliability with which the specified quality of pavement service will be satisfied. It is a statistical parameter which indicated, for this analysis, that 20 percent of the pavements constructed to comply with a particular design situation would not maintain the desired serviceability index before the scheduled placement of an overlay. This input accounts for the variability of materials, construction methods and traffic. The interest rate of 6 percent for funds is used to discount future expenditures in order to have a valid comparison of design strategies.

A value of $15.00* was established as the maximum funds available per square yard for initial construction. For purposes of this analysis, it was assumed that adequate funds were available for construction. Therefore, the above noted figure was set as a realistic amount to control the number of feasible designs, rather than to act as a constraint. A maximum allowed total thickness of initial construction was set at 34* inches which is the total maximum thickness specified for the individual layers. The accumulated maximum depth of all overlays was set at 5.00* inches excluding level-up courses. The program computes and includes the cost of a level-up courses equal to 0.5* in. thickness of asphaltic concrete pavement in each overlay, although no structural value is attributed to the level-up course.

Traffic was assumed to increase uniformly from an average daily traffic (ADT) of 8,000 vehicles per day to 16,000 vehicles per day at the end of the 20 year analysis period. This information is used in the traffic equation to determine the distribution of equivalent 18 kip single axle loads as a function of time, and is used for the calculation of traffic delay costs during overlay construction. The one directional 20 year accumulated number of equivalent 18 kip single axle loads was assumed to be 5 million. The proportion of trucks in the ADT was set at 15 percent. Highways carrying more trucks in the ADT have higher user costs during overlay construction because the cost of slowing down and stopping of trucks is greater than that of passenger cars. The average approach speed to the overlay zone was 55* mph which is used in the computation of the cost of delaying traffic during overlay operations. During the construction of overlays, vehicles may be required to travel through the restricted zone at reduced speeds in both the overlay and non-overlay direction. The average speed through the overlay zone in the overlay direction was established as 30* mph while the non-overlay direction speed was 55* mph since the highway was considered to be four lanes. The proportion of ADT arriving each hour of construction was set at 7 percent which is used in calculating user costs during overlay construction.

*15.00 per square yard = $18 per square metre
1 inch = 25.4 millimetres
1 mph = 1.6 kilometres per hour

A temperature constant of 22 was used for this analysis. This constant is based upon mean monthly temperatures above 32°F (0°C), and represents the increased susceptibility of asphaltic concrete to cracking under traffic in cold weather (120). These temperature constants range between 9 and 38 for Texas. A constant of 22 is considered representative of the Fort Worth, Texas area. The swelling probability, potential vertical rise, and swelling rate constant are parameters used in calculating the reduction of serviceability index with time due to expansive soils. For this analysis, values of zero were assigned to the noted parameters since the subgrade soils were considered to be nonexpansive.

As discussed subsequently in this report, serviceability index is a measure of the momentary ability of a pavement to serve traffic. A value of 4.2 was used as the serviceability index of the initial structure and the structure immediately after an overlay. In Texas, initial serviceability indices have a statewide average of about 4.2 (120). The minimum overlay thickness is usually based upon aggregate gradation of the mixture, and was established as 2.0 in. (51 mm) for this project as noted previously, the program automatically adds a one-half inch level-up to the overlay thickness when determining overlay costs. The overlay construction time of 10 hours per day was used in this analysis for calculating traffic delay costs. The compacted density of 1.95*tons per cubic yard and production rate of 200 tons per hour for the asphalt concrete were also used within the program to calculate traffic delay costs. The width of each lane was set at 12*feet for this analysis. A value of $50.00*per lane mile was used as the first year cost of routine maintenance. In Texas, the statewide value varies between $25.00 and $50.00 (120). The annual incremental increase in maintenance cost was established as $20.00 for this analysis.

Some method of handling traffic must be used during the construction of overlays. The method used depends on highway geometrics and affects user costs. For the analysis discussed in this report, traffic model number 3 was used. This model number indicates that one lane at a time would be closed for overlay construction of a four lane roadway. The traffic in the closed lane would be detoured onto the adjacent lane traveling in the same direction. As noted previously, the total number of main lanes was set at 4 for this analysis. The number of open lanes in the overlay and non-overlay directions were set at 1 and 2, respectively, in order to comply with the requirements of the traffic model number. The distances the traffic was slowed in the overlay and non-overlay directions were set at 0.5*and 0.0*miles, respectively, and the detour distance around the overlay zone was set at 0.0 miles. This information is used in calculating user costs.

The Texas FPS-BISTRO program required cost data for the material used in construction to be input in terms of cost per compacted cubic yard of material. In this analysis, the costs of the asphaltic concrete

* 1.95 tons per cubic yard = 2.31 tonnes per cubic metre
1 foot = 0.30 metre
$50 per lane mile = $31 per lane km
1 mile = 1.6 km

and sulphur-asphaltic concrete were set at $38.00* per cubic yard, crushed limestone base was set at $16.00* per cubic yard and sand-asphalt-sulphur base course was set at $28.00* per cubic yard. These costs assume that the aggregate for the asphaltic concrete, sulphur-asphaltic concrete and base is high quality limestone material, whereas the aggregate for the sand-asphalt-sulphur mixture is local field (blow) sand. Obviously, these costs would be greatly influenced by the distance the aggregate would have to be transported to the project site. The costs assigned to the mixtures containing sulphur do not include any modifications to the batch plant, paving vehicles, and paving equipment. These material cost data are based upon the recently completed Kenedy County Test Section and current highway construction bid prices in Texas (16, 122). Salvage values of 25 percent were used for the asphaltic concrete, sulphur-asphaltic concrete and sand-asphalt sulphur base material. A salvage value of 70 percent was applied to the crushed limestone base course. These are the estimated values of the materials (in terms of percentages of original construction value) at the end of the 20 year analysis period. The salvage values used in this study are within the ranges recommended for Texas highways (120).

The program also required that minimum and maximum depths be specified for the various layers. These inputs determine the range of thicknesses to be considered for each material, and act as a control in preventing thicknesses which are impractical to construct. The minimum and maximum depths of the surfacing materials were set at 1.0 and 10.0 in. (25.4 and 254 mm), respectively, whereas the minimum and maximum depths of the base materials were set at 4.0 and 10.0 inches (102 and 254 mm), respectively.

Program Statistical Relations for Texas FPS-BISTRO Program

This portion of the project required programming of the statistical relations developed in the screening tests and characterization tests into the Texas FPS-BISTRO program. Specific relationships required for this program included elastic moduli (stiffnesses) and Poisson's ratios of all layers as functions of temperature and material variables, fatigue parameters of asphalt type surfaces and bases as a function of temperature and material variables, and strength parameters of the base course and subgrade.

The laboratory test data contained in Tables 17 and 18 and the Appendices were used in developing the relationships required for this program. Data published in the literature and engineering judgment were also used as bases of comparison when selecting values to be used as input. The material properties used as input for the Texas FPS-BISTRO program are presented in Table 26. The input in Table 26 is in accordance with the design situations analyzed for this project and discussed in the next chapter.

Pavement design methods based upon layered-elastic theory require stiffness (elastic modulus) values for the materials. There are many

*$50, $21, and $37 per cubic metre

different test methods used for determination of stiffness. These include Schmidt tests, uniaxial or triaxial compression tests, and beam flexure tests. Often, there is little correlation between results obtained by the different methods. The stiffness is also a function of stress and strain rate. In addition, many of the layered-elastic design methods are not explicit in the type of elastic modulus required as input. Since the use of layered-elastic design methods is becoming increasingly popular, a test method which is relatively easy and inexpensive (such as the Schmidt test) should be standardized for determination of stiffness and incorporated in the design methods in a model which would provide accurate predicted performance. The selection of the stiffness values for the analysis used in this program was based upon evaluation of the resilient moduli as determined by the Schmidt test, dynamic moduli as determined by the repetitive load uniaxial compression tests, and modulus of elasticity values found in the literature (35, 98, 101). A study by Edris and Lytton indicates that the resilient modulus of clay varies with temperature (123). The values of Poisson's ratio listed on Table 26 were estimated from published values since determination of Poisson's ratios was not part of this project (98, 101).

The selection of values for the fatigue parameters K_1 and K_2 posed a somewhat greater problem for two primary reasons. The amount of flexural fatigue data available from this project was rather limited, and Rauhut's study indicated that laboratory measured fatigue parameters did not represent realistic fatigue behavior in the field (52). The values for K_1 and K_2 used in the analyses are listed in Table 26. These values were selected by transforming actual laboratory data to expected field performance data.

The basis for this transformation bears some further explanation. Fatigue life predicted from lab test data is usually considerably less than that experienced in the field. This is because lab tests do not take into account a number of important factors such as healing of the pavement between stress applications, rest time between stresses, variability in the position of the load within the wheel path resulting in a reduction of stress due to the passage of a certain number of vehicles, etc. (14). Although laboratory flexural fatigue tests provide information about the relative fatigue lives of different materials, there is little data available which relates laboratory fatigue life to field fatigue life (15).

Several methods of transforming laboratory fatigue data into field fatigue data have been proposed. Results of the wheel tracking tests made by the Shell Laboratorium show that fatigue cracking in bituminous pavements occurs in several sequential stages as shown in Figure 38 (15). These stages are the progressive development of fatigue cracks which eventually cause the pavement failure. It is believed that the fatigue lives measured in the laboratory more adequately describe the number of cycles for initial crack formation (N_1 in Figure 38). From a pavement design point of view, the more important fatigue life occurs

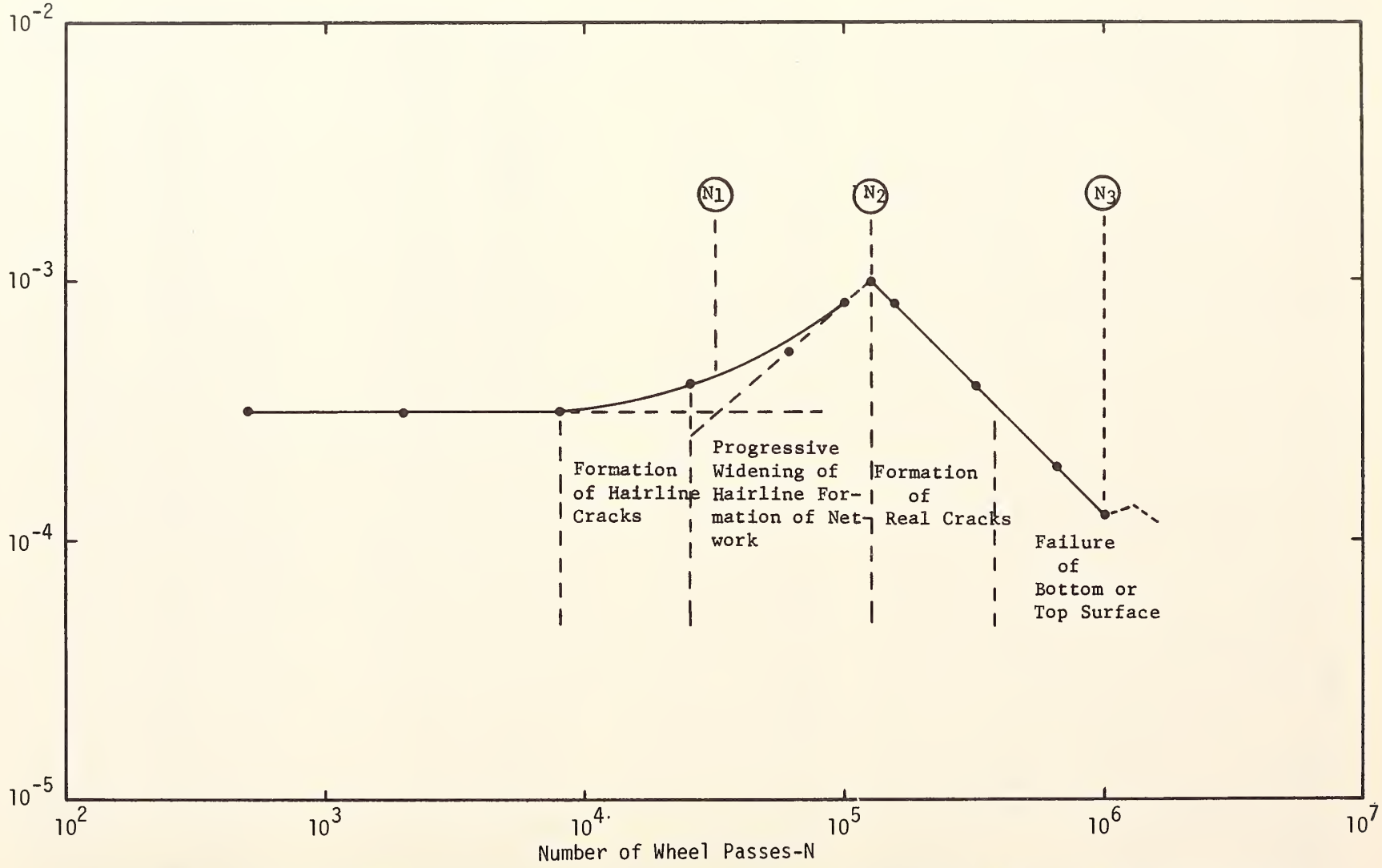

Fig. 38. - Crack Development as a Function of Strain Readings at Equivalent Number of Wheel Passes (15).

1 cm = 0.394 in.

when major cracks form and initiate a loss in pavement serviceability (N_2 in Figure 38). This is the fatigue life which should be used in design as the field fatigue life.

It has been suggested that the field fatigue curves can be approximated from the laboratory curves by using a horizontal shift as shown in Figure 39. The ratio of load applications in the field to those in the lab is termed the shift factor. Van Dijk suggested a shift factor of 3 (15). That is:

$$N_{field} = 3 \times N_{lab}$$

Finn has suggested a shift factor of 13.03 (132). Santucci suggested a shift of the form (118):

$$N_{field} = N_{lab} \times 10^{M}$$

where N_{field} = corrected number of repetitions to failure

N_{lab} = number of repetitions to failure at a given strain level, ε_t, and modulus, E_1.

$$M = 4.84\left(\frac{V_B}{V_V+V_B} - 0.69\right)$$

V_B = asphalt volume

V_V = air voids volume

For the range of V_B and V_V studied in this testing program, this would give shift factors which range from about .02 to 31.7.

This is the type of shift factor that was used on this project for the mixes containing sulphur. The shifting rule developed is:

$$N_{field} = g \times N_{lab}$$

where

$$g = 0.516 \times 10^{0.0147T}$$

T = temperature (°F)

The shift factor was assumed to get larger as temperature increased in order to account for the greater possibility of healing at higher temperatures. This type of a shift implies that:

$$K_{1\ field} = g \times K_{1\ lab}$$

$$K_{2\ field} = K_{2\ lab}$$

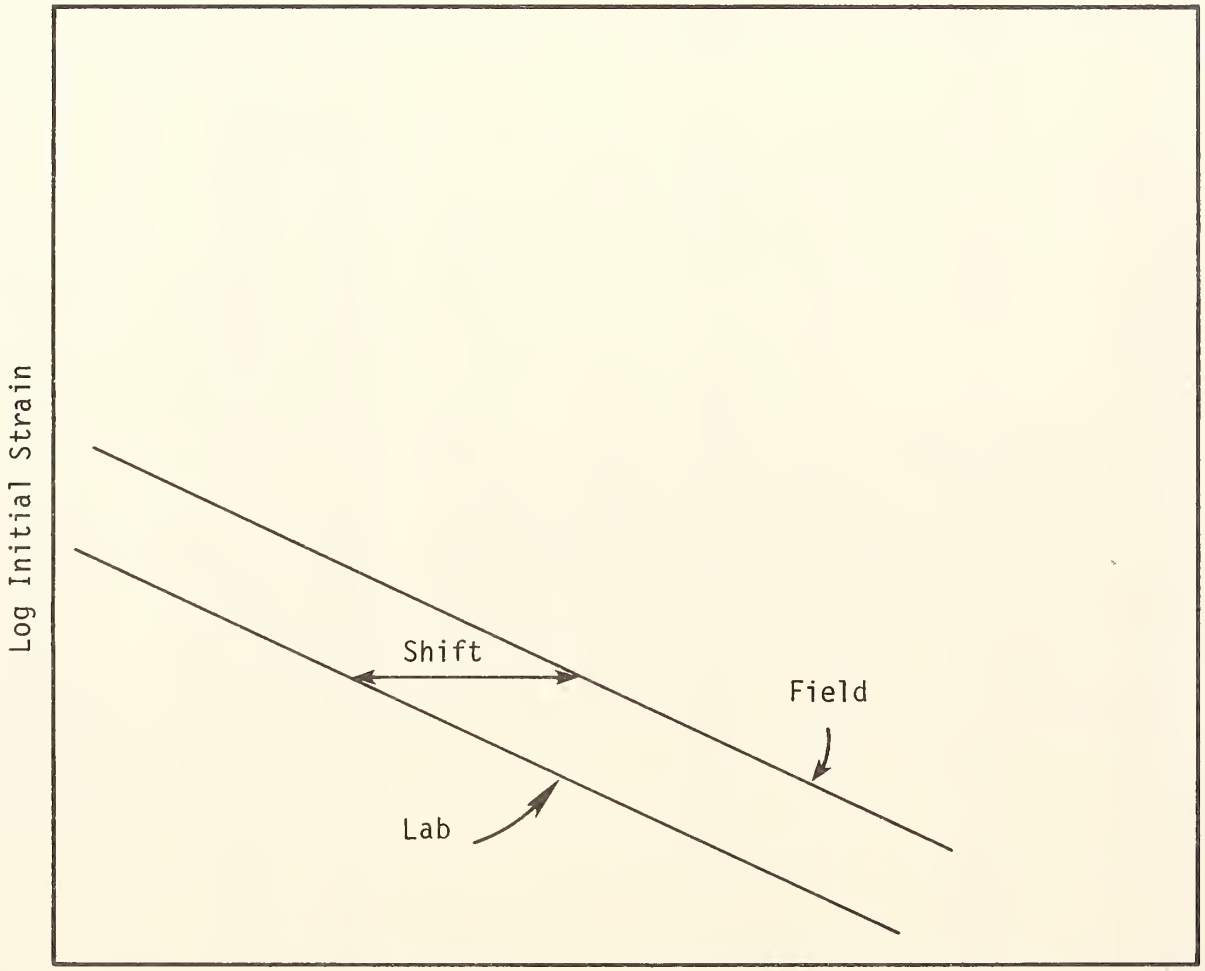

Fig. 39 - Shifting Fatigue Data from Laboratory to Field Conditions.
(As Done with Sulphur Asphalt Concrete)

Another type of shift was used on this project for asphalt concrete. This type of shift, shown in Figure 40, assumed that a given mix in the field will have less compaction than can be achieved in the lab. Published data (52, 118, 119) also suggest an intersection point between laboratory and field curves at about 10^7 to 10^8 repetitions. These two assumptions form the basis for the shifting rule adopted for asphalt concrete:

$$K_1 \text{ field} = 10^n \left(\frac{K_1 \text{ lab}}{10^n}\right)^f$$

$$K_2 \text{ field} = f \times K_2 \text{ lab}$$

where

$f = 0.745 + 0.001\ (T-35)$

$n = 7$

T = temperature (°F)

This rule produces shifting factors as shown in Table 27 for a variety of temperatures. Also shown in the table are values of the sulphur asphalt shift factors used in the analyses. As can be seen from these figures, the higher temperatures are assumed to favor the sulphur asphalt. In all other respects, the shift factors used are fairly comparable between asphalt concrete and sulphur asphalt and they are all within the range of values reported in the literature.

The determination of more precise values of shift factors for sulphur asphalt must await the completion of field tests such as have been placed in Texas in Brazos, Kenedy, and Angelina Counties (16, 131, 138) or extensive wheel tracking tests such as have been conducted at the Shell Laboratorium (15).

Since laboratory flexural fatigue tests were performed at different temperatures for only two of the materials studied in this project (AC (0.0S/4.5A), AAS (4.1S/3.9A)), it was necessary to find relationships between temperature and K_1 and K_2 for the other materials used in the analyses. The sulphur recycled material was assumed to have a temperature dependence like that of asphaltic concrete:

$$\log |\log K_1| = -0.375 \log T + A_1 - 5.4577 \left(\log \frac{T}{35}\right)^{3.3707}$$

$$\log K_2 = -0.25 \log T + B_1 - 3.616 \left(\log \frac{T}{35}\right)^{3.396}$$

where

T = temperature (°F)

A_1 = 1.9936 for AC (0.0S/4.5A) and
1.5243 for sulphur recycled

B_1 = 1.3411 for AC (0.0S/4.5A) and
1.012 for sulphur recycled

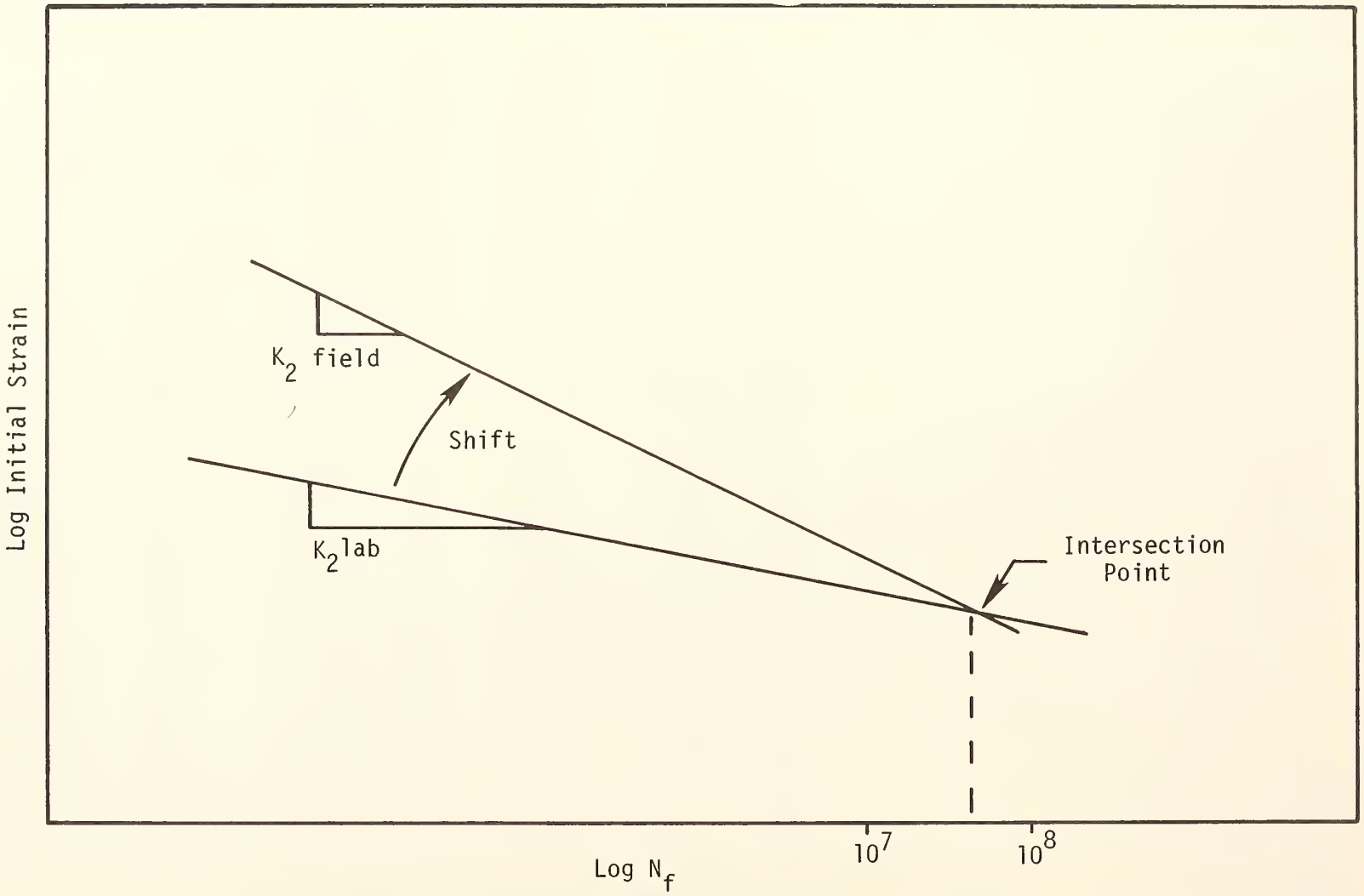

Fig. 40 - Shifting Fatigue Data from Laboratory to Field Conditions
(As Done with Asphalt Concrete)

TABLE 27

SHIFT FACTORS FOR ASPHALT CONCRETE

N_{lab}	Shift Factors		
	T = 35°F (1.7°C)	T = 68° (20°C)	T = 110°F (43.3°C)
10^2	18.8	12.9	7.9
10^3	10.5	7.7	5.3
10^4	5.8	4.6	3.5
10^5	3.2	2.8	2.3
10^6	1.8	1.7	1.5
10^7	1.0	1.0	1.0
10^8	0.56	0.60	0.66
Sulphur Asphalt	3.3	10.0	41.4

The constants were determined by passing the temperature - dependent curve through the only known values of K_1 and K_2. The other sulphur mixes were assumed to have temperature dependency like that of the AAS (4.1S/3.9A):

$$\log|\log K_1| = A_2 - 1.536 \log T$$

$$\log K_2 = B_2 - 3.893 \log T + 0.8875 (\log T)^2$$

where

T = temperature (°F)

A_2 = constant shown in Table 28

B_2 = constant shown in Table 28

Although the numerical values may not be precise, they are reasonable and these relationships permit a comparison of designs and predicted performance of pavements built with the different materials studied in this project. The flexural fatigue relationships at various temperatures need further study.

The base course material properties listed at the bottom of Table 26 are typical of those expected for a good quality crushed limestone base material. An allowable permanent deformation of 0.5 in. was set for the base course as the rutting failure criterion.

The optimum pavement designs selected by FPS-BISTRO are shown in Table 34 in a later section.

Assemble Input Data For VESYS IIM Program

Use of the VESYS IIM structural design program requires input of data in the form of pavement and loading geometry, environment, traffic characteristics, material properties, and pavement system performance bounds. A listing of the input data used for the VESYS IIM analysis is contained in Tables 29, 30, 31 and 32.

The length of analysis period of 20 years was identical to that set for the analysis using the Texas FPS-BISTRO program. Traffic was assumed to increase 3,000 heavy vehicle axles per day to 8,000 heavy vehicle axles per day within the analysis period. The tire pressure was about 74 psi (0.5MPa) over a circular area with a radius of 6.4 in. (163mm) for a duration of 0.1 second. These traffic conditions are considered to simulate a heavily traveled roadway. The program also requires input of statistical information such as the mean and variance of the tire pressure and duration of the repeated loadings. These data were obtained from the VESYS IIM Users Manual (51).

The major environmental influences on pavement response are temperature and moisture (51). The version of VESYS IIM used for this

TABLE 28

TEMPERATURE CONSTANTS FOR SULPHUR MIXES

Material	A_2	B_2
AAS (4.1S/3.9A)	3.503	4.596
AE (4.1S/3.9A)	3.718	4.732
AE (1.8S/5.1A)	3.363	4.580
AES (4.1S/3.9A)	3.053	4.287
AES (1.8S/5.1A)	3.475	4.565

TABLE 29

SUMMARY OF VESYS IIM INPUT DATA

Length of the analysis period in years	20
Initial heavy vehicle axles per day	3,000
Final heavy vehicle axles per day	8,000
Radius of loaded circular area, inches	6.4
Intensity of loading, psi	74
Duration of load, seconds	0.1
Thickness of surface course, inches	2.0 and 3.0
Thickness of base course, inches	8.0 and 10.0
Mean serviceability index at time zero	4.2
Standard deviation of serviceability index at time zero	0.3
Minimum serviceability index	2.5
Tolerance, percent	70%

1 cm = 0.394 in.
1 kPa = 0.1451 psi

TABLE 30

ASSUMED CLIMATIC TEMPERATURE VARIATIONS
FOR VESYS IIM INPUT

Month	Temperature, (^{o}F)*		
	Cool	Moderate	Warm
1	11.5	21.5	41.5
2	13.5	23.5	43.5
3	15.5	25.5	45.5
4	35.5	45.5	65.5
5	50.5	60.5	80.5
6	59.0	69.0	89.0
7	63.0	73.0	93.0
8	65.0	75.0	95.0
9	61.0	71.0	91.0
10	57.5	67.5	87.5
11	34.5	44.5	64.5
12	29.0	39.0	59.0

* ^{o}C = 0.56^{o}F - 17.78

TABLE 31

MATERIAL PROPERTIES USED IN VESYS IIM PROGRAM

Type Material	Asphalt Content (w/o)	Sulfur Content (w/o)	Fatigue Parameters at 70°F		BETA β	Permanent Deformation Parameters	
			K_1	K_2		ALPHA α	GNU μ
Asp. Conc. with Limestone Agg. Surface	6.0	0.0	9.95×10^{-12}	5.14	0.113	0.714	0.127
Sulfur-Asp. Conc. with Limestone Agg. Surface (AAS)	3.9	4.1	1.21×10^{-4}	2.72	0.079	0.805	0.156
Sulfur-Asp. Conc. with Limestone Agg. Surface (AE)	3.9	4.1	1.24×10^{-7}	3.72	0.079	0.806	0.198
Sulfur-Asp. Conc. with Limestone Agg. Surface (AE)	5.1	1.8	2.31×10^{-3}	2.62	0.079	0.760	0.150
Sulfur-Asp. Conc. with Limestone Agg. Surface (AES)	3.9	4.1	1.22×10^{-1}	1.34	0.079	0.790	0.057
Sulfur-Asp Conc. with Limestone Agg. Surface (AES)	5.1	1.8	2.36×10^{-4}	2.53	0.079	0.629	0.131
Sulfur-Asp. Conc. with Beach Sand Base Course	6.0	13.5	1.09×10^{-12}	4.09	0.071	0.674	0.078
Recycled Mix with Sulphur Surface	5.0 (orig.)	1.5	1.93×10^{-5}	3/-0	0.05	0.562	0.023
Crushed Limestone Base			- -	- -	- -	0.730	0.055
Soft Clay Subgrade			- -	- -	- -	0.640	0.036
Medium Clay Subgrade			- -	- -	- -	0.750	0.010
Hard Clay Subgrade			- -	- -	- -	0.850	0.0075

TABLE 32

CREEP PROPERTIES USED IN VESYS IIM PROGRAM

Time (Seconds)	Creep Compliance @ 70°F, psi^{-1}							
	Asp. Conc. w/ Limestone Agg.	Sulphur-Asp. Conc. w/Limestone Aggregate	Sulphur-Asp. Conc. w/ Beach Sand	Recycled Mix w/Sulphur	Crushed Limestone Base	Soft Clay Subgrade	Medium Clay Subgrade	Hard Clay Subgrade
.03	6.53×10^{-7}	5.43×10^{-7}	1.40×10^{-6}	4.00×10^{-7}	1.66×10^{-5}	4.00×10^{-4}	1.00×10^{-4}	6.6×10^{-5}
.10	1.68×10^{-6}	6.62×10^{-7}	2.15×10^{-6}	5.13×10^{-7}	1.66 x 10-5	4.00×10^{-4}	1.00×10^{-4}	6.6×10^{-5}
.30	3.26×10^{-6}	8.15×10^{-7}	2.75×10^{-6}	5.57×10^{-7}	1.66×10^{-5}	4.00×10^{-4}	1.00×10^{-4}	6.6×10^{-5}
1.00	8.77×10^{-6}	1.09×10^{-6}	3.15×10^{-6}	6.65×10^{-7}	1.66×10^{-5}	4.00×10^{-4}	1.00×10^{-4}	6.6×10^{-5}
3.00	1.15×10^{-5}	1.31×10^{-6}	3.70×10^{-6}	7.76×10^{-7}	1.66×10^{-5}	4.00×10^{-4}	1.00×10^{-4}	6.6×10^{-5}
10.00	1.36×10^{-5}	1.61×10^{-6}	4.30×10^{-6}	9.99×10^{-7}	1.66×10^{-5}	4.00×10^{-4}	1.00×10^{-4}	6.6×10^{-5}
30.00	1.36×10^{-5}	1.85×10^{-6}	5.00×10^{-6}	1.29×10^{-6}	1.66×10^{-5}	4.00×10^{-4}	1.00×10^{-4}	6.6×10^{-5}
100.00	1.57×10^{-5}	2.14×10^{-6}	5.80×10^{-6}	1.67×10^{-6}	1.66×10^{-5}	4.00×10^{-4}	1.00×10^{-4}	6.6×10^{-5}
1000.00	1.95×10^{-5}	3.19×10^{-6}	7.30×10^{-6}	3.14×10^{-6}	1.66×10^{-5}	4.00×10^{-4}	1.00×10^{-4}	6.6×10^{-5}

$^{o}C = (^{o}F - 32) \times 5/9$

$1\ KPa^{-1} = 0.1451\ psi^{-1}$

TABLE 32 (CONTINUED)

Time (Sec)	Creep Compliance @ 70°F, psi^{-1}			
	AE (4.1S/3.9A)	AE (1.8S/5.1A)	AES (4.1S/3.9A)	AES (1.8S/5.1A)
.03	$1.12x10^{-6}$	$4.25x10^{-6}$	$1.38x10^{-6}$	$2.64x10^{-6}$
0.1	$1.99x10^{-6}$	$7.18x10^{-6}$	$2.45x10^{-6}$	$4.43x10^{-6}$
0.3	$2.96x10^{-6}$	$8.86x10^{-6}$	$3.57x10^{-6}$	$6.34x10^{-6}$
1.0	$4.08x10^{-6}$	$1.03x10^{-5}$	$4.78x10^{-6}$	$8.42x10^{-6}$
3.0	$4.73x10^{-6}$	$1.31x10^{-5}$	$5.74x10^{-6}$	$1.00x10^{-5}$
10.0	$5.58x10^{-6}$	$1.51x10^{-5}$	$6.23x10^{-6}$	$1.14x10^{-5}$
30.0	$6.58x10^{-6}$	$1.66x10^{-5}$	$6.70x10^{-6}$	$1.29x10^{-5}$
100.0	$7.60x10^{-6}$	$1.84x10^{-5}$	$7.14x10^{-6}$	$1.48x10^{-5}$
500.0	$9.70x10^{-6}$	$2.17x10^{-5}$	$7.86x10^{-6}$	$1.73x10^{-5}$
1000.0	$1.07x10^{-5}$	$2.35x10^{-5}$	$8.45x10^{-6}$	$2.03x10^{-5}$

$^{o}C = (^{o}F - 32) \times 5/9$

1 kPa^{-1} = 0.1451 psi^{-1}

analysis considers moisture through the variation of material properties. The pavements analyzed by this program were assumed to be placed in three different climates whose temperature variations are shown in Table 30.

Pavement system performance bounds included selection of the mean and standard deviation of serviceability index at the beginning of the analysis period. Values for these parameters were selected as 4.5 and 0.3, respectively. Also required was the minimum level of serviceability index which could be tolerated before overlay of the surface. This value was set at 2.5 for these analyses. A value of 70 was used as the tolerance. This is the minimum acceptable reliability of the pavement, expressed as a percent. The reliability is the probability that the actual serviceability index has not reached the specified minimum value at or before some given time during the period of analysis.

Program Statistical Relations for VESYS IIM

This portion of the project required programming of the statistical relations developed in the screening tests and characterization tests into the VESYS IIM program. The program requires that material properties, as a function of mixture variables, be of the type which express stress-strain relationships (primary response) and those which describe a failure characteristic (distress). In this program, response properties are expressed in terms of elastic and viscoelastic behavior whereas distress properties are expressed in terms of parameters which represent permanent deformation or fatigue life.

The laboratory test data contained in Tables 18 and 21 and the Appendices were used in developing the relationships required for this program. The material properties used as input for the VESYS IIM analyses are listed in Tables 31 and 32. As discussed for the Texas FPS-BISTRO program, published data were also used as a basis of comparison when selecting values to be used as input to the VESYS IIM program. The same fatigue characteristics as used in FPS-BISTRO were used in VESYS IIM.

A considerable amount of variation exists in the properties of materials within in-situ pavements. Even though extraordinary quality control of materials and construction procedures was exercised during construction of the American Association of State Highway and Transportation Officials road test sections, it was found that the materials within the completed pavements possessed a significant variability of properties (124). Such variations in a completed pavement result from the variability of materials at the source, during mixing, and during construction. In addition, different compaction techniques, temperatures, moistures, and construction practices contribute to this variability. These variations in material properties have a significant effect on the behavior of the pavement throughout its service life because the probability of pavement distress increases with variability

of material properties (125). The VESYS IIM program considers this variability (uncertainty) of materials and construction procedures by utilization of statistical estimates of the means and variances of the material properties expected to occur in the field.

The values listed in Table 31 for the fatigue parameters K_1 and K_2 are identical to those used in the Texas FPS-BISTRO program. The BETA values were estimated from characterization test data listed in Table 21. Values for the permanent deformation parameters ALPHA and GNU were estimated from characterization test data contained in Table 18. The creep compliance values listed in Table 32 were established from characterization test data for all materials except the crushed limestone base and the clay subgrade. Since characterization of the latter two materials was not part of this project, the respective values for ALPHA, GNU, and creep compliance were estimated from information contained in the VESYS IIM Users Manual (51). Values of BETA are not used for the crushed limestone base course and the clay subgrade since the VESYS IIM program assumes that these two materials are not temperature dependent. Fatigue parameters K_1 and K_2 are not used for the limestone base course and clay subgrade since layers of these materials are not considered to fail by a fatigue cracking mode.

CHAPTER VII

TASK E: SENSITIVITY ANALYSES

This task was used to evaluate various combinations of pavement materials and layer thicknesses in different climates for a selected loading condition. The Texas FPS-BISTRO program was utilized to screen a large number of possible designs and determine the most economical design for a given combination of materials in a given climate. The VESYS IIM program was then used to evaluate the optimum pavement designs with respect to various distress mechanisms.

Screening Analyses by Texas FPS-BISTRO

After the input data listed in Chapter 6 were assembled, 14 combinations of pavement materials were evaluated in each of three temperature conditions. These temperature conditions were 40, 72, and 120°F (4, 22, and 49°C), which were considered to represent cool, moderate, and warm climates, respectively. The 14 material combinations that were evaluated in each climate are shown in Table 33.

Thus, a total of 42 individual cases was evaluated. The Texas FPS-BISTRO computer program was then used to determine the optimum design for the specified design period, materials and other constraints. For each individual case, the computer considers many designs, with the number depending upon the specified minimum and maximum thicknesses for the surface and base layers. The program compares the calculated primary response with the appropriate failure criteria for each layer. The design is rejected as infeasible if any of the criteria are not met.

As noted in Chapter 6, the traffic considered by the Texas FPS-BISTRO program is equivalent to 18 kip single axle loads. The loading configuration and magnitude are presented in Figure 41. Also shown are point locations at which the primary response is calculated by the program. The dual-wheels create a deflection basin typical of that shown in Figure 42. The surface curvature index is a parameter used in the Texas FPS-BISTRO performance equation to calculate serviceability index. The surface curvature index, s, is computed from:

$$s = \frac{W_A - W_B}{20} \times 1000$$

where W_A is the deflection in inches at point A, and

W_B is the deflection in inches at point B

Linear elasticity is used to calculate the deflections.

TABLE 33

MATERIAL COMBINATIONS CONSIDERED IN THE ANALYSES

Surface	Base	Subgrade
AC (0.0S/4.5A)	Limestone	Clay
AC (0.0S/4.5A)	SAS	Clay
AAS (4.1S/3.9A)	Limestone	Clay
AAS (4.1S/3.9A)	SAS	Clay
AE (4.1S/3.9A)	Limestone	Clay
AE (4.1S/3.9A)	SAS	Clay
AE (1.8S/5.1A)	Limestone	Clay
AE (1.85/5.1A)	SAS	Clay
AES (4.1S/3.9A)	Limestone	Clay
AES (4.1S/3.9A)	SAS	Clay
AES (1.8S/5.1A)	Limestone	Clay
AES (1.8S/5.1A)	SAS	Clay
Recycled	Limestone	Clay
Recycled	SAS	Clay

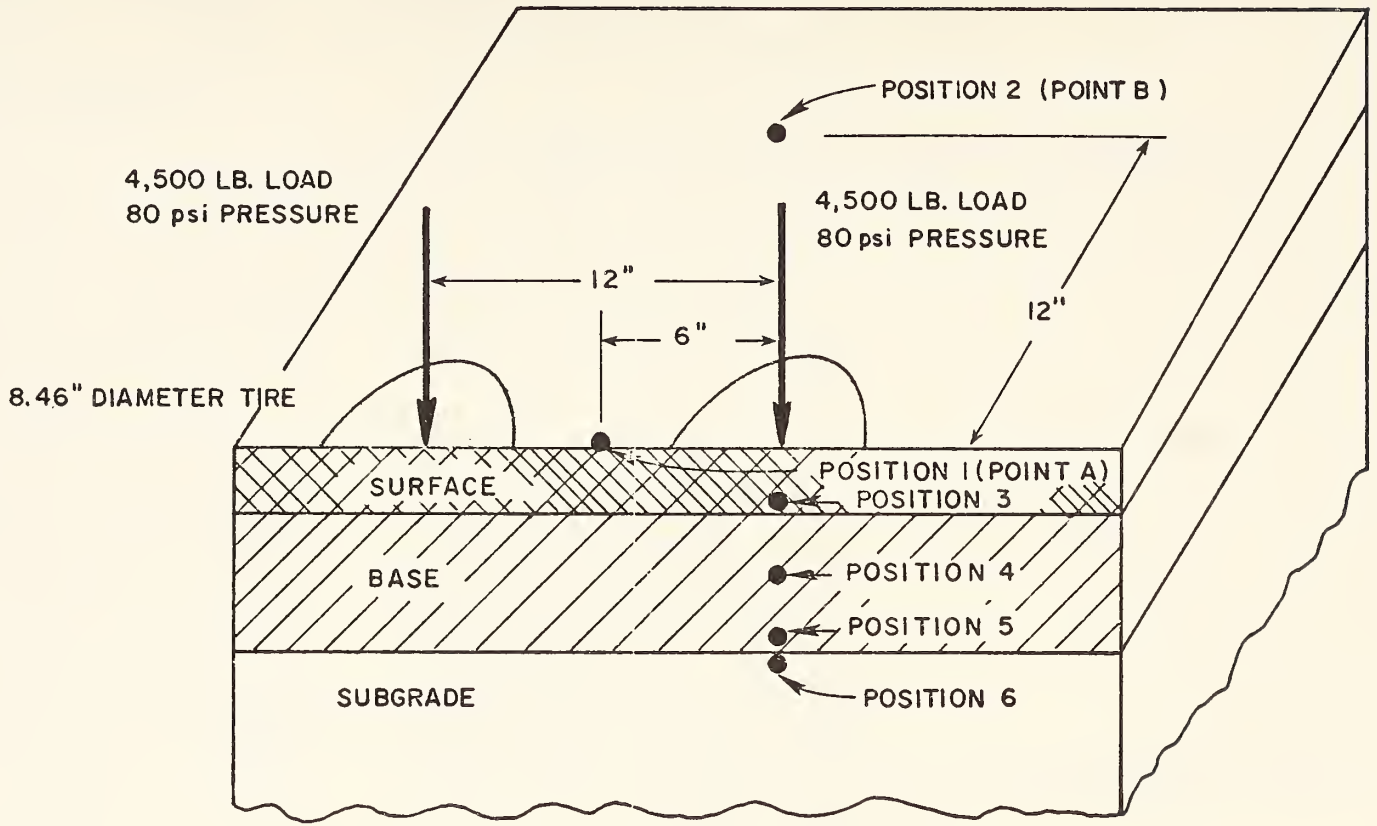

FIG. 41--Dual-wheel load configuration and primary response positions for Texas FPS-BISTRO program.

1 k_g = 0.45 lb.

1 kPa = 0.1451 psi

1 cm = 0.394 in.

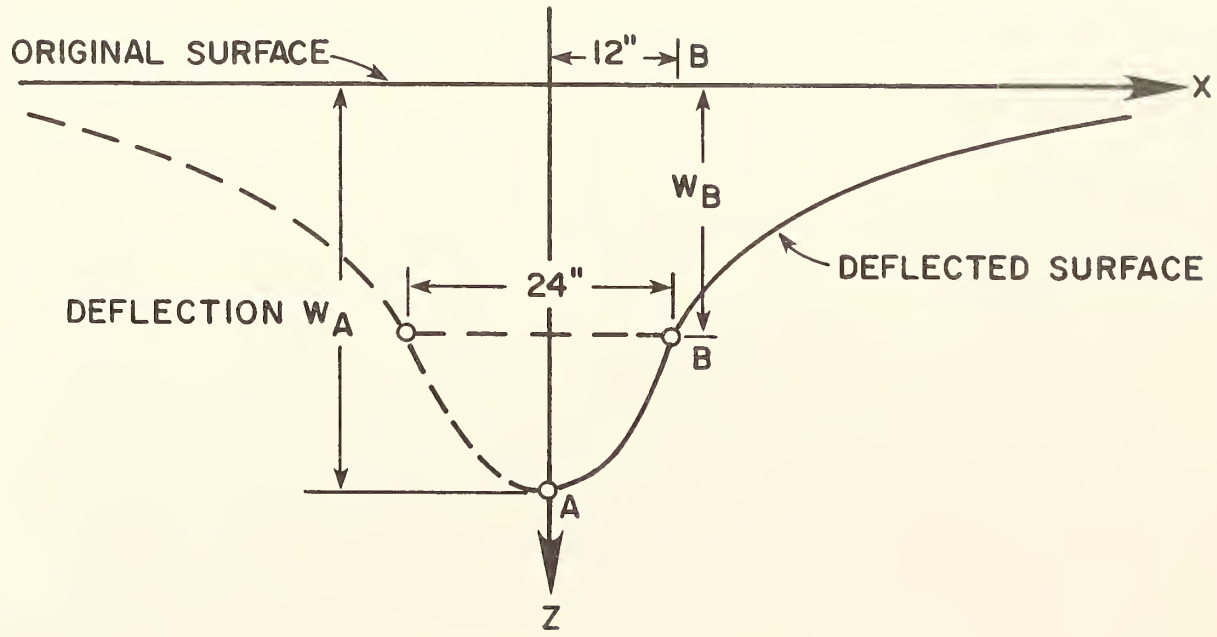

FIG. 42 --Typical deflection basin of the dual-wheel load as it would appear on a vertical plane through the points A and B (59).

1 cm = 0.394 in.

The performance equation was developed from AASHO Road Test Data by Scrivner (127). The equation is

$$P = P_1 - \left[\sqrt{5 - P_1} + 53.6 \frac{N S^2}{\alpha}\right]^2$$

where N is the number of equivalent 18-kip axle loads at time, t,

S is the surface curvature index,

α is the temperature constant,

P_1 is the initial serviceability index, and

P is the serviceability index at time, t.

A typical output for one of the cases evaluated by the Texas FPS-BISTRO program is presented in Table 34. The designs determined to be feasible for the specified conditions are listed by the computer as the best design strategies in order of increasing total cost. This output permits the engineer an immediate overall view of the most cost effective design strategies. In the material arrangement listing in the table, the "A" and "B" refer to the surface and base courses, respectively. The listing of costs includes values for initial construction, overlay construction, user, routine maintenance, and salvage. All costs, with the exception of initial construction costs, are discounted to their present worth. All these cost components are combined to form the total cost for each design. A value of two for number of layers indicates that two types of materials (surfacing and base course) were considered to overlie the subgrade. In the layer depth listing, the values for D(1) and D(2) indicate the initial thicknesses of the surface and base courses, respectively.

A performance period is a time during which the serviceability index is maintained above its minimum acceptable value. Every time a pavement must be overlaid, a new performance period begins. Thus, the number of performance periods is the number of initial construction and major rehabilitation efforts that must be applied to a given pavement for it to last through the specified analysis period of twenty years.

The values of T(1) and T(2) listed in the performance time indicate the cumulative length of time, starting at the initial construction, before the initial construction and subsequent overlay, respectively, reach the specified minimum serviceability index. The overlay policy is a listing of the thicknesses of overlay layers placed after the initial construction. The swelling clay loss is the loss of serviceability caused by expansive clay during the appropriate performance period.

TABLE 34

TYPICAL OUTPUT FOR TEXAS FPS-BISTRO PAVEMENT SYSTEM DESIGN

Summary of the Best Design Strategies
in Order of Increasing Total Cost

	1	2	3	4	5	6	7	8
Material Arrangement	AB	AB	AB	AB	AB	AB	AB	AB
Init. Const. Cost	5.74	5.21	6.14	4.94	8.11	8.29	6.99	5.75
Overlay Const. Cost	1.97	2.51	1.97	3.10	0.0	0.0	1.97	3.10
User Cost	0.02	0.03	0.02	0.03	0.0	0.0	0.02	0.03
Routine Maint. Cost	0.24	0.25	0.24	0.27	0.35	0.35	0.24	0.27
Salvage Value	-0.86	-0.86	-0.99	-0.88	-0.88	-0.96	-1.21	-1.13
Total Cost	7.11	7.13	7.39	7.47	7.58	7.68	8.01	8.02
Number of Layers	2	2	2	2	2	2	2	2
Layer Depth (Inches)								
D(1)	3.75	3.25	3.50	3.00	6.00	5.75	3.25	2.50
D(2)	4.00	4.00	5.50	4.00	4.00	5.00	8.00	7.00
No. of Perf. Periods	2	2	2	2	2	2	2	2
Perf. Time (Years)								
T(1)	5.5	3.7	5.3	3.1	21.8	20.2	5.5	3.2
T(2)	21.6	20.5	20.5	22.2			20.3	20.2
Overlay Policy (Inch) (Including Level-Up)								
D(1)	2.5	3.0	2.5	3.5			2.5	3.5
Swelling Clay Loss (Serviceability)								
SC(1)	0.0	0.0	0.0	0.0	0.0	0.0	0.0	0.0
SC(2)	0.0	0.0	0.0	0.0			0.0	0.0

AAS (4.1S/3.9A) Surface with Limestone Base at 72°F

Material Properties: $K_1 = 1.04 \times 10^{-3}$ $K_2 = 2.67$

$E_1 = 750{,}000$ psi $E_2 = 40{,}000$ psi $E_3 = 10{,}000$ psi

$\nu_1 = 0.35$ $\nu_2 = 0.39$ $\nu_3 = 0.40$

1 cm = 0.394 in.

$^{o}C = (^{o}F - 32) \times 5/9$

1 KPa = 0.1451 psi

Tables 35, 36, and 37 summarize the best design strategy for each of the 42 individual cases evaluated. For each of the three temperatures, the best design strategy is listed for the 14 combinations of materials discussed previously. The material properties used for the asphaltic concrete surface course were those of a high quality mixture such as would be expected of a well graded crushed limestone asphaltic concrete. Similarily, the properties of the sulphur-asphaltic concrete surface material were those of a mixture of well graded crushed limestone, sulphur, and asphalt cement. The sand-asphalt-sulphur base course was considered to contain beach or field sand as the aggregate. The properties of the limestone base course were those of a high quality crushed limestone.

Examination of the information contained in Tables 35, 36, and 37 indicate that the total cost of the pavement structure increases as the temperature increases.

This does not include the important consideration of pavement costs due to climatic causes such as thermal cracking or thermal fatigue in the cold regions nor does it include the beneficial effect of crack healing in the warm climates. As a result, these costs are probably too low in the cold climates and possibly too high in the warm climates. Within each temperature category, a design with the sulphur-asphaltic concrete surfacing is the most economical. For temperatures of 40 and 72°F (4 and 22°C) a design containing the sand-asphalt-sulphur base course is the most economical whereas use of the crushed limestone base course results in the most cost effective pavement at a temperature of 120°F (49°C). No feasible pavement sections were found for the conventional asphaltic concrete pavements at 120°F (49°C) primarily because of the layer deflections in the pavement. These are due to the deflection of the base course and subgrade, the consequent large fatigue strains in the surface course, and the larger permanent deformations in the base and subgrade. The warm conventional asphaltic concrete exhibits a greater fatigue rate than the warm sulphur-asphalt concrete. There were also no feasible designs for sulphur recycled material at 120°F (49°C) for the same reason. No feasible designs were found for AES(4.1S/3.9A) at all three temperatures and AES(1.8S/5.1A) at 72°F (22°C) primarily due to the fatigue properties of the surface course.

The Texas FPS-BISTRO analyses performed for this project indicate that the use of sulphur in the pavement construction would result in a more economical pavement structure. In particular, a substantial savings would result from the use of sulphur-asphaltic concrete surface in combination with sand-asphalt-sulphur base course.

Performance Prediction by VESYS IIM

After design strategies were developed by the Texas FPS-BISTRO program, the VESYS IIM program was used to assess the structural integrity of the optimum thickness combinations of surface and base material

TABLE 35

SUMMARY OF BEST DESIGN STRATEGIES FOR FOURTEEN CASES

EVALUATED AT 40°F BY TEXAS FPS-BISTRO PROGRAM

Surface Material	Base* Material	Layer Thickness (IN)				Total Cost ($ per sq. yd.)	Performance Period (Years)
		Surface	Base	1st Overlay	2nd Overlay		
AC(OS/4.5A)	LS	4 in	4 in	0	0	$5.63	21.3
AC(OS/4.5A)	SAS	1 in	4 in	0	0	4.19	38.9
AAS(4.1S/3.9A)	LS	3 in	4 in	0	0	4.66	20.9
AAS(4.1S/3.9A)	SAS	1 in	4 in	0	0	4.19	29.5
AE(4.1S/3.9A)	LS	7 in	4½ in	0	0	8.73	99.9
AE(4.1S/3.9A)	SAS	1 in	7 in	0	0	6.34	99.9
AE(1.8S/5.1A)	LS	3 in	4 in	0	0	4.66	20.9
AE(1.8S/5.1A)	SAS	1 in	4 in	0	0	4.19	38.9
AES(4.1S/3.9A)	LS	**					
AES(4.1S/3.9A)	SAS	**					
AES(1.8S/5.1A)	LS	8¼ in	4 in	0	0	9.77	99.9
AES(1.8S/5.1A)	SAS	1½ in	10 in	0	0	8.98	99.9
Recycled	LS	2 in	4 in	2.5	0	5.54	22.4
Recycled	SAS	1 in	4 in	0	0	4.19	29.5

*LS - limestone base
SAS - sand-asphalt-sulphur

**No feasible design

1 cm = 0.394 in.

1 m^2 = 1.196 yd^2

TABLE 36

SUMMARY OF BEST DESIGN STRATEGIES FOR FOURTEEN CASES EVALUATED AT 72°F BY TEXAS FPS-BISTRO PROGRAM

Surface Material	Base* Material	Layer Thickness (IN)				Total Cost ($ per sq. yd.)	Performance Period (Years)
		Surface	Base	1st Overlay	2nd Overlay		
AC(OS/4.5A)	LS	4½ in	4 in	2.5	0	$7.61	20.8
AC(OS/4.5A)	SAS	1 in	4 3/4 in	2.5	0	6.22	21.5
AAS(4.1S/3.9A)	LS	3 3/4 in	4 in	2.5	0	7.11	21.6
AAS(4.1S/3.9A)	SAS	1 in	4¼ in	2.5	0	5.97	20.1
AE(4.1S/3.9A)	LS	3 3/4 in	4 in	2.5	0	7.11	21.6
AE(4.1S/3.9A)	SAS	1 in	4¼ in	2.5	0	5.97	20.1
AE(1.8S/5.1A)	LS	3 3/4 in	4 in	2.5	0	7.11	21.6
AE(1.8S/5.1A)	SAS	1 in	4¼ in	2.5	0	5.97	20.1
AES(4.1S/3.9A)	LS	**					
AES(4.1S/3.9A)	SAS	**					
AES(1.8S/5.1A)	LS	**					
AES(1.8S/5.1A)	SAS	**					
Recycled	LS	2 in	4 in	2.5	0	8.34	20.3
Recycled	SAS	1 in	4 3/4 in	2.5	0	6.22	21.5

*LS - limestone base
SAS - sand-asphalt-sulphur base

**No feasible design

1 cm = 0.394 in.

1 m^2 = 1.196 yd^2

TABLE 37

SUMMARY OF BEST DESIGN STRATEGIES FOR FOURTEEN CASES
EVALUATED AT 120°F BY TEXAS FPS-BISTRO PROGRAM

Surface Material	Base* Material	Layer Thickness (IN)				Total Cost ($ per sq. yd.)	Performance Period (Years)
		Surface	Base	1st Overlay	2nd Overlay		
AC(OS/4.5A)	LS	**					
AC(OS/4.5A)	SAS	**					
AAS(4.1S/3.9A)	LS	6¼ in	4 in	3.0	0	$ 9.50	20.0
AAS(4.1S/3.9A)	SAS	5 3/4 in	4 in	2.5	0	10.20	20.3
AE(4.1S/3.9A)	LS	6¼ in	4 in	3.0	0	9.50	20.0
AE(4.1S/3.9A)	SAS	5 3/4 in	4 in	2.5	0	10.20	20.3
AE(1.8S/5.1A)	LS	6¼ in	4 in	3.0	0	9.50	20.0
AE(1.8S/5.1A)	SAS	5 3/4 in	4 in	2.5	0	10.20	20.3
AES(4.1S/3.9A)	LS	**					
AES(4.1S/3.9A)	SAS	**					
AES(1.8S/5.1A)	LS	6¼ in	4 in	3.0	0	9.50	20.0
AES(1.8S/5.1A)	SAS	5 3/4 in	4 in	2.5	0	10.20	20.3
Recycled	LS	**					
Recycled	SAS	**					

*LS - limestone base
SAS - sand-asphalt-sulphur base

** No feasible design

1 cm = 0.394 in.

1 m^2 = 1.196 yd^2

shown in Tables 35, 36, and 37. Evaluations were made using a soft clay subgrade in the warm climate, a medium clay subgrade in the moderate climate, and a hard clay subgrade in the cool climate. The VESYS IIM program computes pavement distress in terms of rutting, roughness, and crack damage. These distress indicators are then used in the distress - performance relationship given later in this chapter to predict the serviceability history of the selected pavement.

The results of the VESYS IIM evaluation of the optimum pavements are shown in Appendix I. In the analysis of some of the designs, the calculated radial strain at the bottom of the surface layer was found to be compressive. VESYS IIM did not predict performance of these pavements because an internal constraint in the program terminates analysis if the radial strain is not a tensile strain. It was found that minor increases in the surface layer thickness of some of these pavements would result in tensile radial strain and produce a VESYS IIM analysis. The results of these analyses are also shown in Appendix I. A few of the pavements could not be analyzed without significantly altering their design; therefore, no VESYS IIM analysis is shown for a few of the optimum designs. These are indicated in Appendix I by the notation, "Compressive Radial Strain Calculated."

Rut depth is a measure of the permanent deformation in the wheel path created by traffic loads. The values of rut depth determined for various combinations of pavement materials and climates are listed in Appendix I. Figure 43 presents the predicted increase of rut depth with time for the optimum AC, AAS, and sulphur recycled pavement designs in a moderate climate. Both the AAS and the sulphur recycled materials have predicted rut depths about the same as or less than conventional asphaltic concrete. It should also be noted that the pavements with a SAS base experienced greater predicted rut depths than those with limestone bases. Examination of the VESYS IIM output indicates a similar trend in the rut depth data for all other combinations evaluated except the AES optimum designs which had predicted rut depths greater than the conventional asphaltic concrete. Although the optimum sulphur-asphalt pavements are thinner and less expensive than optimum asphaltic concrete pavements the rut depths predicted by VESYS IIM were generally the same or less than those predicted for the asphaltic concrete.

A rut depth of less than 0.5 inches (12.7 mm) in 20 years is considered excellent rutting performance.

Roughness of the pavement surface can be expressed in terms of the variance of the slope measurements of deformation taken along the longitudinal profile of the roadway in accordance with the AASHTO definition (51). In the VESYS IIM program, the variance of rut depth is computed in the rut depth model and passed automatically to the roughness model. The difference in rut depth is assumed to occur because of material variability of each layer. The roughness output is in the form of slope variance. Figure 44 presents the predicted slope variance as a function of time in the moderate climate for the optimum AC, AAS, and sulphur

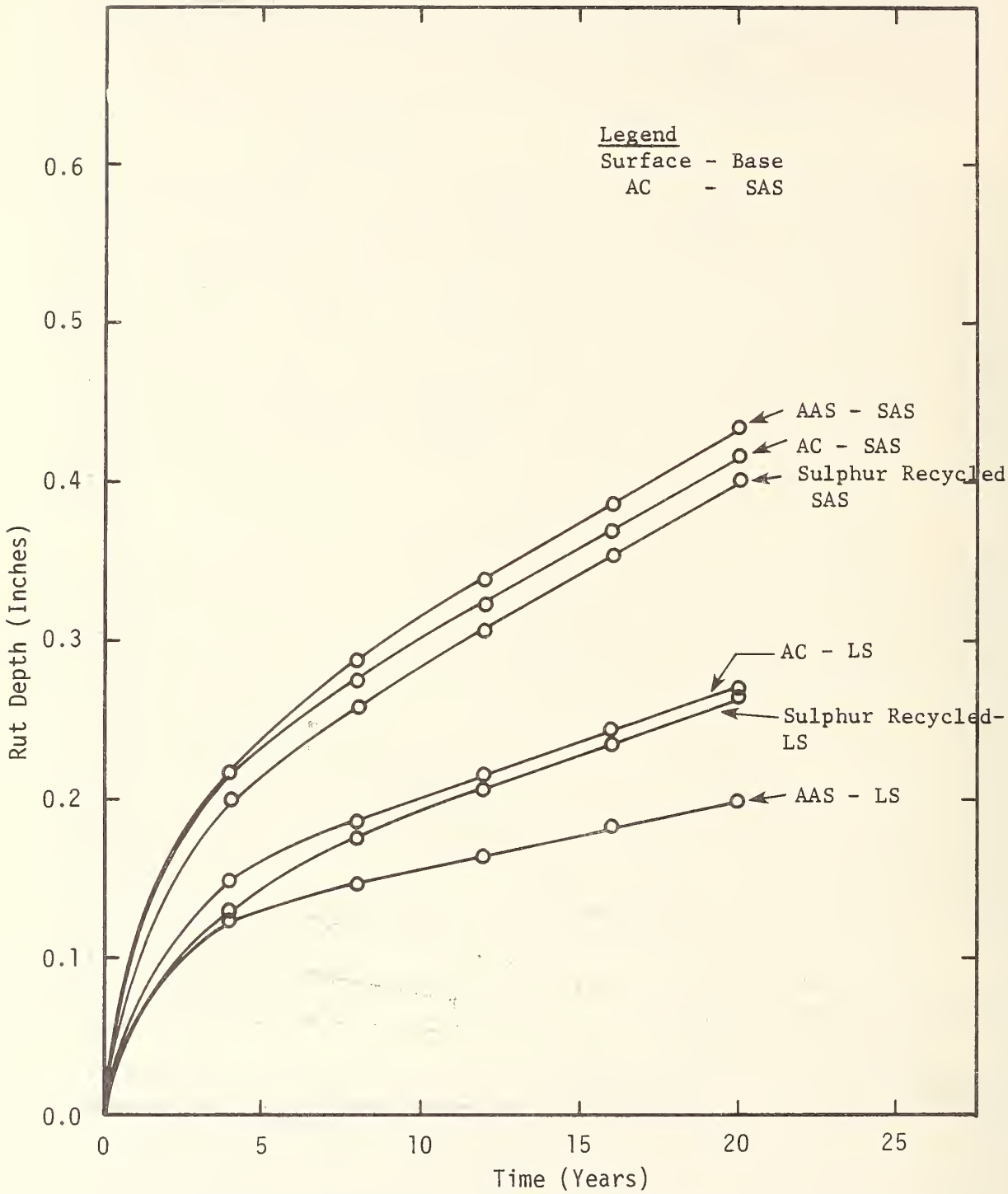

Fig. 43 - Comparison of Rut Depth for AC, AAS, and Sulphur Recycled Optimum Pavement Designs for the Moderate Climate.

1 cm = 0.394 in.

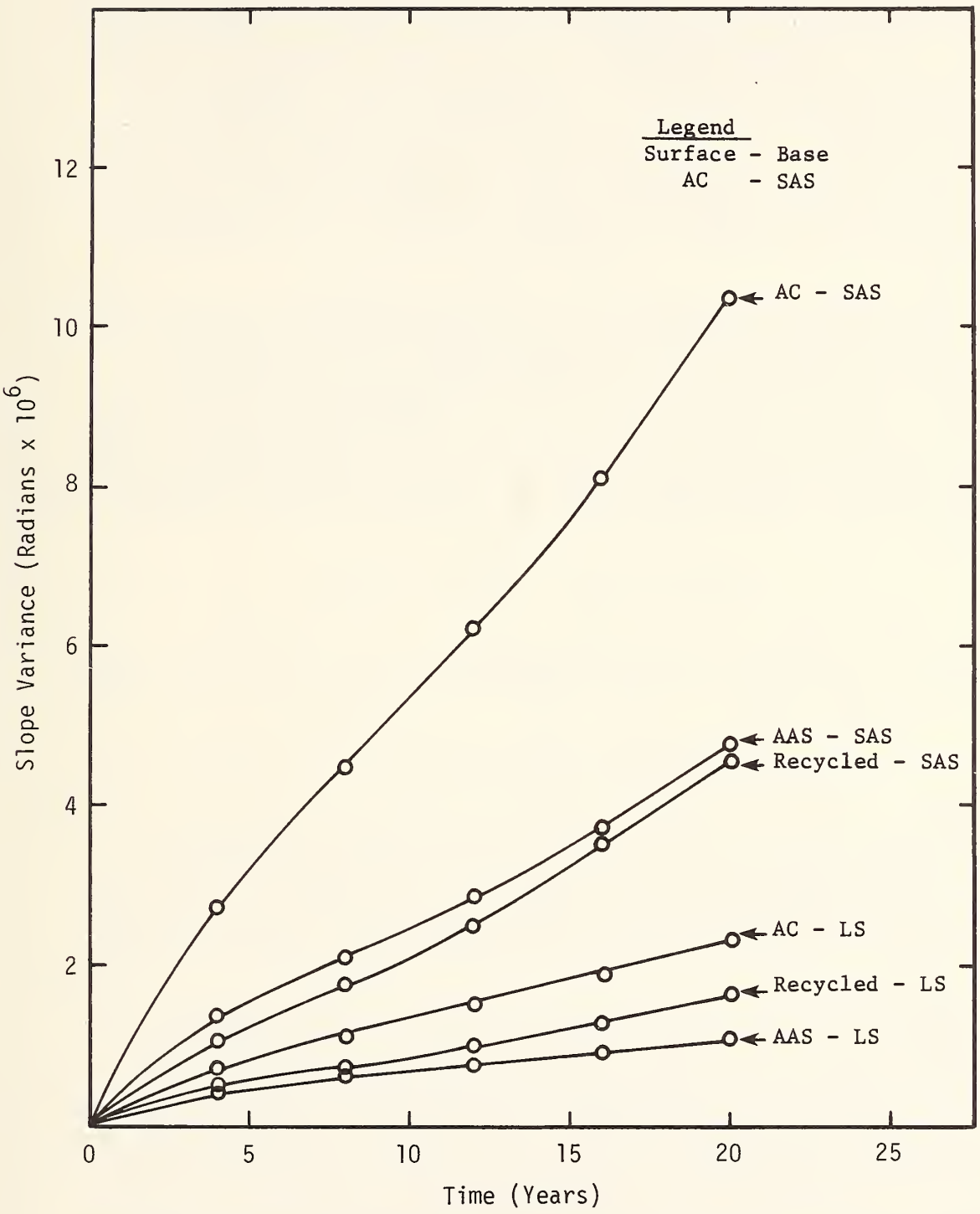

Fig. 44 - Comparison of Slope Variance for AC, AAS, and Sulphur Recycled Optimum Pavement Designs for the Moderate Climate

recycled pavement designs. Both the AAS and the sulphur recycled pavements show predicted slope variances less than that for asphaltic concrete. The pavements with SAS base courses experience greater predicted slope variance than those with a limestone base; indicating that for the optimum pavement thickness, the pavements with a limestone base would be smoother. For all the optimum designs except those with AE and AES surfaces, the pavements constructed with sulphur were indicated to be smoother than conventional asphaltic concrete in each climate. The results of this study indicate that the addition of sulfur to the surface course can result in a smoother as well as a more economical pavement.

The criterion for cracking of the pavement is based on fatigue resulting from the tensile strain at the bottom of the surface layer. This cracking depends upon the fatigue properties of the surfacing layer and the stiffnesses of the underlying materials. The VESYS IIM program calculates a dimensionless cracking index. Although this index cannot be related directly to the area which is cracked, it can be used as an indicator of anticipated damage when comparing different pavement design sections. The cracking index is defined using Miner's damage rule (51):

$$\text{Cracking Index} = \sum \frac{n_i}{N_i}$$

where N_i is the number of passes of wheel load i that will cause fatigue failure, and

n_i is the actual number of passes of wheel load i.

Failure of the pavement is assumed to occur when the sum of these dimensionless ratios is equal to 1.0. In many cases, if laboratory values of K_1 and K_2 are used to determine N_i, the cracking index rises well above 1.0 well before actual experience indicates that a real pavement will be cracked so severely. This is the reason that lab fatigue data must be transformed into field fatigue curves as discussed earlier.

Figure 45 presents a graph of the logarithm of the cracking index as a function of age for the optimum AC, AAS, and sulphur recycled pavement designs at the moderate climate. With the exception of the AE and AES materials and the sulphur recycled material on a limestone base, the optimum sulphur pavements were predicted to experience less cracking than the optimum conventional asphaltic concrete pavements. For the sulphur pavements, the use of an SAS base also tends to reduce cracking. The results indicate that although the optimum sulphur pavements are thinner and less expensive than conventional asphaltic concrete, the cracking performance is probably as good or better than conventional asphaltic concrete.

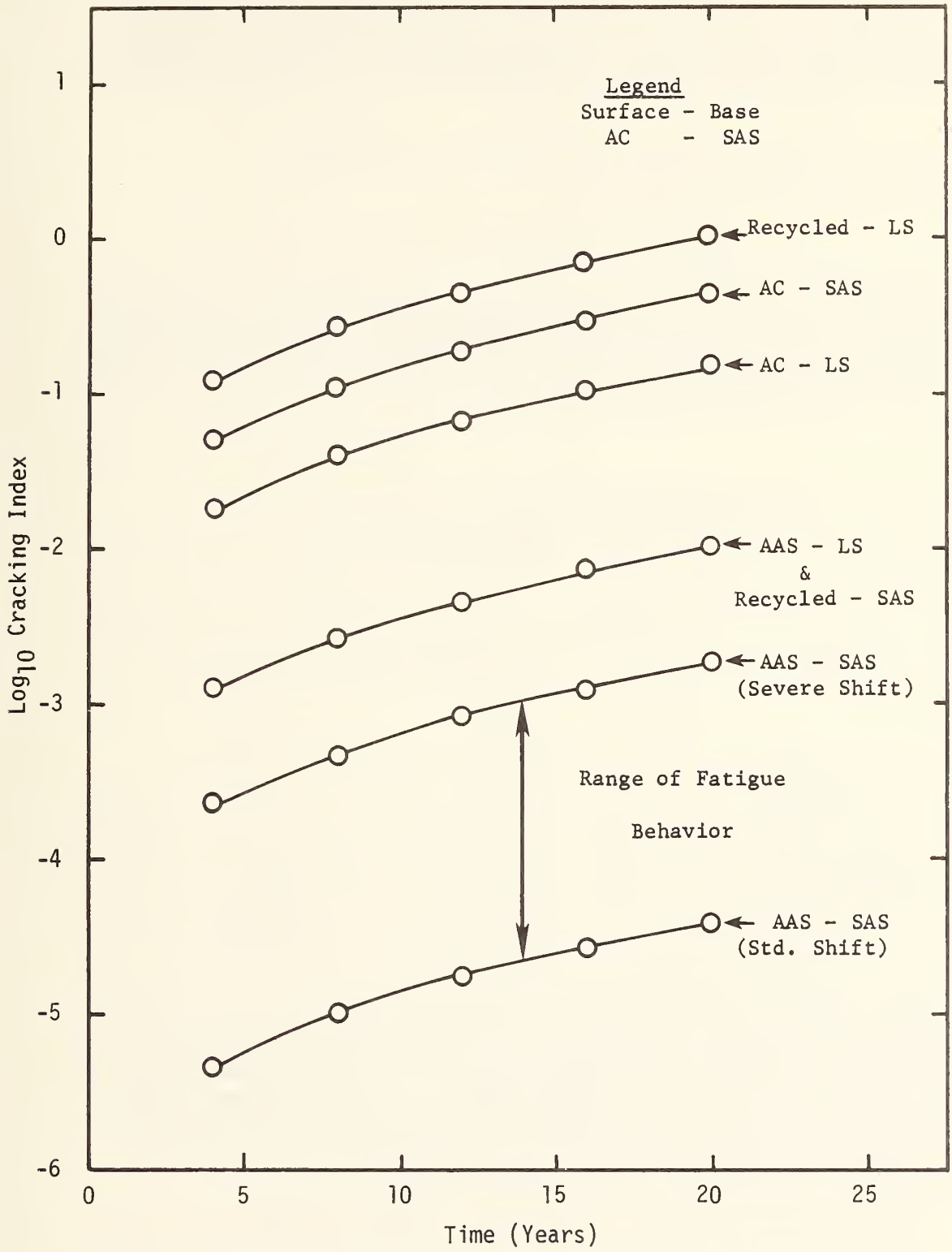

Fig. 45 - Comparison of Cracking Index for AC, AAS, and Sulphur Recycled Optimum Pavement Designs for the Moderate Climate

Also shown in Figure 45 is a graph of the cracking index of the AAS - SAS pavement assuming two different shifts of laboratory fatigue data into field fatigue curves. The standard shift, as explained in the previous chapter, was assumed to be:

$$g = 0.516 \quad 10^{+0.0147T} \qquad \text{(Standard)}$$

The more severe shift took the form

$$g = 0.424 \quad 10^{-0.00708T} \qquad \text{(Severe)}$$

Typical values of g (field K_1 /lab K_1) are shown in Table 38. Because the "severe" shift factors are considered to be conservative, the range of fatigue behavior shown in Figure 45 is believed to enclose the actual behavior that will be observed in the field.

TABLE 38

COMPARISON OF SHIFT FACTORS USED TO COMPUTE SULFUR-ASPHALT FATIGUE BEHAVIOR

Temperature	Shift Factor	
	Standard	Severe
40 (4 °C)	2.00	0.220
60 (16°C)	3.93	0.159
80 (27°C)	7.74	0.115
100 (38°C)	15.23	0.083
120 (49°C)	29.97	0.060

The overall structural adequacy of pavements is given in probabilistic terms of the present serviceability index developed from the AASHTO road test (124). This index, which is a measure of the momentary ability of a pavement to serve traffic, is based on such factors as rut depth, slope variance, cracking and patching of the pavement. The relationship between serviceability index and these pavement distress modes is given by the AASHTO road test equation (124):

$$PSI = 5.03-1.91 \log_{10} (1+SV)-0.01 \sqrt{C+P}-1.38 (RD)^2$$

where PSI is present serviceability index

SV is slope variance

C+P is the amount of cracking and patching on the paving surface

RD is rut depth

This equation is programmed into the VESYS IIM program. Figure 46 presents the anticipated decline of present serviceability index with time for the optimum AC, AAS, and sulphur recycled materials in the moderate climate. The results show that the sulphur systems, except the AE and AES materials, gave a present serviceability index about the same or greater than conventional asphaltic concrete. The optimum pavements with SAS base courses gave lower present serviceability indices than those with limestone bases.

The overall performance of a pavement depends upon the definition of performance. Based upon the present serviceability index, as determined by the AASHTO Road Test equation, the VESYS IIM program predicts that the pavements surfaced with sulphur-asphalt concrete will outperform the conventional asphaltic concrete surfaced pavements. Although all calculations presented here assumed a clay subgrade, it is believed that the sulphur-asphalt surfaced pavements constructed on other subgrades would prove superior to conventional asphaltic concrete pavement.

Two items of data presented here and in Appendix I need further qualification. The first is that none of the optimum pavements performed well in the warm climate. The shift factors estimated for the fatigue data in the warm climate are probably smaller than what will actually be experienced because of the crack healing that will occur at the higher temperatures. This will result in better performance of these pavements than was predicted. This problem emphasizes the need for actual field performance studies so that actual lab-to-field data transformations can be determined. The other item needing further qualification is the performance of the AE and AES materials. For the purposes of the FPS-BISTRO and VESYS IIM evaluations, the AE and AES materials were assumed to have the same form of temperature dependency as the AAS material. This may not necessarily be true. Further testing is needed before more accurate conclusions can be drawn regarding the expected performance of both of these materials.

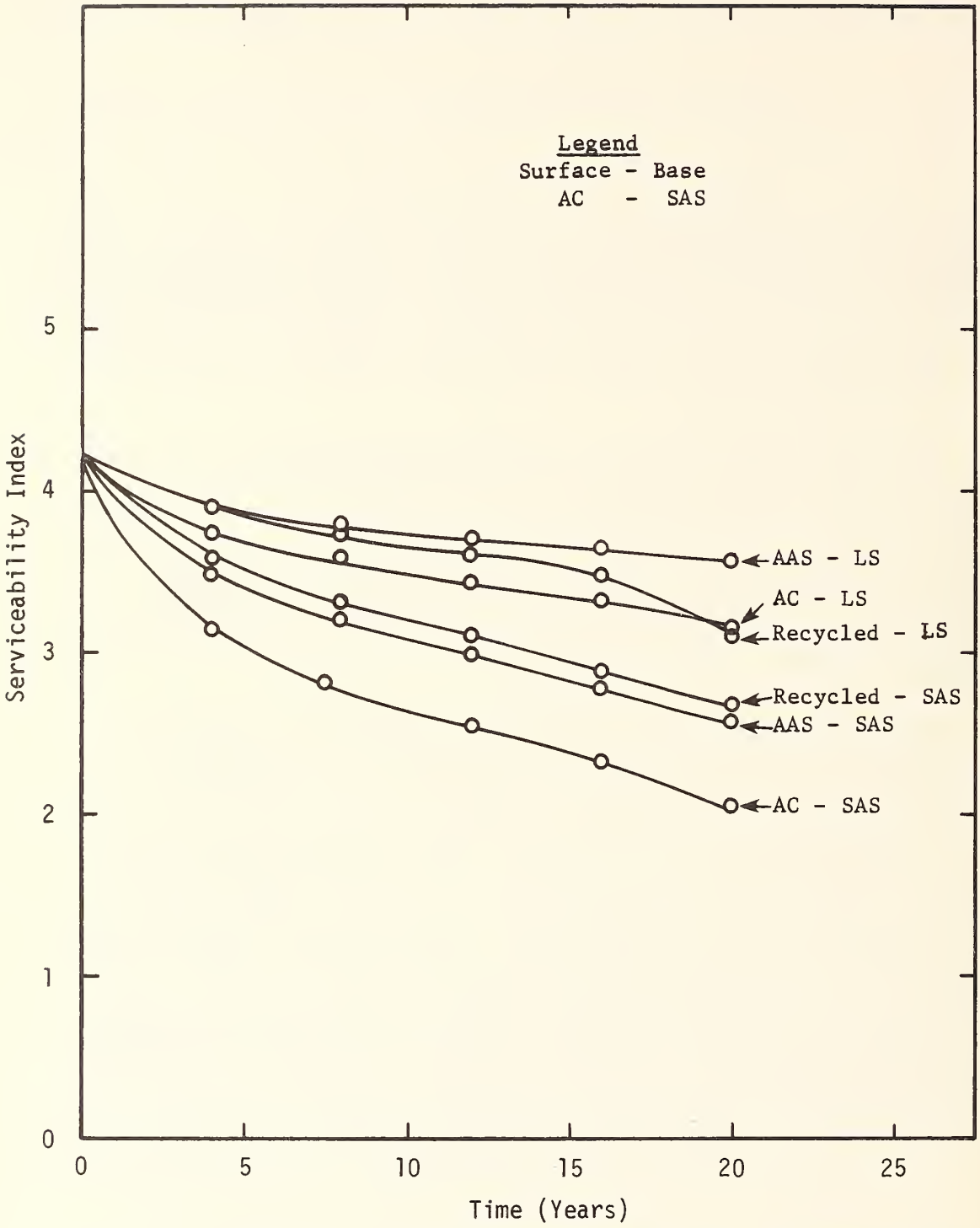

Fig. 46 - Comparison of Serviceability Indices for AC, AAS, and Sulphur Recycled Optimum Pavement Designs for the Moderate Climate.

CHAPTER VIII

CONCLUSIONS AND RECOMMENDATIONS

Conclusions and Summary

Based upon analysis of the experimental data, observations, and other information gained from this research program the following summary remarks and conclusions are made:

1. The availability of asphalt cement, an important ingredient in roadway construction, is decreasing with a resultant rapid increase in price.

2. Efforts are underway in paving related fields to utilize more efficiently available materials in construction of pavements.

3. It has been predicted that elemental sulphur will be in vast oversupply in the very near future. This implies that elemental sulphur will be relatively inexpensive.

4. Elemental sulphur is being evaluated by a number of organizations as a partial substitute for asphalt cement in pavement construction.

5. When mixed with asphalt cement to form an emulsion, sulphur alters the physical properties of the asphalt cement. These properties, as determined by standard laboratory tests, are dependent upon the amount of sulphur added. As determined experimentally for this project, the general trend of the physical properties follows:

    a. The specific gravity of the emulsion increased with sulphur content.

    b. The penetration increased with sulphur content up to about 20 to 30 w/o sulphur, and then decreased as the sulphur content continued to increase.

    c. The ring and ball softening point increased slightly with sulphur content.

    d. Viscosities decrease with increasing sulphur content up to about 20 to 30 w/o sulphur, and then increase rapidly with further increase of sulphur content.

6. As the viscosity of the asphalt cement increased, the amount of sulphur which settled from the sulphur-asphalt emulsion decreased. Very little sulphur settled from emulsions containing 20 w/o or less sulphur. A slightly greater amount of

sulphur settled from emulsions blended and stored at 300°F (148.9°C) than from those at 285°F (140.6°C). Air blown asphalt cements have a much greater capability of maintaining sulphur in suspension than do vacuum-steam or solvent refined asphalt cements.

7. The amount of sulphur which can be dissolved by asphalt cements depends upon the mixing temperature and grade and source of the asphalt cement. The amount of sulphur dissolved by asphalt cement is believed to range between 15 and 20 percent by weight of sulphur-asphalt emulsion. The remainder of the sulphur, if any, remains in suspension or settles from the emulsion.

8. The following systems of preparing mixtures were investigated in this program:

   a. Aggregate-Asphalt-Sulphur (AAS) System

   b. Aggregate-Emulsion (AE) System

   c. Aggregate-Emulsion-Sulphur (AES) System

   The sequence of letters refers to the order in which the individual ingredients were introduced into the mixture.

9. Paving mixtures containing sulphur must be compacted at temperatures in excess of the solidification point of sulphur, or the structuring effect will be destroyed.

10. The size and gradation number (SGN) of aggregate developed for this study can be used as a qualitative indicator of the suitability of aggregates for use in paving mixtures.

11. Specimens of sulphur-asphalt paving mixtures were prepared for this project by the three systems listed in item 8 above. The relative influence of nine materials and mixture variables was investigated by a series of screening tests. An experimental design of a 1/8 factorial experiment was used to determine the combinations of variables to be tested.

12. Results of the screening tests were used to develop statistical relationships between mixture composition and design variables. These results, in the form of regression equation coefficients, are presented in Appendix E and discussed in Chapter 5. These regression equations enable estimation of test results, such as stability and resilient modulus, by use of known values of design variables such as aggregate properties.

13. The optimum values of design variables to maximize resilient modulus are listed in Table 15.

14. A sensitivity analysis indicated that the resilient modulus and Marshall stability are more sensitive to aggregate properties for the AAS system, whereas the two test variables are more sensitive to the degree of compaction for the AE and AES systems.

15. Qualification tests were performed on specimens produced from standard aggregates with variable amounts of sulphur and asphalt cement, These test results, which demonstrated the influence of partial substitution of sulphur for asphalt cement upon the paving mixtures, are presented in Chapter 5 and Appendices F, G, and H.

16. For paving mixtures with approximately constant total binder (sulphur and asphalt cement) content, the bulk specific gravity, Hveem and Marshall stabilities, and resilient moduli increase with increasing sulphur content.

17. The fatigue and permanent deformation characteristics of paving mixtures containing sulphur are listed in Table 18. The value of K_1 decreases whereas the value of K_2 increases as sulphur content increases. The time-temperature parameter BETA decreases with increasing sulphur content up to about 20 w/o of the binder where it increases along with sulphur content.

18. No significant differences exist between the coefficient of thermal expansion of conventional asphaltic concrete and sulphur-asphalt concrete made with crushed limestone aggregate. However, the coefficient of thermal expansion of sulphur-asphalt concrete made with beach sand is about 56 percent larger than that of conventional asphaltic concrete.

19. Micromechanics theory may be used successfully to predict the mechanical properties of the sulphur-asphalt-aggregate mixture. Although more refinement would appear to be desirable, the equations presented in Chapter V may be used to design a mix to produce a desired elastic modulus.

20. The Texas FPS-BISTRO program for pavement system design was used to find optimum combinations of material properties and layer thicknesses which would be least expensive in various climates. Tables 35, 36, and 37 summarize the best design strategies for the cases evaluated in this project. Based upon the conditions, constraints, and material properties used in the study, the total cost for a pavement structure increases as the temperature increases. Within a given temperature category, a design with sulphur-asphalt concrete is the most economical. For temperatures of 40 and 72°F (4 and 22°C), a design containing the sand-asphalt-sulphur base courses proved to be most economical whereas a design with the crushed

limestone base course results in the most effective pavement at a temperature of 120 F°(49°C).

21. The VESYS IIM structural design program was used to evaluate the structural integrity of the optimum pavement designs as determined from the FPS-BISTRO analysis. Results of this evaluation are listed in Appendix I and discussed in Chapter 6. The following can be concluded from the VESYS IIM study:

    a. Based on predicted rut depth, roughness (slope variance), cracking, and present serviceability index, sulphur-asphaltic concrete (AAS) and the sulphur recycled optimum pavements performed as well or better than the optimum conventional asphaltic concrete.

    b. Based on the same criteria, the optimum pavements with a sand-asphalt-sulphur base had poorer predicted performance than the optimum pavements with a limestone base.

22. The results of the screening tests indicate no significant difference in the properties of the paving mixtures containing sulphur prepared by the AAS, AE, and AES systems. In view of the observed differences in pavement performance as predicted by FPS-BISTRO and VESYS IIM, it is apparent that the simple screening tests (stability, flow, strength, and resilient modulus) will not be good indicators of the field performances of these mixtures.

23. On the basis of the VESYS II predictions, it appears that there is no advantage to the use of a sulphur-asphalt emulsion prepared in a colloid mill rather than direct introduction of sulphur and asphalt cement into the mixture.

24. Laboratory and theoretical studies indicate that the addition of sulphur to asphaltic pavements can produce better, more economical pavements.

Recommendations

Based upon the conclusions drawn from this project, the following recommendations for further study are made:

1. Pavement researchers should select the method of measurement of stiffness to be used in layered-elastic and viscoelastic design methods. Correlations among the various methods of determining stiffness should be made.

2. Relationships should be established between fatigue characterization of pavement materials in the laboratory and in the field.

3. To verify the laboratory and theoretical data, full-scale field demonstrations of sulphur-asphalt test sections should be evaluated. These should include the following:

   a. Optimum depth pavements using each of the three methods of combining aggregate, asphalt and sulphur should be built with an optimum depth of asphaltic concrete pavement as a control section. In addition, other sections should be built with paving thicknesses that are expected to fatigue much more quickly than those at optimum depth. This will provide field verification of fatigue properties of the mixes, one of the least known properties of mixes.

   b. Careful measurements of paving temperature, rut depth, and some measure of roughness should be made on these test sections. The input values to the VESYS IIM program require measurements of slope variance and variance of rut depth. Better measures of roughness, such as the roughness amplitude power spectrum, can be determined from Fourier transforms of the profile data. Actual measurements of the profile such as made by the GM Road Profilometer can be used for this purpose.

   c. A thermal cracking model for pavements should be used to predict the sulphur asphalt mixes which should perform the best in resisting transverse cracking that results from sudden temperature drops (thermal cooling) and temperature cycling (reflection cracking and thermal fatigue).

REFERENCES

1. "Asphalt as a Material," Information Series No. 93, The Asphalt Institute, College Park, Maryland, June 1973.

2. Saylak, D., Gallaway, B.M., Epps, J.A., "Recycling Old Asphalt Concrete Pavements", Proceedings of the Fifth Mineral Waste Utilization Symposium, Chicago, Illinois, April 13-14, 1976.

3. Gallaway, B.M., and Saylak, D., "Beneficial Use of Sulphur in Sulphur-Asphalt Pavements, Vol. I," Final Report on Texas A&M Research Project RF-983-IA, Texas A&M Research Foundation, Texas A&M University, College Station, Texas, January 1974.

4. Hammond, R., Deme, I., and McManus, D., "The Use of Sand-Asphalt-Sulphur Mixes for Road Base and Surface Applications," Proceedings, Canadian Technical Asphalt Association, Vol. XVI, November 1971.

5. Deme, I., "Basic Properties of Sand-Asphalt-Sulphur Mixes," presented to the VII International Road Federation World Meeting, Munich, West Germany, October 1973.

6. Deme, I., "The Use of Sulphur in Asphalt Paving Mixes," presented to the Fourth Joint Chemical Engineering Conference, Vancouver, September 1973.

7. Deme, I., "Processing of Sand-Asphalt-Sulphur Mixes," paper presented at the Annual Meeting of the Association of Asphalt Paving Technologists, Williamsburg, Va., February 1974.

8. U. S. Patent No. 3,738,853, June 12, 1973.

9. Kennepohl, G.J.A., Logan, A., and Bean, D.C., "Conventional Paving Mixes with Sulphur-Asphalt Binders," Gulf Oil Canada Limited, presented at the Annual Meeting of the Association of Asphalt Paving Technologists, Phoenix, Arizona, February 1975.

10. Kennepohl, G.J.A., Logan, A., and Bean, D.C., "Sulphur-Asphalt Binders in Paving Mixes," paper presented at the Canadian Sulphur Symposium, Calgary, Alberta, May 1974.

11. Societe Nationale des Petroles d'Aquitaine, "Properties of Sulphur Bitumen Binders," paper presented at the VII International Road Federation World Meeting, Munich, West Germany, October 1973.

12. Garrigues, C., and Vincent, P., "Sulfur/Asphalt Binders for Road Construction," New Uses of Sulfur, Advances in Chemistry Series 140, American Chemical Society, 1975.

13. "Sulphur-Asphalt Binders Pavement Test, U.S. 69, Lufkin, Texas," a paper prepared for The Sulphur Institute, Washington, D.C., by Texas Transportation Institute, Texas A&M University, College Station, Texas, August 1975.

14. Giannini, Franco, and Camomilla, Gabriele, "Procedure for the Structural Design of Pavement Used in Italian Motorways," Proceedings of the Fourth International Converence on the Structural Design of Asphalt Pavements, Vol. I, University of Michigan, Ann Arbor, Michigan, August 22-26, 1977.

15. Van Dijk, W., "Practical Fatigue Characterization of Bituminous Mixes," Proceedings of the Association of Asphalt Paving Technologists, Vol. 44, 1975.

16. Izatt, J.O., Gallaway, B.M., Saylak, D., "Sand-Asphalt-Sulphur Pavement Field Trials, Highway U.S. 77, Kenedy County, Texas," a construction report, FHWA-TS-78-204, April, 1977.

17. Kennedy, T.W., Hass, R., Smith, P., and Kennepohl, G.A., "Engineering Evaluation of Sulphur-Asphalt Mixtures," a paper presented at the Fifty-Sixth Annual Meeting of the Transportation Research Board, Washington, D.C., January 1977.

18. "Sulphur: 1980's Shortage of Glut?," Chemical Engineering, September 27, 1976.

19. "Introduction to Asphalt," Manual Series No. 5, Fourth Edition, The Asphalt Institute, November 1962, pp. 1, 3.

20. Wallace, H.A., and Martin, J.R., Asphalt Pavement Engineering, McGraw-Hill Book Company, New York, p. 5.

21. Neppe, S.L., Proceedings of The Association of Asphalt Paving Technologists, Vol. 22, 1953, pp. 383-427.

22. The Sulphur Data Book, Freeport Sulphur Company, McGraw-Hill Book Company, Inc., 1954, p. 3.

23. Gamble, B.R., Gillott, J.E., Jordaan, I.J., Loov, R.E., and Ward, M.A., "Civil Engineering Applications of Sulfur-Based Materials," New Uses of Sulfur, Advances in Chemistry, Series 140, American Chemical Society, 1975, pp. 154-166.

24. Seymore, R.B., et al., Journal of the American Water Works Association, Paper 43, 1951, p. 1001.

25. Dale, J.M., Ludwig, A.C., "Mechanical Properties of Sulfur", Elemental Sulfur, Chemistry and Physics, John Wiley and Sons, New York, pp. 161-178.

26. Lund, Herbert F., ed., Industrial Pollution Control Handbook, McGraw-Hill Book Company, New York, 1966, pp. 8-18.

27. Stolman, Abran, ed., Progress in Chemical Toxicology, Academic Press, New York, Vol. 1, 1965, p. 10.

28. Elkins, Hervey B., The Chemistry of Industrial Toxicology, John Wiley and Sons, Inc., New York, 1950, pp. 95, 232.

29. Sinko, Michell J., et al., Chemistry: Principles and Properties, McGraw-Hill Book Company, New York, 1966, p. 528.

30. Henderson, Jendell, et al., Noxious Gases, Reinhold Publishing Corporation, New York, 1943, pp. 140, 243-245.

31. Personal telephone conversation with Mr. Horace Adrian, Chief Engineer, Industrial Hygiene Division, Texas State Department of Health, May 27, 1977.

32. "Pave the Way With Sulphur," The Texas Transportation Institute, The Texas A&M University System, College Station, Texas.

33. Day, A.G., U. S. Patent No. 58615, October 9, 1866.

34. Dubbs, J.A., U. S. Patent No. 468867, February 16, 1892.

35. Ahmad, H., "A Laboratory Study of the Use of Sulphur In Sand-Asphalt Mixes for Flexible Pavements," Dissertation for Doctor of Philosophy Degree in Civil Engineering, Texas A&M University, College Station, Texas, May 1974.

36. Gallaway, B.M., and Saylak, D., "Beneficial Use of Sulphur in Sulphur-Asphalt Pavements, Vol. II, Literature Search and Patent Review," Final Report on Texas A&M Research Project RF 983, Texas A&M Research Foundation, College Station, Texas, August, 1974.

37. Duecker, W.W., and Schofield, H.Z., "Results From the Use of Plasticized Sulfur as a Jointing Material for Clay Products," American Ceramic Society Bulletin, Vol. 16, November 1937, pp. 435-438.

38. Bencowitz, Isaac and Boe, E.S., "Effect of Sulfur Upon Some of the Properties of Asphalts," American Society for Testing and Materials, Proceedings of the Forty-First Annual Meeting, Vol. 38, Part II, June 27 - July 1, 1938, p. 539.

39. Williford, C.L., "X-Ray Studies of Paving Asphalts," Bulletin of the Agricultural and Mechanical College of Texas, Engineering Experiment Station, No. 73, 1943.

40. Welborn, J.Y., and Babashak, J.F., Jr., "A New Rubberized Asphalt for Roads," Proceedings of the American Society of Civil Engineers Journal of the Highway Division, 1958.

41. Metcalf, Charles T., "Bituminous Road Surfacing Mass Containing Sulfur," (Shell International Research Maatschappij), Chemical Abstracts, Vol. 72, 1970, 5878r.

42. Nicolau, Albert, et al., "Bitumen Binders Containing Sulfur for Road Surfacing," Societe Nationale des Petroles d'Aquitaine, Chemical Abstracts, Vol. 74, 1971, 5223v.

43. Lee, Day-yinn, "Modification of Asphalt and Asphalt Paving Mixtures," Interim Report, Engineering Research, March 1971.

44. Sadtler, S.S., "Method of Building Roads and in Preparing of the Materials Therefor," U. S. Patent No. 1,830,486, November 3, 1931.

45. Bacon, R.F., and Bencowitz, I., "Method of Paving," U. S. Patent No. 2,182,837, December 13, 1939.

46. Gartarz, Zdzislawa, "Sulfur in Highway Construction," Chemical Abstracts - Applied Chemistry and Chemical Engineering Sections, Vol. 79, No. 8, October 22, 1973.

47. "New Bitumen and Sulphur Composition Based Binders and Their Process of Preparation," British Patent No. 1,303,318, January 17, 1973.

48. Sullivan, T.A., "Study of Sulphur-Asphalt Road Mixes," U. S. Bureau of Mines, Boulder City Metallurgy Research Laboratory, Boulder City, Nevada, Asphalt Research Meeting, August 9 and 10, 1973, Laramie Energy Research Center, Laramie, Wyoming, August 1973.

49. Saylak, D.,Gallaway, B.M., and Noel, J.S., "Evaluation of a Sulphur-Asphalt Emulsion Binder for Road Building Purposes," Final Report on Texas A&M Research Project RF 3146, Texas A&M Research Foundation, Texas A&M University, College Station, Texas, January 1976.

50. "Extension and Replacement of Asphalt Cement With Sulphur, FHWA Contract No. DOT-FH-11-8799, Texas A&M Research Foundation, Project RF3259, Texas A&M University, College Station, Texas.

51. "Predictive Design Procedure, VESYS Users Manual - An Interim Design Method in Flexible Pavement Using the VESYS Structural Subsystem," Federal Highway Administration Offices of Research and Development, Washington, D.C., March 1976.

52. Rauhut, J. B., O'Quin, J.C. and Hudson, W.R., "Sensitivity Analysis of FHWA Model VESYS II," Volumes 1 and 2, Report Nos. FHWA-RD-76-23 and FHWA-RD-76-24, Federal Highway Administration Office of Research and Development, Washington, D.C., March 1976.

53. Kenis, W.J. and McMahon, T.F., "A Flexible Pavement Analysis Subsystem," paper presented at 53rd. Annual Meeting of Highway Research Board, January 1974.

54. Scrivner, F.H., Moore, W.M., McFarland, W.F., and Carey, G.R., "A Systems Approach to the Flexible Pavement Design Problem," Research Report 32-11, Texas Transportation Institute, 1968.

55. Hudson, W. R., McCullough, B.F., Scrivner, F. H., and Brown, J.L., "A Systems Approach Applied to Pavement Design and Research," Research Report 123-1, Texas Highway Department, 1969.

56. Kher, Ramesh, K., Hudson, W.R., and McCullough, B.F., "A Systems Analysis of Rigid Pavement Design," Research Report 123-5, Center for Highway Research, November 1970.

57. Lytton, R.L., McFarland, W.F., and Schafer, D.L., "A Systems Approach to Pavement Design-Implementation Phase," Final Report NCHRP Project 1-10A, Texas Transportation Institute, March 1974.

58. Lu, Danny, "Strategic Approach for the Design and Future Maintenance of Pavement Systems," Doctoral Dissertation, Texas A&M University, May 1974.

59. Lu, D. Y., Shih, C.S., and Scrivner, F.H., "The Optimization of a Flexible Pavement System Using Linear Elasticity," Research Report 123-17, Texas Transportation Institute, 1973.

60. Gallaway, B.M., and Saylak, D., "Beneficial Uses of Sulphur In Sulphur-Asphalt Pavement, Volume III," Final Report on Texas A&M Research Project RF 983-1A, Texas A&M Research Foundation, Texas A&M University, College Station, Texas, January 1974.

61. Saylak, D., Gallaway, B.M., Ahmad, H., "Beneficial Use of Sulfur in Sulfur-Asphalt Pavements", New Uses of Sulfur, Advances in Chemistry Series 140, American Chemical Society, 1975.

62. Saylak, D., Lytton, R.L., Gallaway, B.M, and Pickett, D.E., "Prediction of In-Service Performance of Sulfur-Asphalt Pavements," paper presented at 170th Meeting of the American Chemical Society, New Orleans, Louisiana, March 21-24, 1977.

63. AASHTO Designation: M226-73, Standard Specifications for Highway Materials and Methods of Sampling and Testing, Part I, American Association of State Highway and Transportation Officials, 1974.

64. AASHTO Designation: T-49-74, Standard Specifications for Highway Materials and Methods of Sampling and Testing, Part II, American Association of State Highway and Transportation Officials, 1974.

65. Test Method - Tex-527-C, Texas Highway Department Manual of Testing Procedures, Vol. 1, Bituminous Section, 1968.

66. AASHTO Designation: T-202-74, Standard Specifications for Highway Materials and Methods of Sampling and Testing, Part II, American Association of State Highway and Transportation Officials, 1974.

67. AASHTO Designation: T-201-74, Standard Specification for Highway Materials and Methods of Sampling and Testing, Part II, American Association of State Highway and Transportation Officials, 1974.

68. AASHTO Designations: T-53-74, Standard Specifications for Highway Materials and Methods of Sampling and Testing, Part II, American Association of State Highway and Transportation Officials, 1974.

69. ASTM Designation: D-70-72, 1975 Annual Book of ASTM Standards, Part 15, American Society for Testing and Materials.

70. Krumbein, W.C., "Measurement and Geological Significance of Shape and Roundness of Sedimentary Particles," Journal of Sedimentary Petrology, Vol. 13, No. 2, August 1941, pp. 64-72.

71. Rittenhouse, Gordon, "A Visual Method of Estimating Two-Dimensional Sphericity", Journal of Sedimentary Petrology, Vol. 13, No. 2, August 1943, pp. 79-81.

72. Mather, Bryant, "Shape, Surface Texture, and Coatings of Aggregates", Misc. Paper No. 6-710, U.S. Army Engineers, Waterways Experiment Station, Vicksburg, Mississippi, February 1965.

73. ASTM Designation: C136-71, 1975 Annual Book of ASTM Standards, Part 15, American Society for Testing and Materials.

74. ASTM Designation: C117-69, 1975 Annual Book of ASTM Standards, Part 15, American Society for Testing and Materials.

75. ASTM Designation: D1559-73, 1975 Annual Book of ASTM Standards, Part 15, American Society for Testing and Materials.

76. Handbook of Chemistry and Physics, 33rd Edition, p. 2041, 1952-1953.

77. Kempthorne, O., Design and Analysis of Experiments, John Wiley and Sons, Inc., New York, 1952.

78. "The Asphalt Handbook", Manual Series No. 4, April 1965 Edition, The Asphalt Institute, May 1968.

79. Deme, I., "Guidelines for Sand-Asphalt-Sulphur Mix Design", paper presented at the Annual Meeting of the Association of Asphalt Paving Technologists, Phoenix, Arizona, February 1975.

80. Burgess, R.A., and Deme, I., "Sulfur in Asphalt Paving Mixes", New Uses of Sulfur, Advances in Chemistry Series 140, American Chemical Society, 1975.

81. Gallaway, B.M., and Saylak, Donald, "Sulphur/Asphalt Mixture Design and Construction Details - Lufkin Field Trials", Interim Report 512-1, Study No. 1-10-75-512, Texas Transportation Institute, Texas A&M University, College Station, Texas, January 1976.

82. Litehiser, R.R., and Schofield, H.Z., "Progress Report on Brick Road Experiments in Ohio", Proceedings of the Sixteenth Annual Meeting of the Highway Research Board, November 1936, p. 182.

83. "Patching a Road With Sulphur", Sulphur Institute Journal, Volume 11, Number 2, Summer 1975, p. 2.

84. "Sulphur and Asphalt - Renewed Interest in an Old Subject", Sulphur Institute Journal, Volume 9, Number 2, Summer 1973, p. 10.

85. "New Markets for Tomorrow's Sulphur", The Sulphur Institute, Washington, D.C., 1975, p. 11.

86. Glascock, Lacey A., "A Laboratory Evaluation of Sulphur-Asphalt Paving Mixtures", Research Report No. 100, Research Project No. 74-1B (B), Louisiana HPD 1 (13), Louisiana Department of Highways, February 1976.

87. Bacon, Raymond F., and Davis, Harold S., Chemical and Metallurgical Engineering, Volume 24, January 12, 1921, pp. 65-72.

88. "The Asphalt Handbook", Manual Series No. 4, The Asphalt Institute, College Park, Maryland, April 1965, p. 66.

89. ASTM Designation: C33-71, 1975 Annual Book of ASTM Standards, Part 14, American Society for Testing and Materials.

90. ASTM Designation: D2726-73, 1974 Annual Book of ASTM Standards, Part 15, American Society for Testing and Materials.

91. ASTM Designation: D2041-71, 1974 Annual Book of ASTM Standards, Part 15, American Society for Testing and Materials.

92. "Mix Design Methods for Asphalt Concrete and Other Hot-Mix Types", Manual Series No. 2, Fourth Edition, The Asphalt Institute, College Park, Maryland, March 1974.

93. Schmidt, R.J., "A Practical Method for Measuring the Resilient Modulus of Asphalt-Treated Mixes", Highway Research Record No. 404, Highway Research Board, 1972, pp. 22-32.

94. "Operating Instructions, Mark III Resilient Modulus Device", Instruction Manual for Mark III Resilient Modulus Device, Retsina Company, El Cerrito, California.

95. Schmidt, R.J., U. S. Patent No. 3,854,328, December 17, 1974.

96. Yeager, Larry L., and Wood, Leonard E., "A Recommended Procedure for the Determination of the Dynamic Modulus of Asphalt Mixtures", Joint Highway Research Project No. C-36-6AA, Purdue University, West Lafayette, Indiana, December 17, 1975.

97. Personal communication with Mr. Newell Brabston, Research Engineer, U. S. Army Corps of Engineers Waterways Experiment Station, Vicksburg, Mississippi, June 10, 1977.

98. Gallaway, B.M., and Saylak, D., "Beneficial Use of Sulphur in Sulphur-Asphalt Pavement, Vol. I", Final Report on Texas A&M Research Project RF-983-1B, Texas A&M Research Foundation, Texas A&M University, College Station, Texas, August 1974.

99. ASTM Designation: D1560-71, 1975 Annual Bood of Standards, Part 15, American Society for Testing and Materials.

100. Fox, R.L., Optimization Methods for Engineering Design, Addison-Wesley Publishing Company, Reading, Mass., June 1973.

101. Nair, Keshavan, and Chang, C-Y, "Flexible Pavement Design and Management, Materials Characterization", National Cooperative Highway Research Program Report 140, Highway Research Board, 1973, p. 12.

102. ASTM Designation: E11-70, 1974 Annual Book of ASTM Standards, Part 15, American Society for Testing and Materials.

103. ASTM Designation: C127-73, 1974 Annual Book of ASTM Standards, Part 15, American Society for Testing and Materials.

104. ASTM Designation: C128-73, 1974 Annual Book of ASTM Standards, Part 15, American Society for Testing and Materials.

105. "Test Procedures for Characterizing Dynamic Stress-Strain Properties of Pavement Materials", Special Report 162, Transportation Research Board, National Research Council, National Academy of Sciences, Washington, D.C., 1974.

106. Epps, J.A., and Monismith, C.L., "Fatigue of Asphalt Concrete Mixtures - Summary of Existing Information", Fatigue of Compacted Bituminous Aggregate Mixtures, Special Technical Publication No. 508, American Society for Testing and Materials, 1972, pp. 19-45.

107. Irwin, L.H., and Gallaway, B.M., "Influence of Laboratory Test Method on Fatigue Test Results for Asphaltic Concrete", Fatigue and Dynamic Testing of Bituminous Mixtures, ASTM STP 561, American Society for Testing and Materials, 1974, pp. 12-46.

108. Aklonis, John J., Macknight, William J., and Shen, Mitchell, Introduction to Polymer Viscoelasticity, Wiley-Interscience, New York, 1972, p. 47.

109. Witczak, M.W., and Root, R.E., "Summary of Complex Modulus Laboratory Test Procedures and Results", Fatigue and Dynamic Testing of Bituminous Mixtures, ASTM STP561, American Society for Testing and Material, 1974, pp. 67-94.

110. ASTM Designation: D696-10, 1975 Annual Book of ASTM Standards, Part 35, American Society for Testing and Materials.

111. Monismith, C.L., "Influence of Shape, Size, and Surface Texture on the Stiffness and Fatigue Response of Asphalt Mixtures", Highway Research Board Special Report 109, "Effects of Aggregate Size, Shape, and Surface Texture on Properties of Bituminous Mixtures", Washington, D.C., 1970, pp. 4-11.

112. Griffith, J.M., and Kallas, B.F., "Influence of Fine Aggregates on Asphaltic Concrete Paving Mixtures", Proceedings of the Highway Research Board, Vol. 37, 1958, pp. 219-255.

113. Hargett, Emil R., "Effects of Size, Surface Texture, and Slope of Aggregate Particles on the Properties of Bituminous Mixtures", Highway Research Board Special Report 109, "Effects of Aggregate Size, Shape, and Surface Texture on Properties of Bituminous Mixtures", Washington, D.C., 1970, p. 25.

114. Benson, Fred J., "Effects of Aggregate Size, Shape, and Surface Texture on the Properties of Bituminous Mixtures - A Literature Survey", Highway Research Board Special Report 109, "Effects of Aggregate Size, Shape, and Surface Texture on Properties of Bituminous Mixtures", Washington, D.C., 1970, pp. 12-21.

115. Livneh, M. and Greenstein, J., "Influence of Aggregate Shape on Engineering Properties of Asphaltic Paving Mixtures", Highway Research Record Number 404, Highway Research Board, Washington, D.C., 1972, pp. 42-56.

116. Kenis, W.J., "Material Characterizations for Rational Pavement Design", Fatigue and Dynamic Testing of Bituminous Mixtures, ASTM STP 561, American Society for Testing and Materials, 1974, pp. 132-152.

117. Sharma, M.G. and Kim, K.S., "Non-linear Viscoelastic Properties of Bituminous Concretes", Journal of Testing and Evaluation, JTEVA, Vol. 3, No. 3, May 1975, pp. 182-190.

118. Santucci, L.E., "Thickness Design Procedure for Asphalt and Emulsified Asphalt Mixes," Proceedings of the Fourth Internationa Conference on the Structural Design of Asphalt Pavements, Vol. I, University of Michigan, Ann Arbor, Michigan, August 22-26, 1977.

119. Sharma, Jatinder, et al., "Implementation and Verification of Flexible Pavement Design Methodology," Proceedings of the Fourth International Conference on the Structural Design of Asphalt Pavements, Vol. I, University of Michigan, Ann Arbor, Michigan, August 22-26, 1977.

120. Texas Highway Department Pavement Design System, Part I, Flexible Pavement Designer's Manual, Highway Design Division, Texas State Department of Highways and Public Transportation, 1972.

121. Epps, J.A., "Influences of Mixture Variables on the Flexural Fatigue and Tensile Properties of Asphaltic Concrete," thesis, University of California, Berkeley, 1968.

122. "Highway Information Service," a monthly tabulation of highway construction bid data published by Whitley & Siddons, Austin, Texas, May 1977.

123. Edris, Earl V. and Lytton, Robert L., "Dynamic Properties of Subgrade Soils, Including Environmental Effects," Research Report 164-3, Texas Transportation Institute, Texas A&M University, College Station, Texas, May 1976.

124. "The AASHO Road Test: Report 5- Pavement Research", Special Report 61E, Highway Research Board, National Academy of Sciences, National Research Council, 1962.

125. Hudson, Ronald W., "State-of-the-Art In Predicting Pavement Reliability From Input Variability," Contract Report S-75-7 (FAA-RD-75-207), U.S. Army Engineer Waterways Experiment Station, Soils and Pavements Laboratory, Vicksburg, Mississippi, August 1975.

126. Flavius, Josephus, "The Antiquities of the Jews," first published in 93 or 94 A.D., translated by William Whiston, Kregel Publications, Grand Rapids, Michigan, 1971, p. 33.

127. Scrivner, F.H., and Michalak, C.H., "Flexible Pavement Performance Related to Deflection, Axle Applications, Temperature and Foundation Movements", Research Report 32-13, Texas Transportation Institute, 1969.

128. Fox, T.G., Gratch, S. and Loshaek, S., "Viscosity Relationships for Polymers in bulk and in Concentrated Solution," Chapter 12 in Rheology, Theory and Applications, Vol. I, F.R. Eirich, editor, Academic Press, 1956, p. 431-493.

129. Hashin, Z., "Theory of Composite Materials," Mechanics of Composite Materials, Proceedings of the Fifth Symposium on Naval Structural Mechanics, Pergamon Press, 1970, pp. 201-242.

130. Fung, Y.C., Fundamentals of Solid Mechanics, Prentice-Hall, 1965.

131. Gallaway, B.M., Saylark, D., "Sulphur/Asphalt Mixture Design and Construction Details - Lufkin Field Trials," a construction report on Highway U.S. 69, Angelina County, Texas, FHWA-TS-78-203, January, 1976.

132. Finn, F., et al., "The use of Distress Prediction Subsystems for the Design of Pavement Structures," Proceedings of the Fourth International Conference on the Structural Design of Asphalt Pavements, Vol. I, University of Michigan, Ann Arbor, Michigan, August 22-26, 1977.

133. Clark, S.P., Handbook of Physical Constants, Geological Society of America, Inc., Revised Edition, 1966, p. 123.

134. O'Rourk, General Engineering Handbook, McGraw-Hill Book Co., Inc., Second Edition, 1940, p. 181.

135. Hashin, Z, "The Elastic Moduli of Heterogeneous Materials," Journal of Applied Mechanics, Vol. 29E, 1962, pp. 143-150.

136. Schapery, R.A., "Viscoelastic Behavior of Composite Materials, Mechanics of Composite Materials, Vol. 2, G.P. Sendeckyj, ed., Academic Press, 1974, pp. 85-168.

137. Ferry, J.D., Viscoelastic Properties of Polymers, 2nd Ed., Wiley, 1970.

138. Sulphur Asphalt Project MH-153, Brazos County, Texas, 1978.

APPENDICES TABLE OF CONTENTS

Appendix A. Gradation Curves for Aggregates Used in Screening Tests

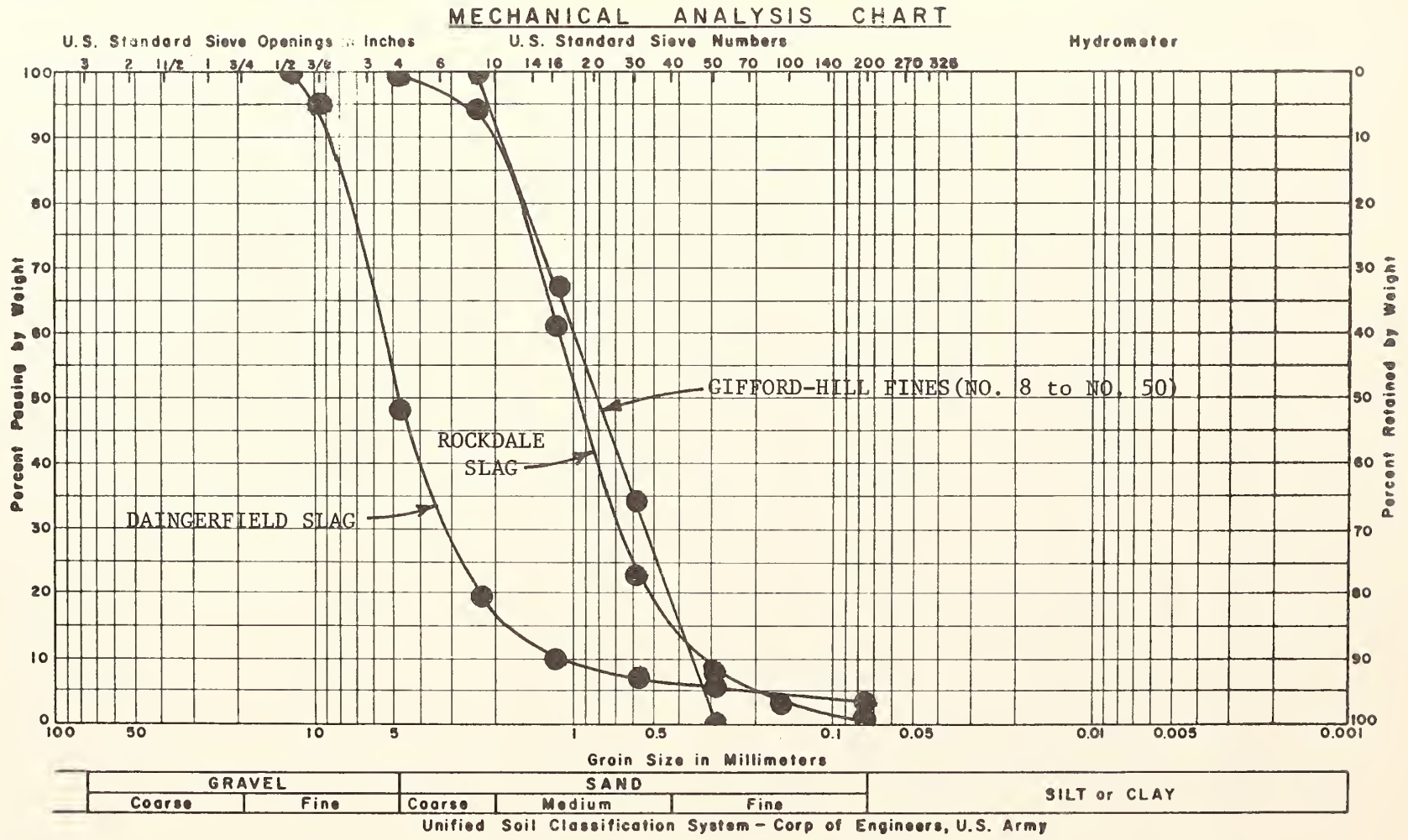

Fig. 47 --GRADATION OF AGGREGATES USED IN SCREENING TESTS

1 inch = 25.4 mm

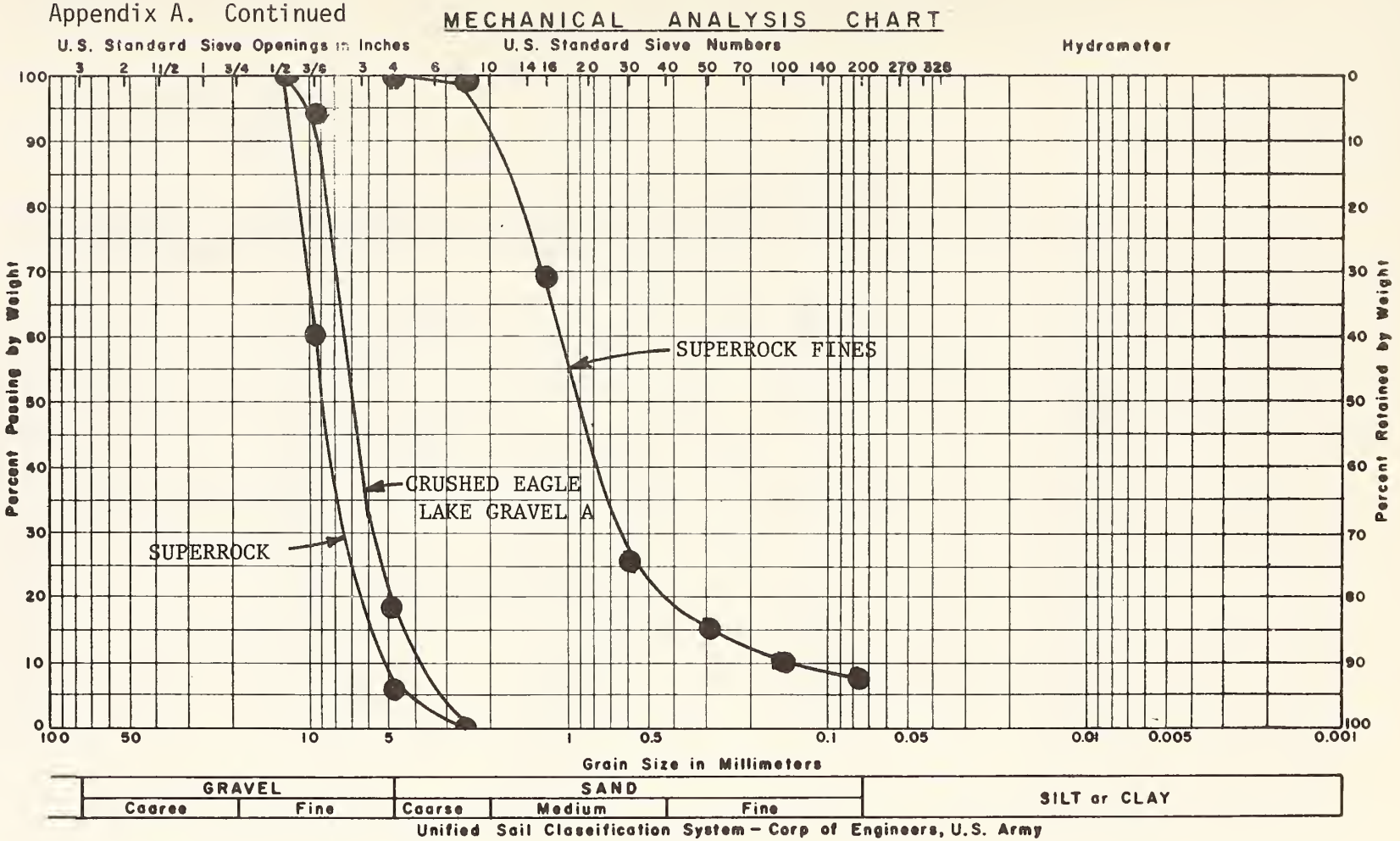

Fig. 48 -- GRADATION OF AGGREGATES USED IN SCREENING TESTS

1 inch = 25.4 mm

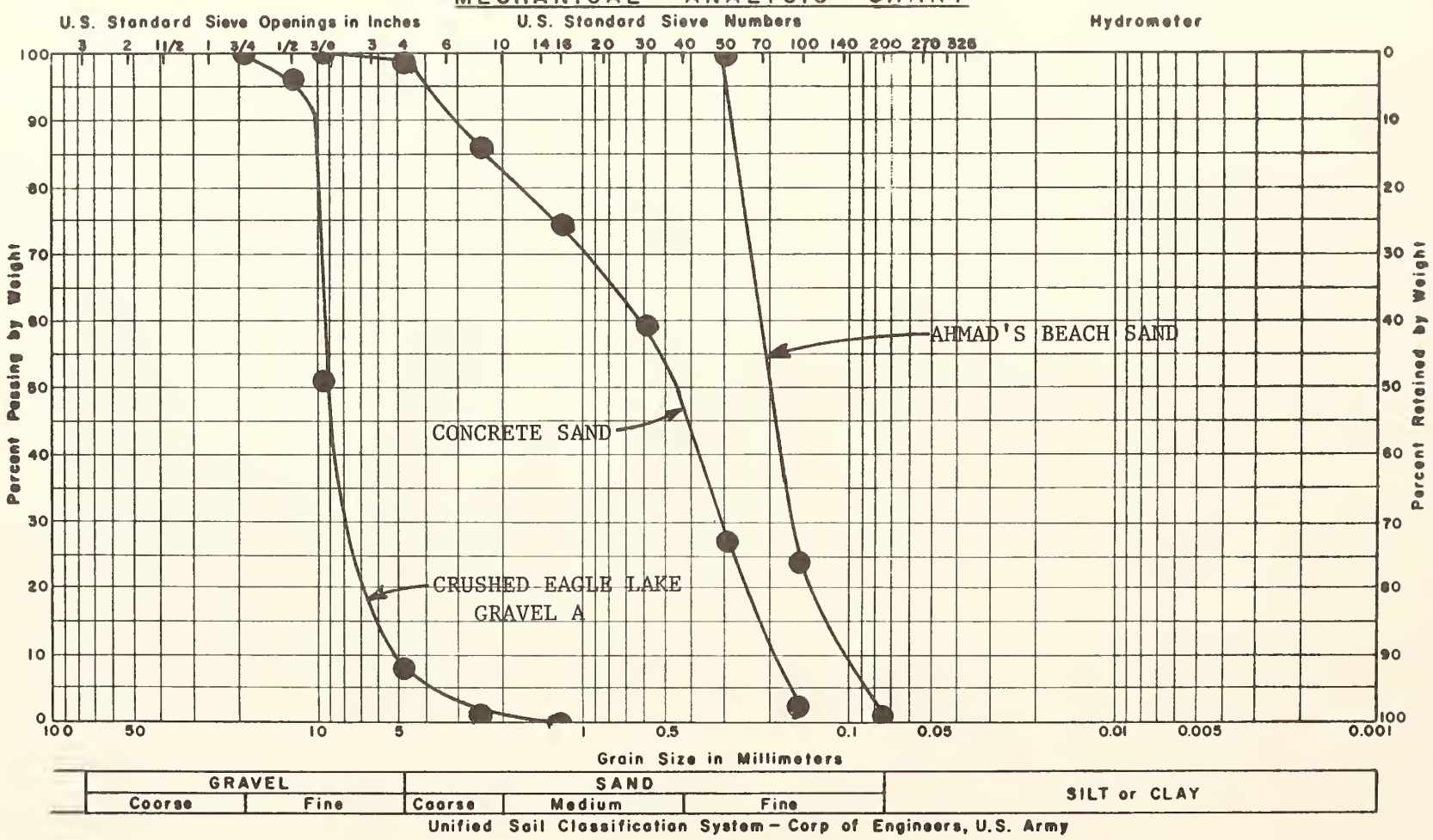

FIG. 49 GRADATION OF AGGREGATES USED IN SCREENING TESTS

1 inch = 25.4 mm

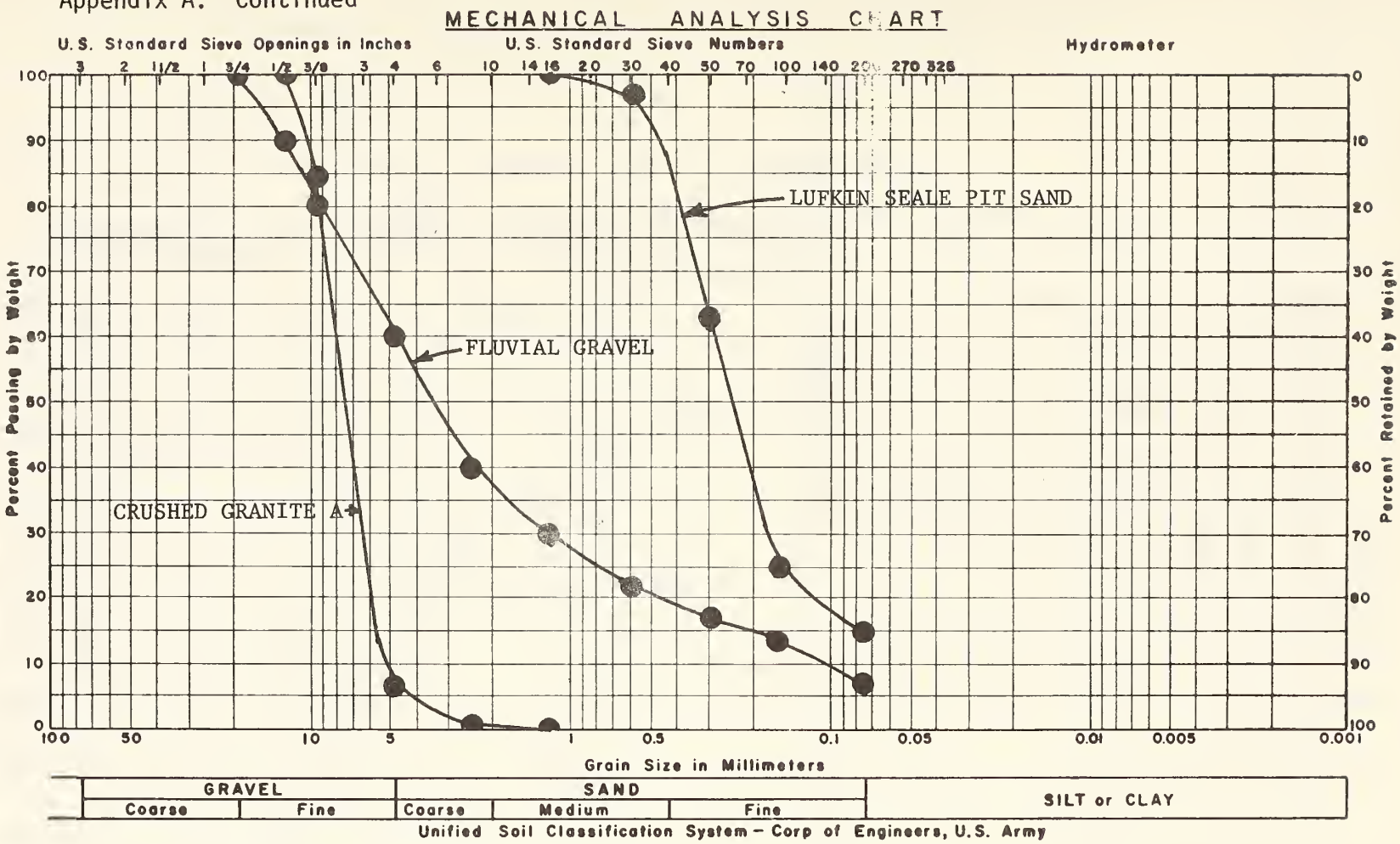

FIG. 50 -- GRADATION OF AGGREGATES USED IN SCREENING TESTS

1 inch = 25.4 mm

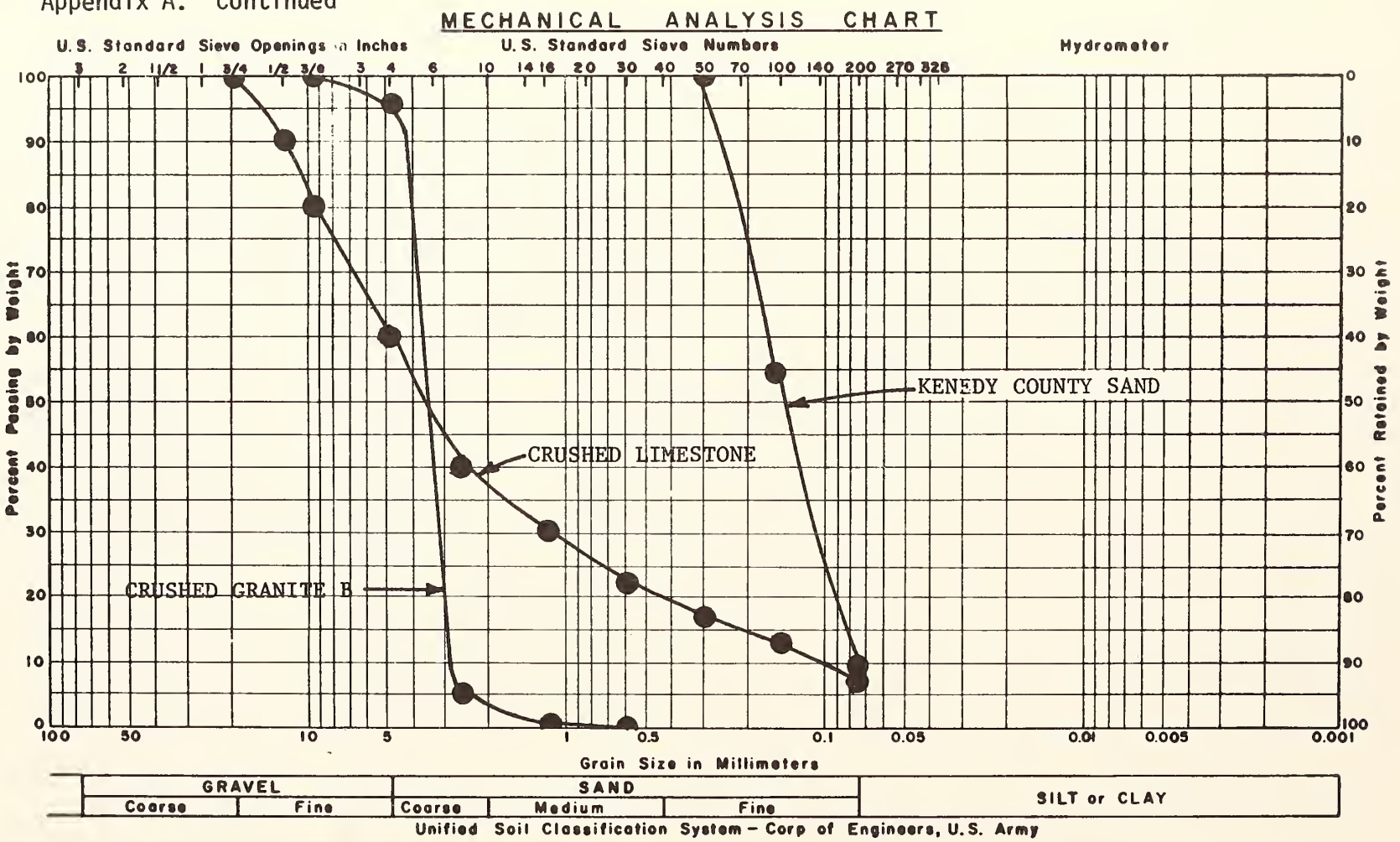

FIG. 51 -- GRADATION OF AGGREGATES USED IN SCREENING TESTS

1 inch = 25.4 mm

Appendix B. Physical Properties of Sulphur-Asphalt Emulsions

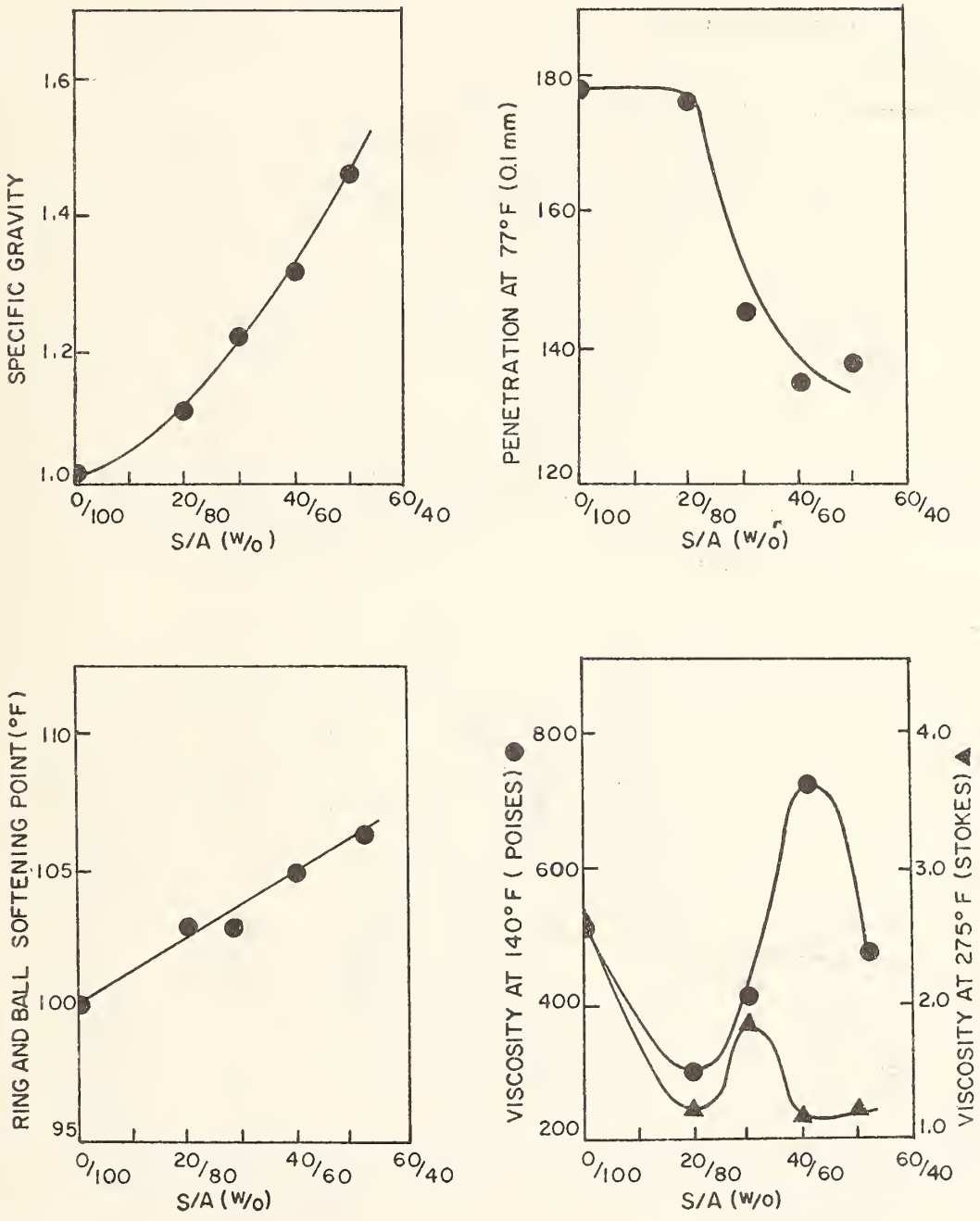

FIG. 52 -- SULPHUR-ASPHALT EMULSION PHYSICAL PROPERTIES
ET AC-5 ASPHALT CEMENT 285°F MIXING TEMPERATURE

°C = (F-32) x 5/9

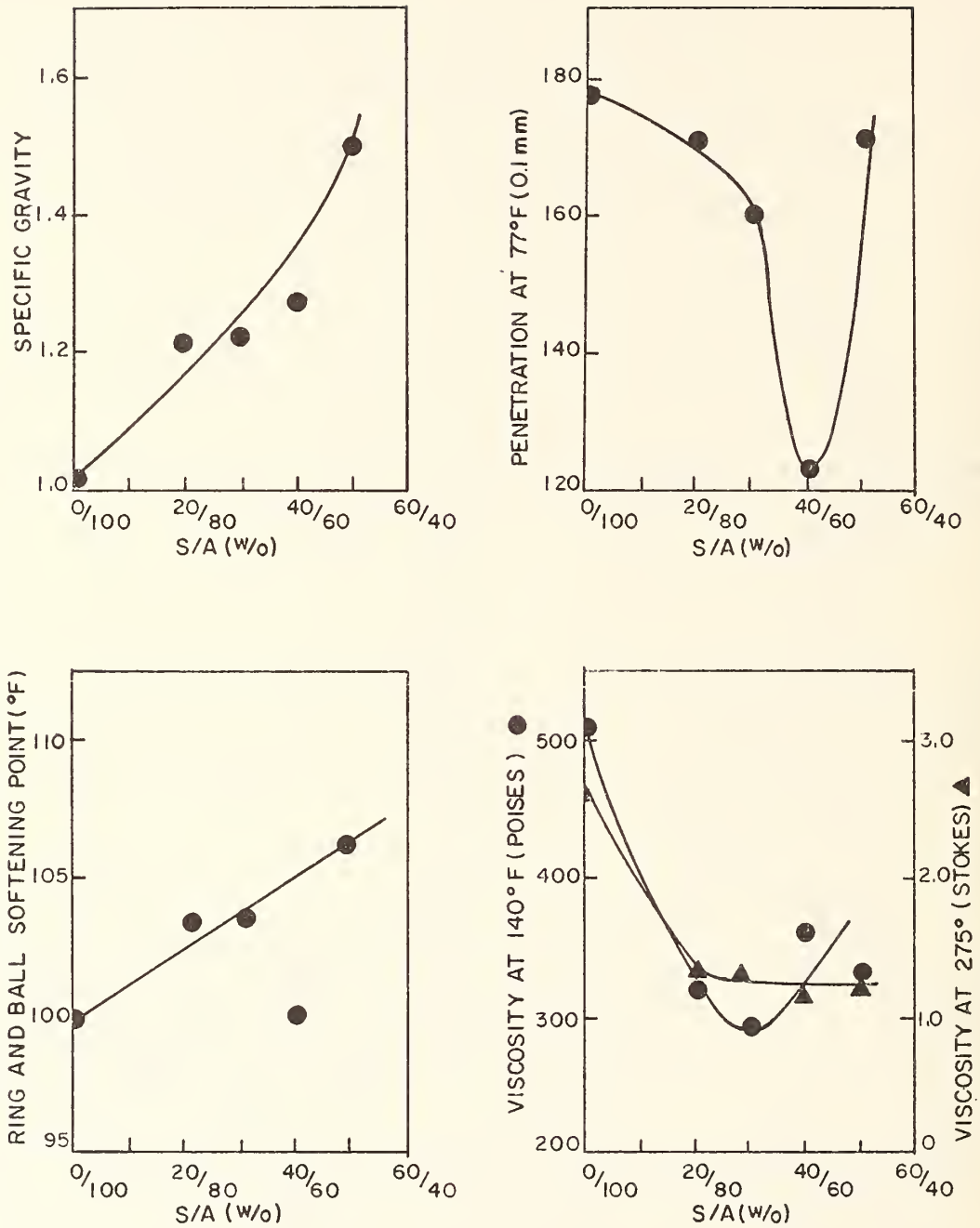

FIG. 53--SULPHUR-ASPHALT EMULSION PHYSICAL PROPERTIES ET AC-5 ASPHALT CEMENT 300°F MIXING TEMPERATURE

°C = (F-32) x 5/9

Appendix B. Continued

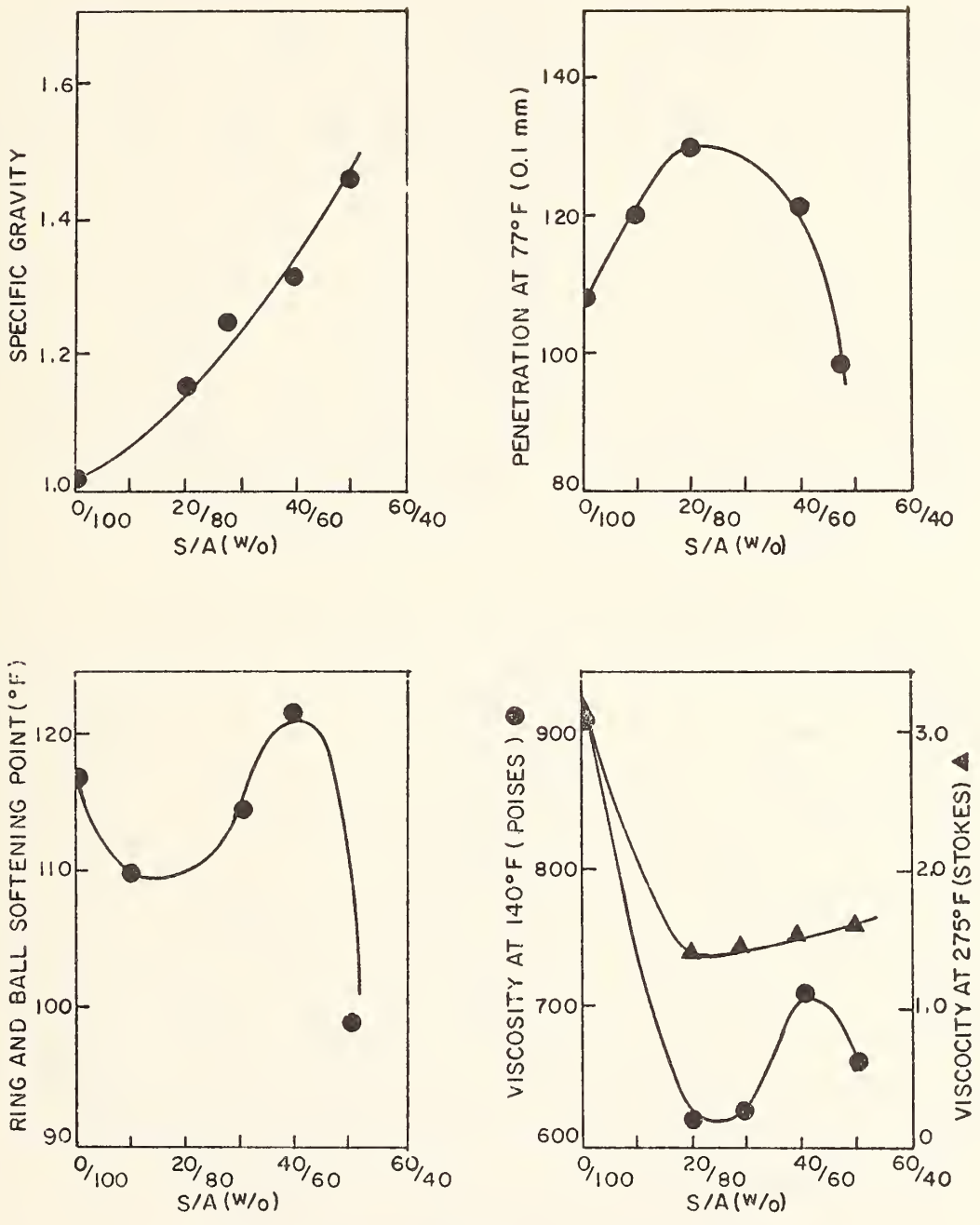

FIG. 54 SULPHUR-ASPHALT EMULSION PHYSICAL PROPERTIES
ET AC-10 ASPHALT CEMENT 285°F MIXING TEMPERATURE

°C = (F-32) x 5/9

Appendix B. Continued

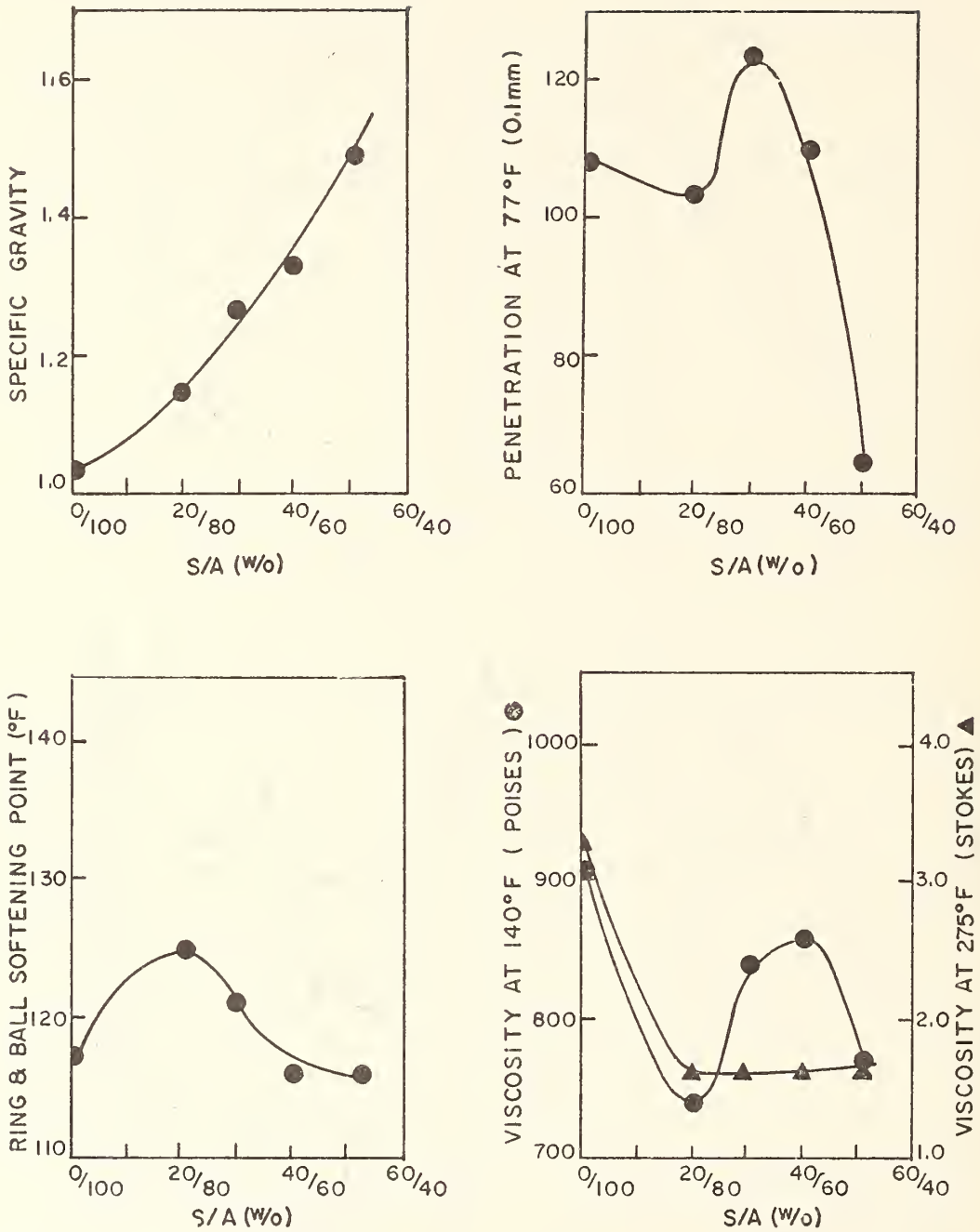

FIG. 55 SULPHUR-ASPHALT EMULSION PHYSICAL PROPERTIES ET AC-10 ASPHALT CEMENT 300°F MIXING TEMPERATURE

°C = (F-32) x 5/9

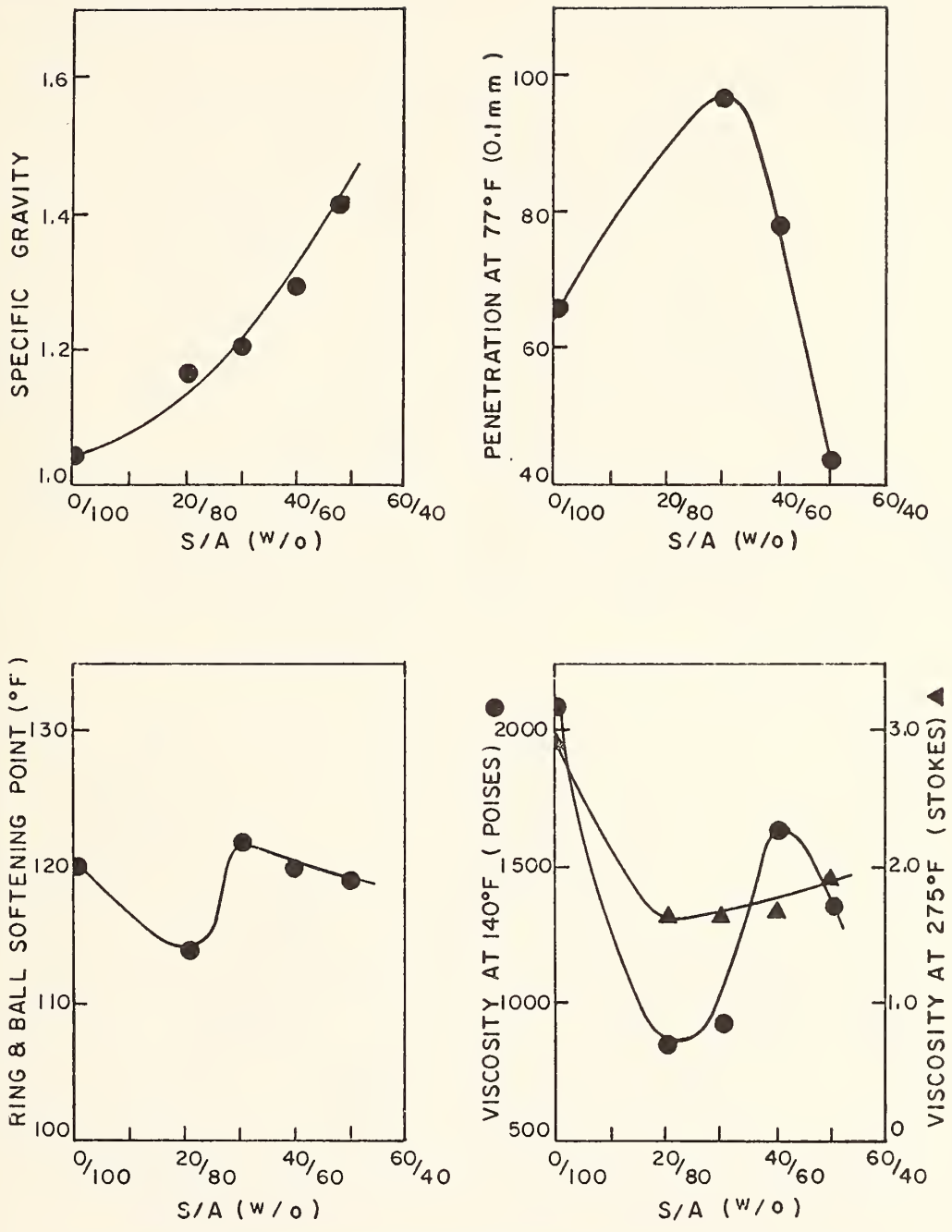

FIG. 56 SULPHUR-ASPHALT EMULSION PHYSICAL PROPERTIES ET AC-20 ASPHALT CEMENT 285°F MIXING TEMPERATURE

°C = (F-32) x 5/9

Appendix B. Continued

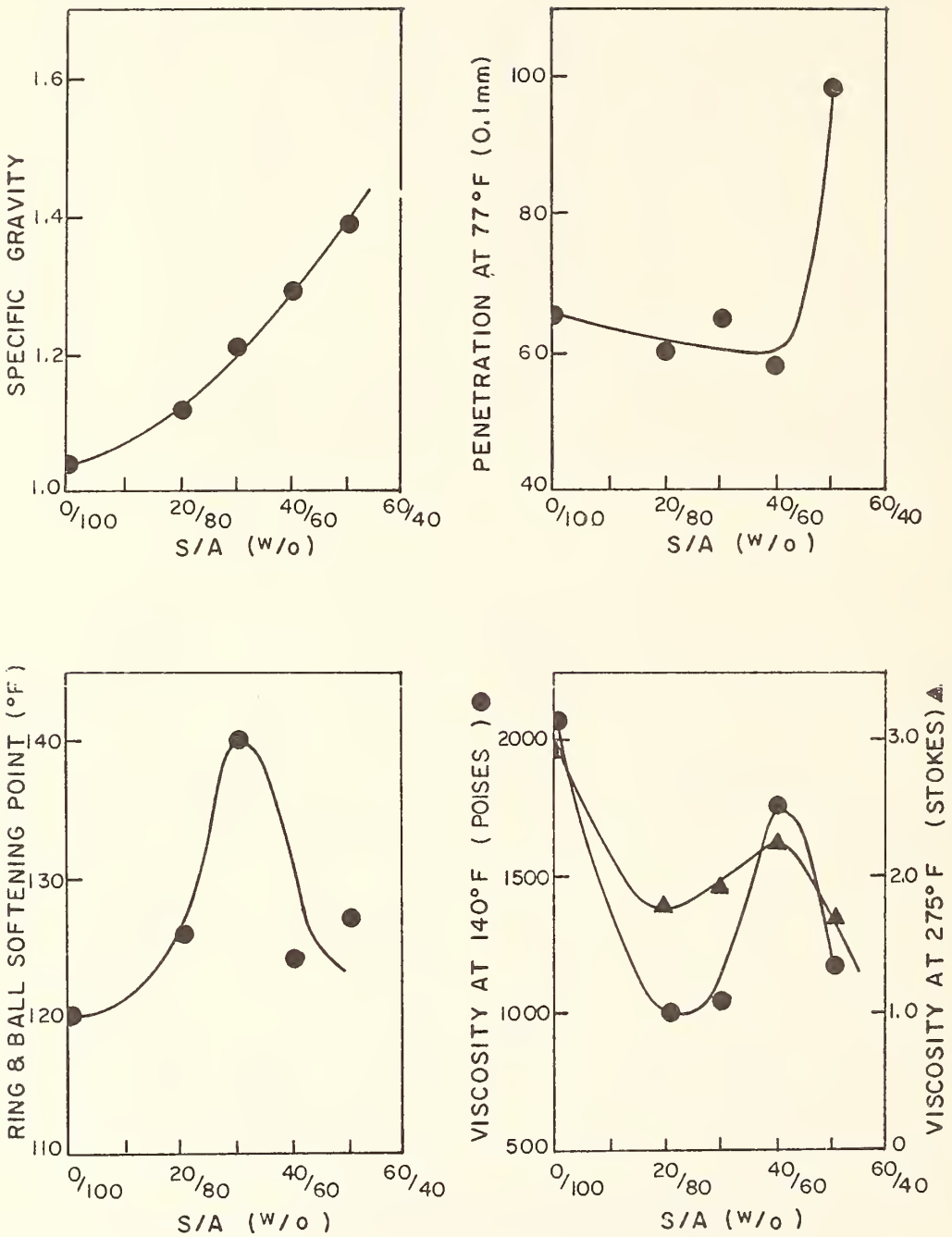

FIG. 57 SULPHUR-ASPHALT EMULSION PHYSICAL PROPERTIES ET AC-20 ASPHALT CEMENT 300°F MIXING TEMPERATURE

°C = (F-32) x 5/9

Appendix B. Continued

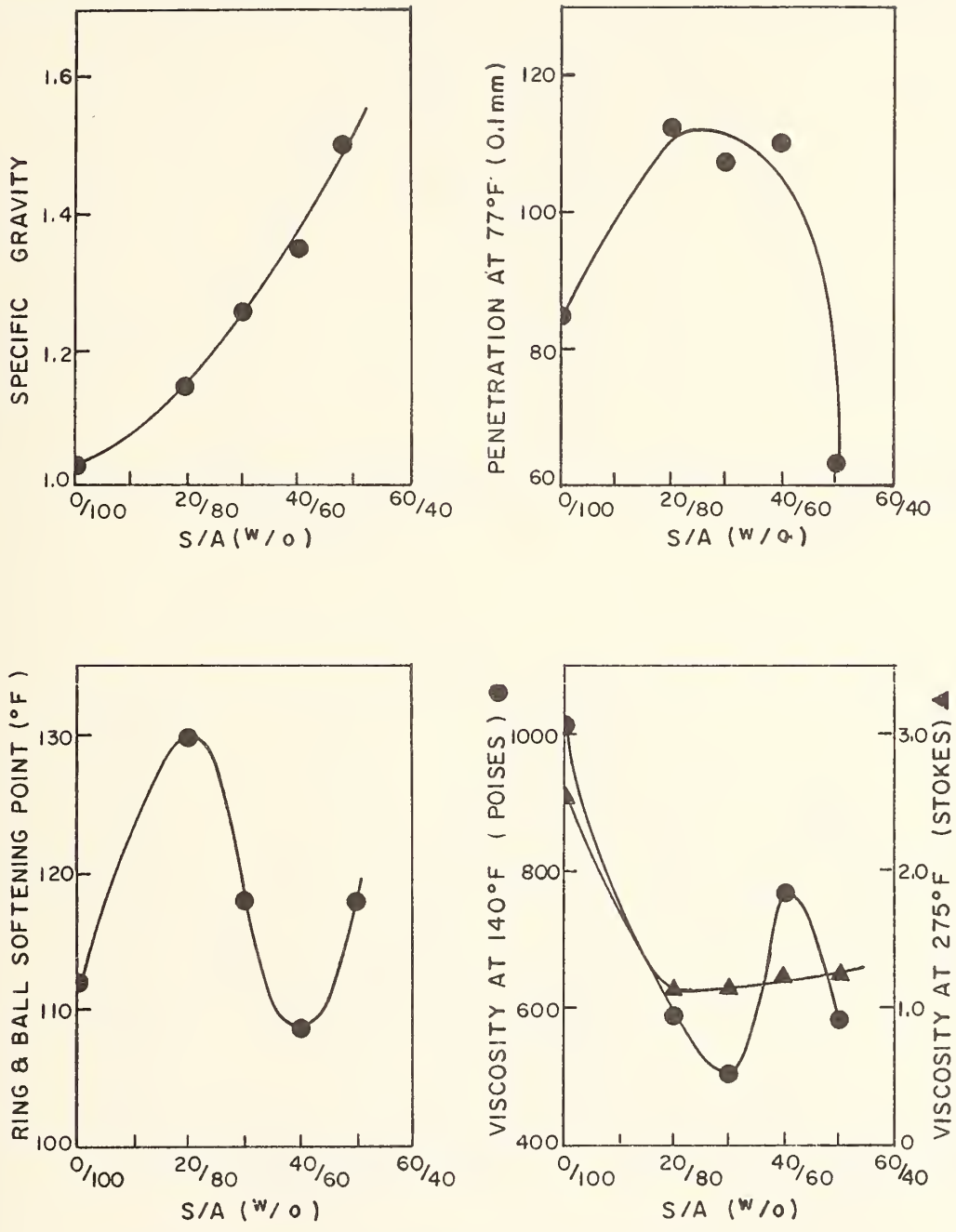

FIG. 58 SULPHUR-ASPHALT EMULSION PHYSICAL PROPERTIES
WT AC-10 ASPHALT CEMENT 285°F MIXING TEMPERATURE

°C = (F-32) x 5/9

Appendix B. Continued

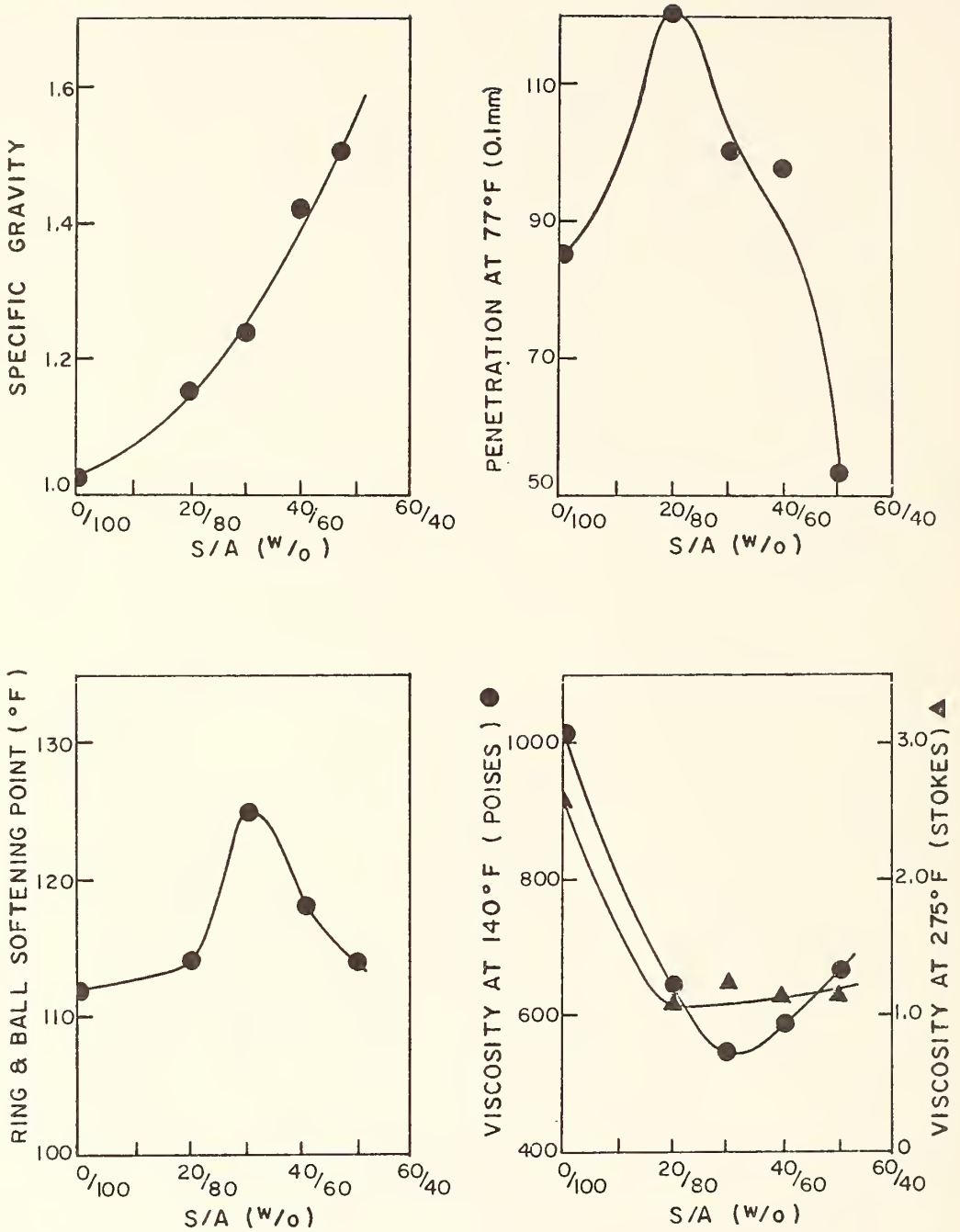

FIG. 59 SULPHUR-ASPHALT EMULSION PHYSICAL PROPERTIES
WT AC-10 ASPHALT CEMENT 300°F MIXING TEMPERATURE

°C = (F-32) x 5/9

Appendix B. Continued

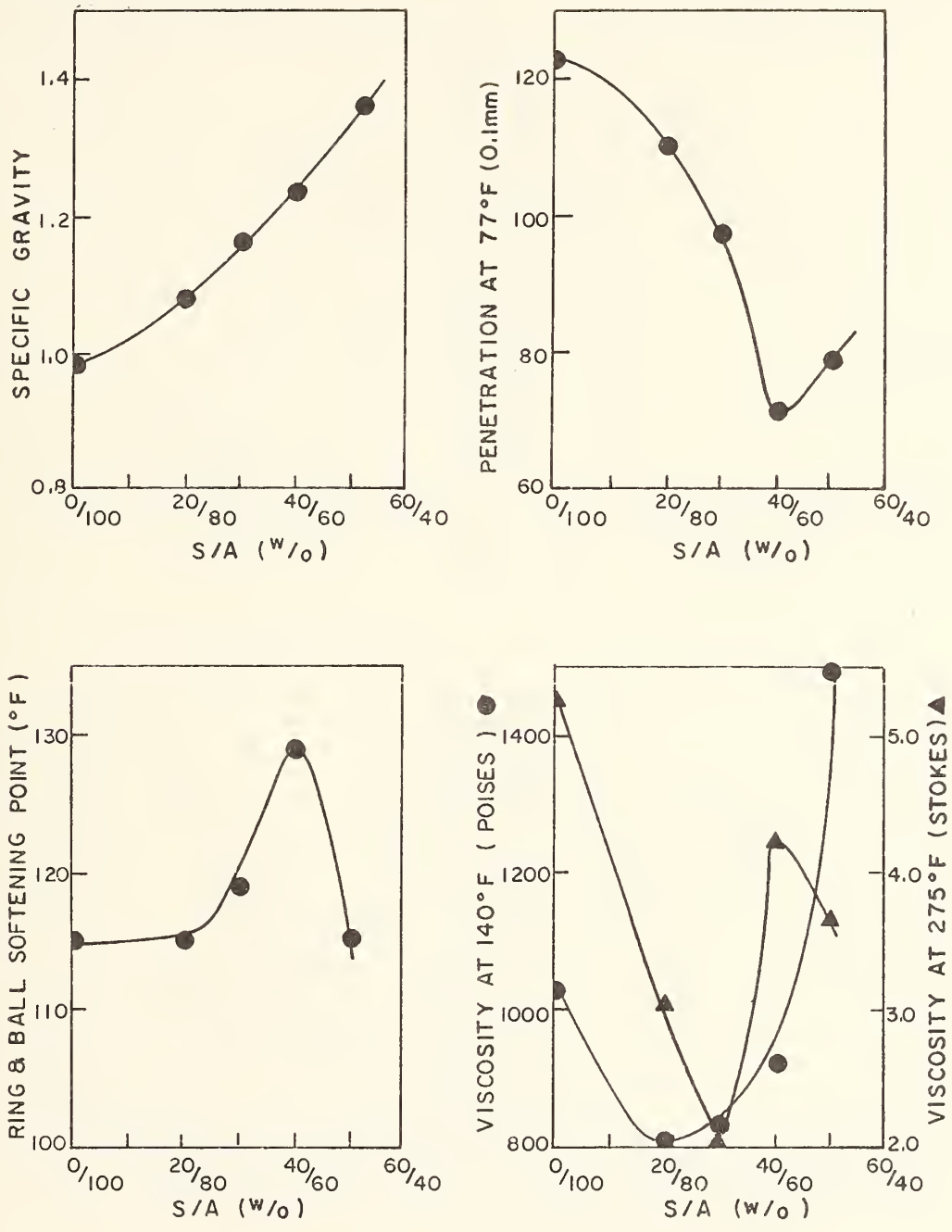

FIG. 60 SULPHUR-ASPHALT EMULSION PHYSICAL PROPERTIES
DS AC-10 ASPHALT CEMENT 285°F MIXING TEMPERATURE

°C = (F-32) x 5/9

Appendix B. Continued

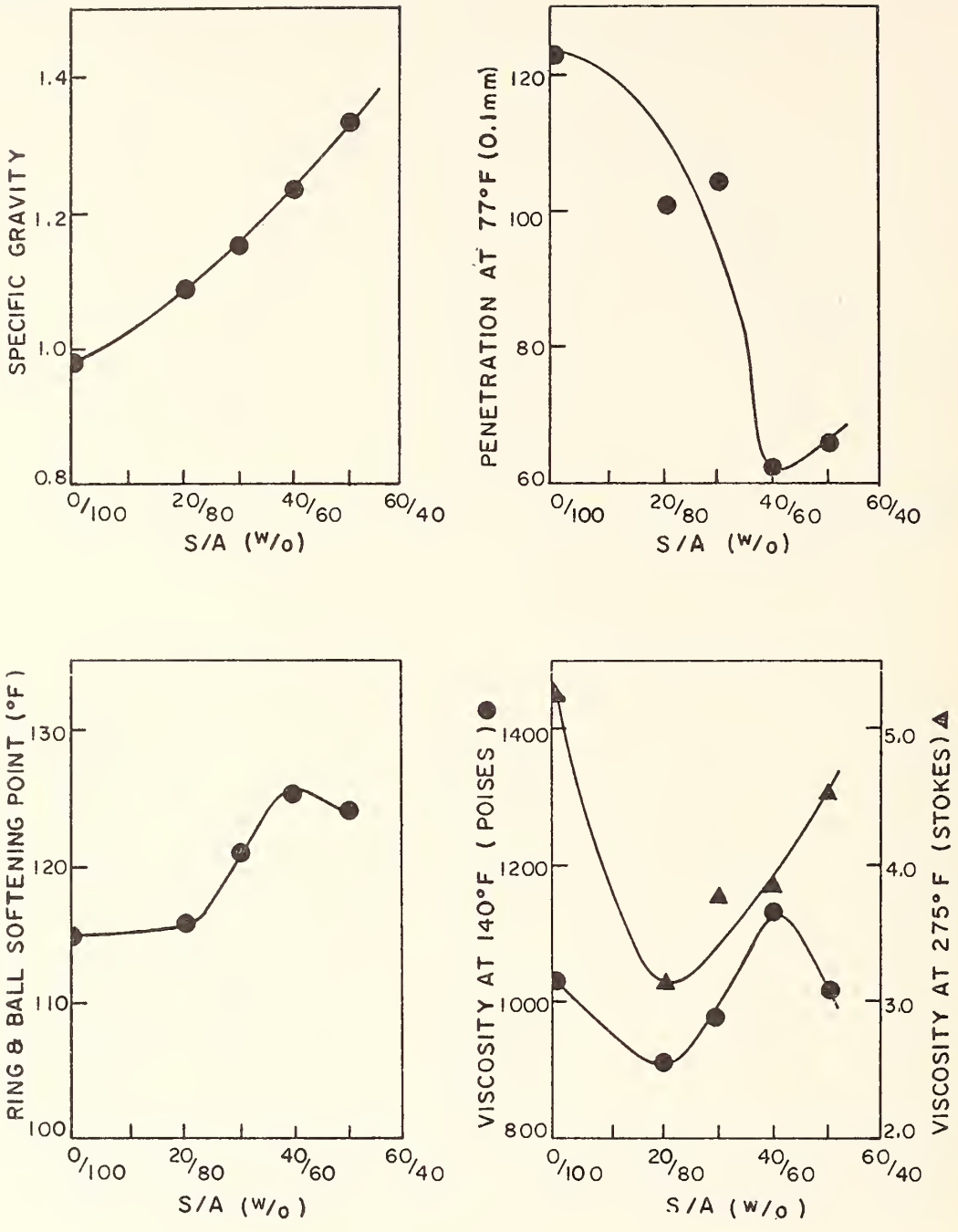

FIG. 61 SULPHUR-ASPHALT EMULSION PHYSICAL PROPERTIES
DS AC-10 ASPHALT CEMENT 300°F MIXING TEMPERATURE

$°C = (F-32) \times 5/9$

Appendix B. Continued

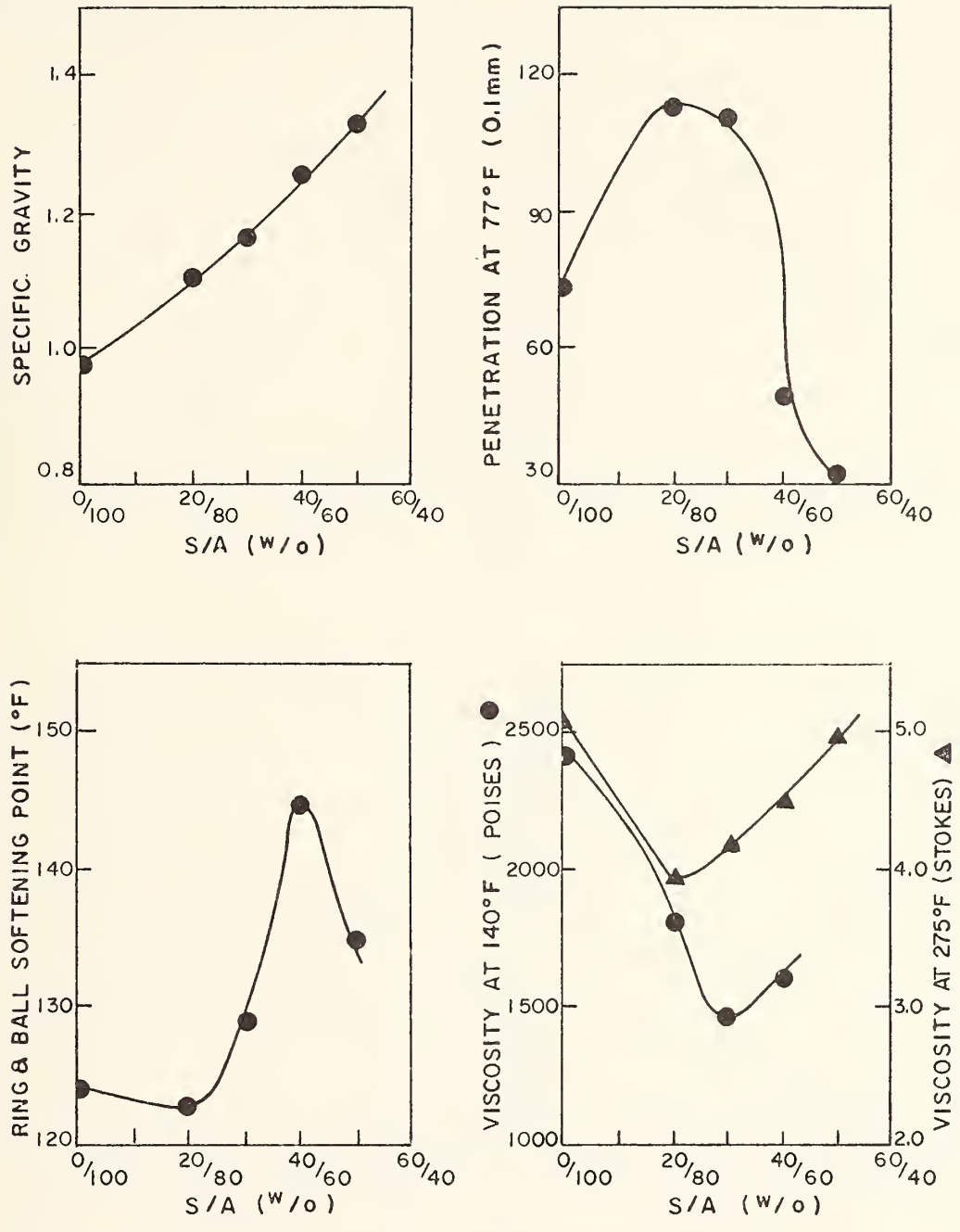

FIG. 62 SULPHUR-ASPHALT EMULSION PHYSICAL PROPERTIES
DS AC-20 ASPHALT CEMENT 285°F MIXING TEMPERATURE

°C = (F-32) x 5/9

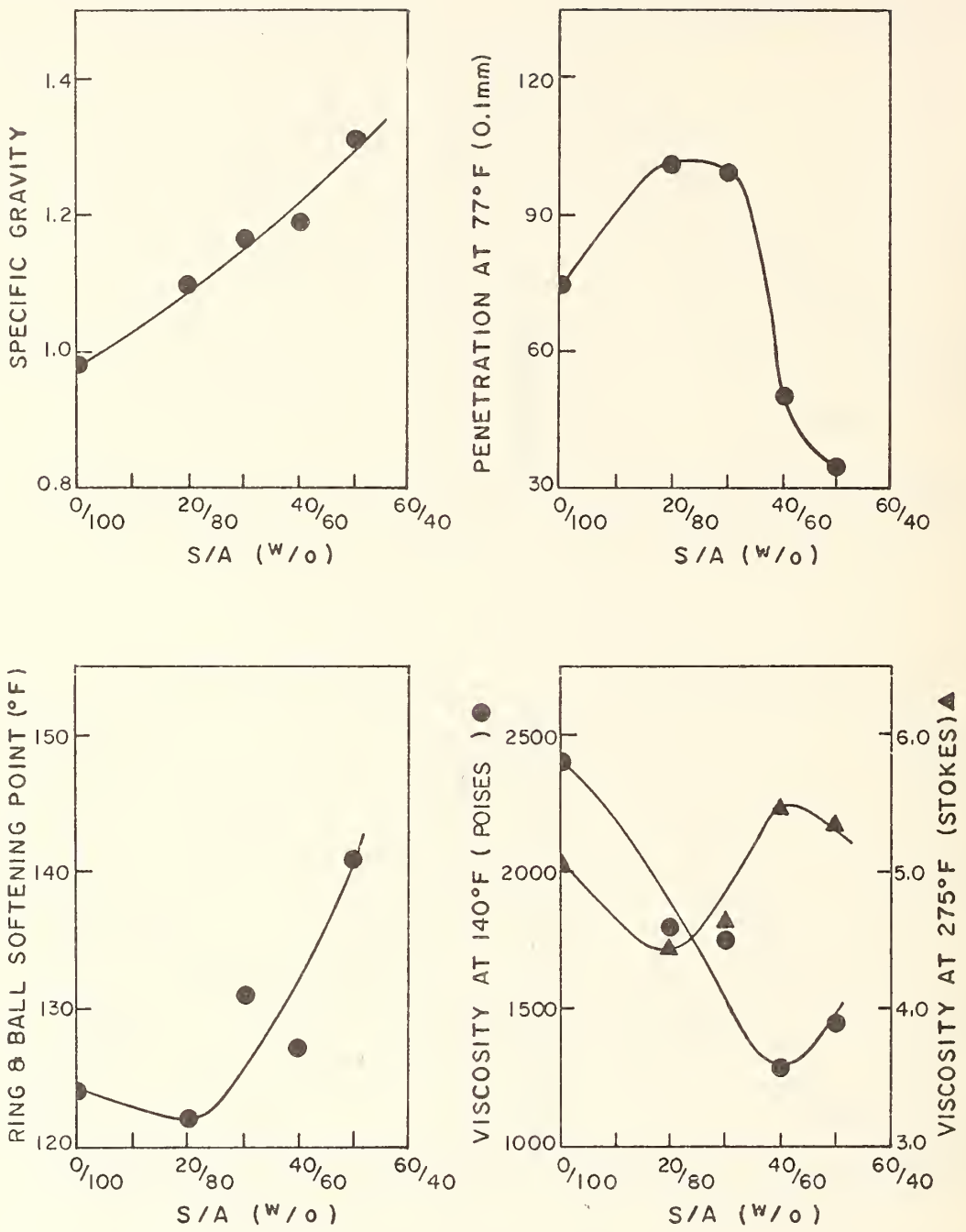

FIG. 63 SULPHUR-ASPHALT EMULSION PHYSICAL PROPERTIES
DS AC-20 ASPHALT CEMENT 300°F MIXING TEMPERATURE

°C = (F-32) x 5/9

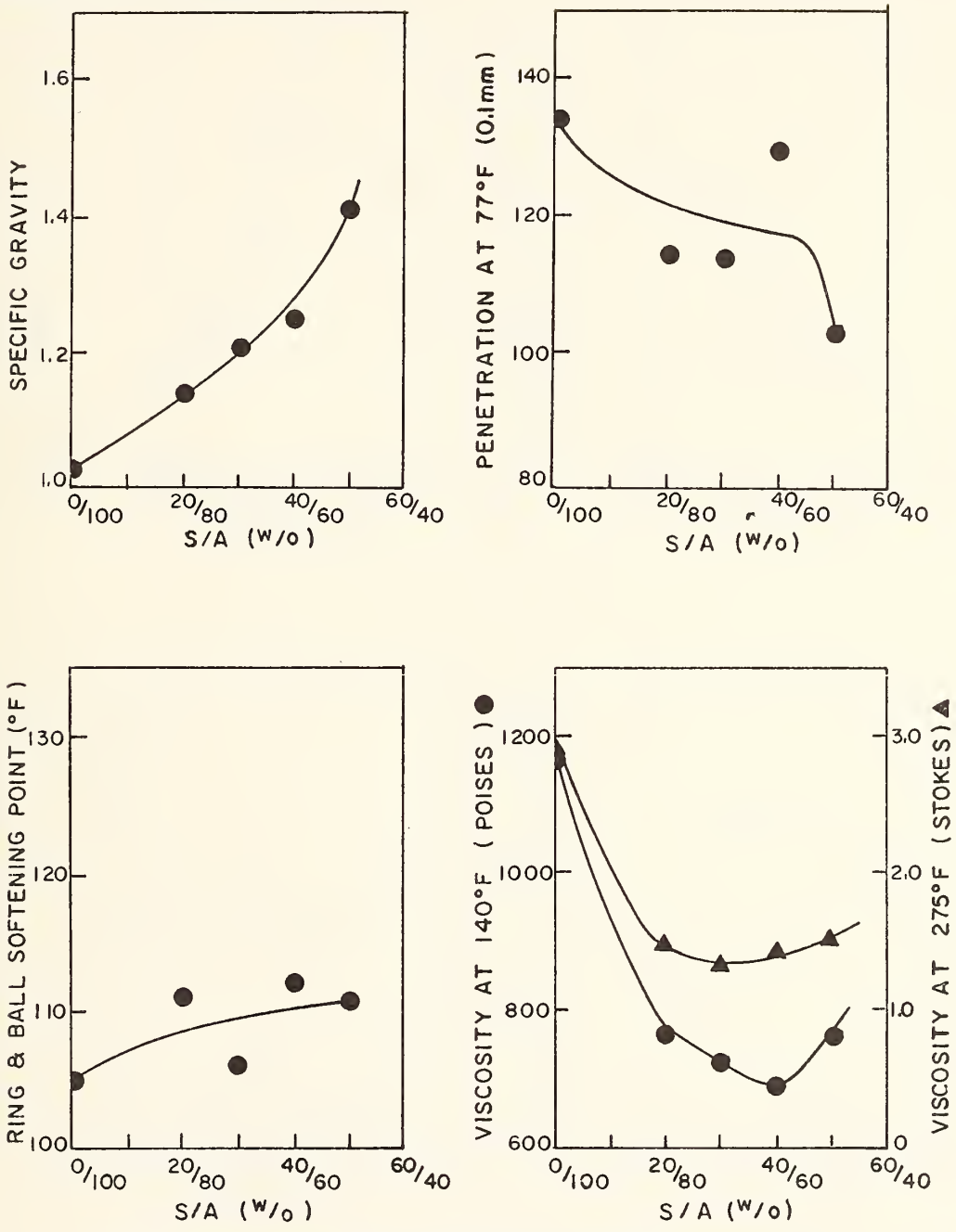

FIG. 64 SULPHUR-ASPHALT EMULSION PHYSICAL PROPERTIES
SM AC-10 ASPHALT CEMENT 285°F MIXING TEMPERATURE

°C = (F-32) x 5/9

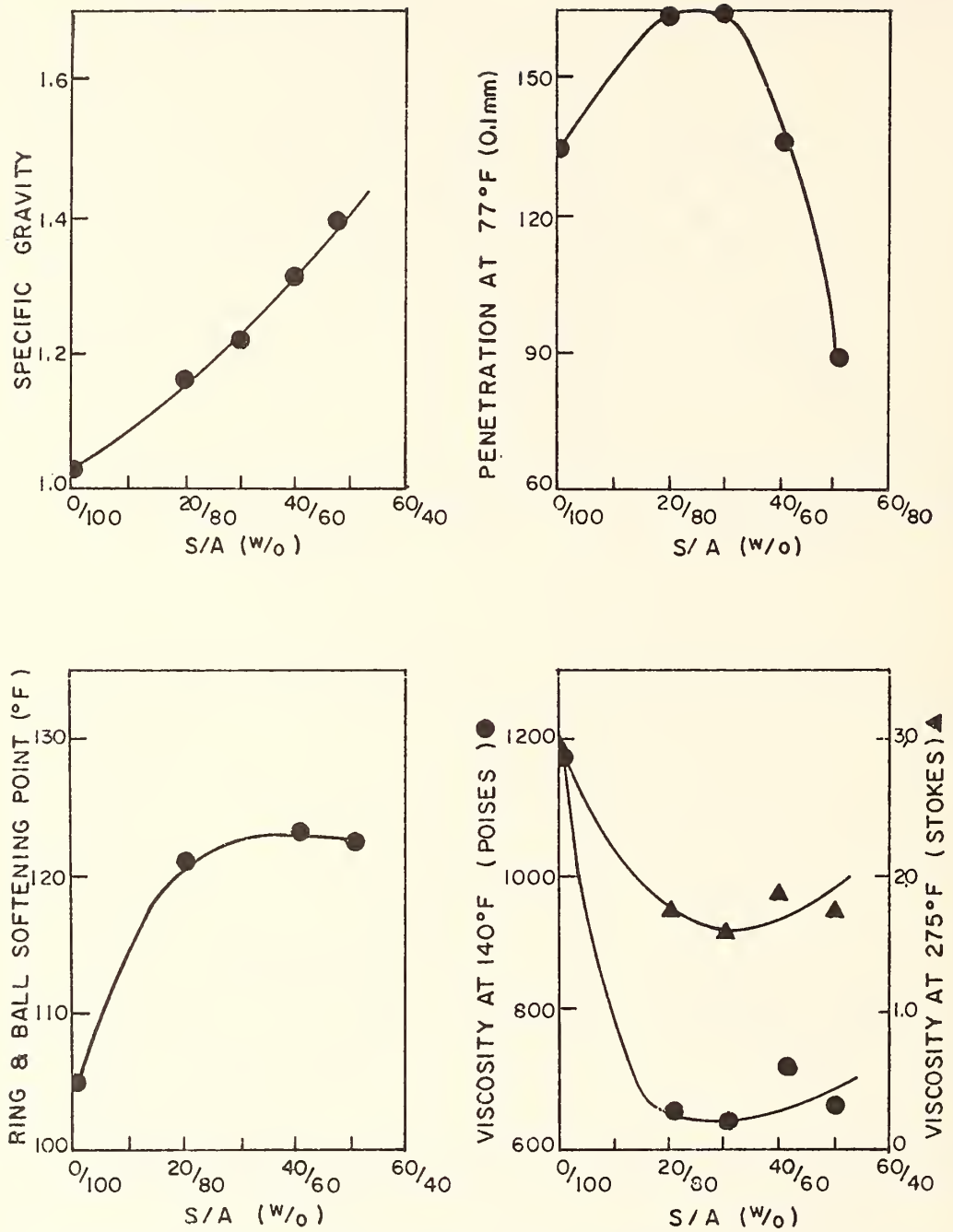

FIG. 65 SULPHUR-ASPHALT EMULSION PHYSICAL PROPERTIES
SM AC-10 ASPHALT CEMENT 300°F MIXING TEMPERATURE

°C = (F-32) x 5/9

Appendix B. Continued

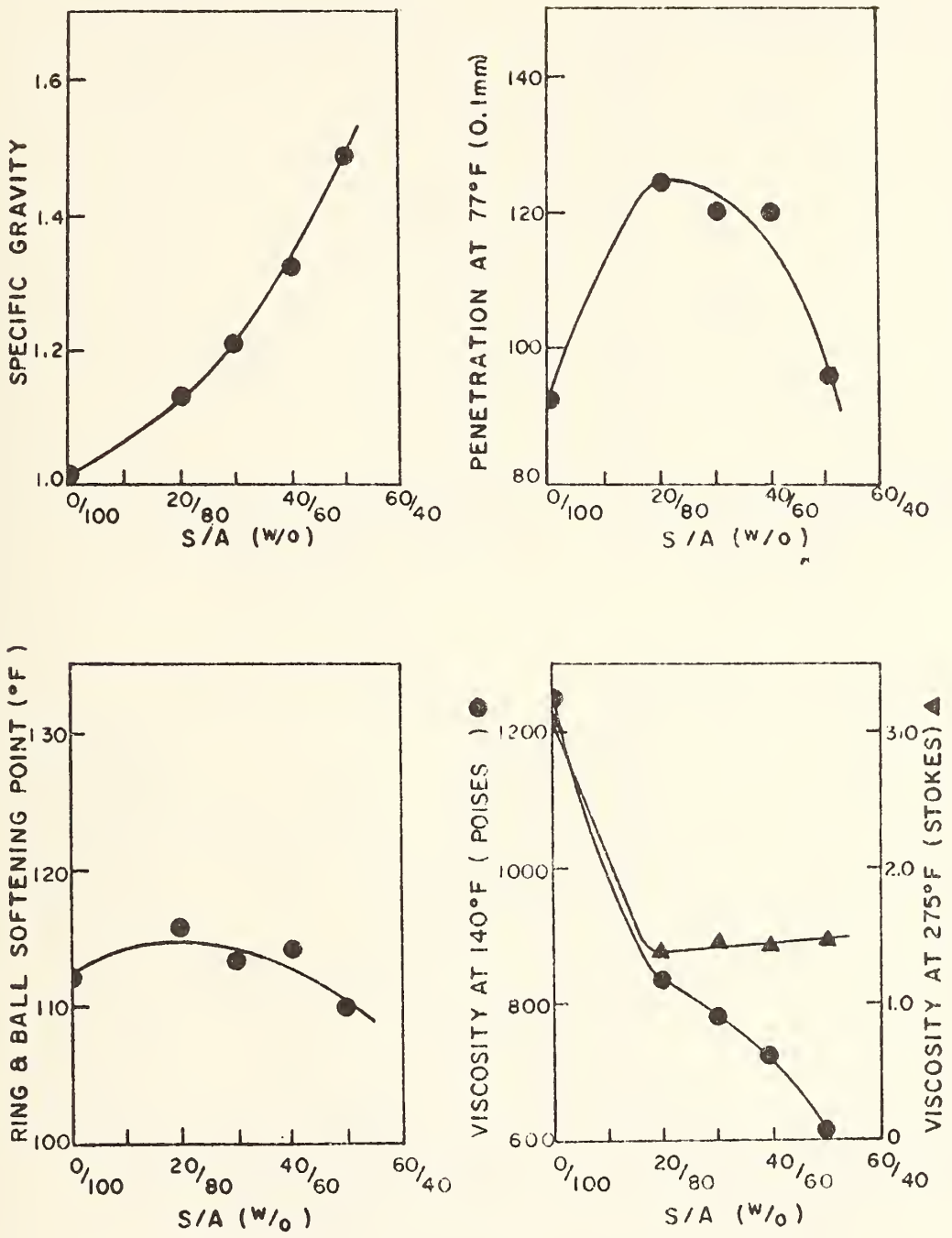

FIG. 66 SULPHUR-ASPHALT EMULSION PHYSICAL PROPERTIES
DENV AC-10 ASPHALT CEMENT 255°F MIXING TEMPERATURE

°C = (F-32) x 5/9

Appendix B. Continued

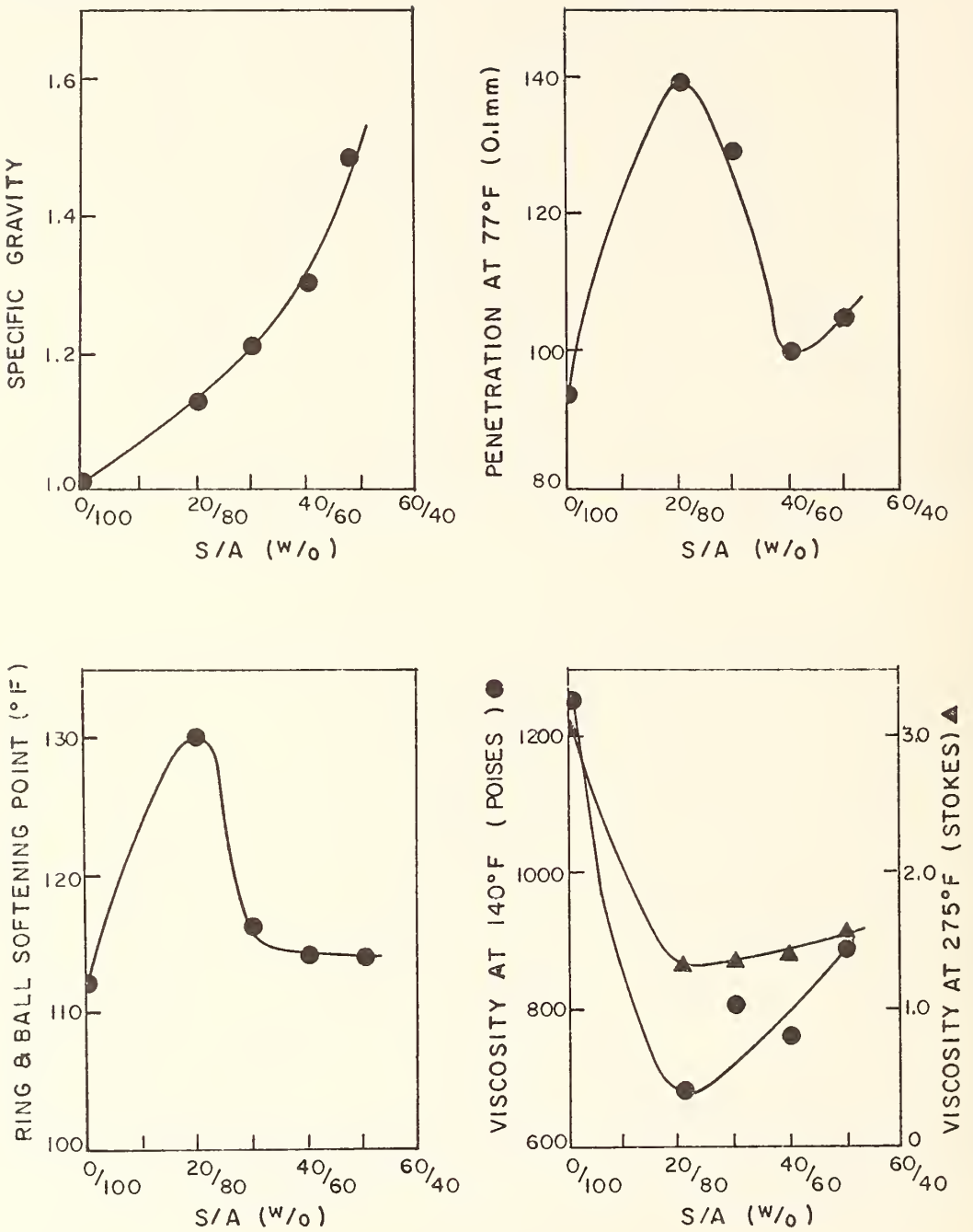

FIG. 67 SULPHUR-ASPHALT EMULSION PHYSICAL PROPERTIES
DENV AC-10 ASPHALT CEMENT 300°F MIXING TEMPERATURE

°C = (F-32) x 5/9

Appendix B. Continued

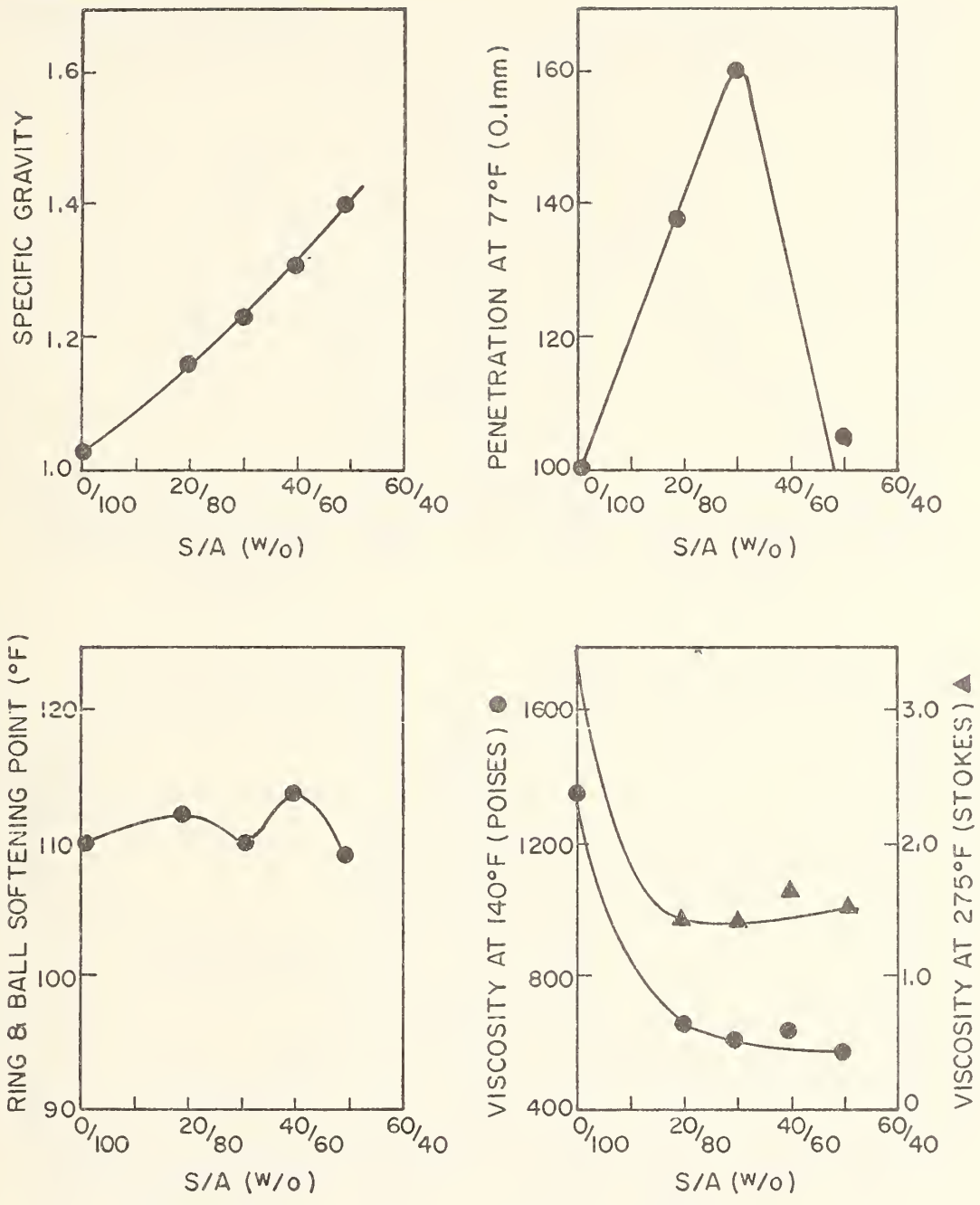

FIG. 68 SULPHUR-ASPHALT EMULSION PHYSICAL PROPERTIES
WC AC-10 ASPHALT CEMENT 285°F MIXING TEMPERATURE

°C = (F-32) x 5/9

Appendix B. Continued

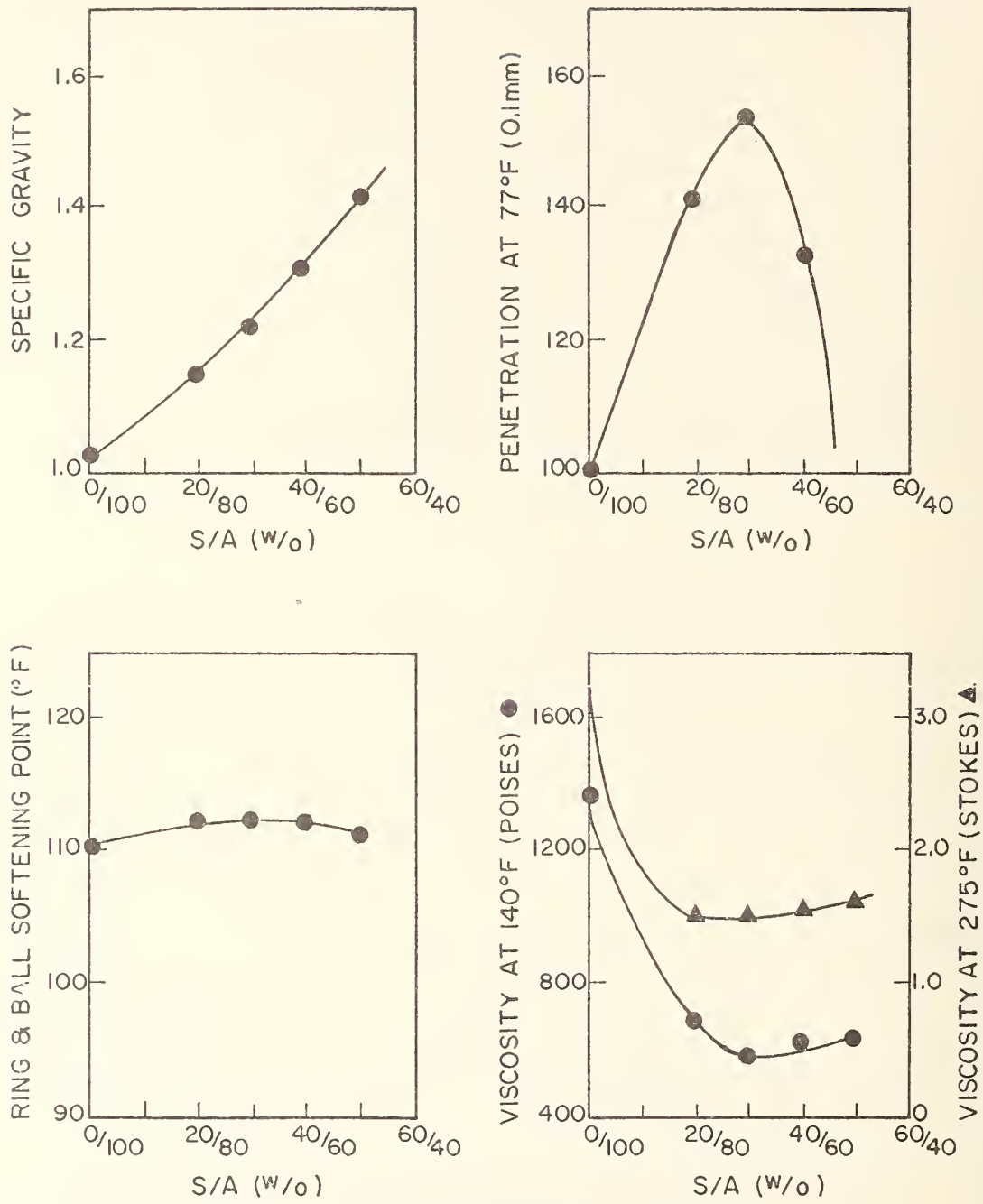

FIG. 69 SULPHUR-ASPHALT EMULSION PHYSICAL PROPERTIES
WC AC-10 ASPHALT CEMENT 300°F MIXING TEMPERATURE

°C = (F-32) x 5/9

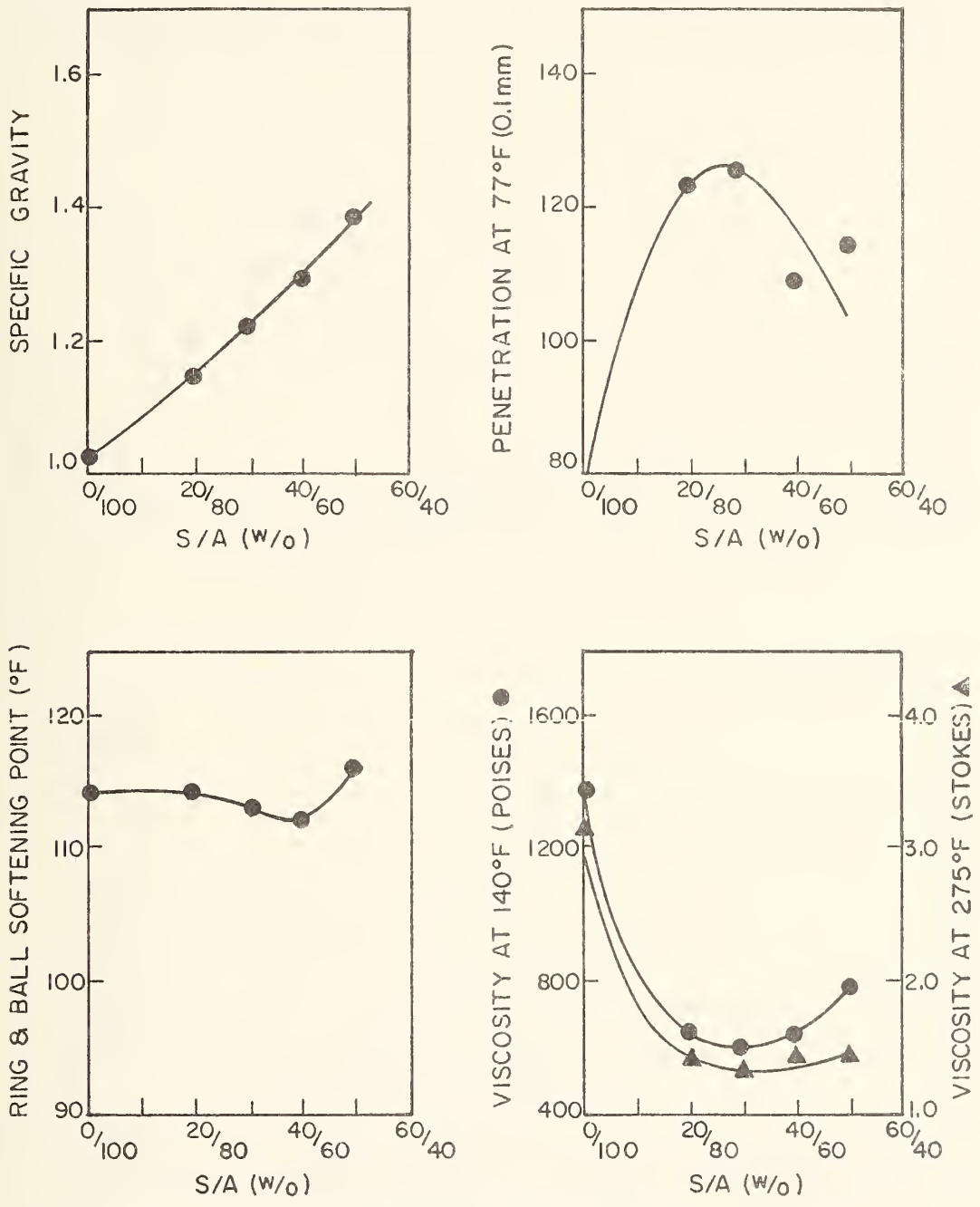

FIG. 70 SULPHUR-ASPHALT EMULSION PHYSICAL PROPERTIES
ME AC-10 ASPHALT CEMENT 285°F MIXING TEMPERATURE

°C = (F-32) x 5/9

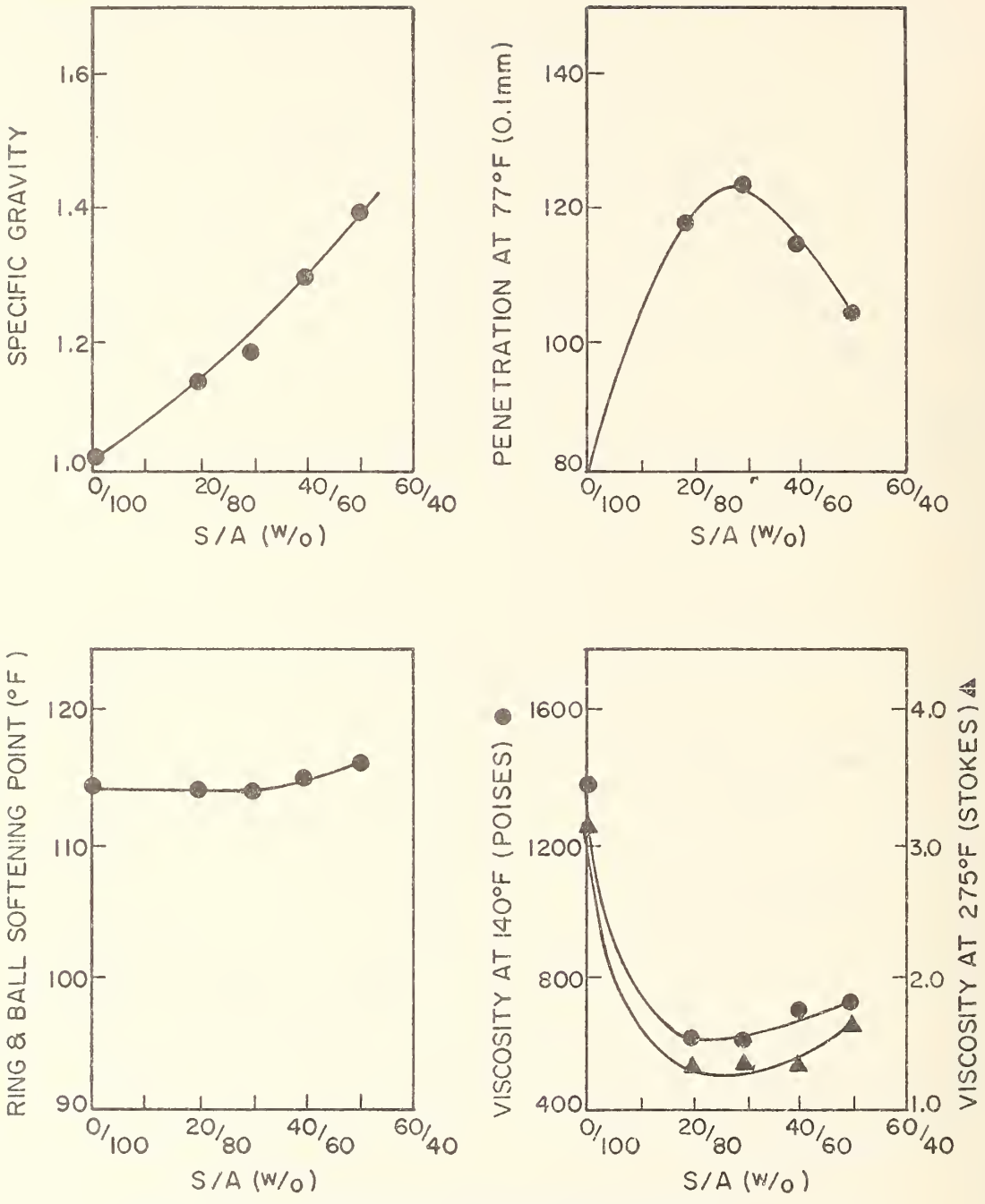

FIG. 71 SULPHUR-ASPHALT EMULSION PHYSICAL PROPERTIES
ME AC-10 ASPHALT CEMENT 300°F MIXING TEMPERATURE

°C = (F-32) x 5/9

Appendix C. Sulphur Settling Heights of Sulphur-Asphalt Emulsions

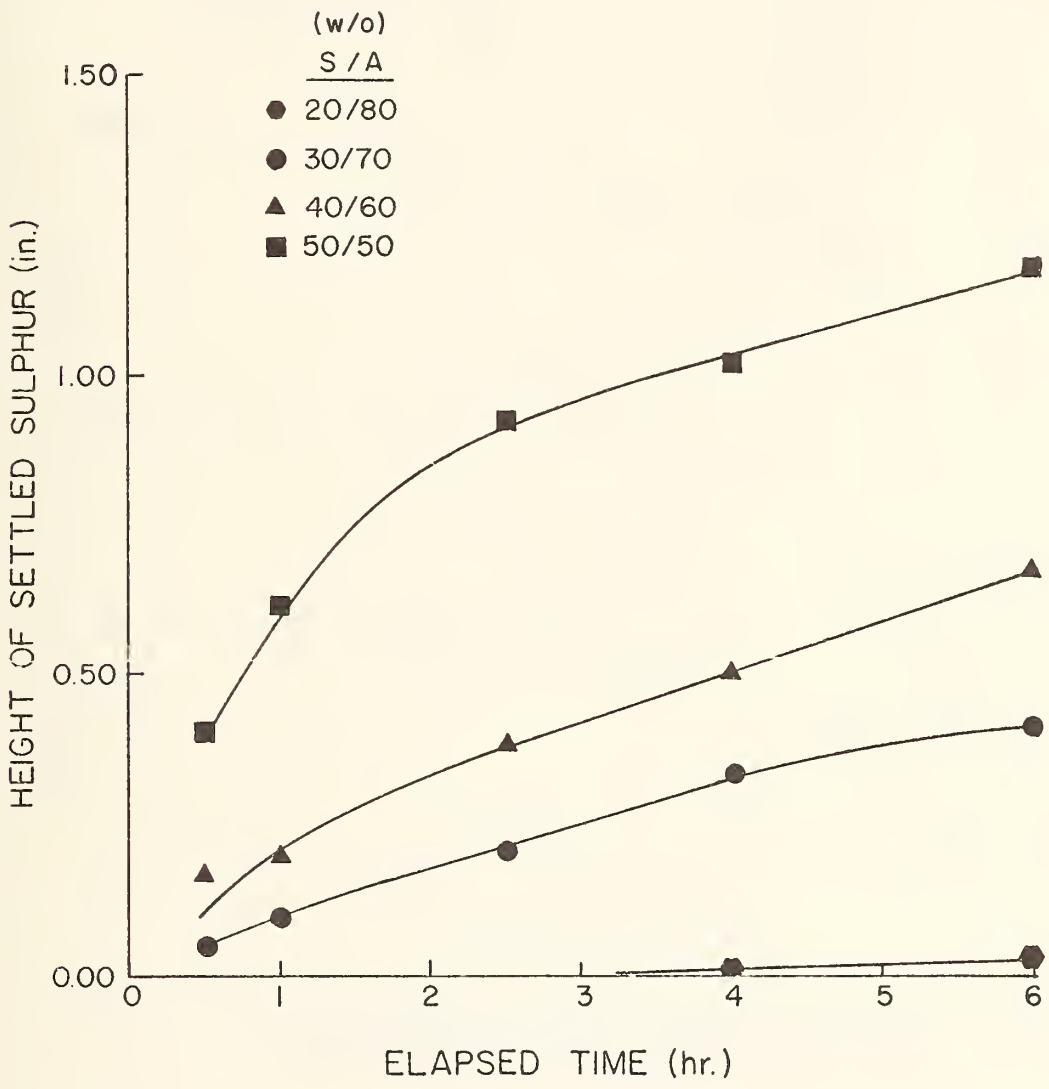

FIG. 72 SULPHUR SETTLING HEIGHT OF SULPHUR-ASPHALT EMULSION ET AC-5 ASPHALT CEMENT 285°F (140.6°C) Mixing and Oven Storage Temperature

1 inch = 25.4 mm

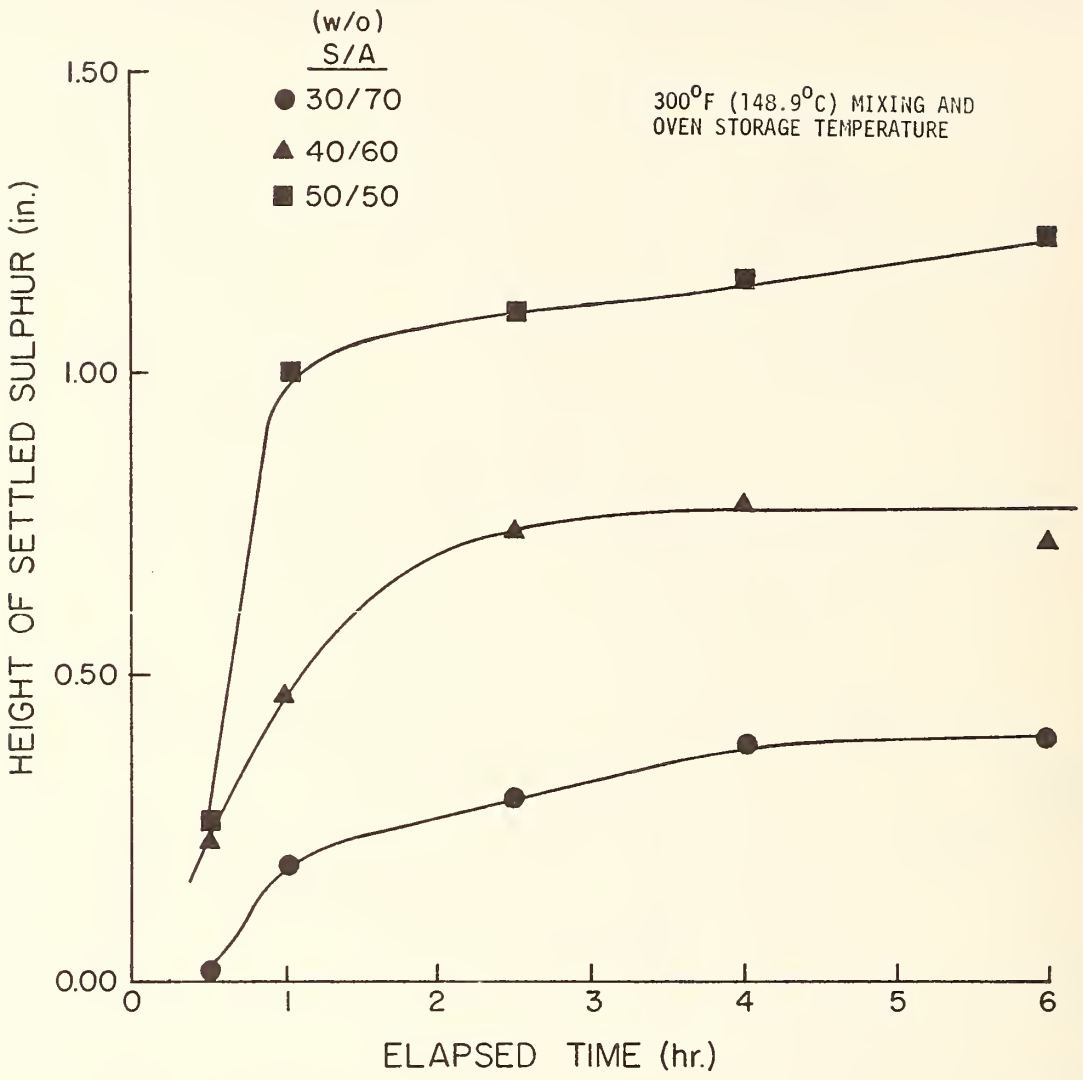

FIG. 73 SULPHUR SETTLING HEIGHT OF SULPHUR-ASPHALT EMULSION ET AC-5 ASPHALT CEMENT 300°F (148.9°C) Mixing and Oven Storage Temperature

1 inch = 25.4 mm

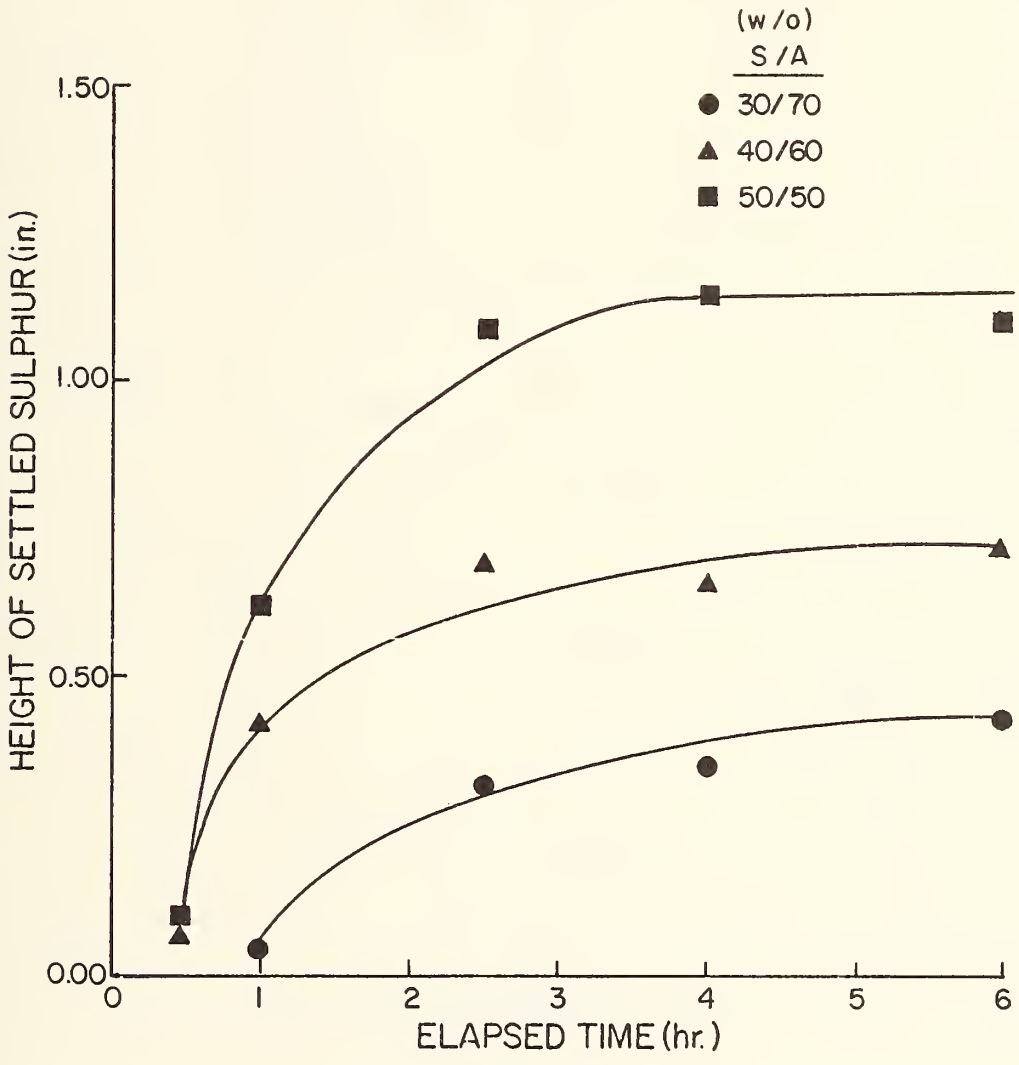

FIG. 74 SULPHUR SETTLING HEIGHT OF SULPHUR-ASPHALT EMULSION ET AC-10 ASPHALT CEMENT 285°F (141.4°C) Mixing and Oven Storage Temperature

1 inch = 25.4 mm

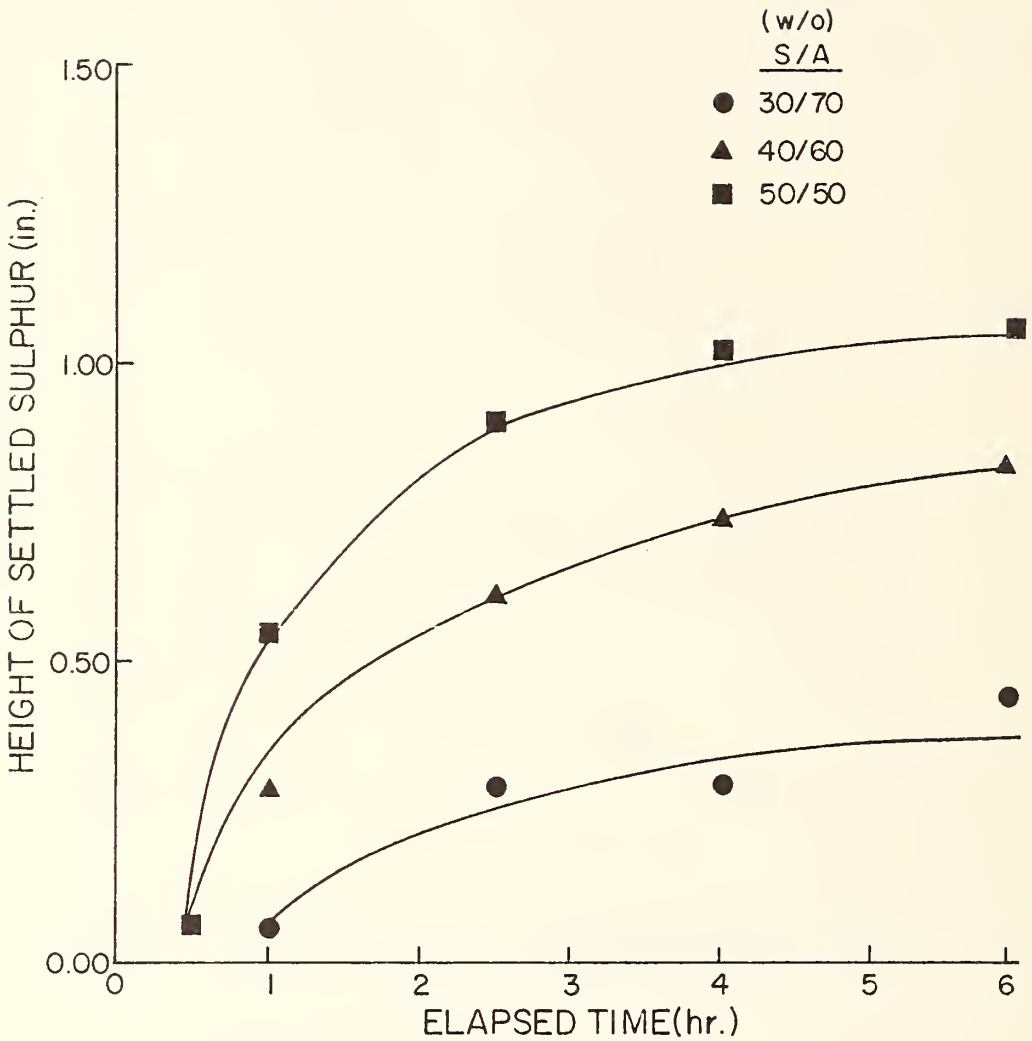

FIG. 75 SULPHUR SETTLING HEIGHT OF SULPHUR-ASPHALT EMULSION ET AC-10 ASPHALT CEMENT 300°F (148.9°C) Mixing and Oven Storage Temperature

1 incn = 25.4 mm

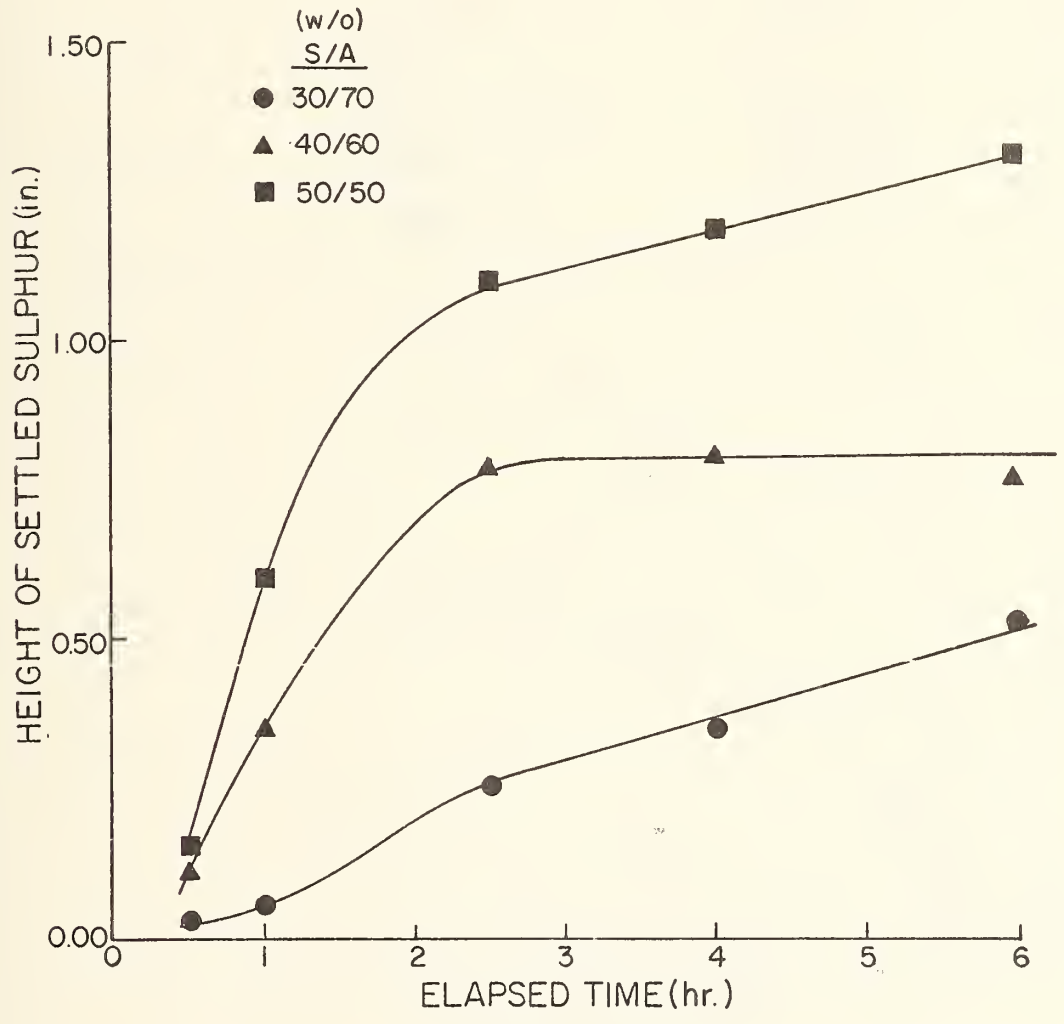

FIG. 76 SULPHUR SETTLING HEIGHT OF SULPHUR-ASPHALT EMULSION ET AC-20 ASPHALT CEMENT 285°F (140.6°C) Mixing and Oven Storage Temperature

1 inch = 25.4 mm

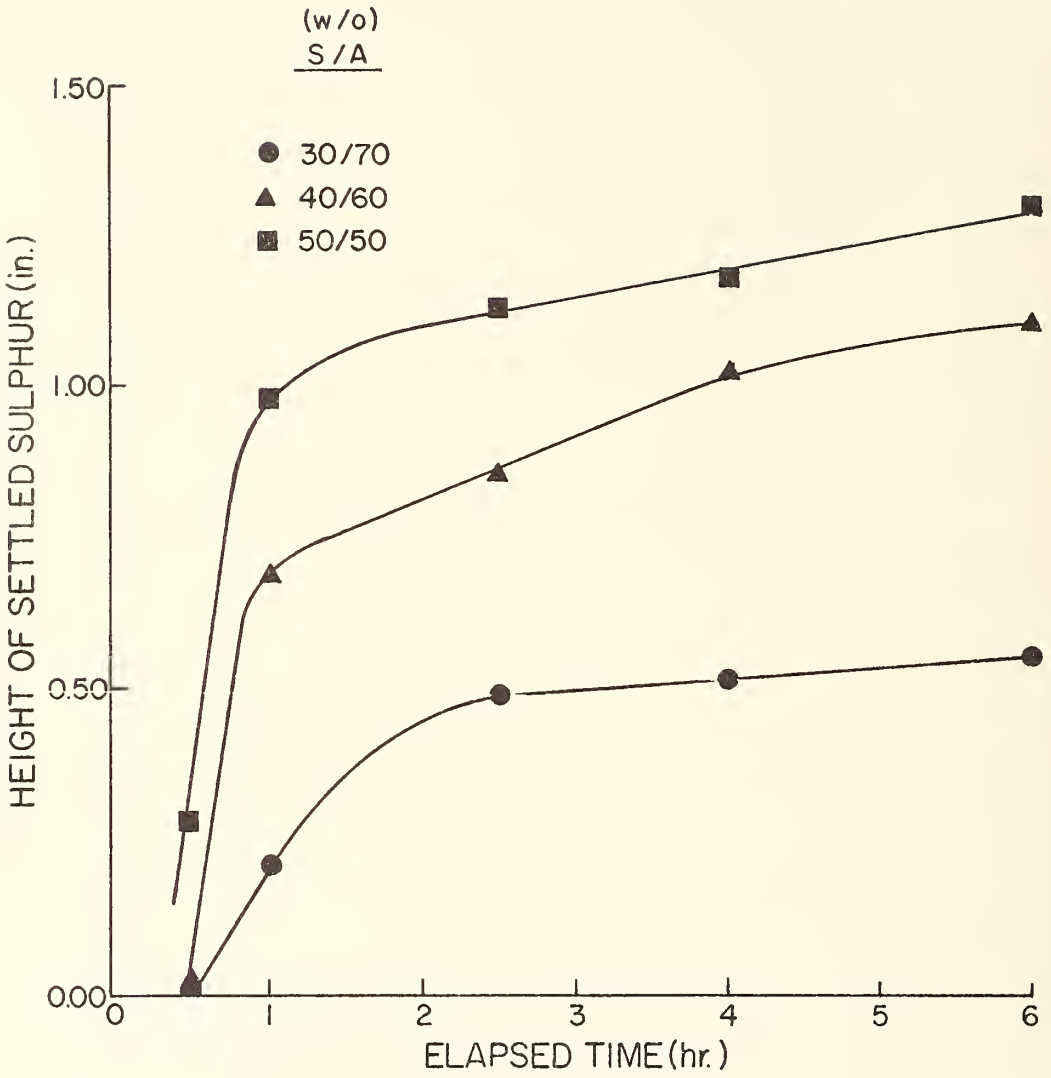

FIG. 77 SULPHUR SETTLING HEIGHT OF SULPHUR-ASPHALT EMULSION ET AC-20 ASPHALT CEMENT 300°F (148.9°C) Mixing and Oven Storage Temperature

1 inch = 25.4 mm

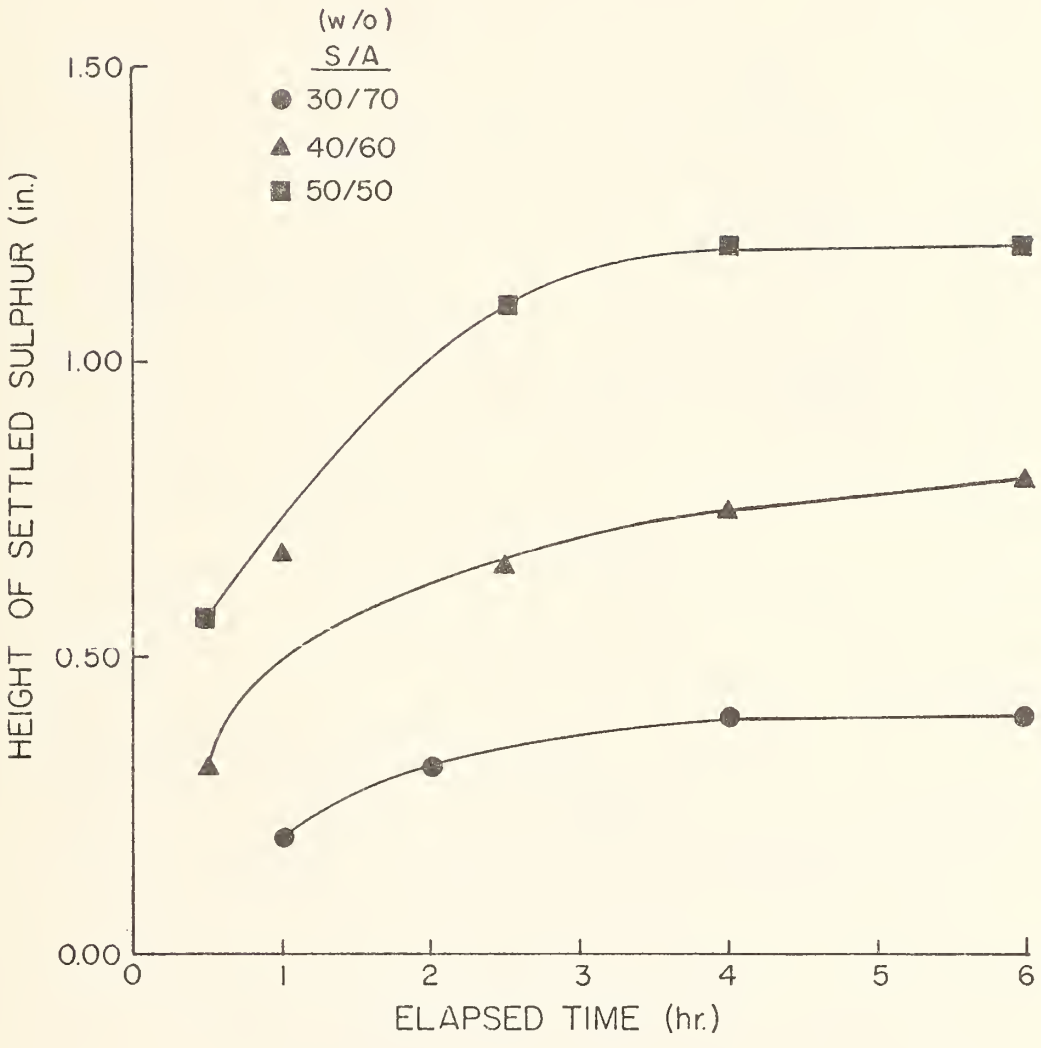

FIG. 78 SULPHUR SETTLING HEIGHT OF SULPHUR-ASPHALT EMULSION
WT AC-10 ASPHALT CEMENT 285.°F (141.4°C) Mixing and Oven Storage Temperature

1 inch = 25.4 mm

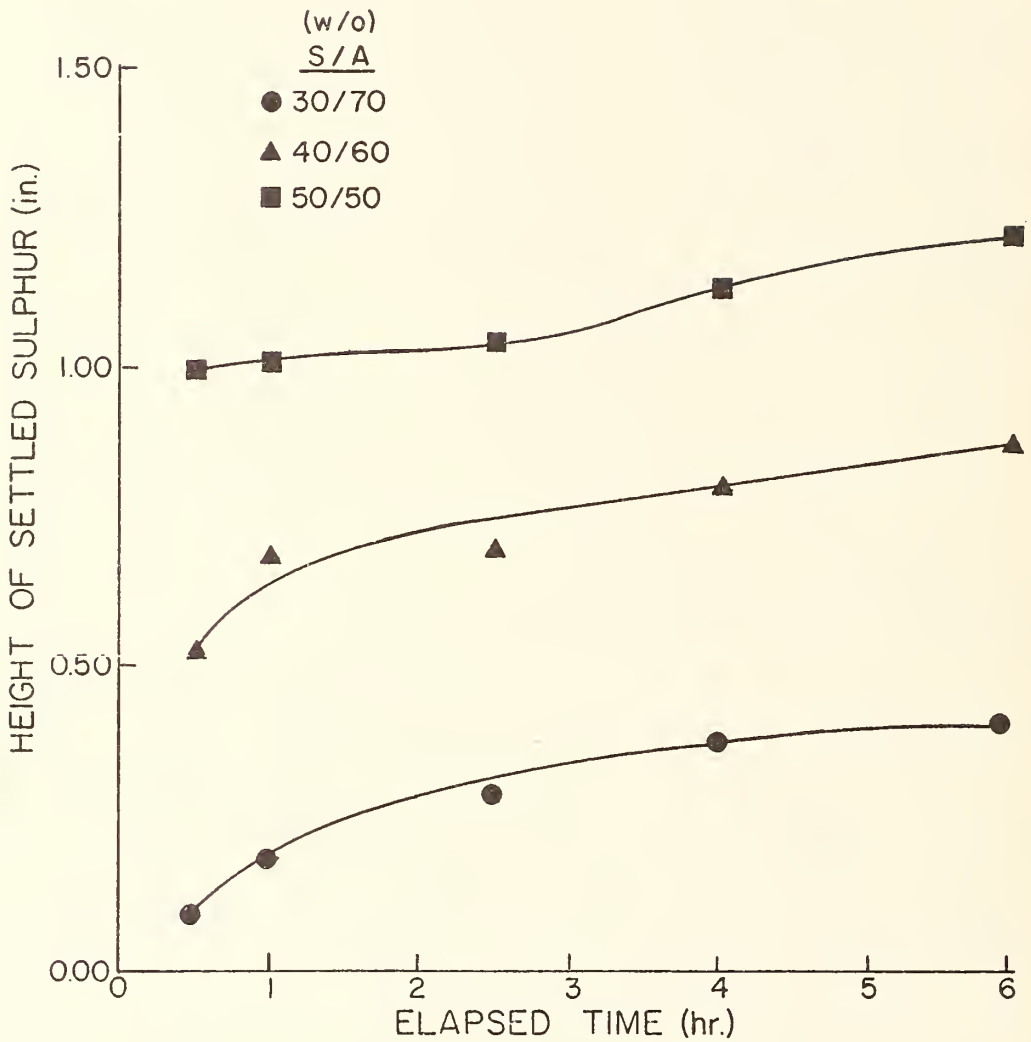

Fig. 79 -- SULPHUR SETTLING HEIGHT OF SULPHUR-ASPHALT EMULSION WT AC-10 ASPHALT CEMENT 300°F (148.9°C) Mixing and Oven Storage Temperature

1 inch = 25.4 mm

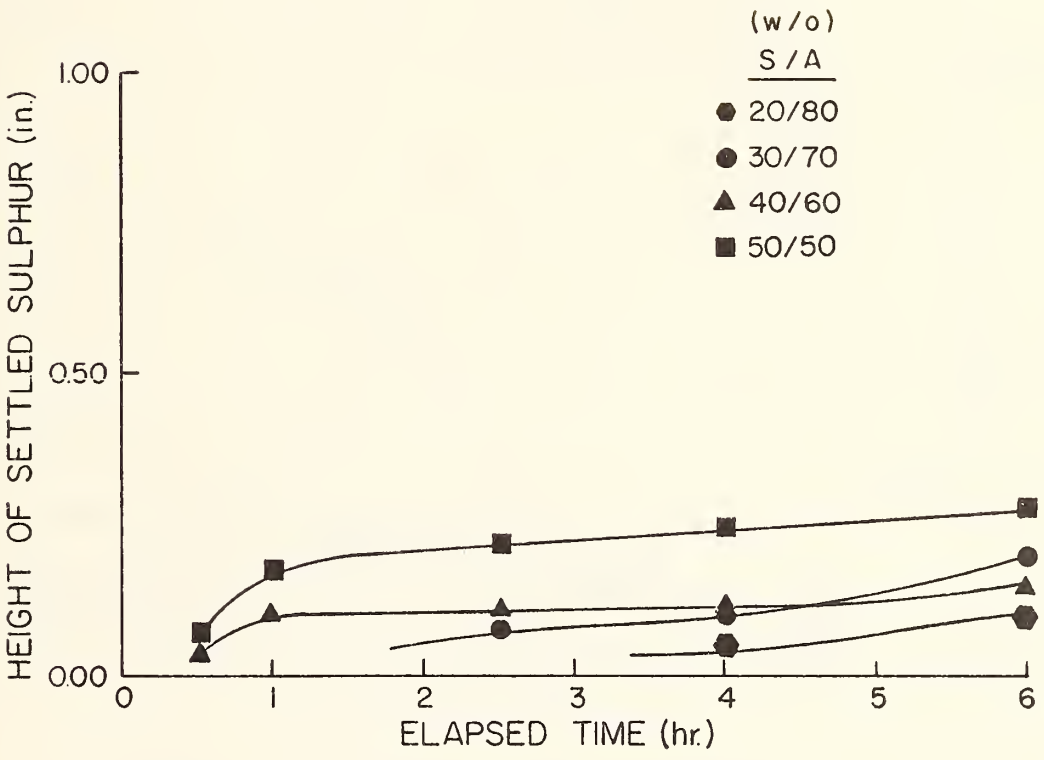

Fig. 80 SULPHUR SETTLING HEIGHT OF SULPHUR-ASPHALT EMULSION
DS AC-10 ASPHALT CEMENT 285°F(140.6°C) Mixing and Oven
Storage Temperature

1 inch = 25.4 mm

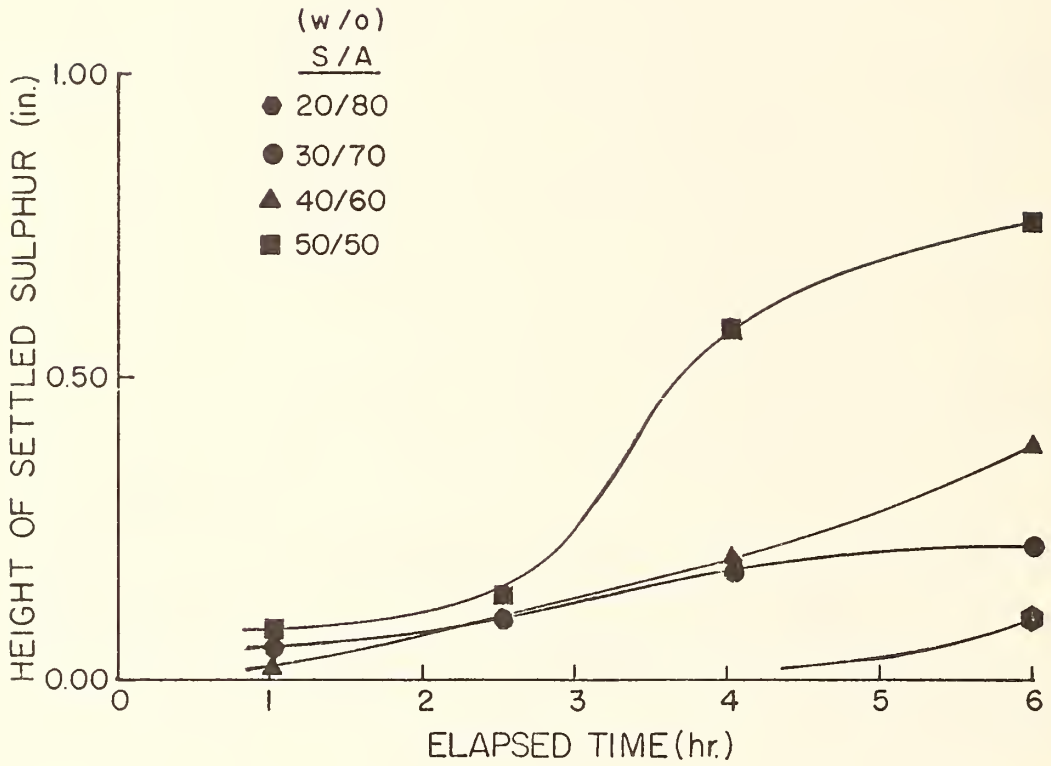

Fig. 81 SULPHUR SETTLING HEIGHT OF SULPHUR-ASPHALT EMULSION DS AC-10 ASPHALT CEMENT 300°F (148.9°C) Mixing and Oven Storage Temperature

1 inch = 25.4 mm

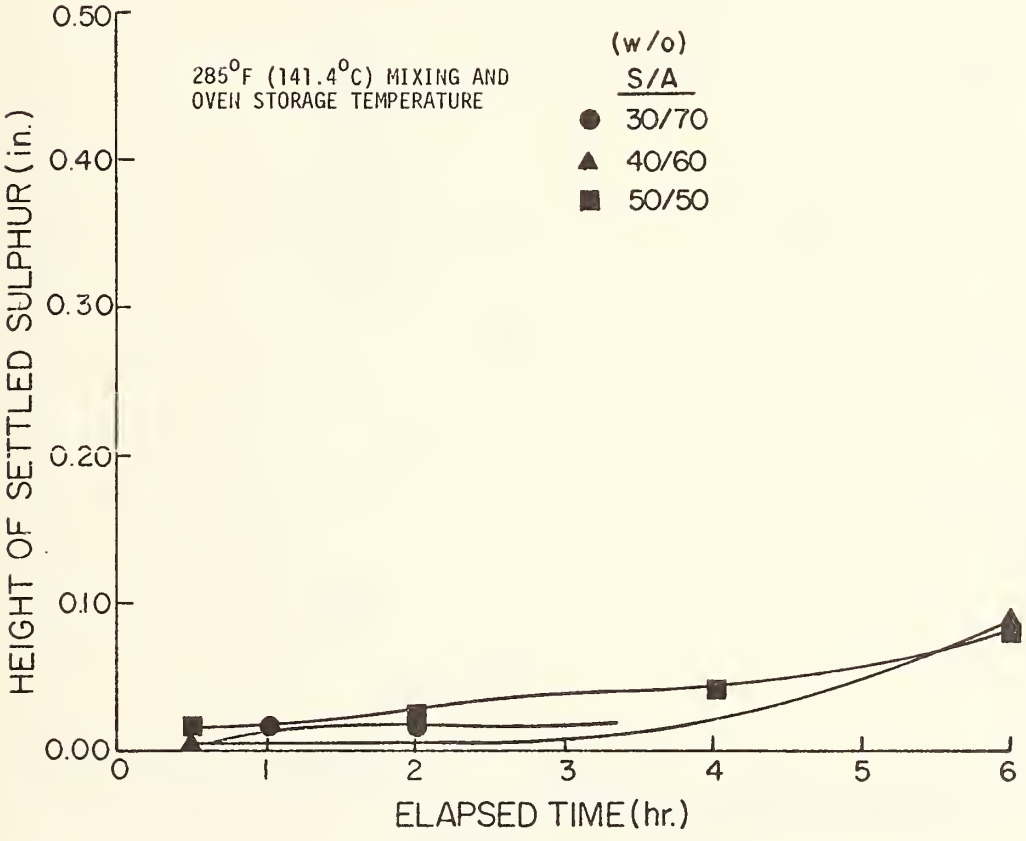

FIGURE 82 SULPHUR SETTLING HEIGHT OF SULPHUR-ASPHALT EMULSION DS AC-20 ASPHALT CEMENT 285°F (141.4°C) Mixing and Oven Storage Temperature

1 inch = 25.4 mm

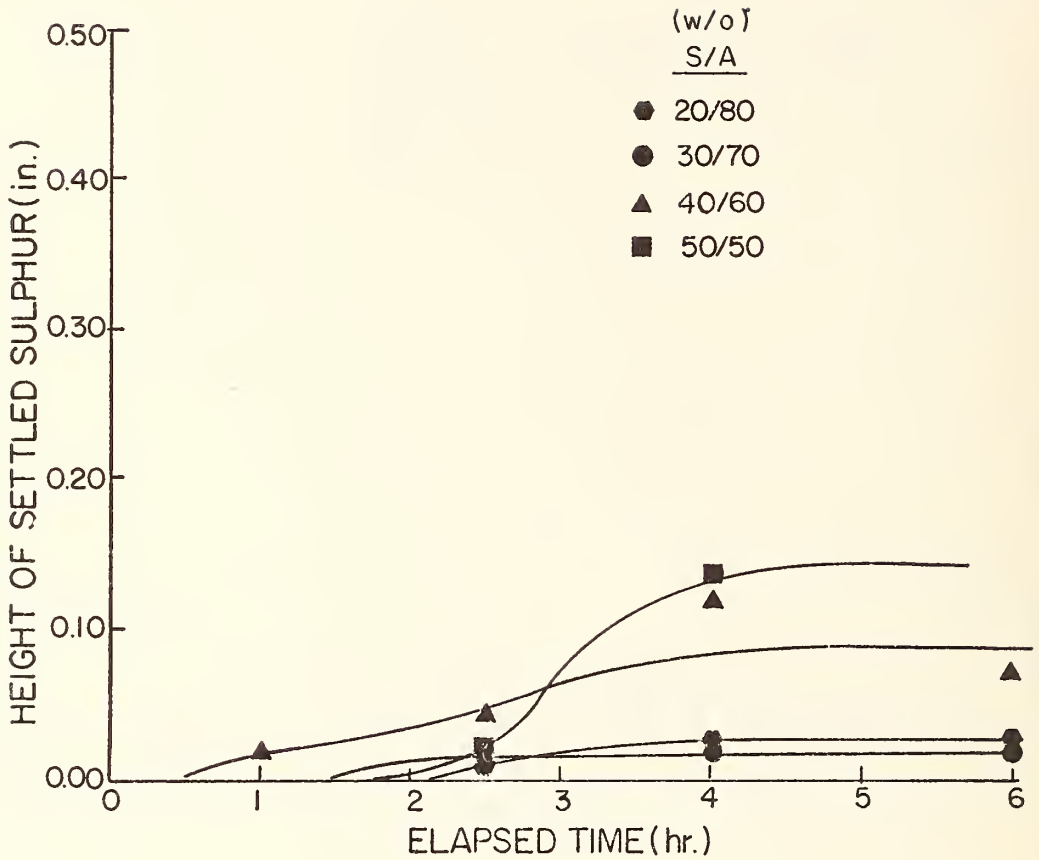

Fig. 83 SULPHUR SETTLING HEIGHT OF SULPHUR-ASPHALT EMULSION
DS AC-20 ASPHALT CEMENT 300°F(148.9°C) Mixing and Oven Storage Temperature

1 inch = 25.4 mm

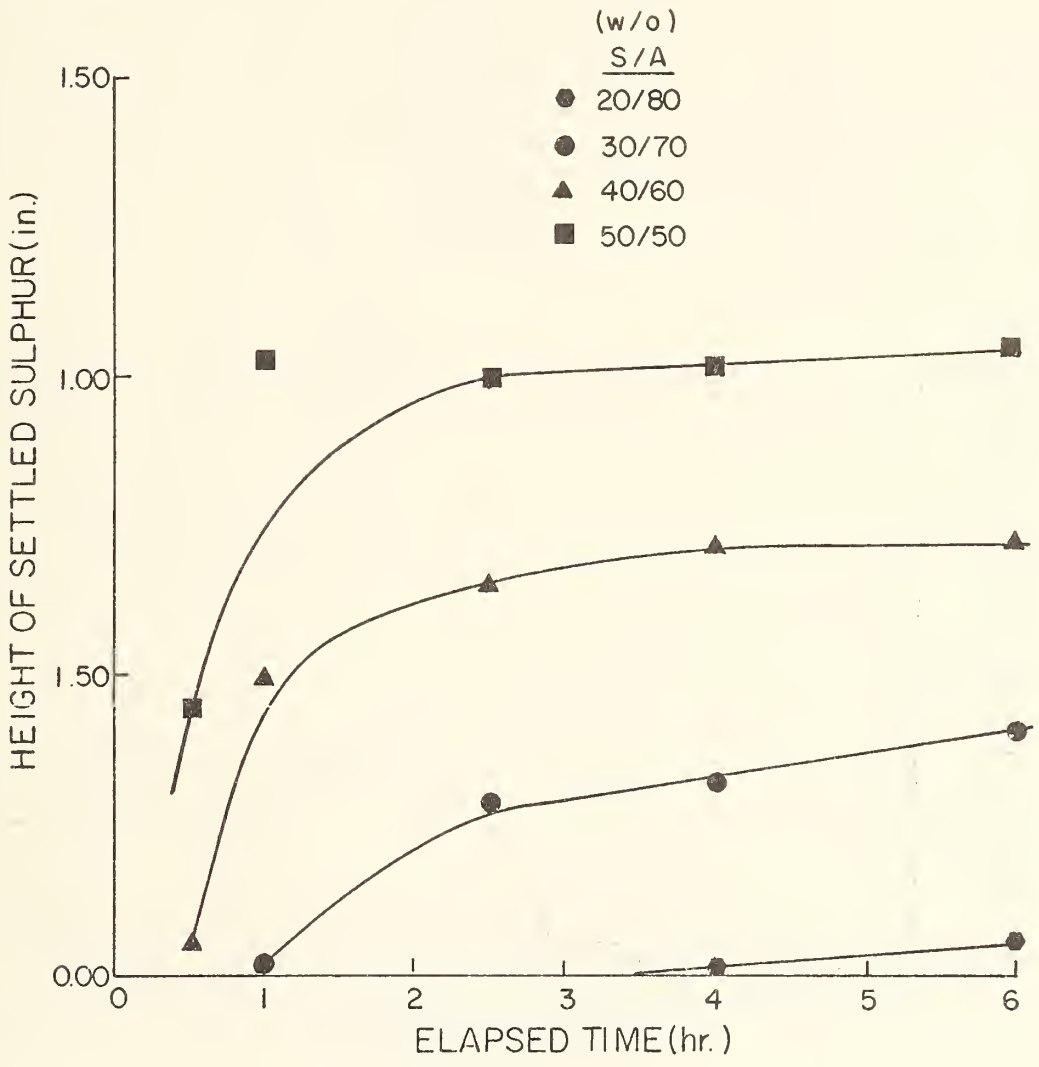

Fig. 84 SULPHUR SETTLING HEIGHT OF SULPHUR-ASPHALT EMULSION DENV AC-10 ASPHALT CEMENT 285°F (140.6°C) Mixing and Oven Storage Temperature

1 inch = 25.4 mm

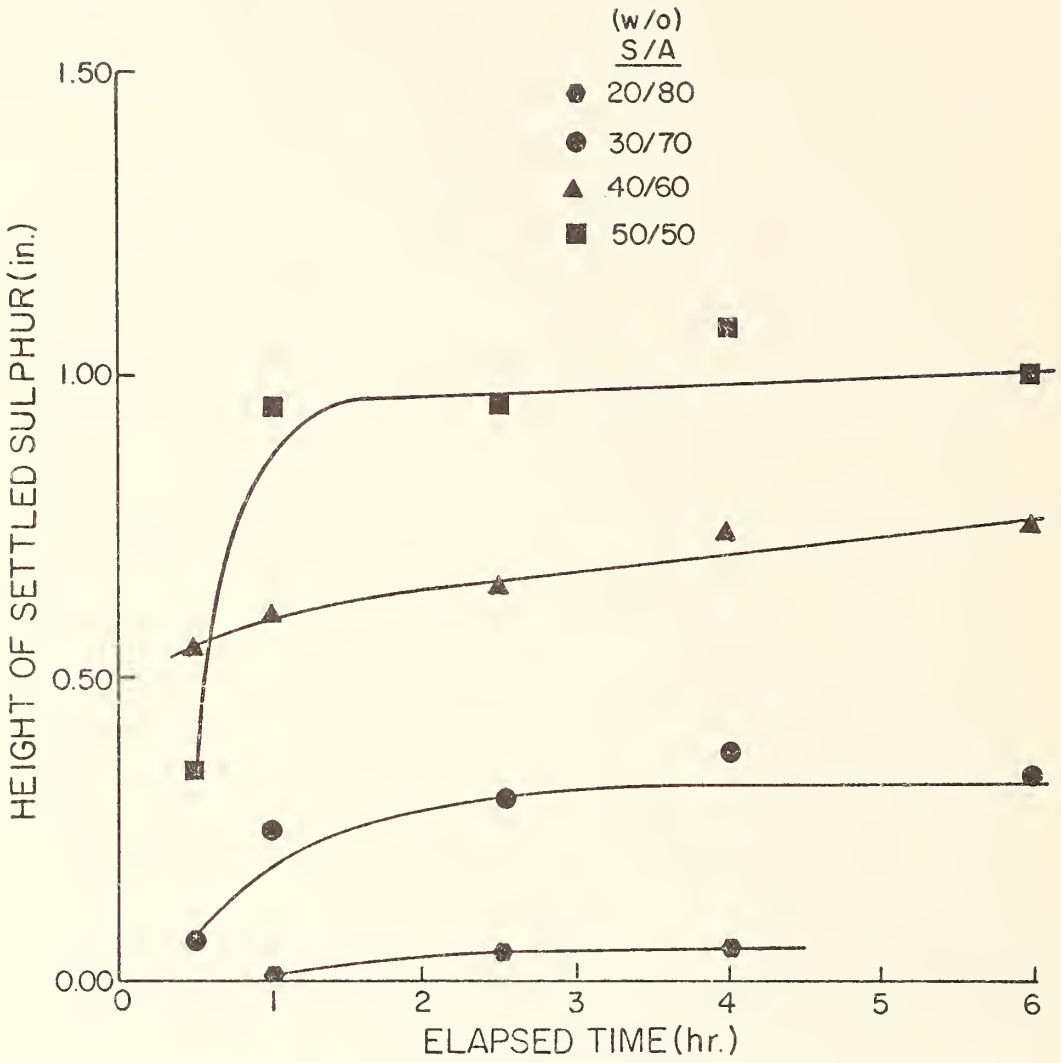

Fig. 85 SULPHUR SETTLING HEIGHT OF SULPHUR-ASPHALT EMULSION DENV AC-10 ASPHALT CEMENT 300°F (148.9°C) Mixing and Oven Storage Temperature

1 inch = 25.4 mm

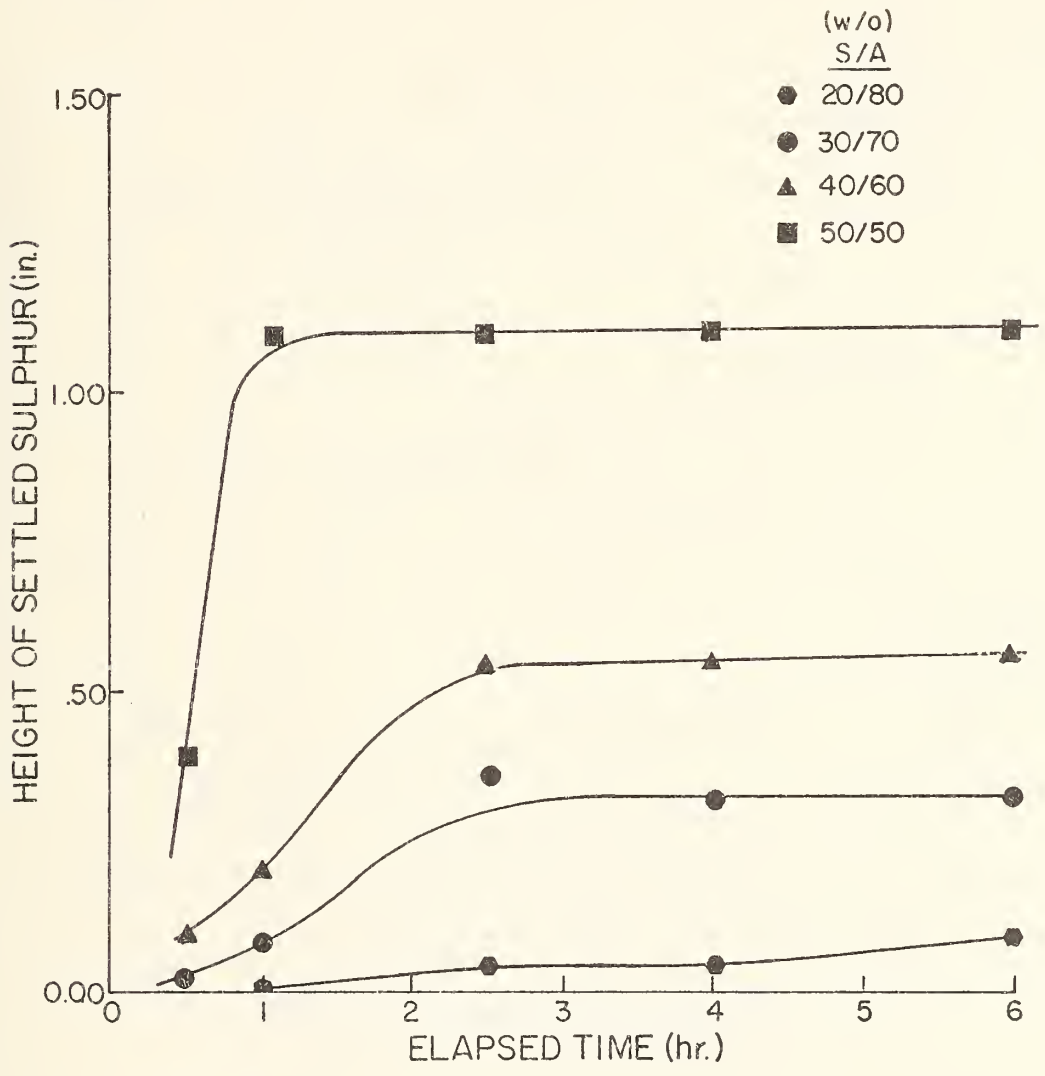

Fig. 86 SULPHUR SETTLING HEIGHT OF SULPHUR-ASPHALT EMULSION
SM AC-10 ASPHALT CEMENT 285°F (140.6°C) Mixing and Oven Storage Temperature

1 inch = 25.4 mm

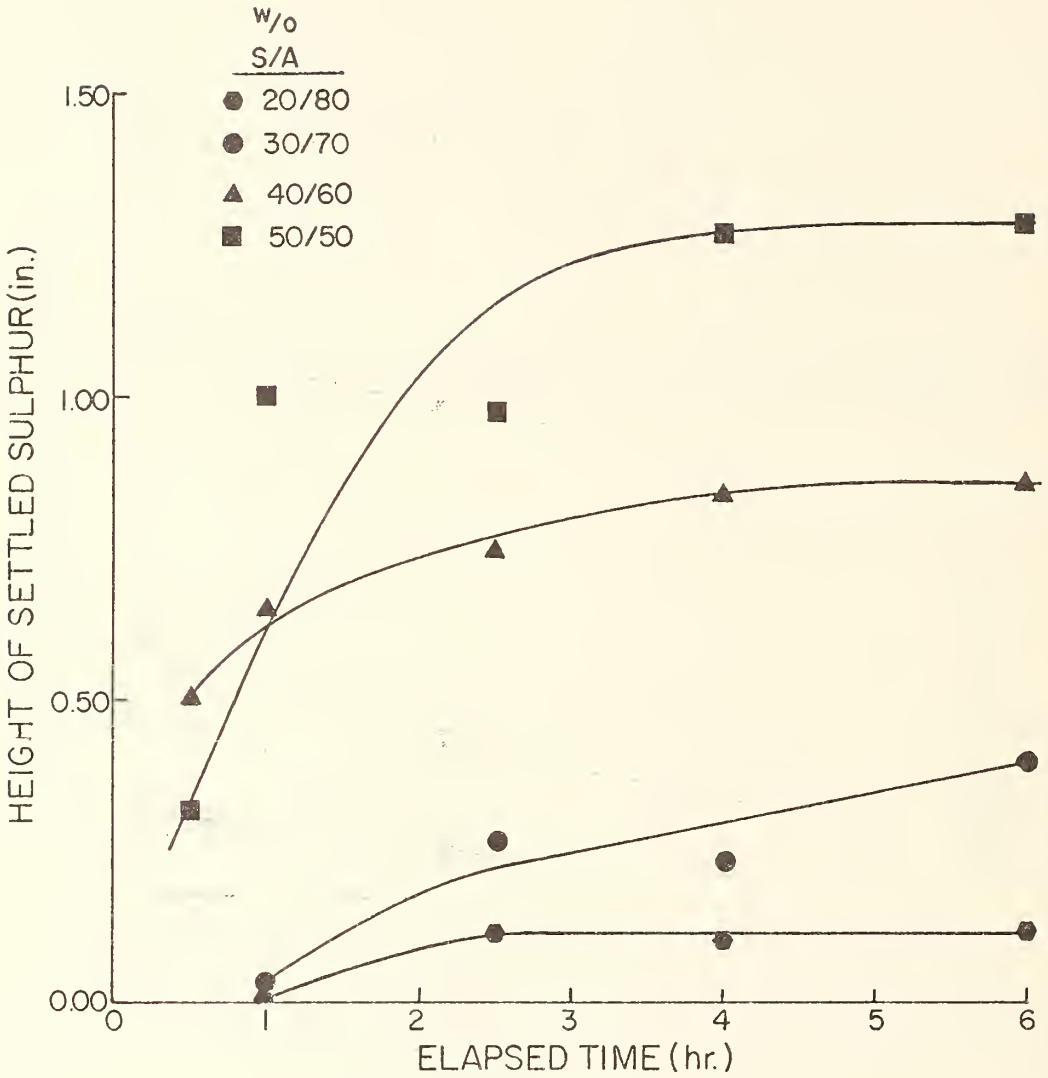

Fig. 87 SULPHUR SETTLING HEIGHT OF SULPHUR-ASPHALT EMULSION
SM AC-10 ASPHALT CEMENT 300°F (148.9°C) Mixing and Oven Storage Temperature

1 inch = 25.4 mm

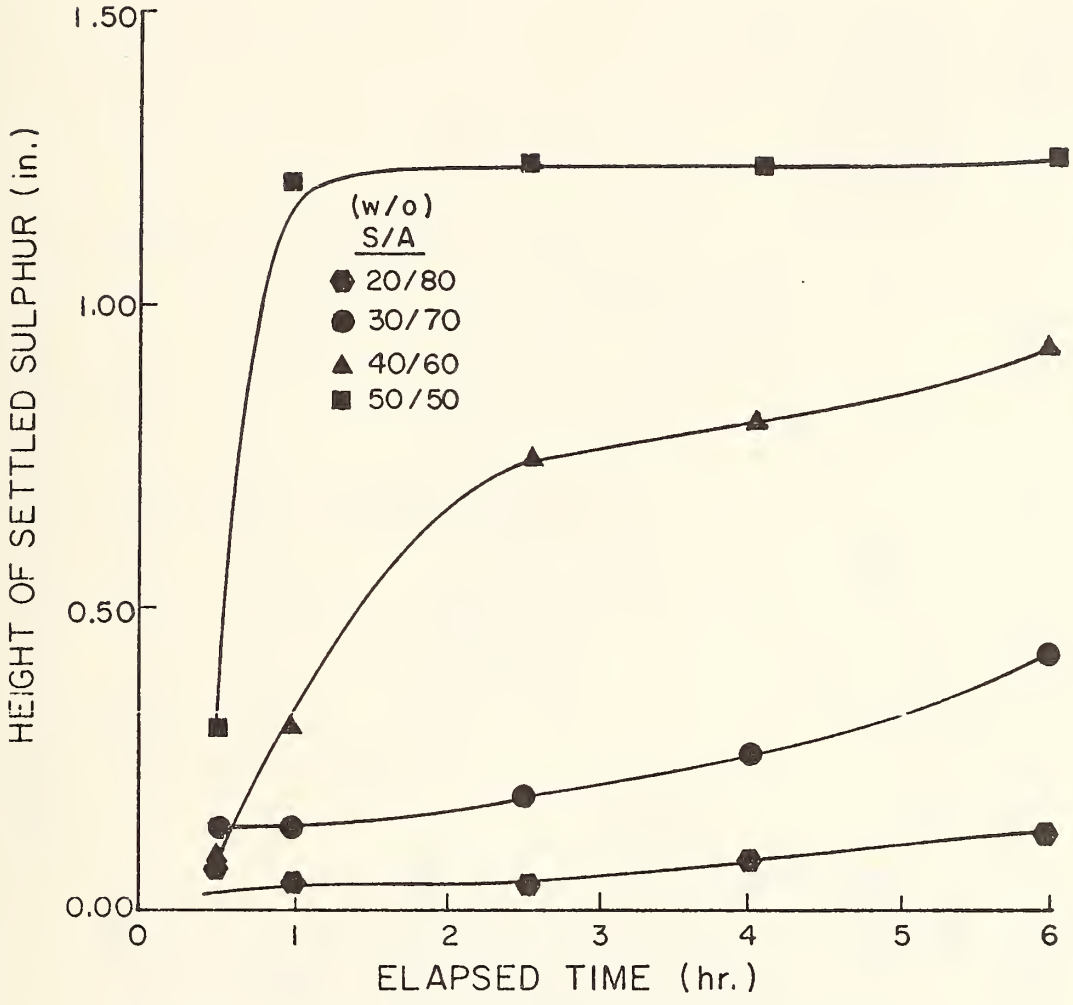

Fig. 88 SULPHUR SETTLING HEIGHT OF SULPHUR-ASPHALT EMULSION WC AC-10 ASPHALT CEMENT 285°F (140.6°C) Mixing and Oven Storage Temperature

1 inch = 25.4 mm

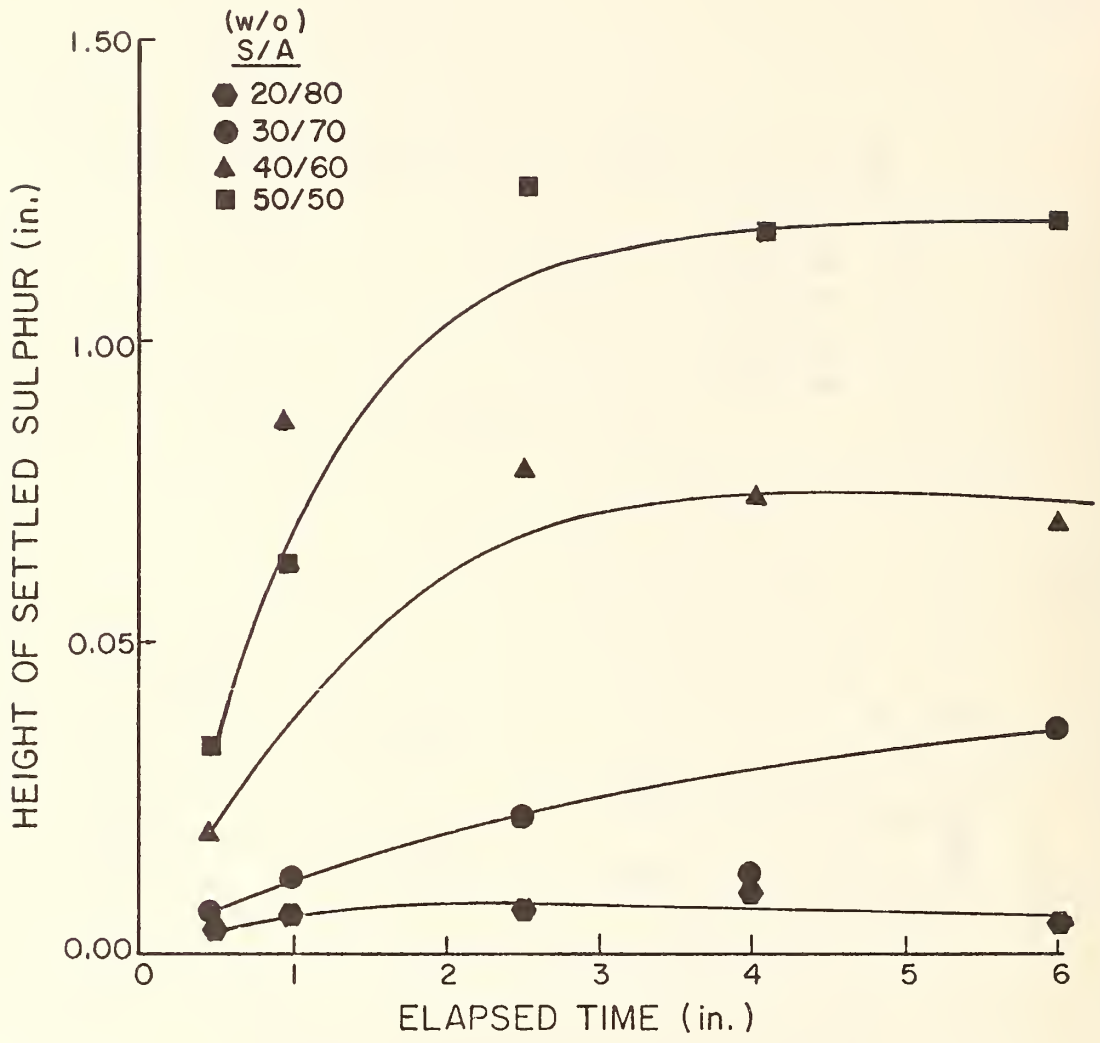

Fig. 89 SULPHUR SETTLING HEIGHT OF SULPHUR-ASPHALT EMULSION
WC AC-10 ASPHALT CEMENT 300°F (148.9°C) Mixing and Oven Storage Temperature

1 inch = 25.4 mm

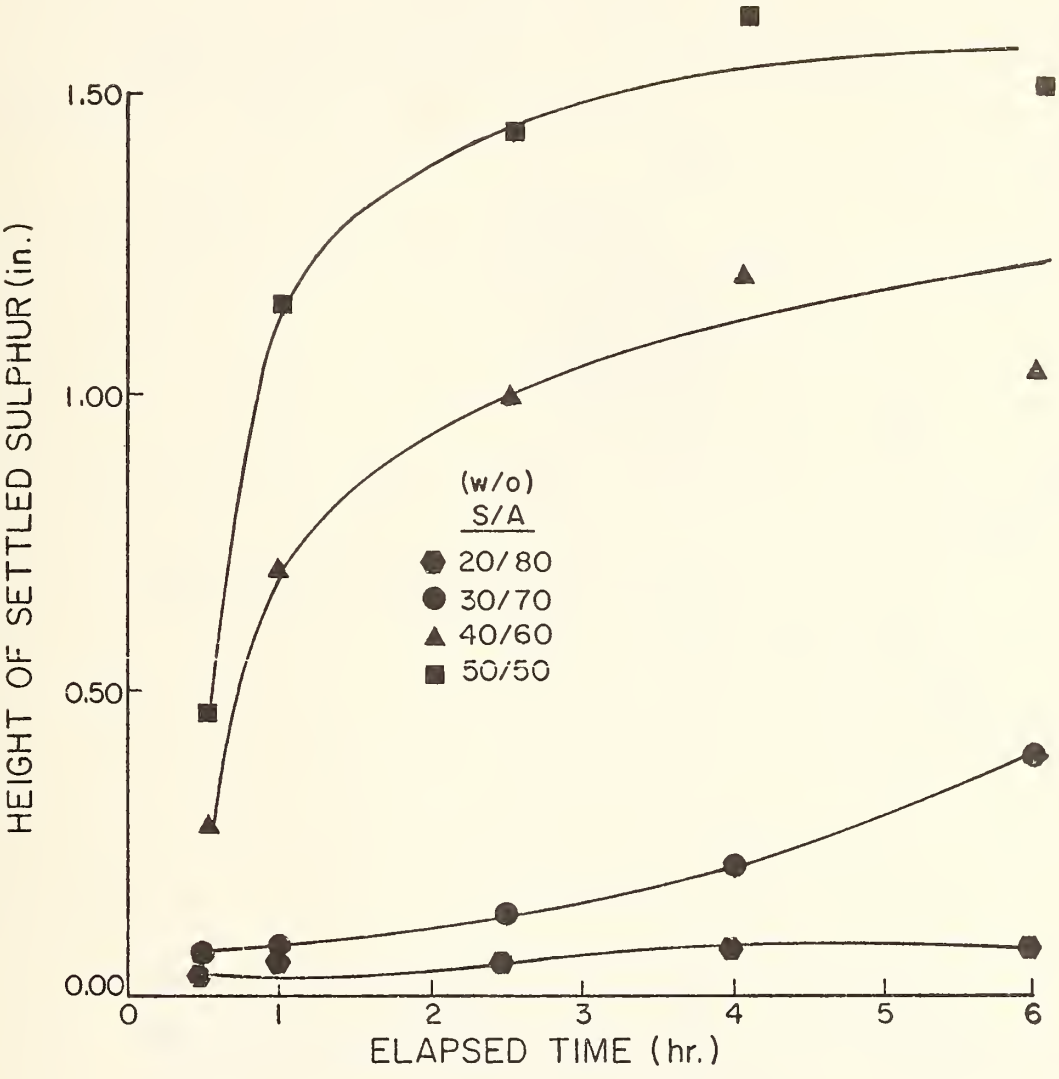

Fig. 90 SULPHUR SELLTING HEIGHT OF SULPHUR-ASPHALT EMULSION ME AC-10 ASPHALT CEMENT 285°F (140.6°C) Mixing and Oven Storage Temperature

1 inch = 25.4 mm

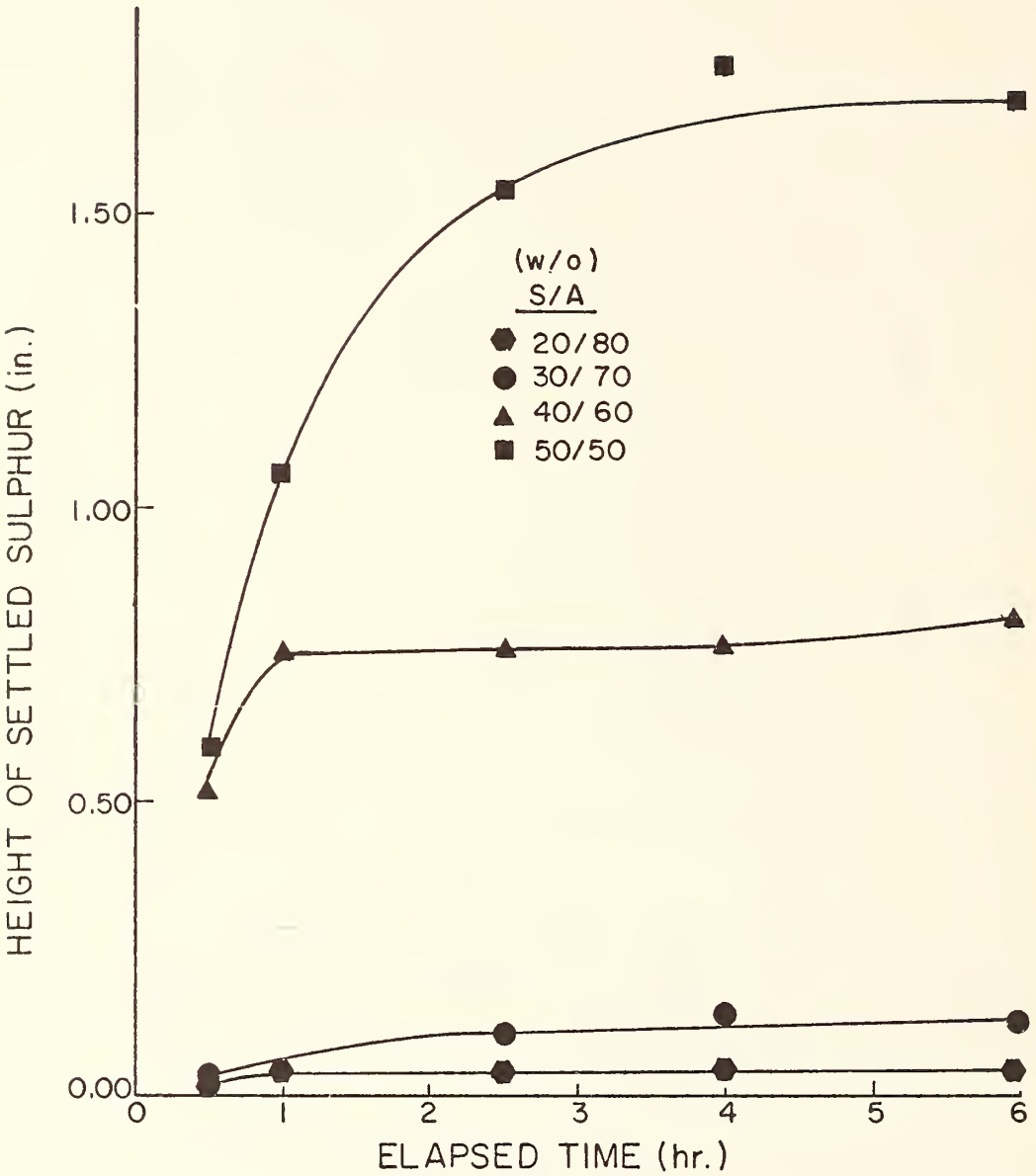

Fig. 91 SULPHUR SETTLING HEIGHT OF SULPHUR-ASPHALT EMULSION ME AC-10 ASPHALT CEMENT 300°F (148.9°C) Mixing and Oven Storage Temperature

1 inch = 25.4 mm

Appendix D. Values of Design and Response Variables for Screening Tests

This appendix presents a tabulation of the decision (design) variables and the response (test) variables resulting from laboratory screening tests performed on the specified treatment combinations for the three systems studied (AAS, AE and AES).

Definitions of the abbreviations and symbols shown on the computer output sheets follow:

SYMBOL	VARIABLE
OBS	Observation number
A	Aggregate roundness
B	Aggregate sphericity
C	Aggregate roughness
D	Aggregate size and gradation number
E	Type of asphalt
F	Volume of binder (% VMA)
G	Volume of sulphur (% Binder)
H	Moisture condition
I	Compaction effort
BLKS	Bulk specific gravity
VMA	Voids in mineral aggregate
AIRV	Air voids
RESMOD	Resilient modulus
HVESTA	Hveem stability
MARST	Marshall stability
MARF	Marshall flow

Appendix D. Continued

TABLE 39 AAS SYSTEM MIXTURES

STATISTICAL ANALYSIS SYSTEM

OBS	A	B	C	D	E	F	G	H	I	BLKS	VMA	AIRV	RESMOD	HVESTA	MARST	MARF
1	.35	.71	2.0	78	0.1	39.3	75.0	0.1	0.1	1.783	42	25.5	0.80	64	4130	6
2	.35	.71	2.0	78	0.1	39.3	75.0	0.1	0.1	1.783	42	25.5	0.69	58	3490	5
3	.35	.71	2.0	78	0.1	40.2	75.0	0.1	0.1	1.804	41	24.5	0.82	64	5030	5
4	.60	.80	2.0	86	0.1	28.3	75.0	0.1	0.1	1.240	46	33.0	0.68	44	1660	8
5	.60	.80	2.0	86	0.1	28.5	75.0	0.1	0.1	1.230	47	33.6	0.68	26	520	11
6	.60	.80	2.0	86	0.1	27.5	75.0	0.1	0.1	1.220	47	34.1	0.68	26	500	10
7	.30	.75	3.0	2	0.1	23.6	75.0	0.1	0.1	1.641	45	34.4	0.06	6	300	15
8	.30	.75	3.0	2	0.1	24.6	75.0	0.1	0.1	1.671	44	33.2	0.06	11	300	15
9	.30	.75	3.0	2	0.1	27.8	75.0	0.1	0.1	1.763	41	29.6	0.06	17	572	13
10	.10	.70	3.5	87	1.0	50.6	75.0	0.1	0.1	2.240	34	16.8	1.30	58	3650	7
11	.10	.70	3.5	87	1.0	45.7	75.0	0.1	0.1	2.180	35	19.0	1.57	50	2680	8
12	.10	.70	3.5	87	1.0	50.6	75.0	0.1	0.1	2.240	34	16.8	1.49	58	4630	9
13	.20	.70	1.5	977	1.0	67.5	75.0	0.1	0.1	2.110	32	10.4	2.85	84	7460	5
14	.20	.70	1.5	977	1.0	67.2	75.0	0.1	0.1	2.107	32	10.5	2.52	76	5850	12
15	.20	.70	1.5	977	1.0	63.9	75.0	0.1	0.1	2.075	33	11.9	2.40	83	8340	5
16	.35	.71	2.0	78	0.1	64.9	50.0	1.0	0.1	1.899	41	14.4	0.12	35	1150	10
17	.35	.71	2.0	78	0.1	67.5	50.0	1.0	0.1	1.931	40	13.0	0.23	43	2000	10
18	.35	.71	2.0	78	0.1	67.3	50.0	1.0	0.1	1.929	40	13.1	0.21	43	1620	8
19	.40	.80	2.2	64	0.1	62.7	81.8	0.1	1.0	2.090	37	13.8	1.24	81	10180	4
20	.40	.80	2.2	64	0.1	62.7	81.8	0.1	1.0	2.090	37	13.8	1.57	73	11000	5
21	.40	.80	2.2	64	0.1	62.7	81.8	0.1	1.0	2.100	37	13.8	1.44	84	12170	6
22	.10	.70	3.5	87	0.1	73.7	50.0	0.1	1.0	2.280	35	9.2	0.33	37	1580	12
23	.10	.70	3.5	87	0.1	73.3	50.0	0.1	1.0	2.260	36	9.6	0.33	41	1640	8
24	.10	.70	3.5	87	0.1	70.6	50.0	0.1	1.0	2.250	36	10.6	0.34	40	1790	8
25	.10	.70	3.5	87	0.1	28.9	75.5	1.0	1.0	2.160	36	25.6	0.57	47	2510	11
26	.10	.70	3.5	87	0.1	28.1	75.5	1.0	1.0	2.130	37	26.6	0.64	40	980	12
27	.10	.70	3.5	87	0.1	28.9	75.5	1.0	1.0	2.180	35	24.9	0.66	48	2380	12
28	.20	.70	1.5	977	0.1	99.9	50.0	0.1	1.0	2.329	28	0.0	0.89	50	3060	11
29	.20	.70	1.5	977	0.1	97.2	50.0	0.1	1.0	2.293	29	0.8	0.73	46	3180	11
30	.20	.70	1.5	977	0.1	96.2	50.0	0.1	1.0	2.286	29	1.1	0.44	33	2000	25
31	.20	.70	1.5	977	0.1	80.9	75.0	1.0	1.0	2.393	22	4.2	4.28	88	26445	12
32	.20	.70	1.5	977	0.1	82.7	75.0	1.0	1.0	2.401	22	3.8	4.23	88	29512	10
33	.20	.70	1.5	977	0.1	77.0	75.0	1.0	1.0	2.365	23	5.3	4.73	88	24966	9
34	.35	.01	2.0	78	1.0	70.3	50.0	0.1	1.0	2.054	36	10.7	0.64	62	4950	9
35	.35	.71	2.0	78	1.0	73.4	50.0	0.1	1.0	2.088	35	9.3	0.77	65	6210	9
36	.35	.71	2.0	78	1.0	70.9	50.0	0.1	1.0	2.067	35	10.2	0.70	60	5390	8
37	.35	.71	2.0	78	1.0	52.6	75.0	1.0	1.0	1.974	35	16.6	0.83	59	3760	10
38	.35	.71	2.0	78	1.0	51.9	75.0	1.0	1.0	1.957	36	17.3	0.66	57	3700	10
39	.35	.71	2.0	78	1.0	52.5	75.0	1.0	1.0	1.962	36	17.1	0.69	57	4340	10
40	.73	.77	3.3	977	0.1	80.5	75.0	0.1	0.1	2.390	22	4.3	2.13	62	3916	8
41	.73	.77	3.3	977	0.1	80.5	75.0	0.1	0.1	2.390	22	4.3	1.77	71	3927	7
42	.73	.77	3.3	977	0.1	79.6	75.0	0.1	0.1	2.380	23	4.7	1.46	66	3885	7
43	.66	.78	3.0	226	1.0	29.6	75.0	0.1	0.1	1.620	47	33.1	0.19	21	144	16
44	.66	.78	3.0	226	1.0	38.5	75.0	0.1	0.1	1.810	41	25.2	0.95	57	1665	12
45	.66	.78	3.0	226	1.0	46.2	75.0	0.1	0.1	1.940	37	19.9	1.18	75	5438	8
46	.78	.87	1.8	56	1.0	43.0	75.0	0.1	0.1	1.140	30	17.1	0.50	15	400	5
47	.78	.87	1.8	56	1.0	42.6	75.0	0.1	0.1	1.130	31	17.8	0.50	15	552	4
48	.78	.87	1.8	56	1.0	43.5	75.0	0.1	0.1	1.150	29	16.4	0.50	15	400	5
49	.78	.87	1.8	56	1.0	46.8	75.0	0.1	0.1	1.170	28	14.9	0.50	18	400	5
50	.60	.80	2.0	86	0.1	37.0	50.0	1.0	0.1	1.300	46	29.0	0.71	68	4420	8
51	.60	.80	2.0	86	0.1	37.0	50.0	1.0	0.1	1.300	46	29.0	0.72	80	4790	5
52	.60	.80	2.0	86	0.1	37.0	50.0	1.0	0.1	1.300	46	29.0	0.82	75	4360	6
53	.70	.75	3.1	64	0.1	89.2	60.0	0.1	0.1	2.220	37	4.0	0.26	38	1400	9
54	.70	.75	3.1	64	0.1	84.0	60.0	0.1	0.1	2.170	38	6.1	0.24	39	1440	8
55	.70	.75	3.1	64	0.1	87.0	60.0	0.1	0.1	2.200	37	4.8	0.30	37	1700	7

Appendix D. Continued

TABLE 39 AAS SYSTEM MIXTURES (CONT.)

STATISTICAL ANALYSIS SYSTEM

OBS	A	B	C	D	E	F	G	H	I	BLKS	VMA	AIRV	RESMOD	HVESTA	MARST	MARF
56	.70	.75	3.1	64	0.1	77.5	81.8	1.0	0.1	2.258	32	7.20	0.95	60	6360	8
57	.70	.75	3.1	64	0.1	77.5	81.8	1.0	0.1	2.259	35	7.20	0.93	73	7085	12
58	.70	.75	3.1	64	0.1	76.3	81.8	1.0	0.1	2.250	32	7.60	0.86	70	6931	10
59	.15	.75	1.2	8	0.1	62.9	50.0	1.0	0.1	2.007	38	14.10	0.48	11	15	18
60	.15	.75	1.2	8	0.1	66.5	50.0	1.0	0.1	2.048	37	12.40	0.22	11	160	18
61	.15	.75	1.2	8	0.1	68.1	50.0	1.0	0.1	2.069	36	11.50	0.19	10	224	18
62	.15	.75	1.2	8	0.1	52.4	81.8	1.0	0.1	2.042	38	18.10	0.50	15	325	15
63	.15	.75	1.2	8	0.1	52.3	81.8	1.0	0.1	2.031	39	18.60	0.69	10	574	15
64	.15	.75	1.2	8	0.1	52.1	81.8	1.0	0.1	2.027	39	18.70	0.66	10	300	15
65	.40	.80	2.2	64	1.0	79.8	60.0	0.1	0.1	2.030	42	8.50	0.57	48	3760	7
66	.40	.80	2.2	64	1.0	74.6	60.0	0.1	0.1	1.970	44	11.20	0.53	44	2040	6
67	.40	.80	2.2	64	1.0	80.7	60.0	0.1	0.1	2.040	42	8.10	0.56	55	5100	6
68	.40	.80	2.2	64	1.0	57.8	81.8	1.0	0.1	2.010	40	16.90	1.13	79	6440	8
69	.40	.80	2.2	64	1.0	59.0	81.8	1.0	0.1	2.030	39	16.00	1.18	80	7500	9
70	.40	.80	2.2	64	1.0	60.0	81.8	1.0	0.1	2.040	39	15.60	1.27	78	8700	8
71	.30	.75	3.0	2	0.1	38.7	50.0	1.0	0.1	1.724	45	27.60	0.09	6	200	10
72	.30	.75	3.0	2	0.1	36.8	50.0	1.0	0.1	1.675	47	29.70	0.09	6	200	10
73	.30	.75	3.0	2	0.1	38.3	50.0	1.0	0.1	1.706	46	28.40	0.09	6	200	10
74	.10	.70	3.5	87	1.0	54.0	50.0	1.0	0.1	2.000	43	19.80	0.41	17	180	21
75	.10	.70	3.5	87	1.0	53.2	50.0	1.0	0.1	1.980	44	20.60	0.40	17	40	26
76	.10	.70	3.5	87	1.0	56.7	50.0	1.0	0.1	2.040	42	18.20	0.52	22	530	17
77	.20	.70	1.5	977	1.0	80.7	50.0	1.0	0.1	2.238	31	6.00	1.18	34	1905	16
78	.20	.70	1.5	977	1.0	75.3	50.0	1.0	0.1	2.191	32	7.90	0.82	29	1459	16
79	.20	.70	1.5	977	1.0	73.6	50.0	1.0	0.1	2.174	33	8.70	0.75	29	1404	15
80	.66	.78	3.0	226	0.1	79.1	50.0	0.1	1.0	2.180	33	6.90	0.86	54	4182	8
81	.66	.78	3.0	226	0.1	79.1	50.0	0.1	1.0	2.180	33	6.90	0.90	51	4214	7
82	.66	.78	3.0	226	0.1	79.1	50.0	0.1	1.0	2.180	33	6.90	0.85	47	3896	8
83	.66	.78	3.0	226	0.1	55.2	75.0	1.0	1.0	2.130	31	13.90	0.12	50	2707	19
84	.66	.78	3.0	226	0.1	56.3	75.0	1.0	1.0	2.150	30	13.10	0.15	60	2792	17
85	.66	.78	3.0	226	0.1	56.3	75.0	1.0	1.0	2.150	30	13.10	0.15	51	2358	19
86	.78	.87	1.8	56	0.1	48.6	50.0	0.1	1.0	1.220	29	14.90	0.71	80	8396	7
87	.78	.87	1.8	56	0.1	98.8	50.0	0.1	1.0	1.430	16	0.20	1.17	85	16856	8
88	.78	.87	1.8	56	0.1	45.7	50.0	0.1	1.0	1.200	30	16.30	1.33	84	6815	6
89	.78	.87	1.8	56	0.1	77.2	50.0	0.1	1.0	1.280	47	10.70	1.21	81	10996	8
90	.78	.87	1.8	56	0.1	1.6	75.0	1.0	1.0	1.130	31	30.50	1.35	70	7681	4
91	.78	.87	1.8	56	0.1	1.0	75.0	1.0	1.0	1.173	28	27.90	1.23	72	7659	6
92	.78	.87	1.8	56	0.1	1.0	75.0	1.0	1.0	1.200	26	26.20	1.32	71	8030	7
93	.60	.80	2.0	86	1.0	50.0	50.0	0.1	1.0	1.400	42	21.00	1.45	77	5640	9
94	.60	.80	2.0	86	1.0	48.4	50.0	0.1	1.0	1.370	44	22.70	1.38	70	3860	5
95	.60	.80	2.0	86	1.0	52.6	50.0	0.1	1.0	1.420	42	19.90	0.65	76	6000	7
96	.60	.80	2.0	86	1.0	38.4	75.0	1.0	1.0	1.330	43	26.50	0.90	74	1380	8
97	.60	.80	2.0	86	1.0	38.1	75.0	1.0	1.0	1.340	42	26.00	0.93	66	2480	8
98	.60	.80	2.0	86	1.0	39.3	75.0	1.0	1.0	1.360	41	24.90	0.76	66	3710	9
99	.70	.75	3.1	64	1.0	82.6	81.8	0.1	1.0	2.307	31	0.54	1.91	79	8600	9
100	.70	.75	3.1	64	1.0	81.0	81.8	0.1	1.0	2.295	31	5.90	1.98	81	7840	9
101	.70	.75	3.1	64	1.0	82.3	81.8	0.1	1.0	2.305	31	5.50	1.96	78	8040	7
102	.30	.80	3.0	2	0.1	36.8	81.8	0.1	1.0	1.809	44	27.80	0.17	25	412	8
103	.30	.80	3.0	2	0.1	36.8	81.8	0.1	1.0	1.808	44	27.80	0.43	27	364	9
104	.30	.80	3.0	2	0.1	37.7	81.8	0.1	1.0	1.794	45	28.40	0.37	25	338	8
105	.15	.75	1.2	8	1.0	57.1	81.8	0.1	1.0	2.160	35	15.00	1.67	57	3876	6
106	.15	.75	1.2	8	1.0	54.9	81.8	0.1	1.0	2.140	35	15.80	1.16	49	3724	8
107	.15	.75	1.2	8	1.0	57.1	81.8	0.1	1.0	2.160	35	15.00	1.97	58	3885	7
108	.40	.80	2.2	64	0.1	82.2	60.0	1.0	1.0	2.080	41	7.30	0.33	44	2250	8
109	.40	.80	2.2	64	0.1	82.2	60.0	1.0	1.0	2.080	41	7.30	0.33	35	3420	9
110	.40	.80	2.2	64	0.1	84.0	60.0	1.0	1.0	2.100	40	6.40	0.40	38	3540	9

Appendix D. Continued

TABLE 39 AAS SYSTEM MIXTURES (CONT.)

STATISTICAL ANALYSIS SYSTEM

OBS	A	B	C	D	E	F	G	H	I	BLKS	VMA	AIRV	RESMOD	HVESTA	MARST	MARF
111	.30	.75	3.0	2	1.0	51.8	50.0	0.1	1.0	1.944	38	18.3	0.23	20	314	22
112	.30	.75	3.0	2	1.0	55.4	50.0	0.1	1.0	1.985	37	16.5	0.31	22	480	18
113	.30	.75	3.0	2	1.0	54.9	50.0	0.1	1.0	1.980	37	16.7	0.40	25	513	11
114	.30	.75	3.0	2	1.0	31.5	75.0	1.0	1.0	1.789	41	28.1	0.54	17	300	10
115	.30	.75	3.0	2	1.0	31.8	75.0	1.0	1.0	1.825	39	26.6	0.59	31	300	10
116	.30	.75	3.0	2	1.0	31.5	75.0	1.0	1.0	1.805	40	27.4	0.00	26	300	10
117	.73	.77	3.3	977	0.1	93.2	50.0	1.0	0.1	2.340	28	1.9	0.26	19	636	11
118	.73	.77	3.3	977	0.1	90.0	50.0	1.0	0.1	2.320	28	2.8	0.20	3	592	9
119	.73	.77	3.3	977	0.1	91.8	50.0	1.0	0.1	2.330	28	2.3	0.18	2	504	13
120	.66	.78	3.0	226	1.0	49.3	50.0	1.0	0.1	1.820	44	22.3	0.10	30	300	15
121	.66	.78	3.0	226	1.0	56.0	50.0	1.0	0.1	1.930	40	17.6	0.21	33	342	16
122	.66	.78	3.0	226	1.0	58.2	50.0	1.0	0.1	1.960	39	16.3	0.20	42	585	15
123	.78	.87	1.8	56	1.0	52.2	50.0	1.0	0.1	1.252	27	12.9	0.49	26	371	14
124	.78	.87	1.8	56	1.0	40.7	50.0	1.0	0.1	1.173	31	18.4	0.48	27	224	14
125	.78	.87	1.8	56	1.0	47.1	50.0	1.0	0.1	1.225	28	14.8	0.41	27	318	9
126	.30	.80	3.0	2	1.0	42.9	60.0	0.1	0.1	1.779	48	27.4	0.10	0	0	20
127	.30	.80	3.0	2	1.0	41.4	60.0	0.1	0.1	1.747	49	28.7	0.10	0	0	20
128	.30	.80	3.0	2	1.0	41.3	60.0	0.1	0.1	1.761	48	28.2	0.08	0	0	20
129	.30	.80	3.0	2	1.0	30.0	81.8	1.0	0.1	1.644	49	34.3	0.22	1	251	10
130	.30	.80	3.0	2	1.0	32.3	81.8	1.0	0.1	1.707	47	31.8	0.39	1	200	10
131	.30	.80	3.0	2	1.0	31.0	81.8	1.0	0.1	1.673	48	33.1	0.28	1	200	10
132	.73	.77	3.3	977	1.0	98.1	50.0	0.1	1.0	2.380	26	0.5	0.51	8	318	11
133	.73	.77	3.3	977	1.0	95.2	50.0	0.1	1.0	2.360	27	1.3	0.47	11	707	10
134	.73	.77	3.3	977	1.0	89.3	50.0	0.1	1.0	2.320	28	3.0	0.30	2	556	8
135	.73	.77	3.3	977	1.0	89.5	75.0	1.0	1.0	2.460	20	2.1	1.12	45	2116	9
136	.73	.77	3.3	977	1.0	86.2	75.0	1.0	1.0	2.440	21	2.9	1.25	42	2250	8
137	.73	.77	3.3	977	1.0	84.3	75.0	1.0	1.0	2.430	21	3.3	1.10	41	2105	8
138	.70	.75	3.1	64	1.0	90.0	60.0	1.0	1.0	2.242	36	3.6	0.35	33	0	11
139	.70	.75	3.1	64	1.0	88.6	60.0	1.0	1.0	2.230	36	4.1	0.42	33	1050	8
140	.70	.75	3.1	64	1.0	90.0	60.0	1.0	1.0	2.242	36	3.6	0.46	38	1090	11
141	.30	.80	3.0	2	0.1	61.7	60.0	1.0	1.0	2.021	41	15.7	0.05	20	500	12
142	.30	.80	3.0	2	0.1	65.6	60.0	1.0	1.0	2.077	39	13.4	0.08	24	571	12
143	.30	.80	3.0	2	0.1	56.1	60.0	1.0	1.0	1.945	43	18.9	0.03	20	515	10
144	.15	.75	1.2	8	1.0	77.2	60.0	1.0	1.0	2.230	36	8.2	0.64	33	0	25
145	.15	.75	1.2	8	1.0	73.2	60.0	1.0	1.0	2.190	37	9.9	0.58	23	714	15
146	.15	.75	1.2	8	1.0	76.1	60.0	1.0	1.0	2.220	36	8.6	1.63	50	2580	8

Appendix D. Continued

TABLE 40 AE SYSTEM MIXTURES

DATA FOR DIFFERENT TYPES OF MIXTURES

OBS	A	B	C	D	E	F	G	H	I	BLKS	VMA	AIRV	RESMOD	HVESTA	MARST	MARF
1	.35	.71	2.0	78	0.1	37.3	30	0.1	0.1	1.779	40.0	25.1	0.02	8	62	12
2	.35	.71	2.0	78	0.1	38.0	30	0.1	0.1	1.786	40.0	24.8	0.02	8	48	12
3	.35	.71	2.0	78	0.1	36.3	30	0.1	0.1	1.770	40.0	25.5	0.01	8	36	10
4	.60	.80	2.0	86	0.1	42.9	30	0.1	0.1	1.270	46.0	26.2	0.03	19	100	15
5	.60	.80	2.0	86	0.1	41.7	30	0.1	0.1	1.240	48.0	28.0	0.03	20	106	10
6	.60	.80	2.0	86	0.1	41.7	30	0.1	0.1	1.250	47.0	27.4	0.03	19	95	7
7	.10	.70	3.5	87	1.0	37.1	30	0.1	0.1	1.990	38.0	23.9	0.12	16	114	15
8	.10	.70	3.5	87	1.0	35.9	30	0.1	0.1	1.960	39.0	25.0	0.13	18	95	15
9	.10	.70	3.5	87	1.0	36.1	30	0.1	0.1	1.980	38.0	24.3	0.12	14	80	13
10	.20	.70	1.5	977	1.0	31.8	30	0.1	0.1	2.041	28.0	19.1	0.58	18	500	14
11	.20	.70	1.5	977	1.0	28.6	30	0.1	0.1	2.001	29.0	20.7	0.78	26	950	13
12	.20	.70	1.5	977	1.0	29.7	30	0.1	0.1	2.007	29.0	20.4	0.99	20	580	17
13	.35	.71	2.0	78	0.1	79.2	30	1.0	0.1	1.998	39.0	8.1	0.01	16	447	8
14	.35	.71	2.0	78	0.1	77.9	30	1.0	0.1	1.986	39.0	8.6	0.01	17	466	11
15	.35	.71	2.0	78	0.1	77.7	30	1.0	0.1	1.984	39.0	8.7	0.01	19	382	12
16	.40	.80	2.2	64	0.1	56.4	70	0.1	1.0	2.002	36.0	15.7	0.61	59	3698	6
17	.40	.80	2.2	64	0.1	55.4	70	0.1	1.0	1.983	37.0	16.5	0.58	53	2937	6
18	.40	.80	2.2	64	0.1	55.4	70	0.1	1.0	1.984	37.0	16.5	0.61	58	3000	6
19	.10	.70	3.5	87	0.1	78.3	30	0.1	1.0	2.240	35.0	7.6	0.04	22	207	9
20	.10	.70	3.5	87	0.1	79.4	30	0.1	1.0	2.250	35.0	7.2	0.02	19	198	10
21	.10	.70	3.5	87	0.1	79.4	30	0.1	1.0	2.250	35.0	7.2	0.03	22	196	8
22	.10	.70	3.5	87	0.1	40.9	30	1.0	1.0	2.150	33.0	19.5	0.69	38	1500	6
23	.10	.70	3.5	87	0.1	38.5	30	1.0	1.0	2.130	33.0	20.3	0.68	45	1325	9
24	.10	.70	3.5	87	0.1	38.5	30	1.0	1.0	2.130	33.0	20.3	0.72	41	1133	8
25	.20	.70	1.5	977	0.1	84.5	30	0.1	1.0	2.350	20.0	3.1	1.58	59	5000	15
26	.20	.70	1.5	977	0.1	85.0	30	0.1	1.0	2.352	20.0	3.0	1.13	57	4620	12
27	.20	.70	1.5	977	0.1	82.5	30	0.1	1.0	2.340	20.0	3.5	0.86	50	4180	13
28	.20	.70	1.5	977	0.1	52.5	30	1.0	1.0	2.264	20.0	9.5	0.46	63	2500	8
29	.20	.70	1.5	977	0.1	51.5	30	1.0	1.0	2.260	20.0	9.7	0.35	66	2580	9
30	.20	.70	1.5	977	0.1	52.6	30	1.0	1.0	2.277	19.0	9.0	0.38	65	3100	10
31	.35	.71	2.0	78	1.0	91.9	30	0.1	1.0	2.085	36.0	2.9	0.03	3	480	15
32	.35	.71	2.0	78	1.0	89.2	30	0.1	1.0	2.062	37.0	4.0	0.03	3	291	15
33	.35	.71	2.0	78	1.0	88.9	30	0.1	1.0	2.060	37.0	4.1	0.03	3	480	15
34	.35	.71	2.0	78	1.0	62.1	30	1.0	1.0	1.952	34.0	12.9	0.04	24	458	12
35	.35	.71	2.0	78	1.0	61.7	30	1.0	1.0	1.939	35.0	13.4	0.04	30	499	12
36	.35	.71	2.0	78	1.0	62.4	30	1.0	1.0	1.954	34.0	12.8	0.04	28	498	11
37	.73	.77	3.3	977	0.1	63.6	30	0.1	0.1	2.317	17.6	6.4	0.01	20	227	11
38	.73	.77	3.3	977	0.1	60.7	30	0.1	0.1	2.298	18.3	7.2	0.01	20	265	12
39	.73	.77	3.3	977	0.1	57.0	30	0.1	0.1	2.271	19.3	8.3	0.01	21	294	13
40	.66	.78	3.0	3554	1.0	45.6	30	0.1	0.1	1.832	39.0	21.2	0.04	11	100	6
41	.66	.78	3.0	226	1.0	45.6	30	0.1	0.1	1.831	39.0	21.2	0.04	11	81	8
42	.66	.78	3.0	226	1.0	45.5	30	0.1	0.1	1.844	38.0	20.7	0.04	11	103	6
43	.78	.87	1.8	56	1.0	19.1	30	0.1	0.1	0.854	49.3	39.9	0.12	8	235	14
44	.78	.87	1.8	56	1.0	19.8	30	0.1	0.1	0.866	48.6	39.0	0.13	14	228	18
45	.78	.87	1.8	56	1.0	21.2	30	0.1	0.1	0.898	46.7	36.8	0.15	9	132	21
46	.60	.80	2.0	86	0.1	64.7	30	1.0	0.1	1.440	47.0	16.6	0.21	23	572	11
47	.60	.80	2.0	86	0.1	62.3	30	1.0	0.1	1.420	47.0	17.7	0.12	26	545	10
48	.60	.80	2.0	86	0.1	63.6	30	1.0	0.1	1.430	47.0	17.1	0.12	32	828	9
49	.70	.75	3.1	64	0.1	84.7	70	0.1	0.1	2.268	32.0	4.9	0.66	46	3871	7
50	.70	.75	3.1	64	0.1	85.6	70	0.1	0.1	2.274	32.0	4.6	0.58	32	3500	6
51	.70	.75	3.1	64	0.1	82.5	70	0.1	0.1	2.251	32.0	5.6	0.77	31	3720	7
52	.70	.75	3.1	64	0.1	42.5	70	1.0	0.1	2.054	32.0	18.4	0.54	30	1992	7
53	.70	.75	3.1	64	0.1	44.5	70	1.0	0.1	2.085	31.0	17.2	0.46	28	2003	9
54	.70	.75	3.1	64	0.1	43.5	70	1.0	0.1	2.077	31.0	17.5	0.62	28	2191	7
55	.40	.80	2.2	64	1.0	79.8	70	0.1	0.1	2.086	41.0	8.3	0.83	65	8300	8

Appendix D. Continued

TABLE 40 AE SYSTEM MIXTURES (CONT.)

DATA FOR DIFFERENT TYPES OF MIXTURES

OBS	A	B	C	D	E	F	G	H	I	BLKS	VMA	AIRV	RESMOD	HVESTA	MARST	MARF
56	.40	.80	2.2	64	1.0	79.3	70	0.1	0.1	2.083	41.0	8.5	0.83	53	8160	8
57	.40	.80	2.2	64	1.0	79.8	70	0.1	0.1	2.086	41.0	8.3	0.93	67	7600	6
58	.40	.80	2.2	64	1.0	49.1	70	1.0	0.1	1.886	39.7	20.2	0.50	37	3071	8
59	.40	.80	2.2	64	1.0	46.6	70	1.0	0.1	1.900	39.3	21.0	0.53	60	2902	7
60	.40	.80	2.2	64	1.0	45.2	70	1.0	0.1	1.902	39.2	21.5	0.53	56	2790	8
61	.10	.70	3.5	87	1.0	68.1	30	1.0	0.1	2.020	42.0	13.4	0.21	19	200	12
62	.10	.70	3.5	87	1.0	68.3	30	1.0	0.1	2.030	41.0	13.0	0.22	21	220	13
63	.10	.70	3.5	87	1.0	69.3	30	1.0	0.1	2.040	41.0	12.6	0.22	19	240	13
64	.20	.70	1.5	977	1.0	57.1	30	1.0	0.1	2.118	28.0	12.0	0.35	21	500	15
65	.20	.70	1.5	977	1.0	53.3	30	1.0	0.1	2.068	30.0	14.0	0.29	18	640	18
66	.20	.70	1.5	977	1.0	55.9	30	1.0	0.1	2.097	29.0	12.8	0.33	18	540	20
67	.66	.78	3.0	226	0.1	89.7	30	0.1	1.0	2.085	36.0	3.7	0.02	3	333	17
68	.66	.78	3.0	226	0.1	91.4	30	0.1	1.0	2.099	36.0	3.1	0.02	3	433	20
69	.66	.78	3.0	226	0.1	59.4	30	1.0	1.0	2.042	31.5	12.8	0.17	27	1222	12
70	.66	.78	3.0	226	0.1	62.5	30	1.0	1.0	2.075	30.4	11.4	0.08	41	1352	11
71	.66	.78	3.0	226	0.1	62.9	30	1.0	1.0	2.081	30.2	11.2	0.10	43	1800	11
72	.78	.87	1.8	56	0.1	22.0	30	0.1	1.0	1.126	25.9	20.2	0.29	48	2470	15
73	.78	.87	1.8	56	0.1	27.9	30	0.1	1.0	1.193	21.5	15.5	0.27	44	2576	13
74	.78	.87	1.8	56	0.1	39.3	30	0.1	1.0	1.271	16.3	9.9	0.34	58	3192	9
75	.78	.87	1.8	56	0.1	15.5	30	1.0	1.0	1.097	34.9	29.5	0.15	42	1854	11
76	.78	.87	1.8	56	0.1	16.7	30	1.0	1.0	1.140	32.4	27.0	0.13	54	2080	12
77	.78	.87	1.8	56	0.1	22.4	30	1.0	1.0	1.177	30.1	24.6	0.14	41	2417	14
78	.60	.80	2.0	86	1.0	69.6	30	0.1	1.0	1.400	48.0	14.6	0.10	23	1584	17
79	.60	.80	2.0	86	1.0	80.7	30	0.1	1.0	1.500	44.0	8.5	0.28	24	1580	14
80	.60	.80	2.0	86	1.0	73.4	30	0.1	1.0	1.435	47.0	12.5	0.13	23	1706	15
81	.60	.80	2.0	86	1.0	39.8	30	1.0	1.0	1.370	42.0	25.3	0.18	71	4800	8
82	.60	.80	2.0	86	1.0	42.0	30	1.0	1.0	1.410	40.0	23.2	1.23	75	4800	8
83	.60	.80	2.0	86	1.0	42.2	30	1.0	1.0	1.400	41.0	23.7	1.09	66	5016	9
84	.70	.75	3.1	64	1.0	52.0	70	0.1	1.0	2.124	30.0	14.4	0.78	41	2160	8
85	.70	.75	3.1	64	1.0	51.3	70	0.1	1.0	2.119	30.0	14.6	1.03	56	1869	8
86	.70	.75	3.1	64	1.0	53.8	70	0.1	1.0	2.148	29.0	13.4	0.88	59	2816	7
87	.40	.80	2.2	64	0.1	70.7	70	1.0	1.0	2.084	41.0	12.0	0.37	42	4316	9
88	.40	.80	2.2	64	0.1	69.8	70	1.0	1.0	2.075	41.0	12.4	0.38	39	4055	9
89	.40	.80	2.2	64	0.1	71.0	70	1.0	1.0	2.086	41.0	11.9	0.37	52	4181	12
90	.73	.77	3.3	977	0.1	90.5	30	1.0	0.1	2.398	18.9	1.8	0.18	8	477	12
91	.73	.77	3.3	977	0.1	94.0	30	1.0	0.1	2.416	18.3	1.1	0.10	13	412	16
92	.73	.77	3.3	977	0.1	86.7	30	1.0	0.1	2.379	19.6	2.6	0.10	13	500	15
93	.66	.78	3.0	226	1.0	70.3	30	1.0	0.1	2.006	38.7	11.5	0.11	7	551	14
94	.66	.78	3.0	226	1.0	71.3	30	1.0	0.1	2.019	38.3	11.0	0.11	22	684	13
95	.66	.78	3.0	226	1.0	70.0	30	1.0	0.1	2.007	38.7	11.6	0.11	28	738	12
96	.78	.87	1.8	56	1.0	37.4	30	1.0	0.1	0.983	49.2	30.8	0.06	10	396	16
97	.78	.87	1.8	56	1.0	46.2	30	1.0	0.1	1.085	43.9	23.6	0.06	9	483	16
98	.78	.87	1.8	56	1.0	41.9	30	1.0	0.1	1.038	46.3	26.9	0.07	10	446	32
99	.73	.77	3.3	977	1.0	85.8	30	0.1	1.0	2.388	19.0	2.7	0.17	5	685	17
100	.73	.77	3.3	977	1.0	90.0	30	0.1	1.0	2.407	19.0	1.9	0.15	10	694	16
101	.73	.77	3.3	977	1.0	86.8	30	0.1	1.0	2.393	19.0	2.5	0.14	11	783	11
102	.73	.77	3.3	977	1.0	82.7	30	1.0	1.0	2.455	12.7	2.2	0.34	45	1824	9
103	.73	.77	3.3	977	1.0	82.7	30	1.0	1.0	2.457	12.7	2.2	0.31	48	1598	9
104	.73	.77	3.3	977	1.0	79.5	30	1.0	1.0	2.442	13.2	2.7	0.33	45	1710	10
105	.70	.75	3.1	64	1.0	73.6	70	1.0	1.0	2.213	33.0	8.7	0.67	52	2568	8
106	.70	.75	3.1	64	1.0	68.6	70	1.0	1.0	2.158	35.0	11.0	0.77	50	1256	8
107	.70	.75	3.1	64	1.0	64.3	70	1.0	1.0	2.105	37.0	13.2	0.55	40	528	9

Appendix D. Continued

TABLE 41 AES SYSTEM MIXTURES

STATISTICAL ANALYSIS SYSTEM

OBS	A	B	C	D	E	F	G	H	I	BLKS	VMA	AIRV	RESMOD	HVESTA	MARST	MARF
1	.35	.71	2.0	78	0.1	76.8	56.8	0.1	0.1	2.017	38.8	9.0	0.28	40	2592	6
2	.35	.71	2.0	78	0.1	72.6	56.8	0.1	0.1	2.014	39.1	10.7	0.38	36	2652	7
3	.35	.71	2.0	78	0.1	72.8	56.8	0.1	0.1	1.998	39.4	10.7	0.39	38	2968	8
4	.60	.80	2.0	86	0.1	49.1	51.9	0.1	0.1	1.319	49.9	25.4	0.39	31	2142	8
5	.60	.80	2.0	86	0.1	51.1	51.9	0.1	0.1	1.365	48.3	23.6	0.84	61	4033	5
6	.60	.80	2.0	86	0.1	52.0	51.9	0.1	0.1	1.374	47.9	23.0	0.66	58	4218	6
7	.10	.70	3.5	87	1.0	60.5	60.2	0.1	0.1	1.902	46.6	18.4	1.00	49	2790	9
8	.10	.70	3.5	87	1.0	59.1	60.2	0.1	0.1	1.895	46.9	19.2	0.81	41	2697	8
9	.10	.70	3.5	87	1.0	58.1	60.2	0.1	0.1	1.873	47.5	19.7	0.73	37	2604	9
10	.20	.70	1.5	977	1.0	65.2	67.4	0.1	0.1	2.131	32.2	11.2	0.78	45	2266	12
11	.20	.70	1.5	977	1.0	61.4	67.4	0.1	0.1	2.143	31.9	12.3	0.93	43	2520	11
12	.20	.70	1.5	977	1.0	66.8	67.4	0.1	0.1	2.168	31.0	10.3	1.00	44	2862	9
13	.35	.71	2.0	78	0.1	76.9	48.7	1.0	0.1	2.028	44.2	10.2	0.29	37	3535	12
14	.35	.71	2.0	78	0.1	73.6	48.7	1.0	0.1	1.996	45.1	11.9	0.62	43	3822	11
15	.35	.71	2.0	78	0.1	80.5	48.7	1.0	0.1	2.046	43.7	8.5	0.39	34	3724	11
16	.40	.80	2.2	64	0.1	76.3	81.9	0.1	1.0	2.196	36.7	8.7	1.25	76	8000	7
17	.40	.80	2.2	64	0.1	79.4	81.9	0.1	1.0	2.210	36.4	7.5	1.04	62	7954	7
18	.40	.80	2.2	64	0.1	74.1	81.9	0.1	1.0	2.199	36.7	9.5	1.07	68	8178	7
19	.10	.70	3.5	87	0.1	89.1	51.3	0.1	1.0	2.135	44.8	4.9	0.18	32	2496	12
20	.10	.70	3.5	87	0.1	87.1	51.3	0.1	1.0	2.120	45.0	5.8	0.21	34	1908	13
21	.10	.70	3.5	87	0.1	84.6	51.3	0.1	1.0	2.081	46.1	7.1	0.20	29	1760	11
22	.10	.70	3.5	87	0.1	70.7	60.2	1.0	1.0	2.082	41.6	12.2	0.33	47	3162	11
23	.10	.70	3.5	87	0.1	69.7	60.2	1.0	1.0	2.083	41.6	12.6	0.47	44	3069	11
24	.10	.70	3.5	87	0.1	68.8	60.2	1.0	1.0	2.076	41.6	13.0	0.36	45	2940	10
25	.20	.70	1.5	977	0.1	90.2	51.2	0.1	1.0	2.274	30.5	3.0	0.44	36	2880	10
26	.20	.70	1.5	977	0.1	88.9	51.2	0.1	1.0	2.266	30.5	3.4	0.59	28	2646	9
27	.20	.70	1.5	977	0.1	88.9	51.2	0.1	1.0	2.266	30.5	3.4	0.54	40	2652	14
28	.20	.70	1.5	977	0.1	81.4	67.4	1.0	1.0	2.397	23.7	4.4	2.26	93	26780	5
29	.20	.70	1.5	977	0.1	80.0	67.4	1.0	1.0	2.391	24.0	4.8	2.34	93	27250	4
30	.20	.70	1.5	977	0.1	83.1	67.4	1.0	1.0	2.403	23.7	4.0	2.76	91	27810	4
31	.35	.71	2.0	78	1.0	84.5	48.7	0.1	1.0	2.043	44.0	6.8	0.31	33	1638	12
32	.35	.71	2.0	78	1.0	86.3	48.7	0.1	1.0	2.051	43.7	6.0	0.48	23	1456	10
33	.35	.71	2.0	78	1.0	84.4	48.7	0.1	1.0	2.053	43.7	6.8	0.33	28	1440	11
34	.35	.71	2.0	78	1.0	78.1	56.8	1.0	1.0	2.138	35.2	7.7	0.81	40	5915	11
35	.35	.71	2.0	78	1.0	73.7	56.8	1.0	1.0	2.122	35.8	9.4	0.62	28	5590	11
36	.35	.71	2.0	78	1.0	74.9	56.8	1.0	1.0	2.119	35.8	9.0	0.89	48	5280	8
37	.73	.77	3.3	977	0.1	88.4	68.7	0.1	0.1	2.353	24.9	2.9	0.99	37	1560	9
38	.73	.77	3.3	977	0.1	98.3	68.7	0.1	0.1	2.377	23.9	0.4	1.11	29	1482	8
39	.73	.77	3.3	977	0.1	96.7	68.7	0.1	0.1	2.359	24.6	0.8	1.09	28	1596	10
40	.66	.78	3.0	226	1.0	76.4	57.5	0.1	0.1	2.094	36.9	8.7	0.79	54	4800	7
41	.66	.78	3.0	226	1.0	74.3	57.5	0.1	0.1	2.089	36.9	9.5	0.68	52	4875	7
42	.66	.78	3.0	226	1.0	76.2	57.5	0.1	0.1	2.099	36.6	8.7	0.64	54	4602	7
43	.78	.87	1.8	56	1.0	56.6	51.1	0.1	0.1	1.102	41.2	17.9	0.24	45	356	34
44	.78	.87	1.8	56	1.0	60.7	51.1	0.1	0.1	1.122	40.2	15.8	0.24	38	250	35
45	.78	.87	1.8	56	1.0	64.0	51.1	0.1	0.1	1.194	36.4	13.1	0.33	48	875	17
46	.60	.80	2.0	86	0.1	83.9	45.2	1.0	0.1	1.617	45.9	7.4	0.49	52	4200	10
47	.60	.80	2.0	86	0.1	78.4	45.2	1.0	0.1	1.575	47.6	10.3	0.28	39	3264	12
48	.70	.75	3.1	64	0.1	87.1	79.6	0.1	0.1	2.259	38.7	5.0	0.54	50	4370	3
49	.70	.75	3.1	64	0.1	86.1	79.6	0.1	0.1	2.205	39.6	5.5	0.56	46	3136	8
50	.70	.75	3.1	64	0.1	89.1	79.6	0.1	0.1	2.256	38.7	4.2	0.49	40	3842	6
51	.70	.75	3.1	64	0.1	68.2	83.4	1.0	0.1	2.190	34.6	11.0	1.28	57	5292	12
52	.70	.75	3.1	64	0.1	70.8	83.4	1.0	0.1	2.245	33.2	9.7	1.08	58	7050	10
53	.70	.75	3.1	64	0.1	79.8	83.4	1.0	0.1	2.265	32.6	6.6	1.16	56	8178	9
54	.40	.80	2.2	64	1.0	86.5	78.4	0.1	0.1	2.117	45.9	6.2	0.76	61	15225	9
55	.40	.80	2.2	64	1.0	85.6	78.4	0.1	0.1	2.115	45.9	6.6	0.69	61	15753	9

Appendix D. Continued

TABLE 41 AES SYSTEM MIXTURES (CONT.)

STATISTICAL ANALYSIS SYSTEM

OBS	A	B	C	D	E	F	G	H	I	BLKS	VMA	AIRV	RESMOD	HVESTA	MARST	MARF
56	.40	.80	2.2	64	1.0	83.9	78.4	0.1	0.1	2.121	45.9	7.4	0.80	59	15840	10
57	.40	.80	2.2	64	1.0	72.1	81.9	1.0	0.1	2.134	38.7	10.8	1.26	72	13350	7
58	.40	.80	2.2	64	1.0	71.7	81.9	1.0	0.1	2.155	38.1	10.8	1.45	73	15470	8
59	.40	.80	2.2	64	1.0	74.6	81.9	1.0	0.1	2.162	37.8	9.6	0.93	78	15510	7
60	.10	.70	3.5	87	1.0	81.0	51.3	1.0	0.1	2.026	47.4	9.0	0.59	32	2100	14
61	.10	.70	3.5	87	1.0	80.3	51.3	1.0	0.1	2.018	47.6	9.4	0.55	31	1900	12
62	.10	.70	3.5	87	1.0	82.9	51.3	1.0	0.1	2.032	47.4	8.1	0.48	34	2000	10
63	.20	.70	1.5	977	1.0	63.9	51.2	1.0	0.1	2.099	35.7	12.9	0.64	43	1584	15
64	.20	.70	1.5	977	1.0	67.5	51.2	1.0	0.1	2.144	34.5	11.2	0.88	45	2530	11
65	.20	.70	1.5	977	1.0	66.4	51.2	1.0	0.1	2.143	34.5	11.6	0.70	45	1854	10
66	.66	.78	3.0	226	0.1	85.4	49.3	0.1	1.0	2.040	43.9	6.4	0.13	32	1010	12
67	.66	.78	3.0	226	0.1	85.3	49.3	0.1	1.0	2.057	43.4	6.4	0.12	27	1050	10
68	.66	.78	3.0	226	0.1	85.3	49.3	0.1	1.0	2.055	43.4	6.4	0.12	26	1160	10
69	.66	.78	3.0	226	0.1	81.1	57.5	1.0	1.0	2.193	33.9	6.4	0.56	34	2912	8
70	.66	.78	3.0	226	0.1	79.9	57.5	1.0	1.0	2.187	33.9	6.8	0.58	37	3150	10
71	.66	.78	3.0	226	0.1	81.0	57.5	1.0	1.0	2.196	33.6	6.4	0.63	39	3808	11
72	.78	.87	1.8	56	0.1	80.5	44.7	0.1	1.0	1.283	26.6	5.2	0.31	41	3132	12
73	.78	.87	1.8	56	0.1	67.1	44.7	0.1	1.0	1.240	28.9	9.5	0.24	42	2842	12
74	.78	.87	1.8	56	0.1	79.4	44.7	0.1	1.0	1.315	24.8	5.1	0.26	49	2990	12
75	.78	.87	1.8	56	0.1	48.6	51.1	1.0	1.0	1.240	35.8	18.4	0.81	53	4675	9
76	.78	.87	1.8	56	0.1	48.6	51.1	1.0	1.0	1.244	35.8	18.4	0.66	62	5432	8
77	.78	.87	1.8	56	0.1	65.6	51.1	1.0	1.0	1.333	31.1	10.7	0.39	55	5460	10
78	.60	.80	2.0	86	1.0	92.3	45.2	0.1	1.0	1.603	46.6	3.6	0.19	27	1664	14
79	.60	.80	2.0	86	1.0	93.5	45.2	0.1	1.0	1.607	46.3	3.0	0.10	30	1998	14
80	.60	.80	2.0	86	1.0	92.3	45.2	0.1	1.0	1.600	46.6	3.6	0.08	31	2109	14
81	.60	.80	2.0	86	1.0	50.5	51.9	1.0	1.0	1.527	41.8	20.7	1.35	93	19500	8
82	.60	.80	2.0	86	1.0	51.2	51.9	1.0	1.0	1.545	41.4	20.2	1.35	93	18000	6
83	.60	.80	2.0	86	1.0	67.5	51.9	1.0	1.0	1.607	38.8	12.6	1.33	93	21528	7
84	.70	.75	3.1	64	1.0	79.3	83.4	0.1	1.0	2.300	31.4	6.5	1.29	72	10290	6
85	.70	.75	3.1	64	1.0	75.2	83.4	0.1	1.0	2.243	33.1	8.2	1.23	72	11040	7
86	.70	.75	3.1	64	1.0	81.7	83.4	0.1	1.0	2.292	31.7	5.8	1.03	73	11280	8
87	.40	.80	2.2	64	0.1	82.9	78.4	1.0	1.0	2.147	45.1	7.7	0.38	42	7350	8
88	.40	.80	2.2	64	0.1	81.2	78.4	1.0	1.0	2.147	45.1	8.5	0.46	55	7500	8
89	.40	.80	2.2	64	0.1	85.8	78.4	1.0	1.0	2.194	45.1	6.4	0.35	40	6726	6
90	.73	.77	3.3	977	0.1	82.2	58.8	1.0	0.1	2.309	29.7	5.3	0.42	30	1488	8
91	.73	.77	3.3	977	0.1	79.5	58.8	1.0	0.1	2.312	29.7	6.1	0.32	24	1316	12
92	.73	.77	3.3	977	0.1	76.3	58.8	1.0	0.1	2.326	29.1	6.9	0.33	22	1056	11
93	.66	.78	3.0	226	1.0	74.5	49.3	1.0	0.1	2.042	44.0	11.2	0.34	35	2728	10
94	.66	.78	3.0	226	1.0	79.8	49.3	1.0	0.1	2.038	44.0	8.9	0.31	33	2223	10
95	.66	.78	3.0	226	1.0	79.8	49.3	1.0	0.1	2.043	44.0	8.9	0.30	28	2242	10
96	.78	.87	1.8	56	1.0	61.6	44.7	1.0	0.1	1.155	46.4	17.8	0.23	45	435	27
97	.78	.87	1.8	56	1.0	66.7	44.7	1.0	0.1	1.159	46.0	15.3	0.09	41	364	31
98	.78	.87	1.8	56	1.0	80.6	44.7	1.0	0.1	1.260	41.3	8.0	0.13	30	791	14
99	.73	.77	3.3	977	1.0	89.7	58.8	0.1	1.0	2.358	28.2	2.9	0.60	25	1224	13
100	.73	.77	3.3	977	1.0	87.2	58.8	0.1	1.0	2.344	28.8	3.7	0.99	30	1313	12
101	.73	.77	3.3	977	1.0	84.2	58.8	0.1	1.0	2.370	27.9	4.4	0.87	28	1560	12
102	.73	.77	3.3	977	1.0	85.7	68.7	1.0	1.0	2.435	22.3	3.2	0.63	30	1545	9
103	.73	.77	3.3	977	1.0	85.5	68.7	1.0	1.0	2.444	22.0	3.2	0.39	26	1122	15
104	.73	.77	3.3	977	1.0	89.2	68.7	1.0	1.0	2.435	22.3	2.4	0.37	25	964	17
105	.70	.75	3.1	64	1.0	86.9	79.6	1.0	1.0	2.284	38.2	5.0	0.74	52	2120	8
106	.70	.75	3.1	64	1.0	74.2	79.6	1.0	1.0	2.160	41.4	10.7	0.80	46	3811	9
107	.70	.75	3.1	64	1.0	84.1	79.6	1.0	1.0	2.252	39.0	6.2	0.84	50	3774	10

Appendix E. Regression Coefficients for Response Surface Fitting

The decision (design) variables and response (test) variables used in the screening test are as follows:

TABLE 42 DECISION AND RESPONSE VARIABLE USED

Variable	Symbol
Decision (design) Variables:	
Roundness	A
Sphericity	B
Roughness	C
Size and Gradation	D
Type of Asphalt	E
Vol. Binder (% VMA)	F
Vol. Sulphur (% Binder)	G
Moisture Condition	H
Compaction Effort	I
Response (test) Variables:	
Bulk Sp. Gravity	J
VMA (%)	K
Air Voids (%)	L
Resilient Modulus ($X10^6$ psi)	M
Hveem Stability	N
Marshall Stability (lb)	O
Marshall Flow (1/100 in.)	P

1 psi = 6.894 kPa
1 lb = 0.454 kg
1 in = 25.4 mm

The second order response surface used for evaluation of the screening tests is of the form:

$$y = \beta_o + \sum_{i=1}^{9} \beta_i x_i + \sum_{i,j=1}^{9} \beta_{ij} x_i x_j + \varepsilon$$

for each response variable

where

β_o, β_i, β_{ij} are the regression coefficients,

x_i are the test variables (A, B, C, . . ., I),

$x_i x_j$ are the first order interactions,

ε is the experimental error and

y is the response variable.

Appendix E. Continued

TABLE 43 RESPONSE SURFACE FITTING FOR AAS SYSTEM MIXTURES

Source	Regression Coefficient (B) for Indicated Response Variable						
	Bulk Sp. Gr.	VMA	Air Voids	Resilient Modulus	Hveem Stability	Marshall Stability	Marshall Flow
Intercept	8.31	99.42	39.45	-12.69	749.83	22785.22	25.56
A	-1.26	-34.97	-19.26	-7.90	24.46	2169.34	55.67
B	10.47	84.32	84.02	24.78	-446.98	-59173.94	-83.63
C	-2.79	-11.84	7.20	12.00	90.02	30100.92	-20.70
D	0.00	-0.14	0.00	0.01	-0.33	42.51	0.20
E	-1.63	22.72	25.89	-7.70	-54.61	-103816.07	19.15
F	-0.02	2.42	0.62	-0.22	-64.9	-2022.76	-0.59
G	0.02	-1.42	-0.75	0.00	-4.48	366.07	0.02
H	2.29	-147.69	-79.52	3.13	-118.63	38640.97	-83.77
I	4.10	-180.83	-112.50	9.57	-288.58	155700.51	-5.92
AC	0.01	-19.17	-9.96	1.10	-38.28	-2824.32	12.18
AD	0.00	0.16	0.12	0.02	0.54	132.06	-0.24
AE	-0.61	20.16	12.15	-0.90	34.61	-16150.90	-11.19
AF	0.00	0.81	0.36	0.05	1.24	6.85	-0.99
AH	0.24	-16.32	-7.71	-1.10	11.25	-3791.69	-6.90
AI	0.35	-21.99	-14.26	-0.78	-103.79	10055.10	25.69
BC	3.26	23.21	-5.38	-19.45	-230.70	-49208.53	58.95
BD	0.00	0.41	0.19	0.00	0.90	-18.80	-0.39
BE	2.38	-58.98	-48.87	8.43	-66.12	115858.32	-6.56
BF	0.04	-4.32	-1.71	0.15	3.22	2428.32	2.12
BH	-0.62	63.40	27.22	0.87	34.56	-5754.10	60.92
BI	-2.86	124.45	71.79	-3.30	511.19	-125576.06	-80.81
CD	0.00	-0.05	-0.03	0.00	-0.19	-44.36	0.08
CE	0.05	0.50	-0.24	0.56	5.87	6903.14	0.00
CF	0.00	0.04	0.02	0.03	0.87	196.77	-0.31
CG	0.00	0.04	0.04	0.01	0.85	49.54	-0.19
CH	-0.07	3.79	1.89	-0.42	-5.33	-2945.31	-0.18
CI	-0.01	-1.90	-0.96	-1.15	-21.50	-11205.04	3.76
DE	0.00	0.00	0.00	0.00	-0.04	6.55	0.00
DF	0.00	0.00	0.00	0.00	0.00	-0.06	0.00
DG	0.00	0.00	0.00	0.00	0.00	0.35	0.00
DH	0.00	-0.01	0.00	0.00	-0.01	3.71	0.00
DI	0.00	0.00	0.00	0.00	0.00	-3.58	0.00
EF	0.00	0.08	0.04	0.02	1.15	139.31	-0.10
EG	0.00	0.08	0.03	0.01	0.91	0.26	-0.24
EH	-0.03	0.84	0.90	-0.51	-3.03	-4024.75	1.42
EI	-0.07	3.30	4.27	-2.36	-62.84	-11150.64	19.50
FG	0.00	0.00	0.00	0.00	0.01	-3.64	0.00
FH	0.00	0.33	0.17	0.00	-0.09	-43.76	0.25
FI	0.00	0.36	0.28	0.00	0.05	-126.94	0.06
GH	-0.02	1.14	0.71	-0.02	1.80	-236.16	0.41
GI	-0.02	1.03	0.64	-0.01	0.69	-164.79	0.51
HI	0.00	4.40	0.08	-1.02	-24.84	-9021.32	-1.80

Appendix E. Continued

TABLE 44 RESPONSE SURFACE FITTING FOR AE SYSTEM MIXTURES

Source	Regression Coefficient (B) for Indicated Response Variable						
	Bulk Sp. Gr.	VMA	Air Voids	Resilient Modulus	Hveem Stability	Marshall Stability	Marshall Flow
Intercept	-136.39	6017.17	3797.56	245.50	18364.47	924758.58	-3741.86
A	-66.22	2770.23	1727.90	94.30	6802.67	324075.50	-1318.33
B	219.89	-9348.10	-5898.36	-403.71	-30305.81	-1507716.56	6216.27
C	57.75	-2255.82	-1475.58	-139.82	-10999.72	-539783.86	2355.76
D	-0.05	1.29	1.03	0.20	16.34	817.45	-3.52
E	9.49	-664.16	-381.00	30.78	2735.04	111664.18	-761.00
F	0.00	0.25	0.23	-0.02	0.17	-494.27	-0.16
G	-0.05	2.09	1.51	0.14	11.20	367.59	-2.43
H	-0.48	28.23	6.49	-4.97	57.21	1114.00	-28.77
I	19.69	-1440.77	-797.04	59.15	5532.22	288982.80	-1386.20
AC	21.52	-812.40	-526.31	-46.84	-3628.39	-171845.80	765.36
AD	-0.00	0.22	0.18	0.03	3.17	163.12	-0.70
AE	6.33	-436.41	-245.42	19.92	1830.67	82737.74	-487.05
AF	0.00	0.08	0.13	0.00	-0.61	-200.62	0.15
AH	0.01	1.23	0.35	-0.10	17.49	1296.44	-3.43
AI	8.14	-585.70	-326.50	25.14	2349.81	117898.15	-587.87
BC	-86.59	3294.10	2169.70	221.52	17515.05	856341.39	-3767.91
BD	0.07	-1.75	-1.44	-0.29	-23.93	-1206.56	5.18
BE	-13.78	961.27	551.96	-43.46	-3958.35	-158967.67	1104.81
BF	0.00	-0.92	-1.25	0.03	-0.29	674.30	0.18
BH	0.59	-18.56	-0.40	1.04	-60.81	-1075.94	31.28
BI	-25.66	1868.01	1029.39	-77.67	-7279.53	-372682.16	1831.75
CD	0.0	0.0	0.0	0.0	0.0	0.0	0.0
CE	-1.37	95.20	53.15	-4.13	-377.79	-18347.18	95.72
CF	0.00	0.10	0.06	0.00	-0.26	-18.35	0.01
CG	0.0	0.0	0.0	0.0	0.0	0.0	0.0
CH	-0.02	-0.27	0.30	0.41	8.44	1082.17	-2.11
CI	-1.83	131.51	72.85	-5.49	-517.47	-26595.74	131.50
DE	0.00	-0.07	-0.03	0.00	0.25	15.12	-0.06
DF	0.00	0.00	0.00	0.00	-0.00	0.01	0.00
DG	0.0	0.0	0.0	0.0	0.0	0.0	0.0
DH	0.00	0.00	0.00	0.00	-0.00	0.13	-0.00
DI	0.0	0.0	0.0	0.0	0.0	0.0	0.0
EF	0.00	0.07	0.01	-0.01	-0.48	-56.70	0.16
EG	0.0	0.0	0.0	0.0	0.0	0.0	0.0
EH	0.00	-4.74	-2.00	0.08	12.41	9.65	-0.06
EI	0.0	0.0	0.0	0.0	0.0	0.0	0.0
FG	0.00	0.00	0.00	0.00	0.02	4.03	0.00
FH	0.00	-0.18	-0.08	0.00	0.18	-20.31	0.06
FI	0.00	0.15	0.13	0.00	0.24	-21.94	-0.10
GH	0.00	0.02	-0.04	-0.01	-0.84	-25.22	0.15
GI	0.0	0.0	0.0	0.0	0.0	0.00	0.0
HI	0.00	0.25	2.60	-0.25	-10.71	-2273.81	0.91

TABLE 45 RESPONSE SURFACE FITTING FOR AES SYSTEM MIXTURES

Source	Regression Coefficient (B) for Indicated Response Variable						
	Bulk Sp. Gr.	VMA	Air Voids	Resilient Modulus	Hveem Stability	Marshall Stability	Marshall Flow
Intercept	49.08	-8319.01	-1737.53	-158.06	-28885.52	-6957106.37	-6536.03
A	24.45	-3757.04	-1092.36	-97.66	-17690.15	-4299039.41	-3088.33
B	-69.73	9378.76	2638.78	198.25	39629.76	9555307.88	7824.35
C	-8.52	855.77	193.63	-28.19	-460.16	-25097.27	428.08
D	-0.01	1.07	0.35	0.10	12.15	2873.96	1.43
E	-22.17	2521.73	904.08	153.89	20057.04	4869409.98	3007.39
F	0.02	1.13	-0.51	-0.01	-2.09	-3623.33	2.27
G	0.03	-3.77	-1.19	0.06	-12.88	-2829.97	-2.54
H	1.15	-108.39	-29.90	3.49	-397.27	-102291.11	-24.74
I	-47.83	6370.42	1972.48	287.63	42997.69	10363942.54	6539.26
AC	-1.18	330.57	76.31	-10.94	-388.97	-60568.11	86.86
AD	0.00	0.20	0.07	0.01	2.37	557.74	0.33
AE	-15.15	1968.28	617.16	95.37	13556.09	3278640.74	2040.37
AF	0.00	0.53	0.15	-0.01	-1.00	-937.15	0.12
AH	0.03	3.93	0.64	0.72	23.77	2329.07	9.29
AI	-21.07	2768.57	854.10	123.57	18498.96	4453411.69	2837.82
BC	2.57	-416.51	-34.94	79.93	6477.14	1437772.53	231.60
BD	0.01	-2.02	-0.66	-0.15	-19.68	-4700.82	-2.49
BE	31.39	-3994.00	-1276.10	-215.20	-25317.84	-6871593.99	-4183.40
BF	-0.01	-1.92	0.04	0.02	2.02	4287.44	-2.69
BH	-0.68	73.42	20.80	-4.87	162.46	49381.23	-13.26
BI	65.53	-8679.72	-2684.85	-384.70	-57877.57	-13917982.74	-8892.40
CD	0.0	0.0	0.0	0.0	0.0	0.0	0.0
CE	3.76	-489.94	-148.85	-20.00	-3179.38	-762202.60	-496.17
CF	0.00	-0.11	0.01	0.00	0.14	11.89	0.01
CG	0.00	-0.29	-0.02	0.00	0.02	-258.13	0.08
CH	-0.02	0.03	0.32	-0.44	-7.81	-3382.35	3.38
CI	4.83	-639.47	-195.42	-26.19	-4199.12	-1005201.66	-649.99
DE	0.00	0.35	0.10	0.01	2.24	531.54	0.35
DF	0.00	0.00	0.00	0.00	-0.00	0.09	0.00
DG	0.00	0.00	0.00	0.00	-0.00	0.09	0.00
DH	0.00	-0.01	0.00	0.00	-0.07	-14.32	-0.01
DI	0.0	0.0	0.0	0.0	0.0	0.0	0.0
EF	0.00	0.15	0.00	-0.01	-1.25	-303.66	-0.36
EG	0.00	0.32	0.03	-0.06	0.06	-123.19	0.17
EH	0.00	-2.74	-0.21	-0.08	-4.67	-3058.90	-3.62
EI	-0.47	34.46	9.24	1.46	121.20	33728.69	-1.56
FH	0.00	0.00	0.00	0.00	0.01	13.08	-0.00
FH	0.00	-0.07	0.00	0.01	0.62	315.24	-0.14
FI	0.00	0.16	0.11	-0.01	-0.61	-249.27	0.58
GH	0.00	0.75	0.17	0.00	3.73	797.66	0.51
GI	-0.03	4.27	1.13	0.03	20.55	4485.02	3.83
HI	-0.09	10.82	2.18	-0.77	-29.38	-8861.70	2.07

Appendix F. Flexure Fatigue Curves

Fatigue parameters used in the fatigue law and the VESYS IIM program are calculated from flexural fatigue test data as follows:

$$N_f = K_1 \left(\frac{1}{\varepsilon}\right)^{K_2}$$

where N_f is the number of repetitions to failure

ε is strain

K_1 and K_2 are fatigue parameters

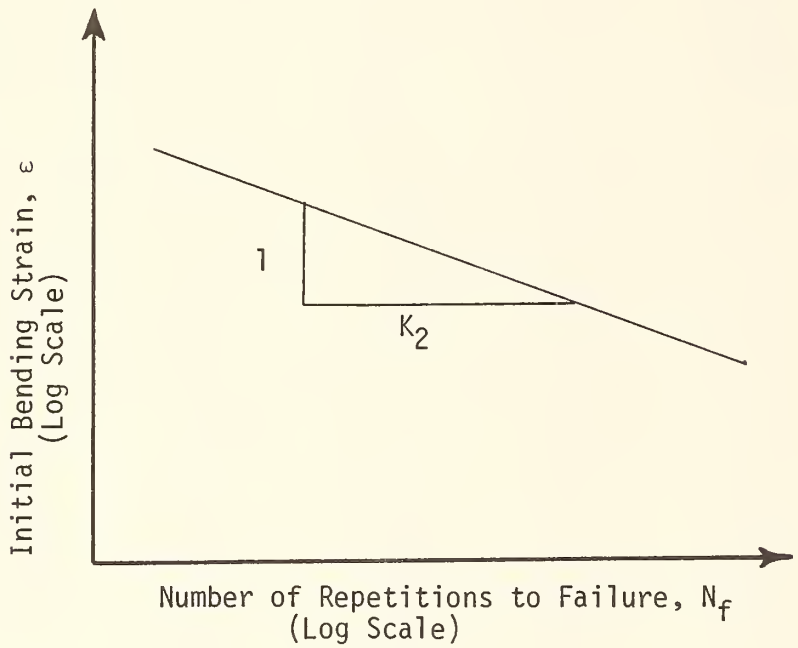

$$\text{Log}_{10}K_1 = \text{Log}_{10}N_f + K_2\text{Log}_{10}\varepsilon$$

Determine the value of K_2 graphically. Select a value for N_f and determine the respective value for ε. Then calculate K_1.

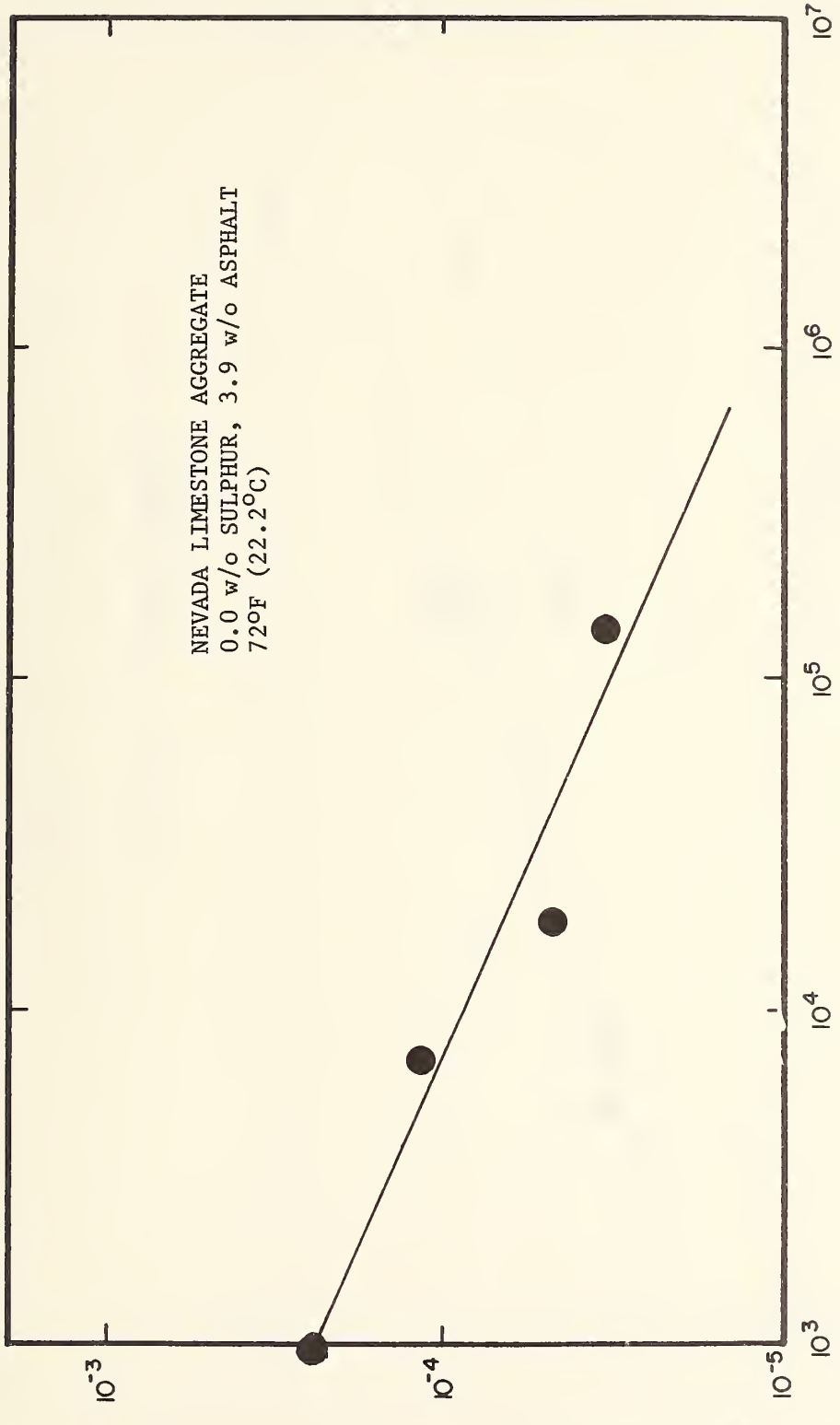

FIG. 92 -- FLEXURAL FATIGUE TEST RESULTS for NEVADA LIMESTONE AGGREGATE (0.0 w/o SULPHUR, 3.9 ASPHALT) AT 72°F (22.2°C)

1 inch = 25.4 mm

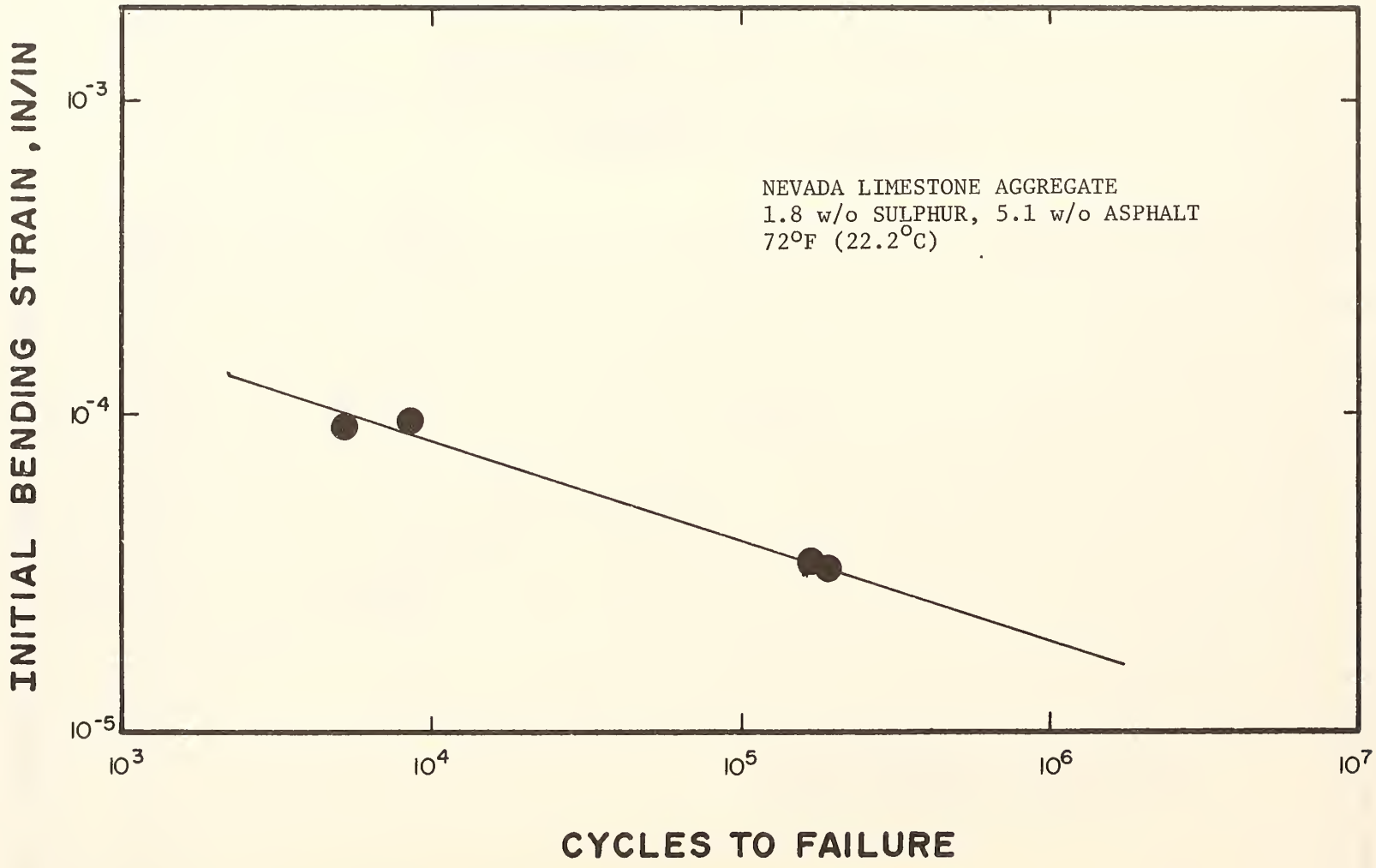

FIG. 93 FLEXURAL FATIGUE TEST RESULTS FOR NEVADA LIMESTONE AGGREGATE (1.8 w/o SULPHUR, 5.1 w/o ASPHALT) at 72°F (22.2°C)

1 inch = 25.4 mm

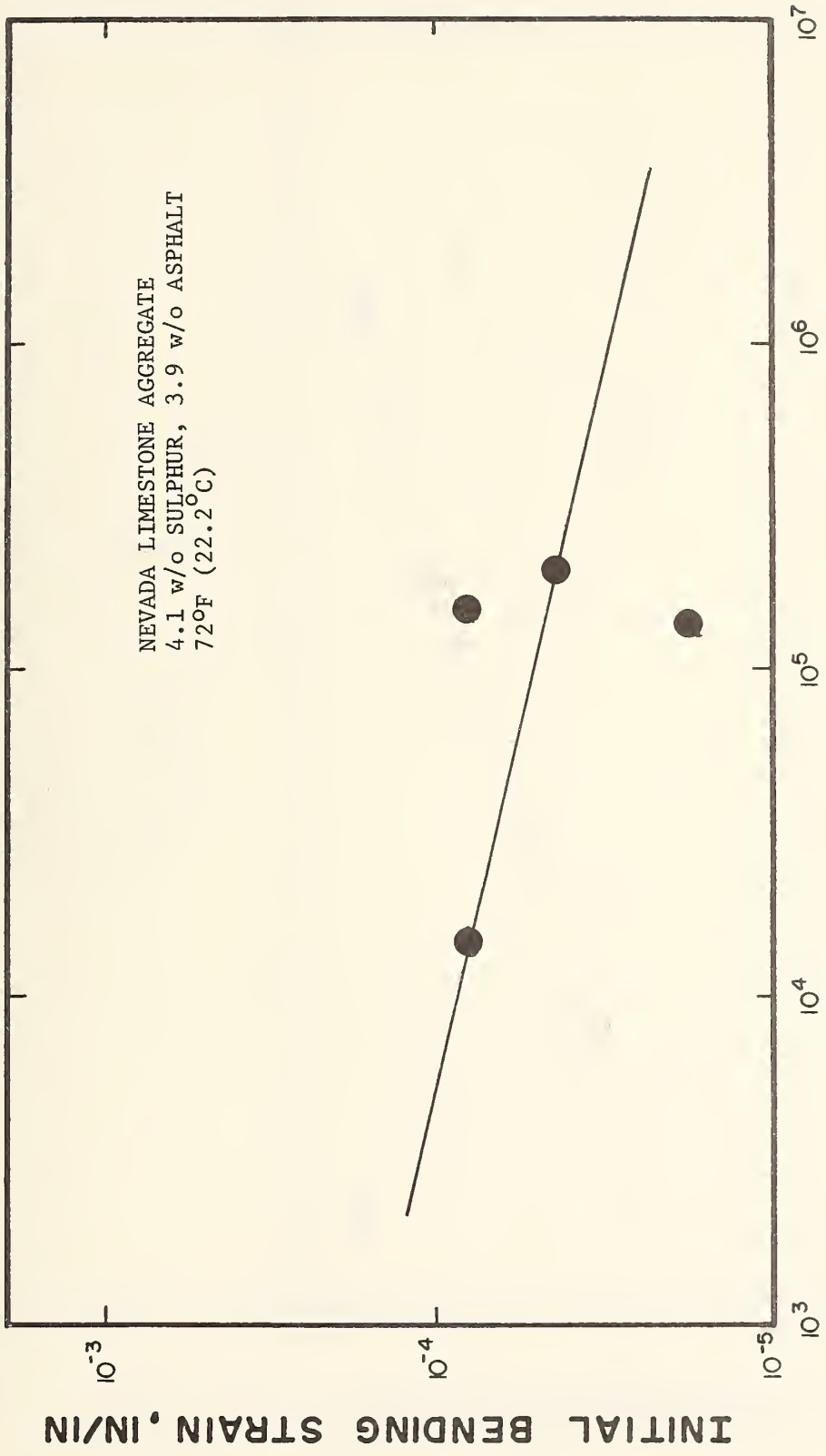

FIG. 94 FLEXURAL FATIGUE TEST RESULTS FOR NEVADA LIMESTONE AGGREGATE (4.1 w/o SULPHUR, 3.9 w/o ASPHALT) at 72°F (22.2°C)

1 inch = 25.4 mm

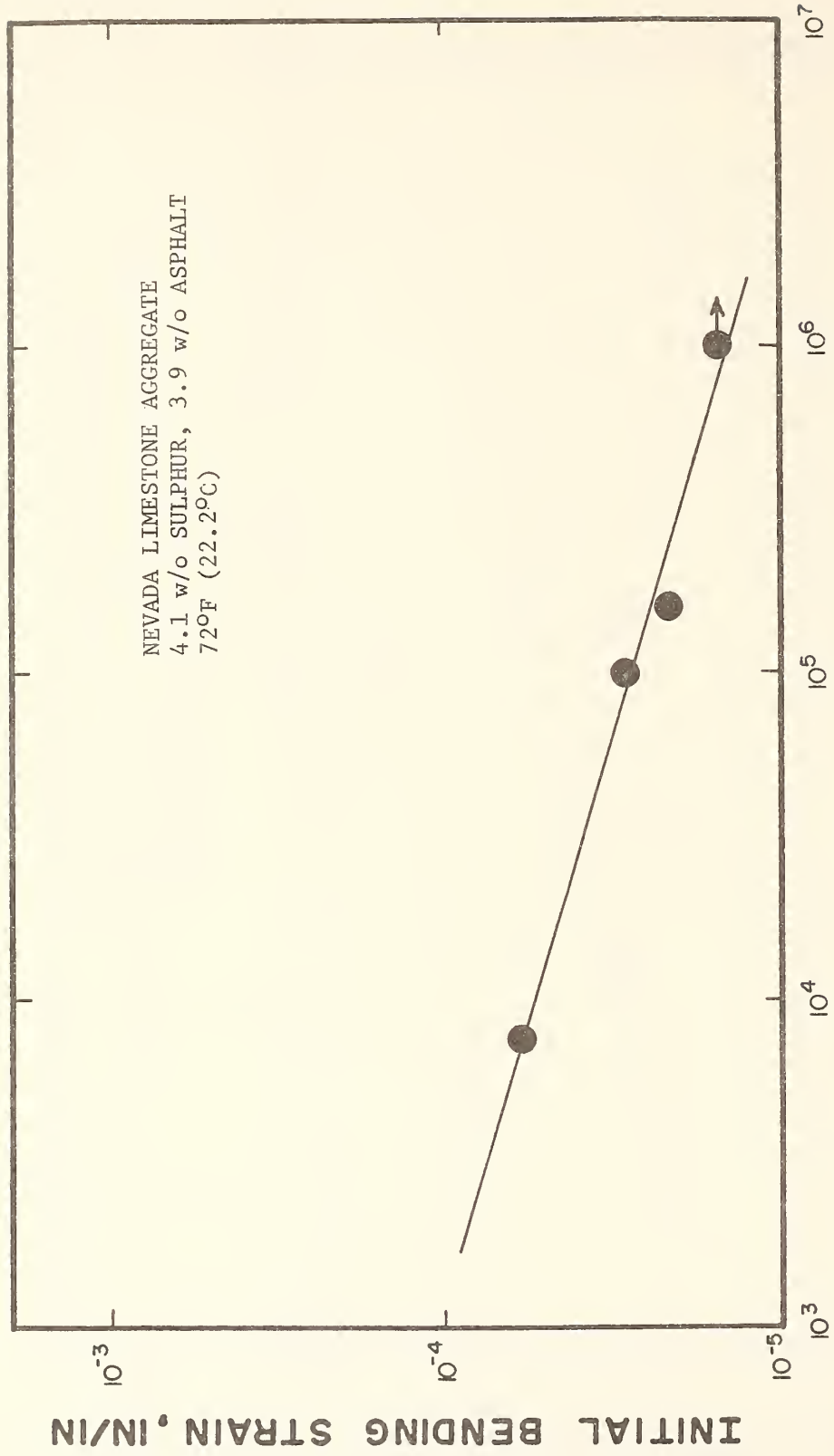

FIG. 95 FLEXURAL FATIGUE TEST RESULTS FOR NEVADA LIMESTONE AGGREGATE (4.1 w/o SULPHUR, 3.9 w/o ASPHALT) at 72°F (22.2°C)

1 inch = 25.4 mm

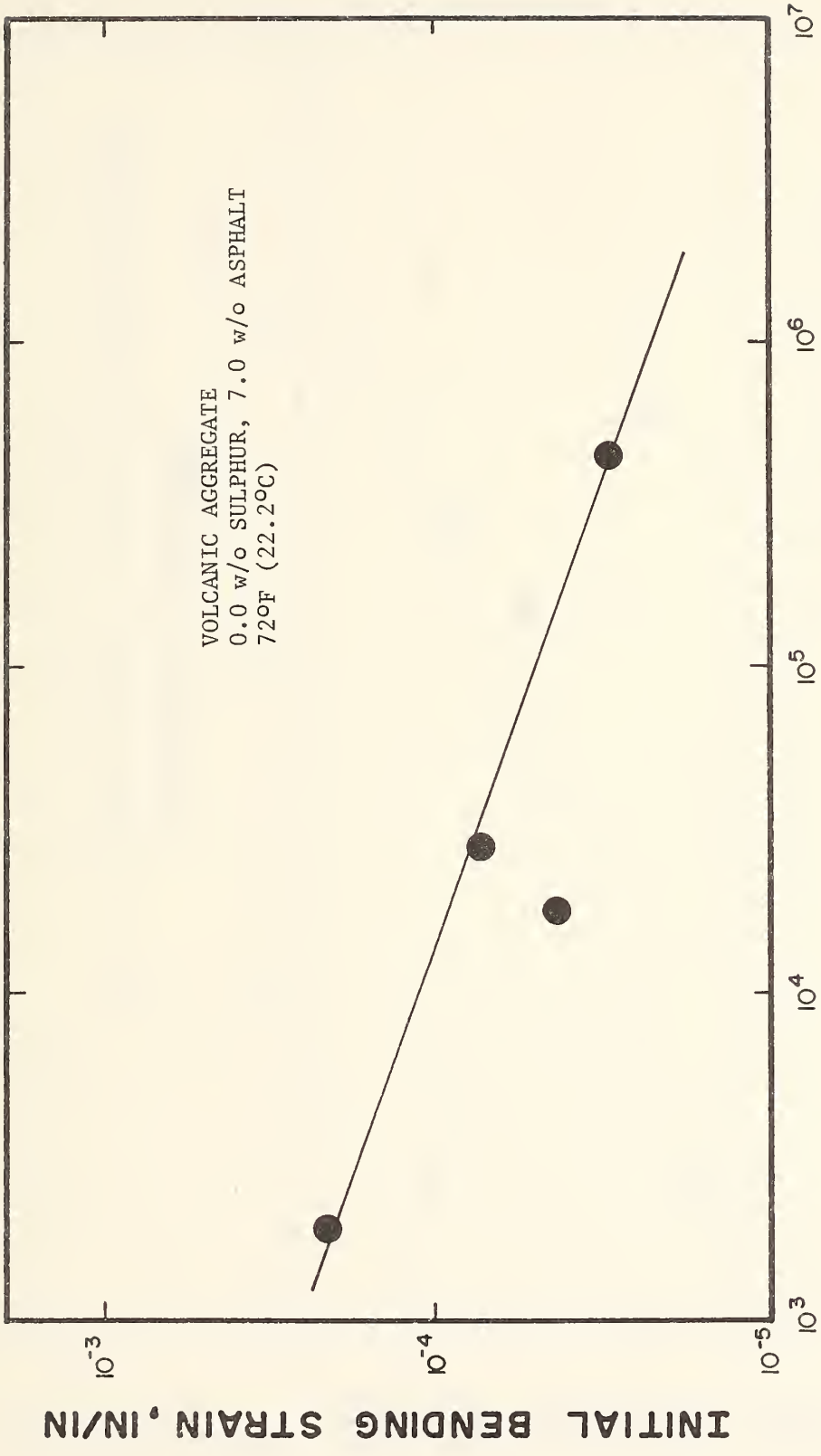

FIG. 96 FLEXURAL FATIGUE TEST RESULTS FOR VOLCANIC AGGREGATE (0.0 w/o SULPHUR, 7.0 w/o ASPHALT) at 72°F (22.2°C)

1 inch = 25.4 mm

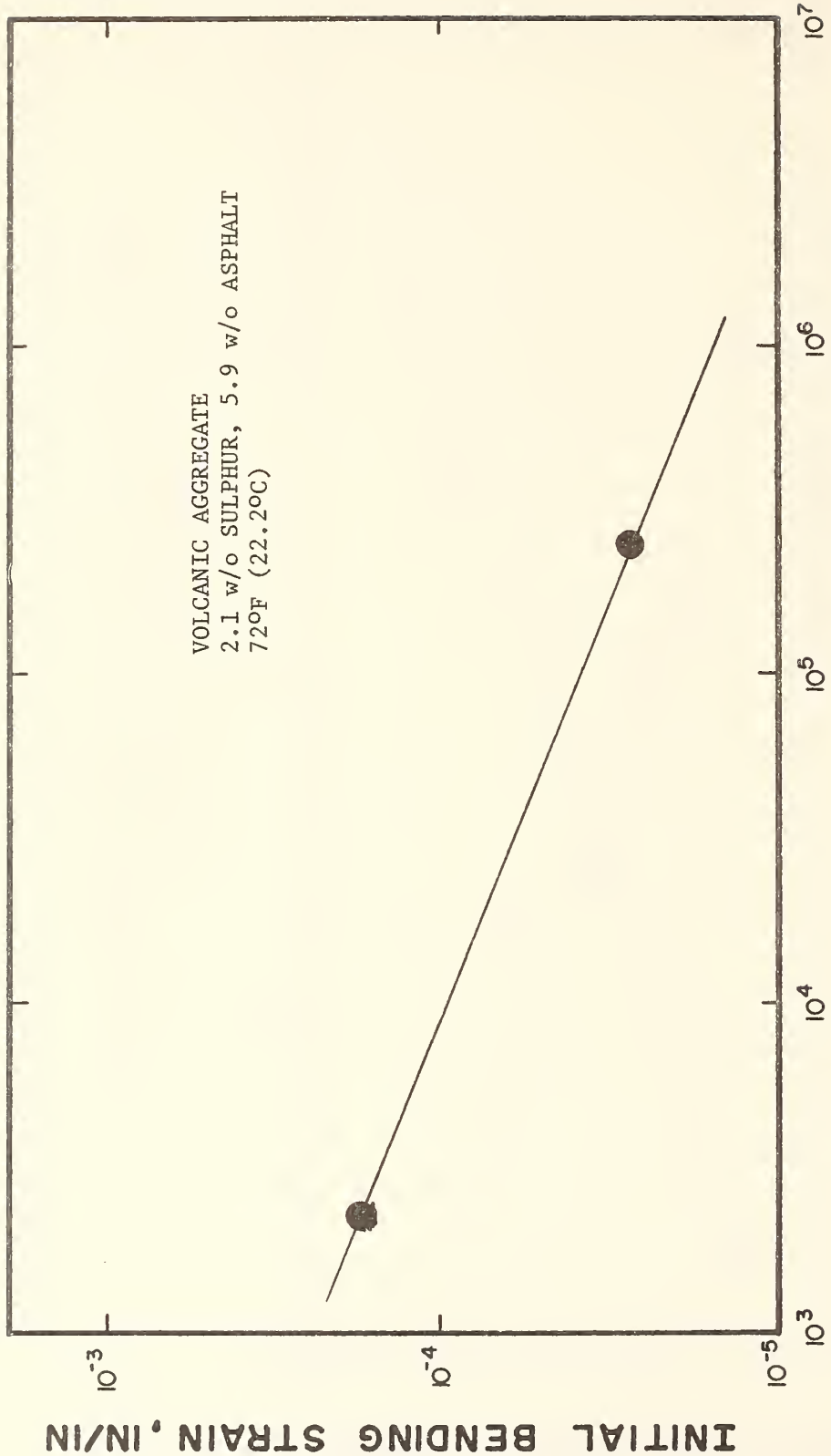

FIG. 97 FLEXURAL FATIGUE TEST RESULTS FOR VOLCANIC AGGREGATE (2.1 w/o SULPHUR, 5.9 w/o ASPHALT) at 72°F (22.2°C)

1 inch = 25.4 mm

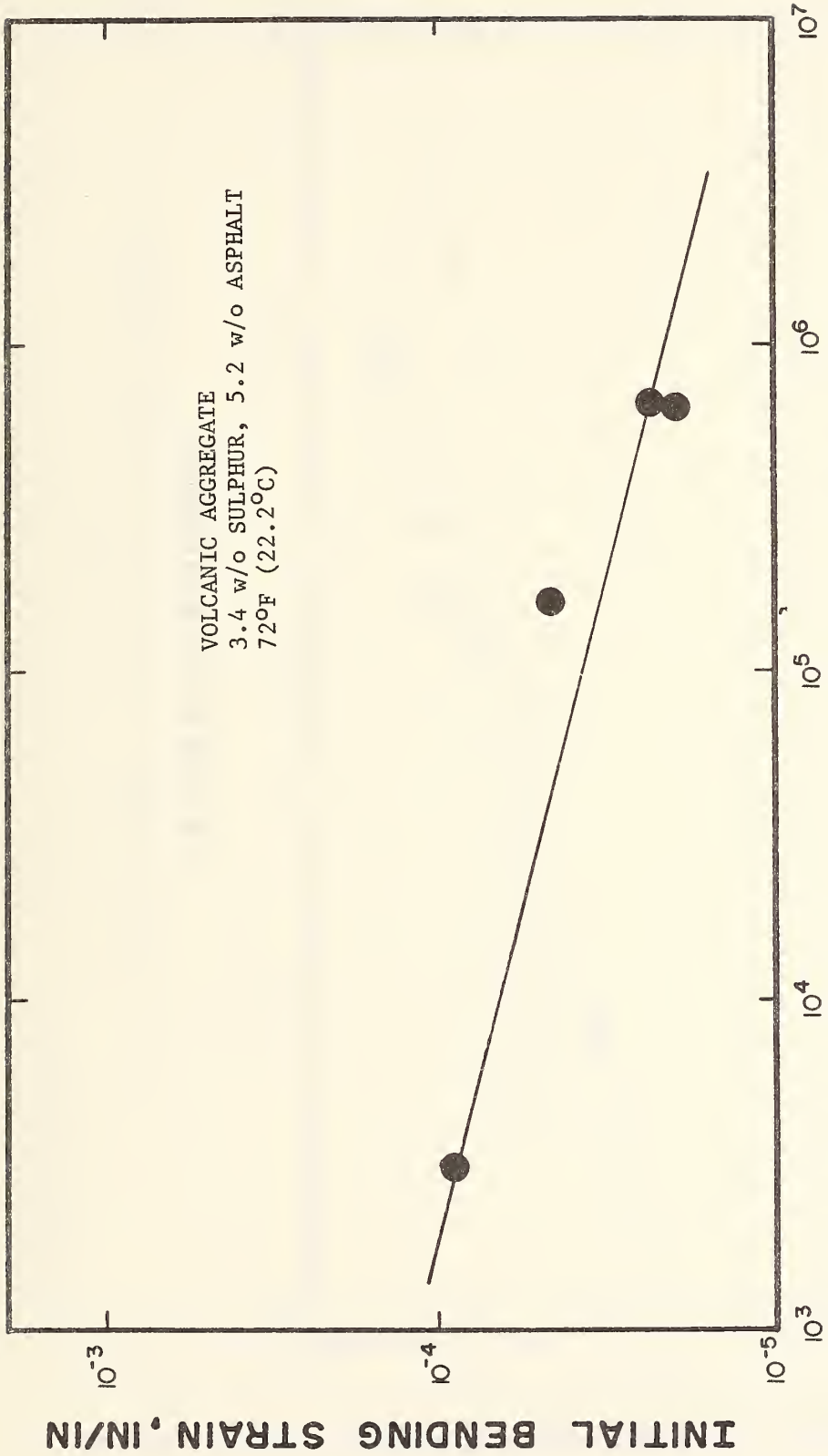

FIG. 98 FLEXURAL FATIGUE TEST RESULTS FOR VOLCANCIL AGGREGATE (3.4 w/o SULPHUR, 5.2 w/o ASPHALT) at 72°F (22.2°C)

1 inch = 25.4 mm

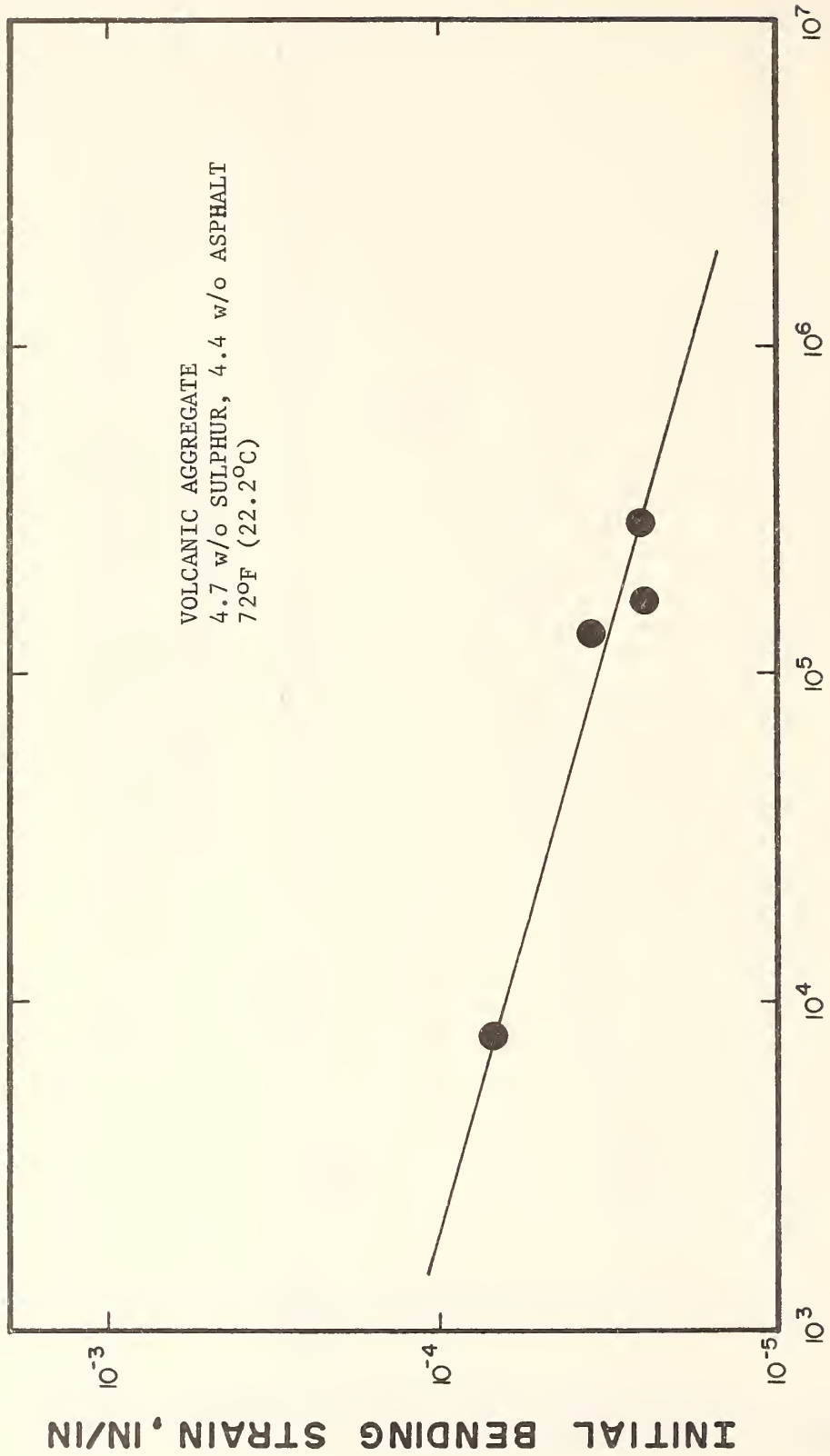

FIG. 99 FLEXURAL FATIGUE TEST RESULTS FOR VOLCANCIC AGGREGATE (4.7 w/o SULPHUR, 4.4 w/o ASPHALT) at 72°F (22.2°C)

1 inch = 25.4 mm

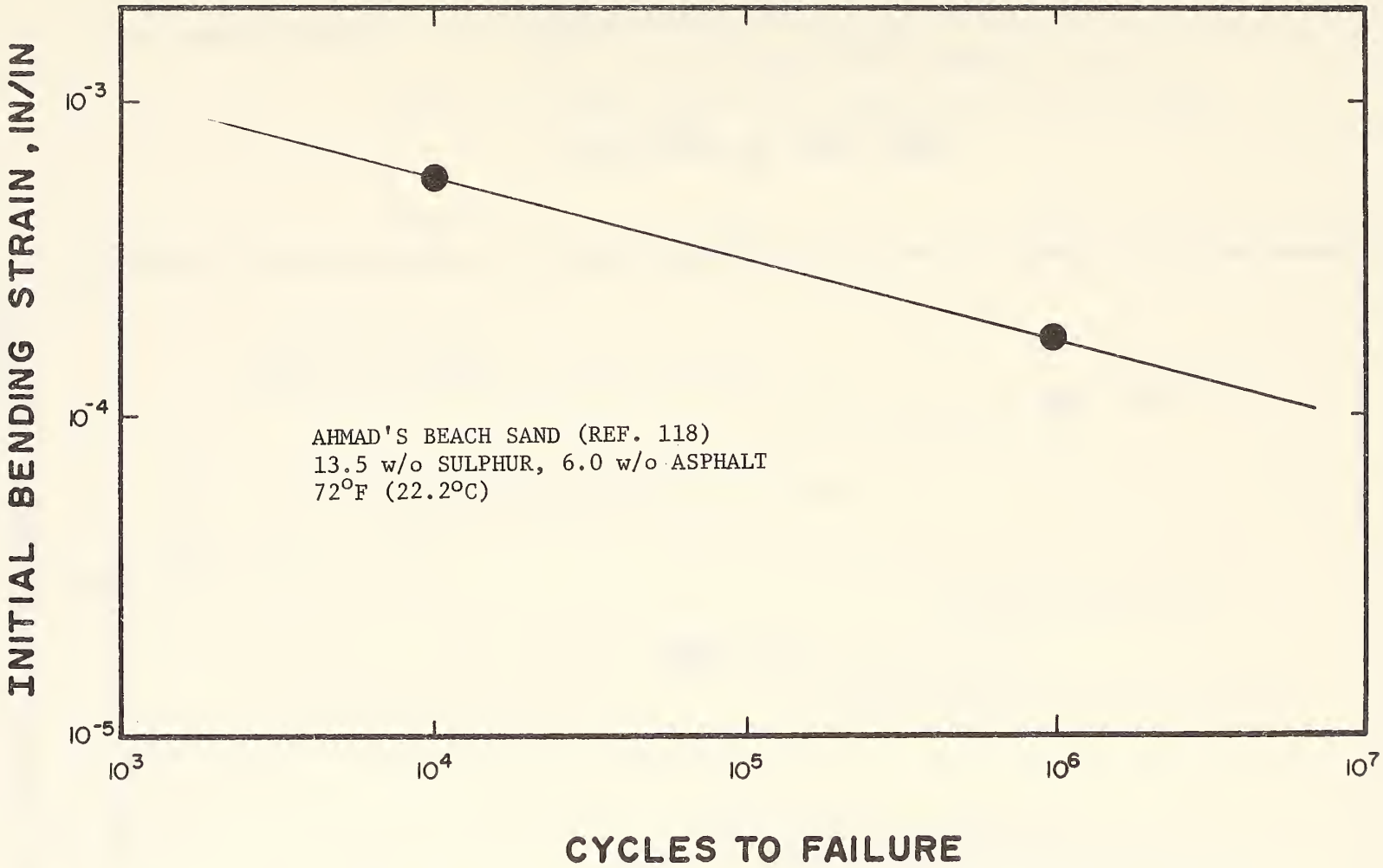

FIG. 100 FLEXURAL FATIGUE TEST RESULTS FOR AHMAD'S BEACH SAND (13.5 w/o SULPHUR, 6.0 w/o ASPHALT) at 72°F (22.2°C)

1 inch = 25.4 mm

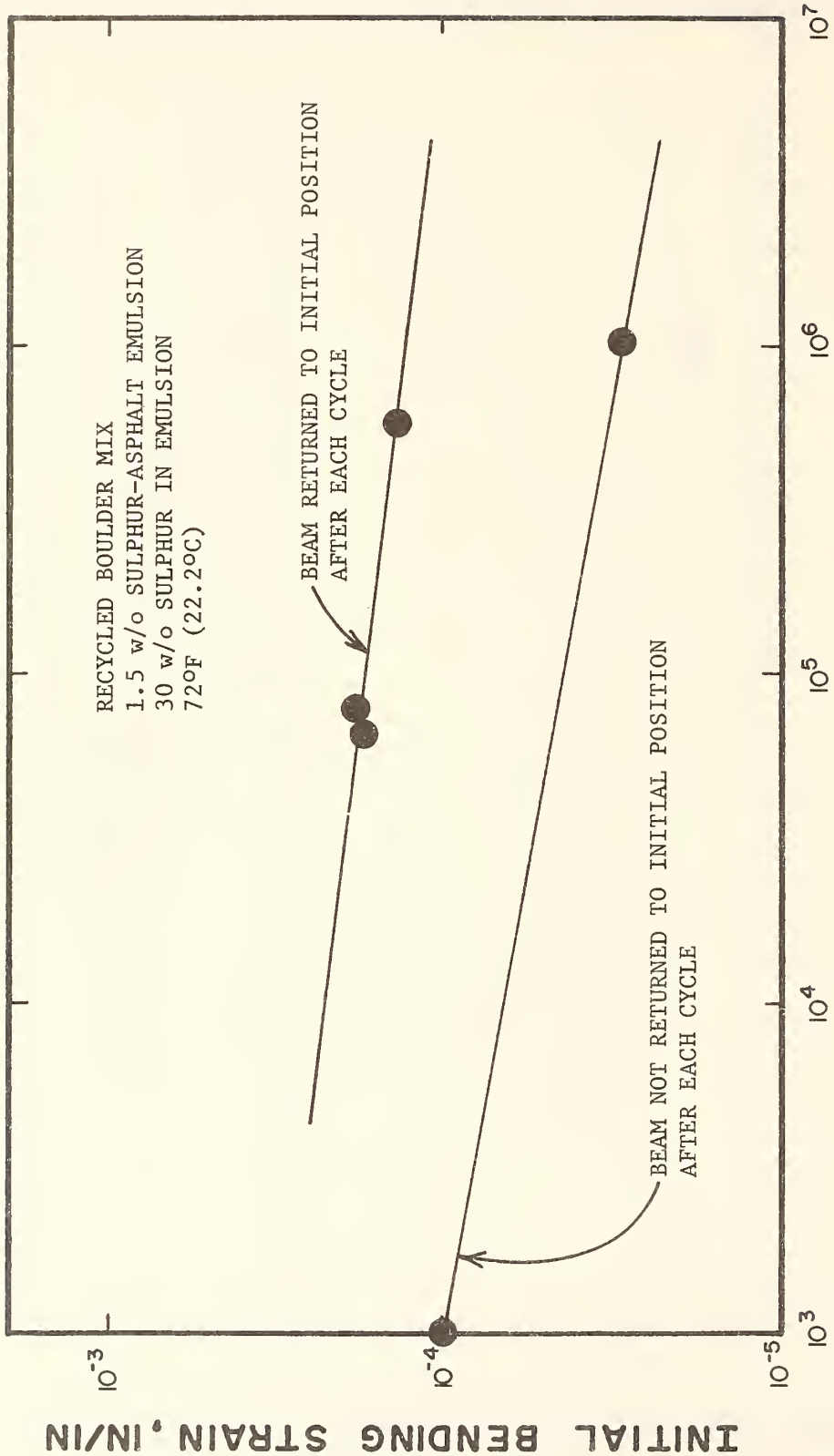

FIG. 101 FLEXURAL FATIGUE TEST RESULTS FOR RECYCLED BOULDER MIX (1.5 w/o SULPHUR-ASPHALT EMULSION, 30 w/o SULPHUR IN EMULSION) at 72°F (22.2°C)

1 inch = 25.4 mm

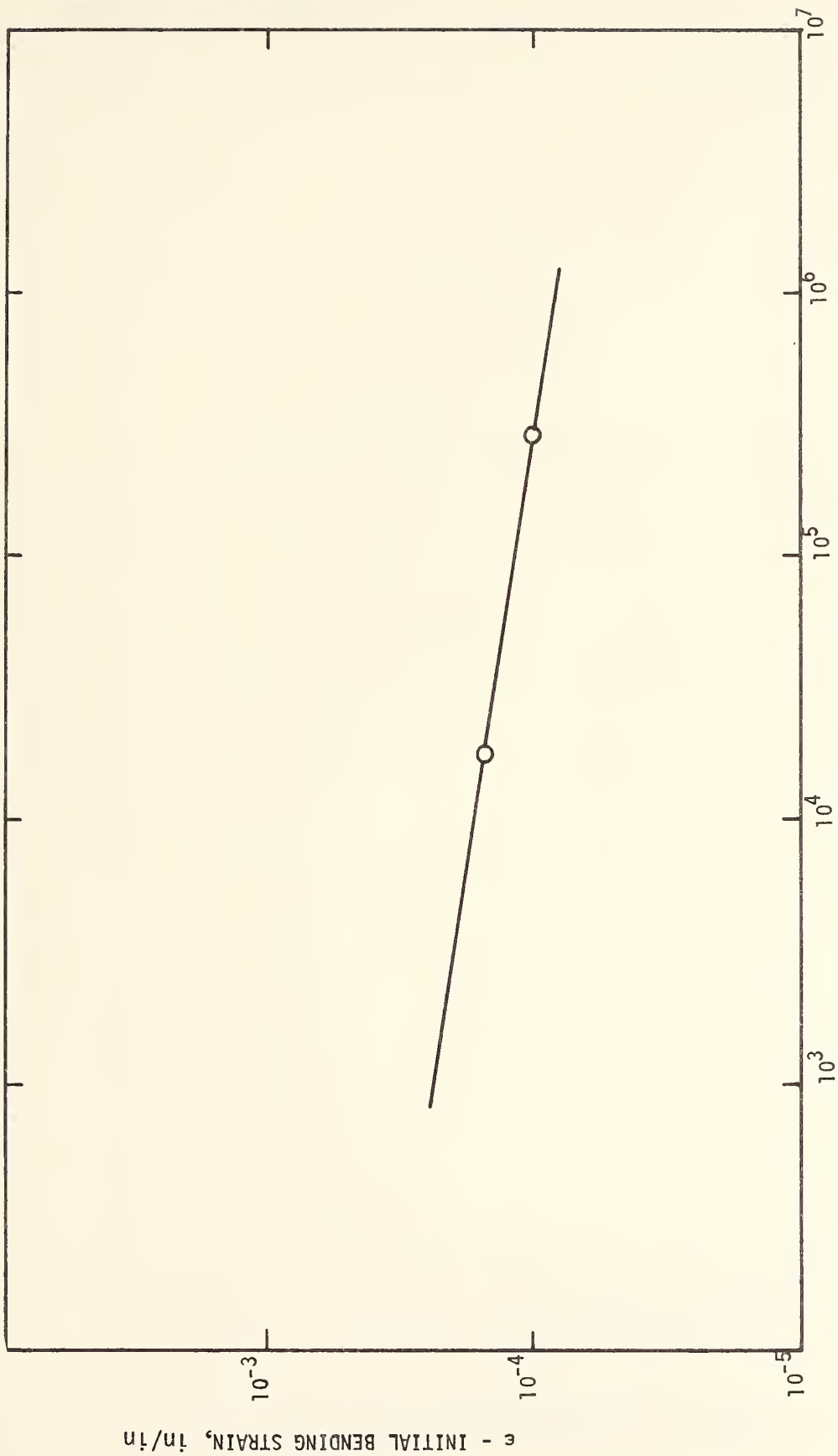

Fig. 102 FLEXURAL FATIGUE TEST RESULTS FOR AE STANDARD LIMESTONE AGGREGATE (0.0 w/o SULPHUR, 4.5 w/o ASPHALT) at 68°F (20°C)

1 inch = 25.4 mm

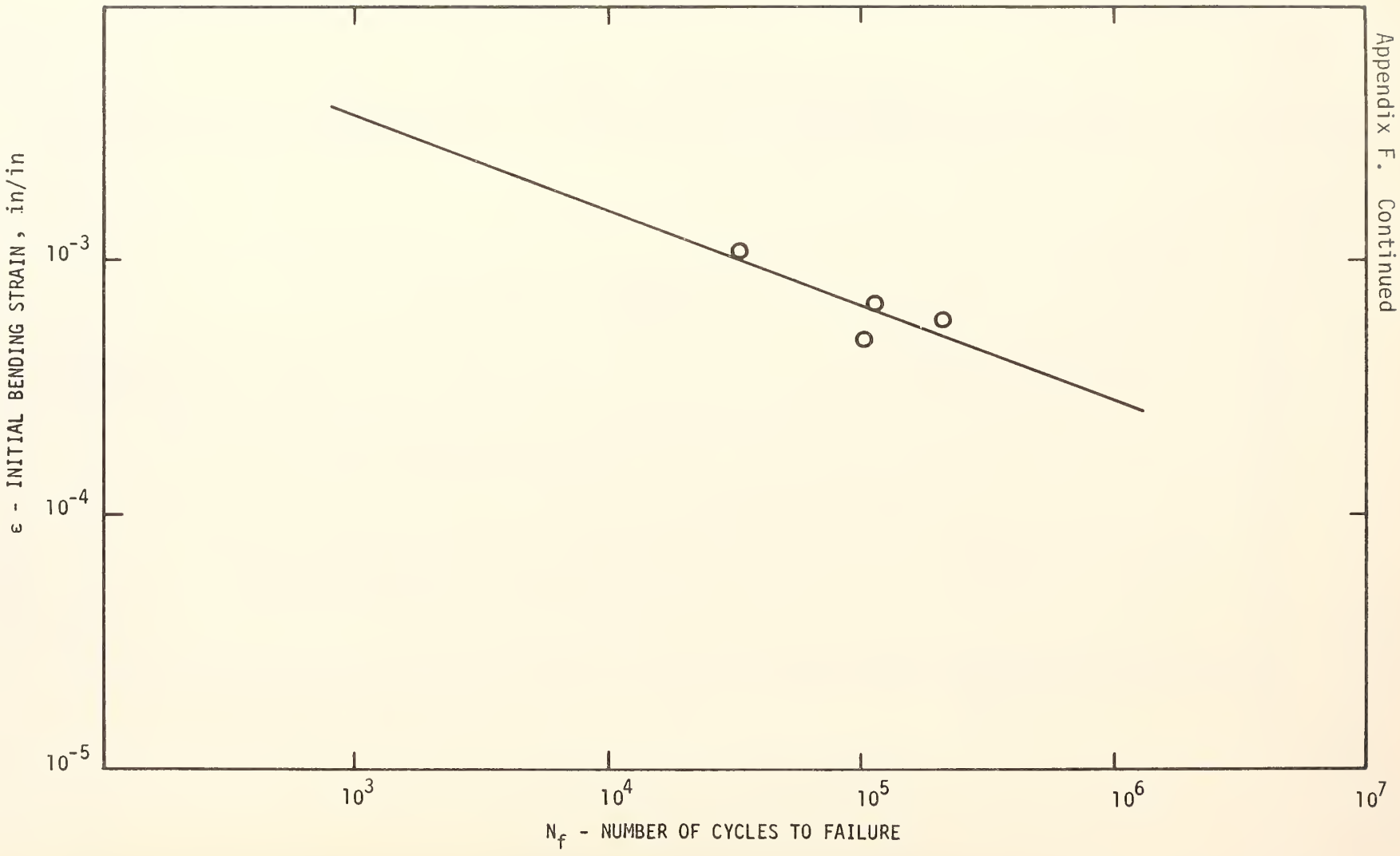

Fig. 103 FLEXURAL FATIGUE TEST RESULTS FOR AE STANDARD LIMESTONE AGGREGATE (1.8 w/o SULPHUR, 5.1 w/o ASPHALT) at 68°F (20°C)

1 inch = 25.4 mm

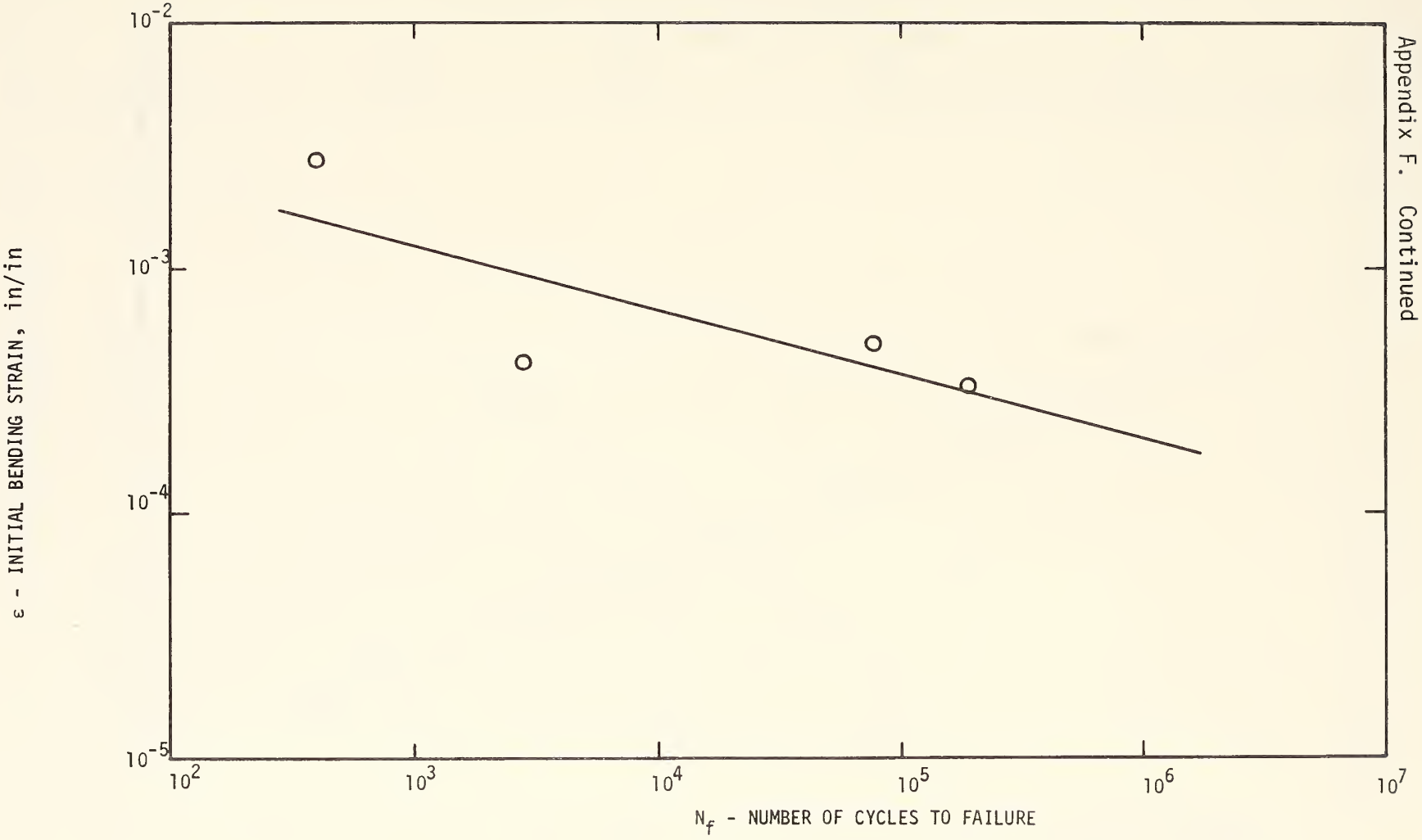

Fig. 104 FLEXURAL FATIGUE TEST RESULTS FOR AE STANDARD LIMESTONE AGGREGATE (4.1 w/o SULPHUR, 3.9 w/o ASPHALT) at 68°F (20°C)

1 inch = 25.4 mm

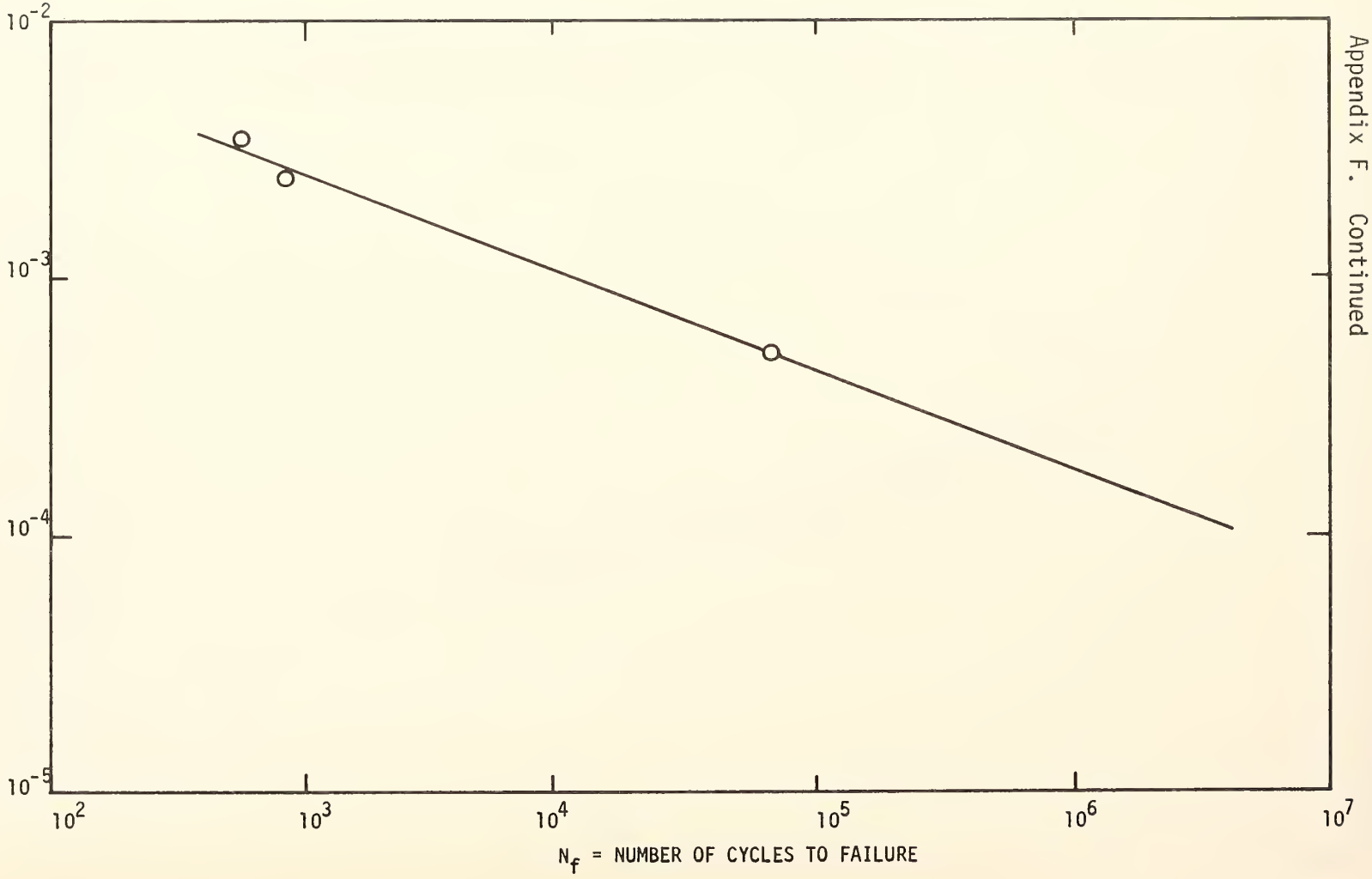

Fig. 105 FLEXURAL FATIGUE TEST RESULTS FOR AES STANDARD LIMESTONE AGGREGATE (1.8 w/o SULPHUR, 5.1 w/o ASPHALT) at 68°F (20°C)

1 inch = 25.4 mm

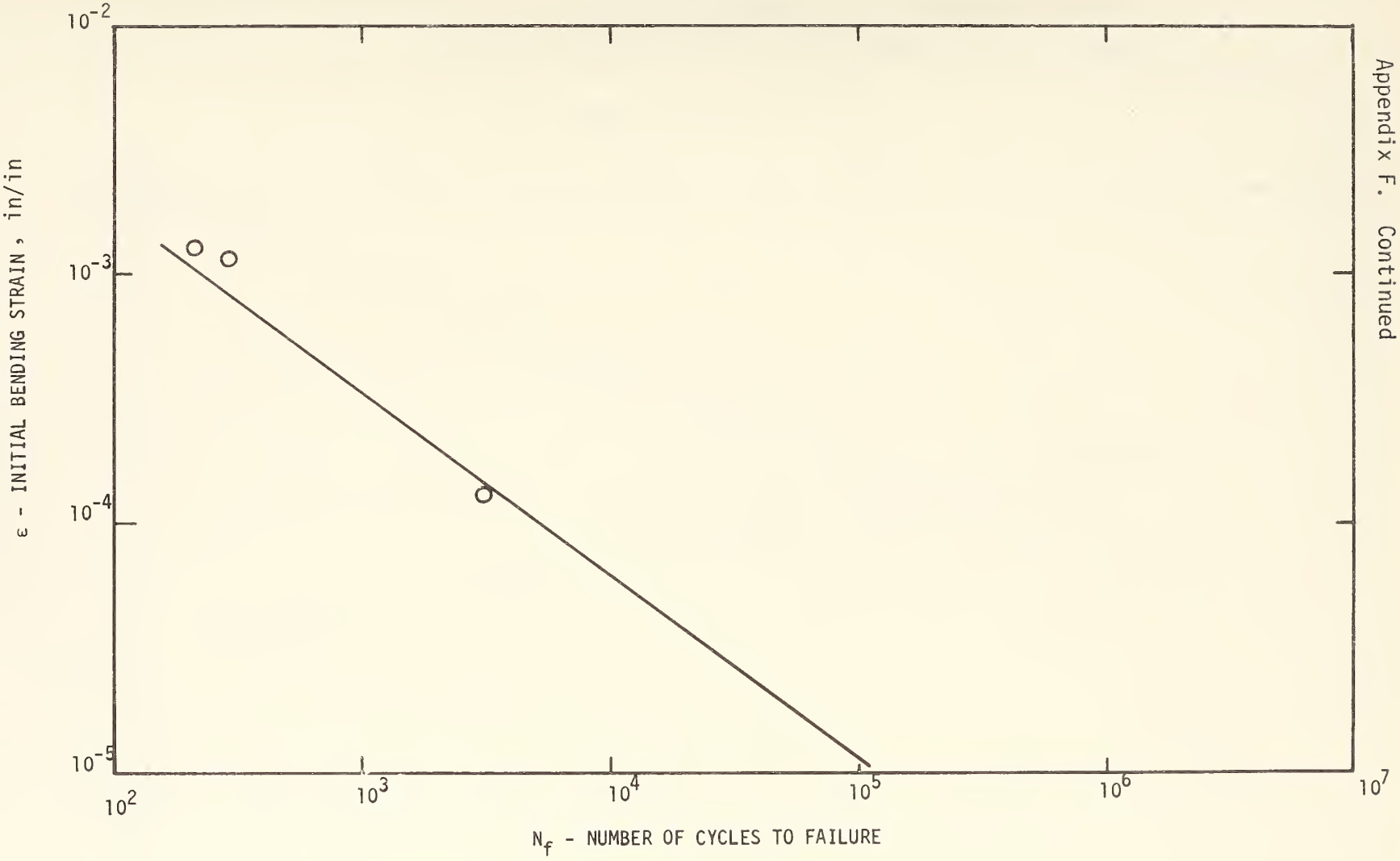

Fig. 106 FLEXURAL FATIGUE TEST RESULTS FOR AES STANDARD LIMESTONE AGGREGATE (4.1 w/o SULPHUR, 3.9 w/o ASPHALT) at 68°F (20°C)

1 inch = 25.4 mm

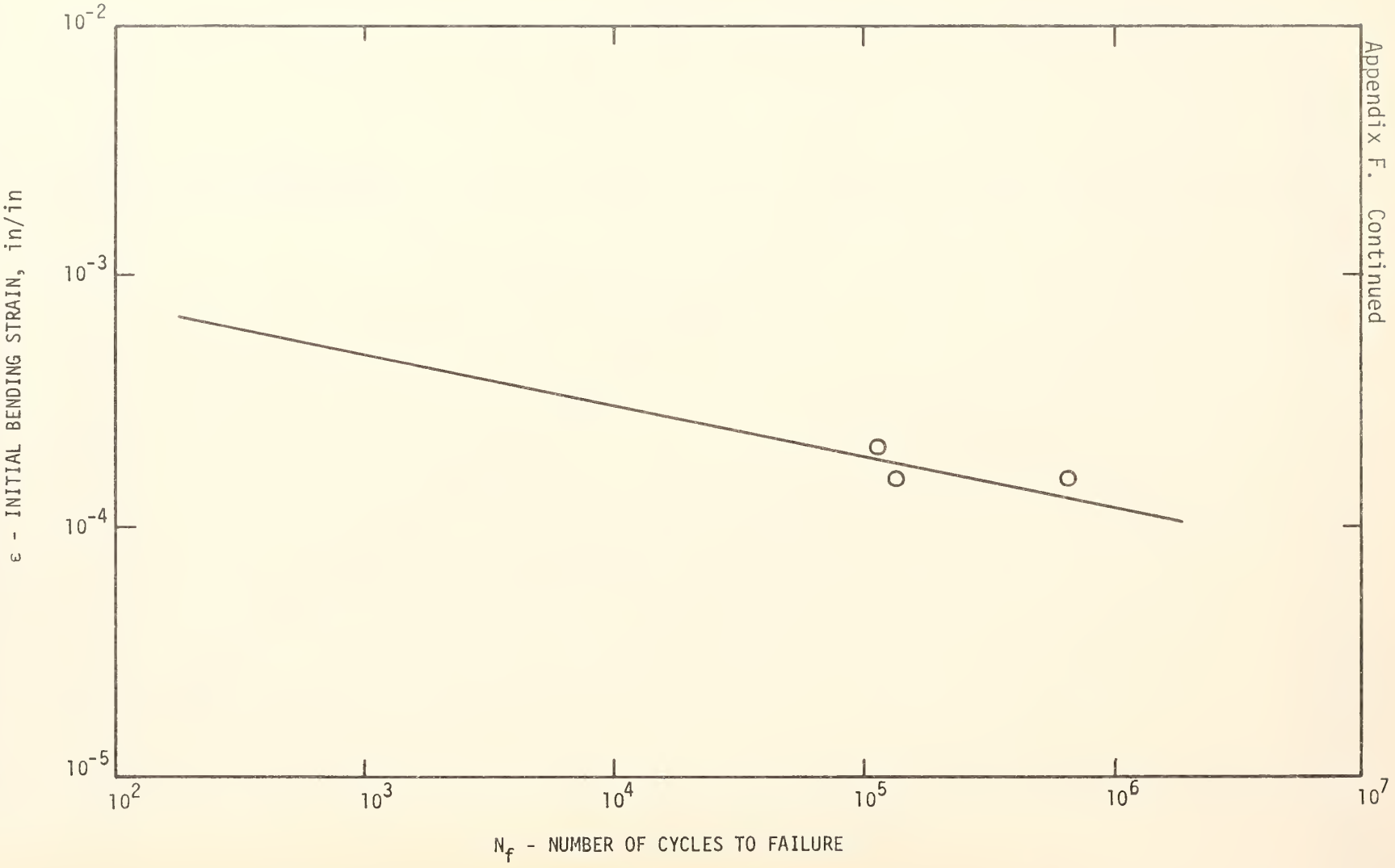

Fig. 107 FLEXURAL FATIGUE TEST RESULTS FOR AAS STANDARD LIMESTONE AGGREGATE (4.1 w/o SULPHUR, 3.9 w/o ASPHALT) at 35°F (1.7°C)

1 inch = 25.4 mm

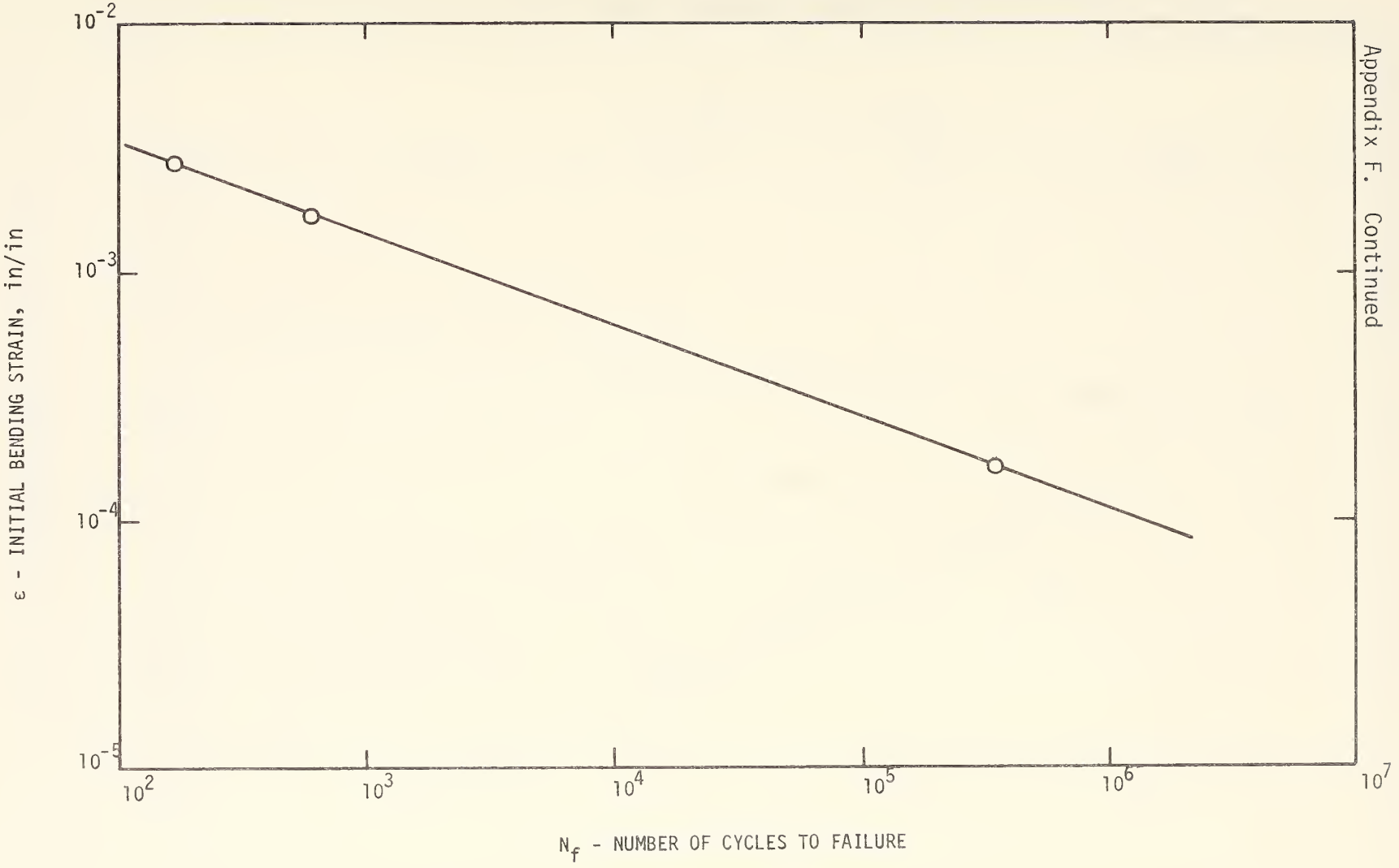

Fig. 108 FLEXURAL FATIGUE TEST RESULTS FOR AAS STANDARD LIMESTONE AGGREGATE (4.1 w/o SULPHUR, 3.9 w/o ASPHALT) at 68°F (20°C)

1 inch = 25.4 mm

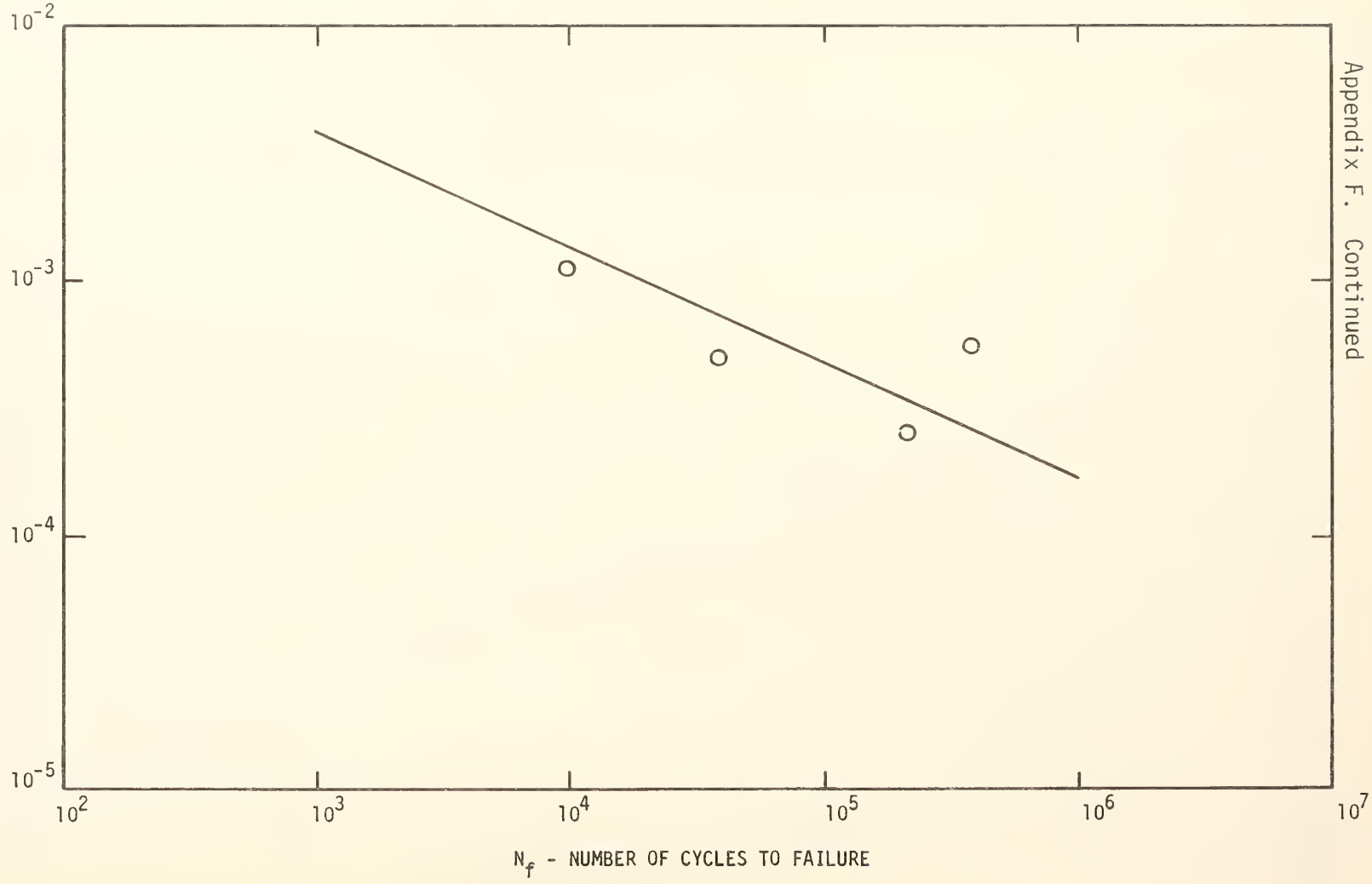

Fig. 109 FLEXURAL FATIGUE TEST RESULTS FOR AAS STANDARD LIMESTONE AGGREGATE (4.1 w/o SULPHUR, 3.9 w/o ASPHALT) at 110°F (92.2°C)

1 inch = 25.4 mm

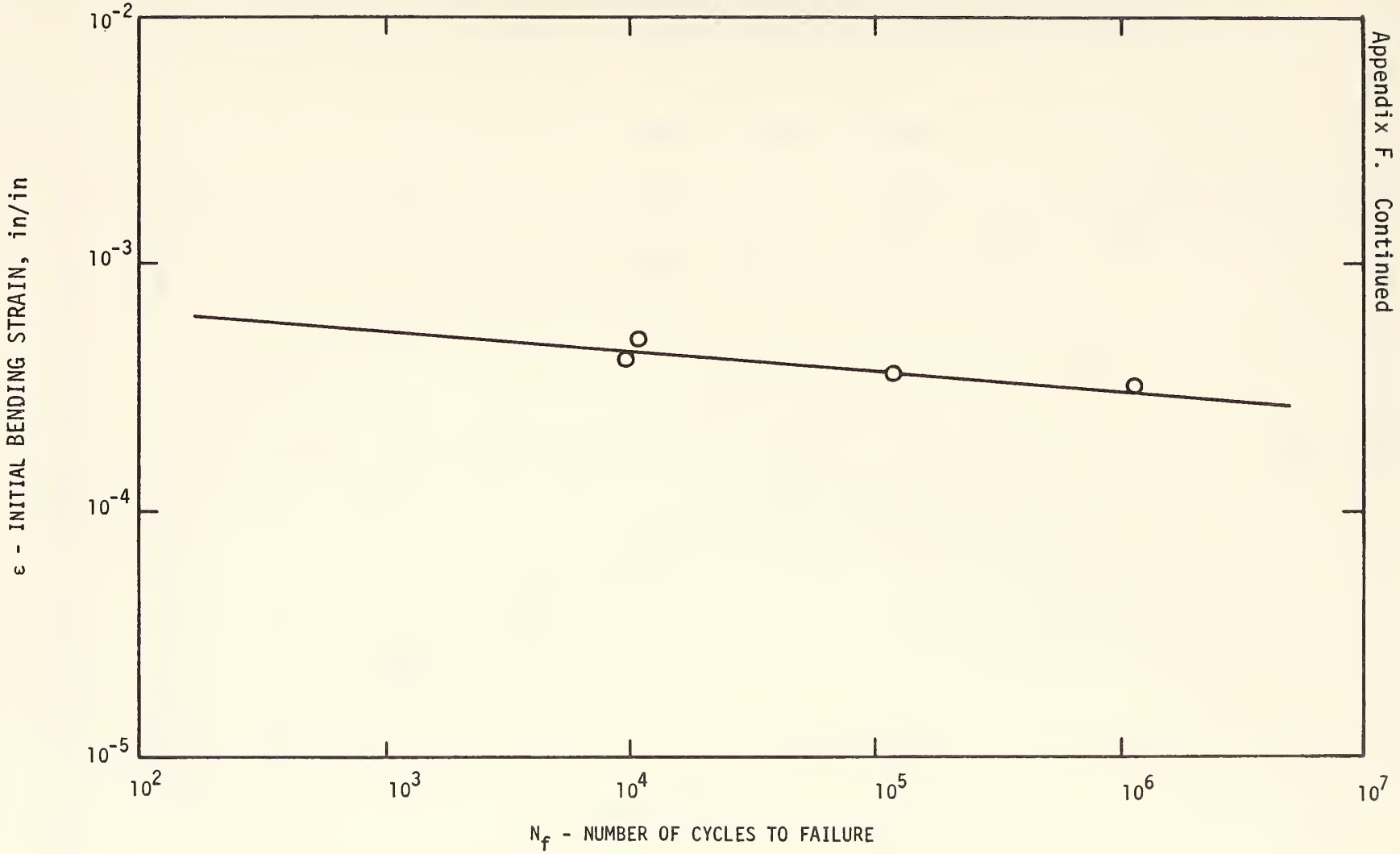

Fig. 110 FLEXURAL FATIGUE TEST RESULTS FOR AAS STANDARD LIMESTONE AGGREGATE (0.0 w/o SULPHUR, 4.5 w/o ASPHALT) at 35°F (1.7°C)

1 inch = 25.4 mm

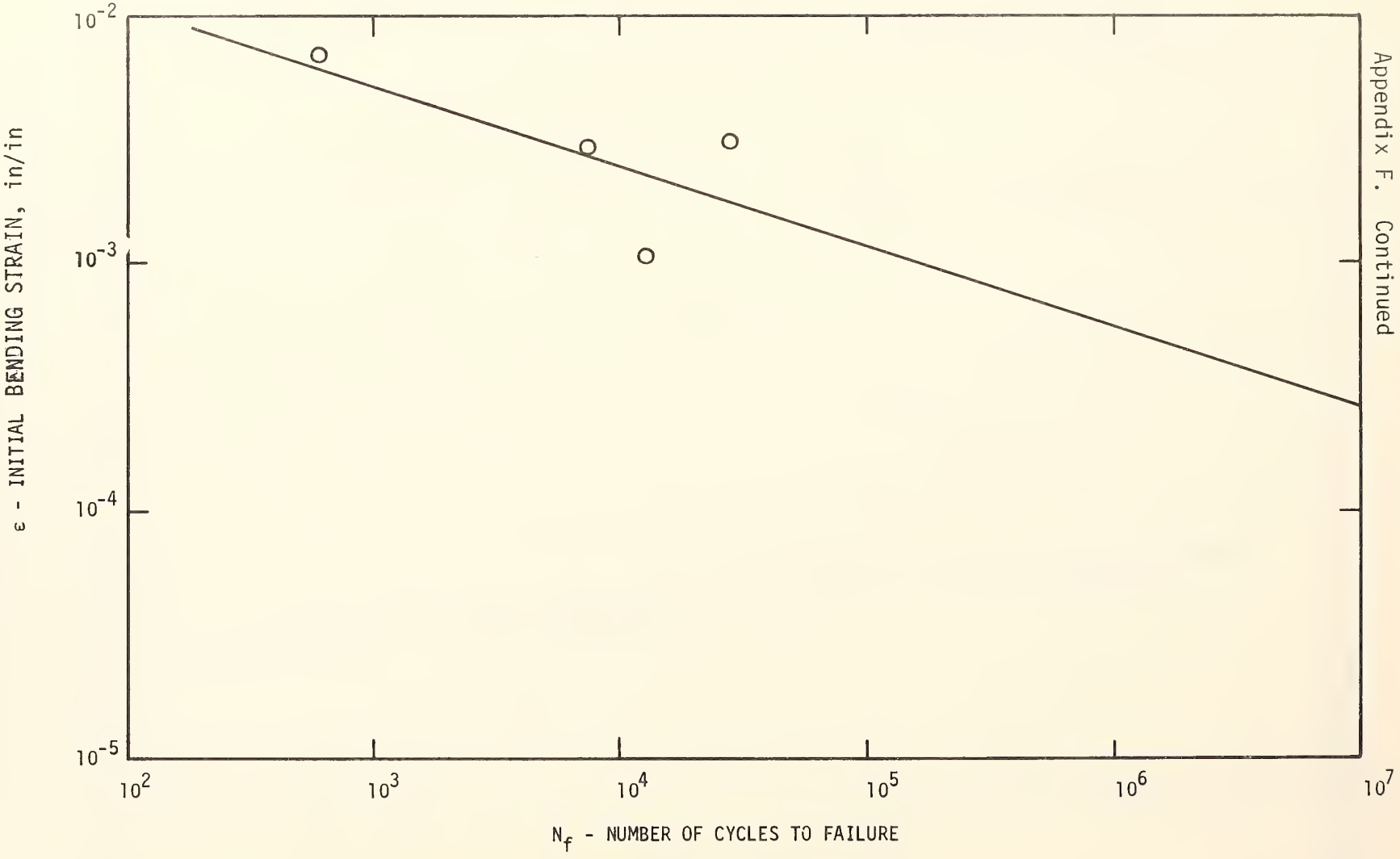

Fig. 111 FLEXURAL FATIGUE TEST RESULTS FOR STANDARD LIMESTONE AGGREGATE (0.0 w/o SULPHUR, 4.5 w/o ASPHALT) at 110°F (92.2°C)

1 inch = 25.4 mm

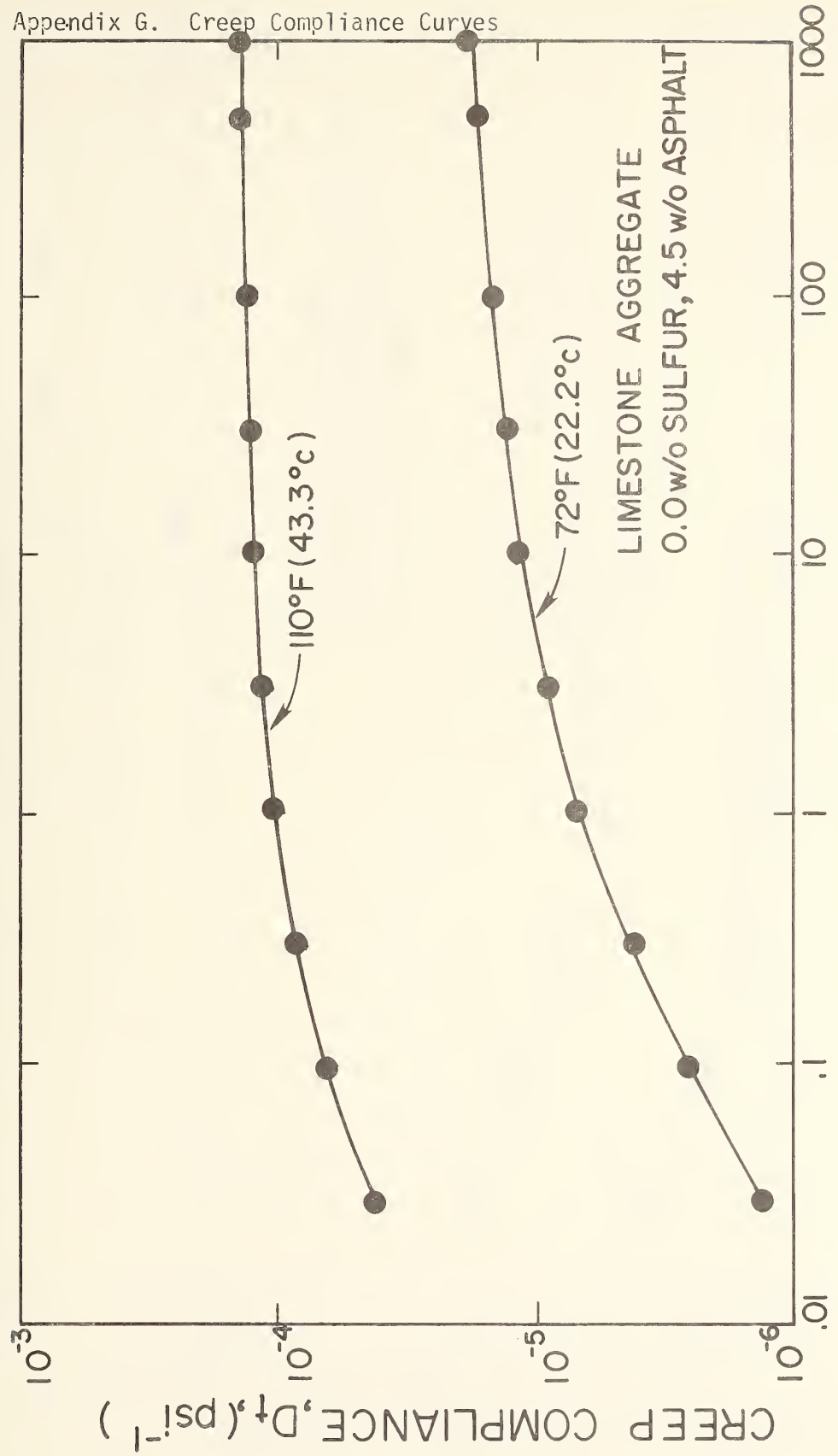

Fig. 112 COMPRESSIVE CREEP TEST RESULTS FOR LIMESTONE AGGREGATE (0.0 w/o SULPHUR, 4.5 w/o ASPHALT)

1 psi = 6.894 kPa

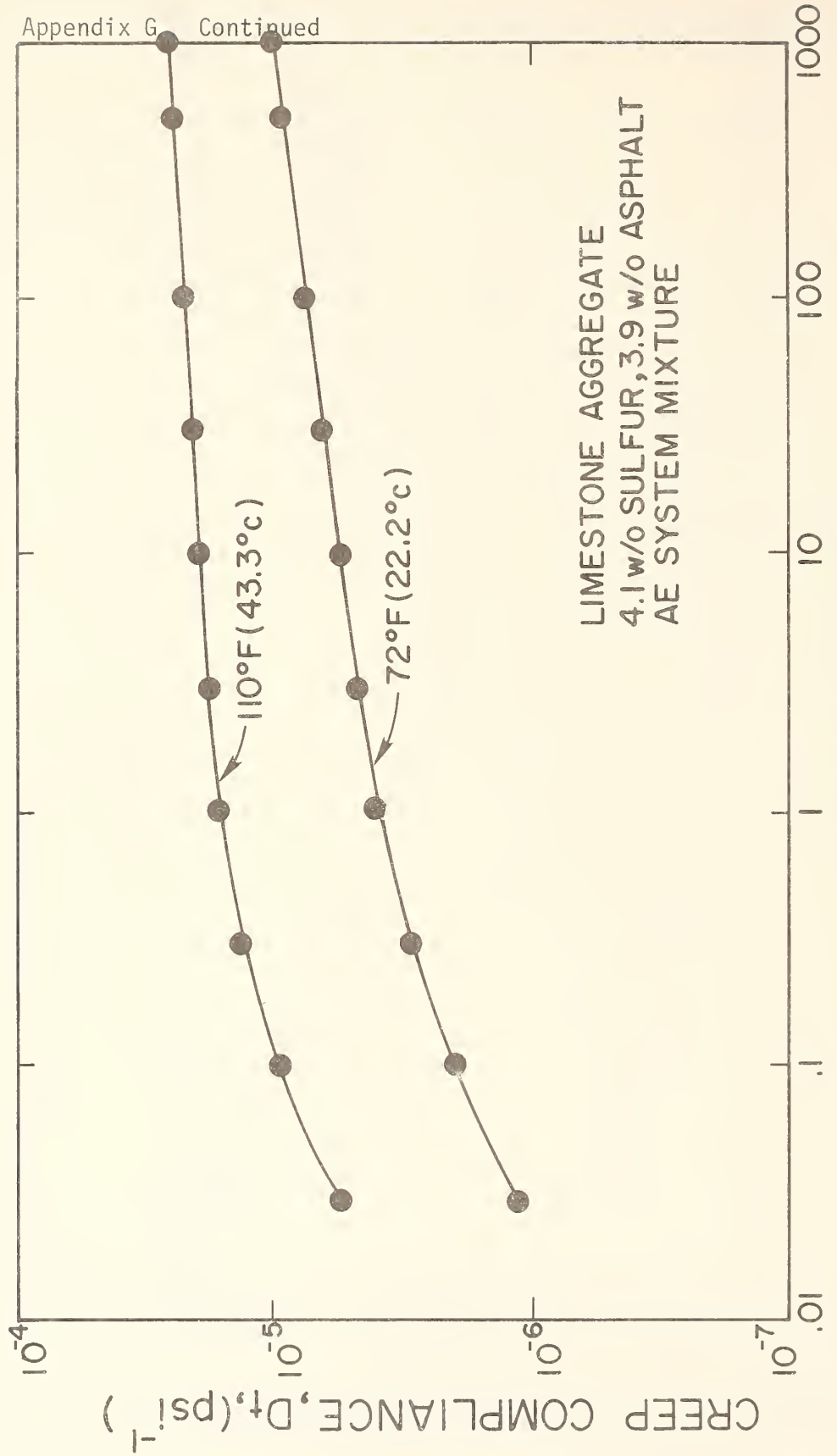

Fig. 113 COMPRESSIVE CREEP TEST RESULTS FOR LIMESTONE AGGREGATE AE (4.1 w/o SULPHUR, 3.9 w/o ASPHALT)

1 psi = 6.894 kPa

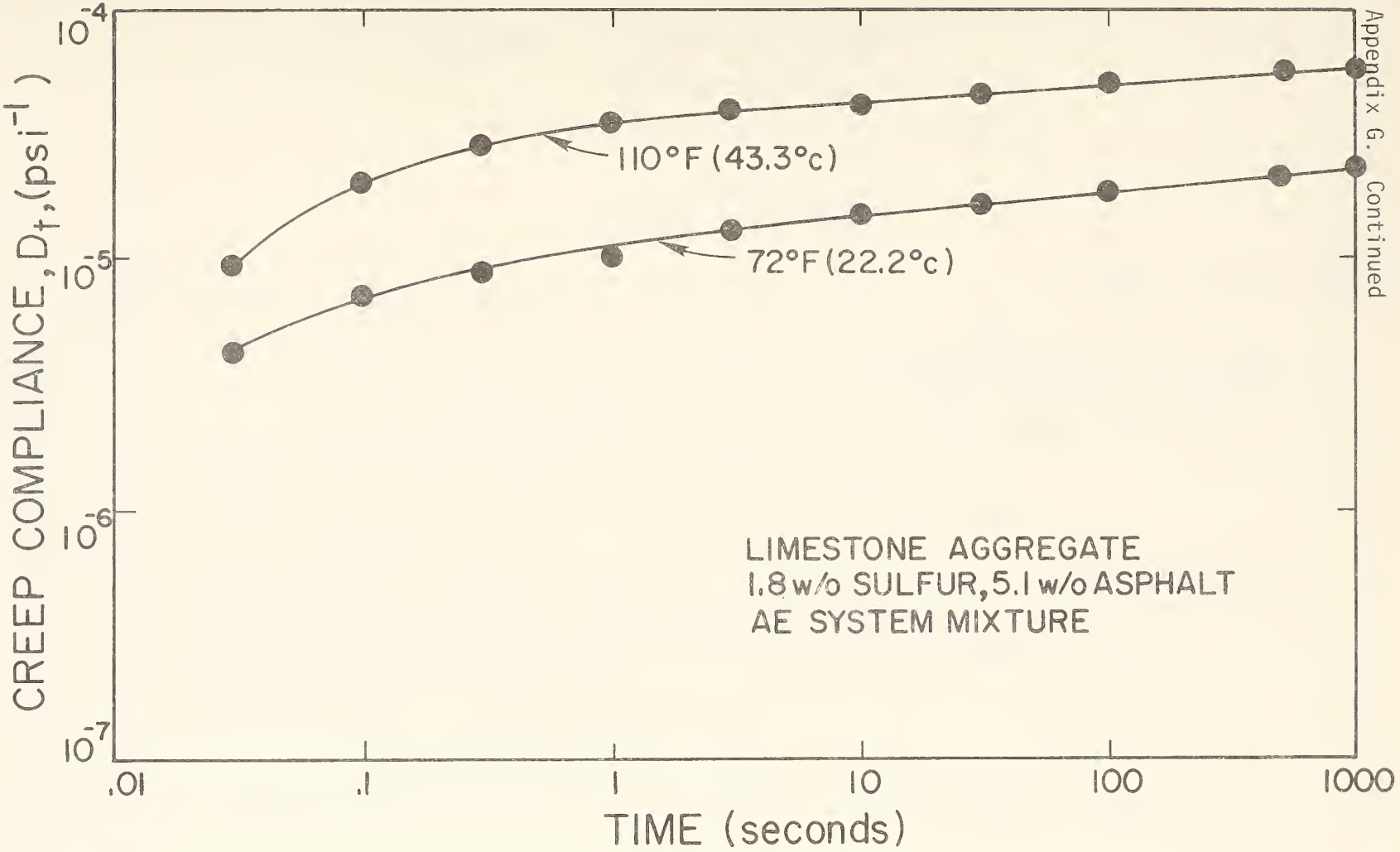

Fig. 114 COMPRESSIVE CREEP TEST RESULTS FOR LIMESTONE AGGREGATE AE (1.8 w/o SULPHUR, 5.1 w/o ASPHALT)

1 psi = 6.894 kPa

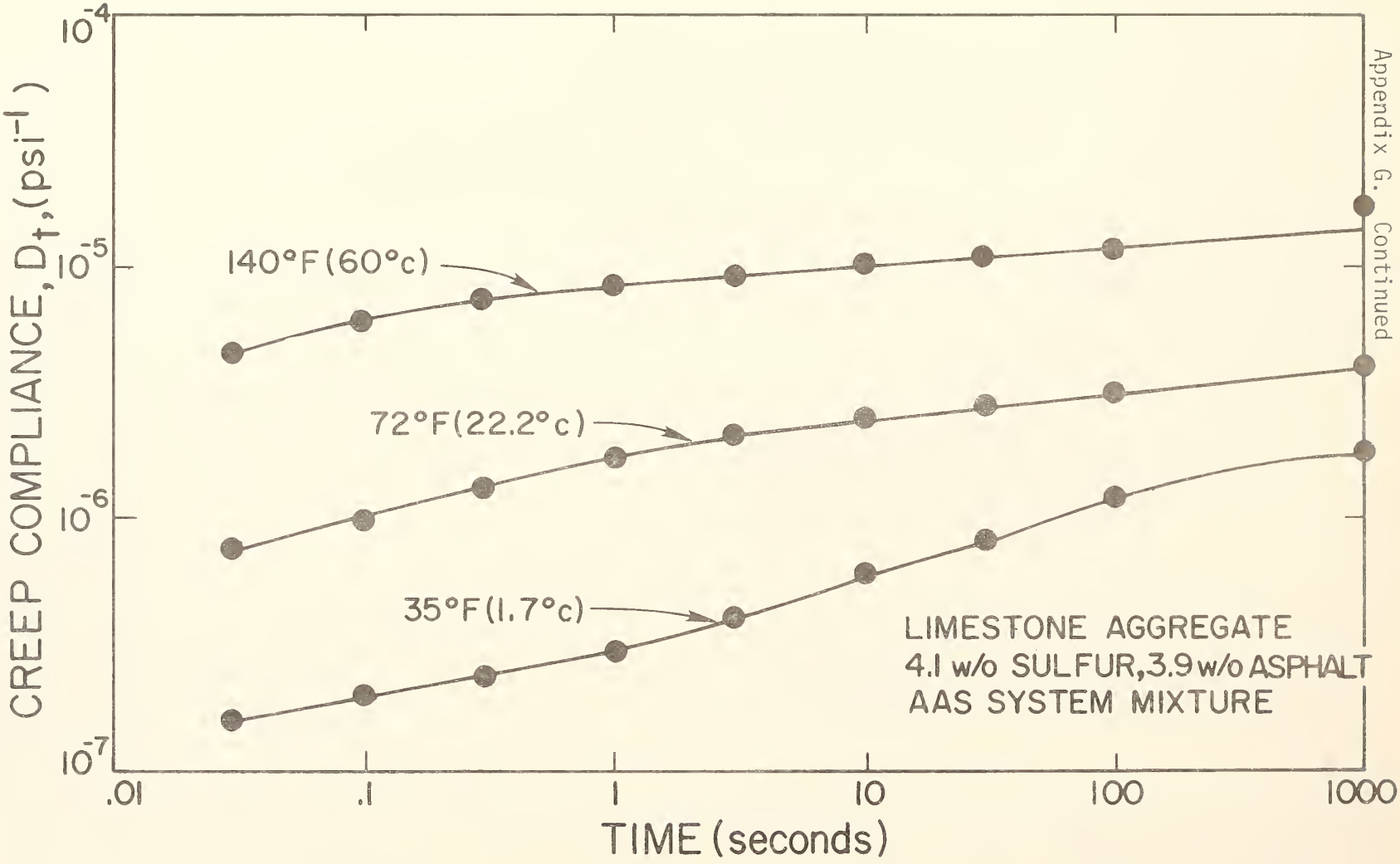

Fig. 115 COMPRESSIVE CREEP TEST RESULTS FOR LIMESTONE AGGREGATE AAS (4.1 w/o SULPHUR, 3.9 w/o ASPHALT)

1 psi = 6.894 kPa

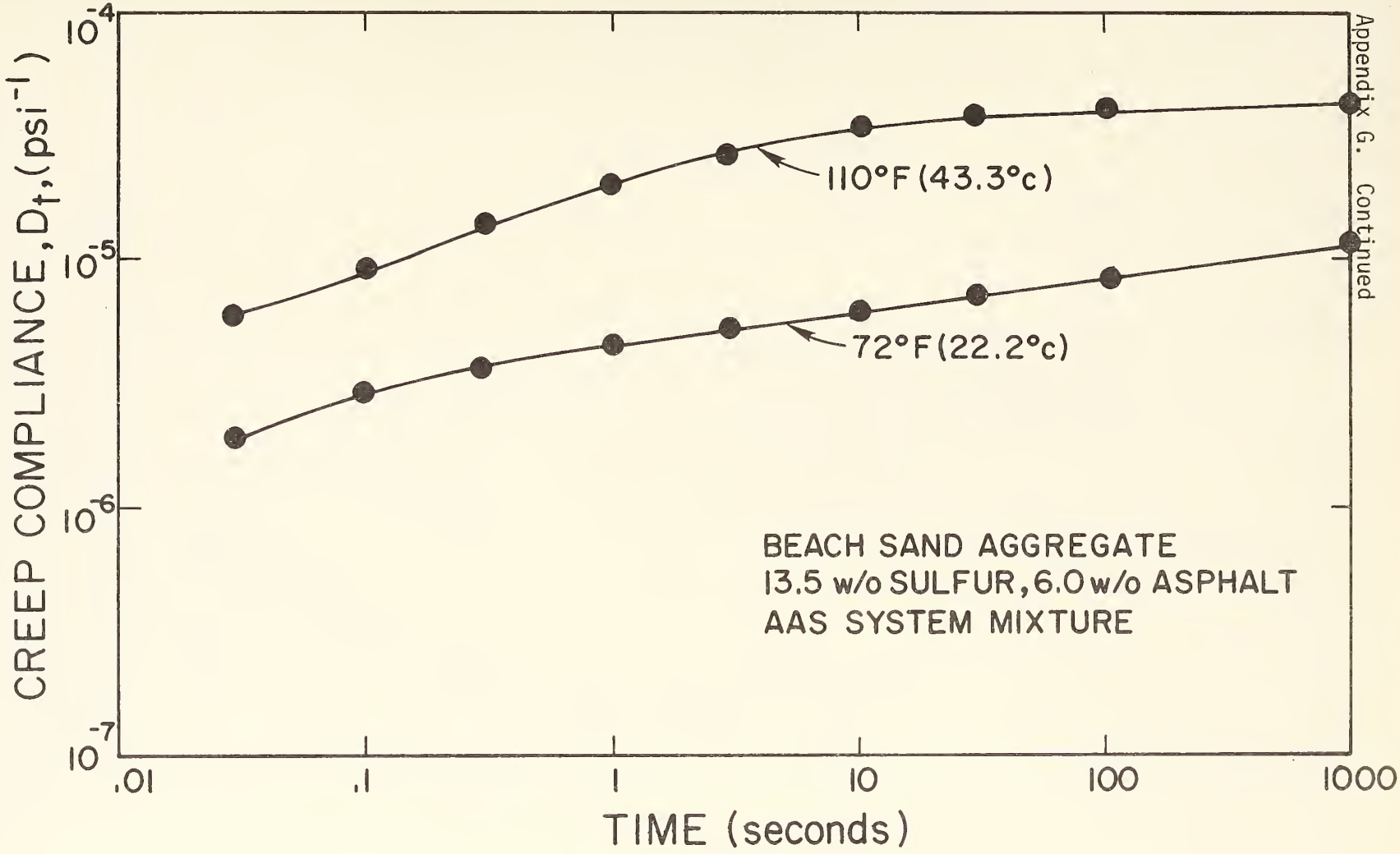

Fig. 116 COMPRESSIVE CREEP TEST RESULTS FOR BEACH SAND AGGREGATE AAS (13.5 w/o SULPHUR, 6.0 w/o ASPHALT)

1 psi = 6.894 kPa

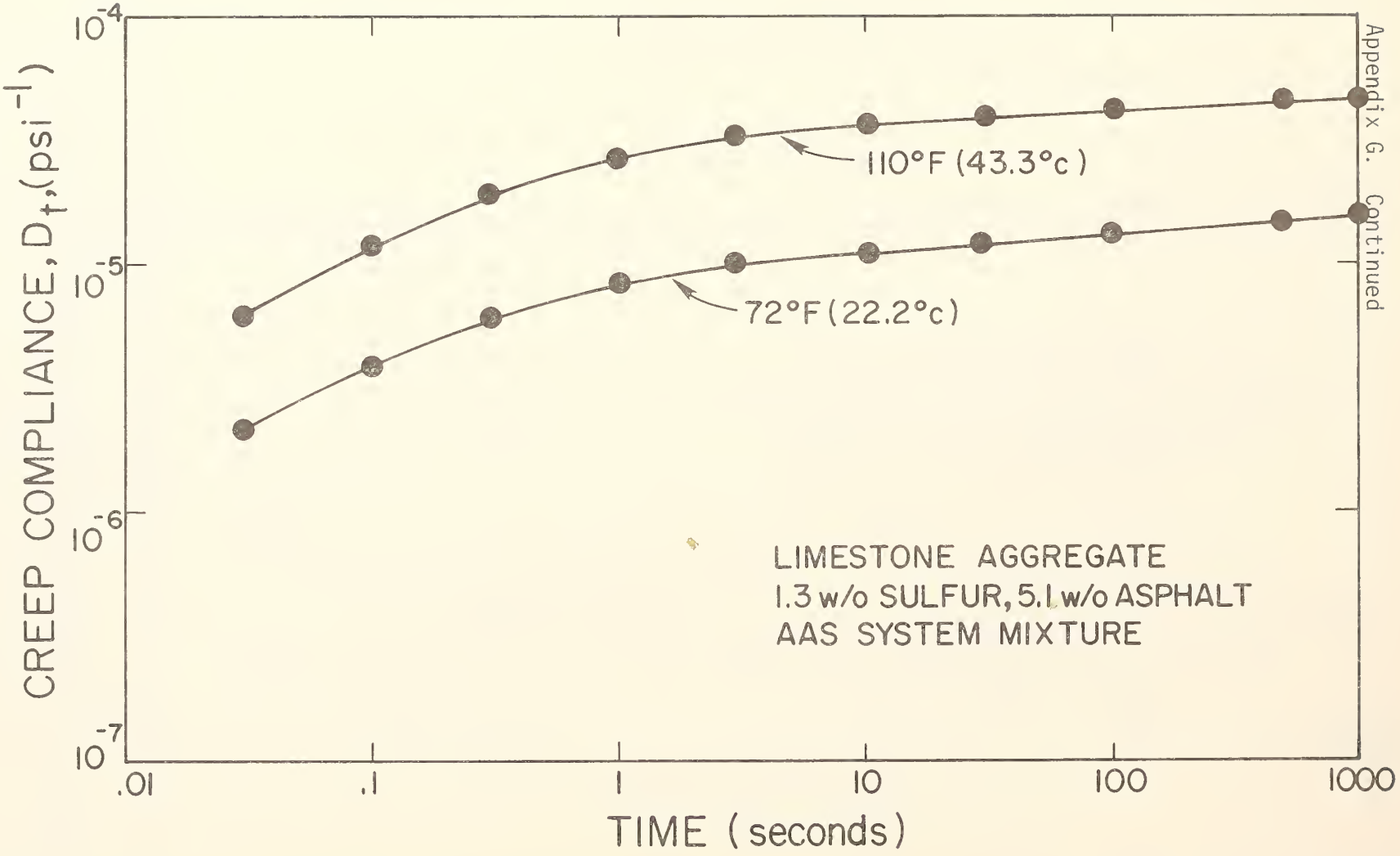

Fig. 117 COMPRESSIVE CREEP TEST RESULTS FOR LIMESTONE AGGREGATE AAS (1.3 w/o SULPHUR, 5.1 w/o ASPHALT)

1 psi = 6.894 kPa

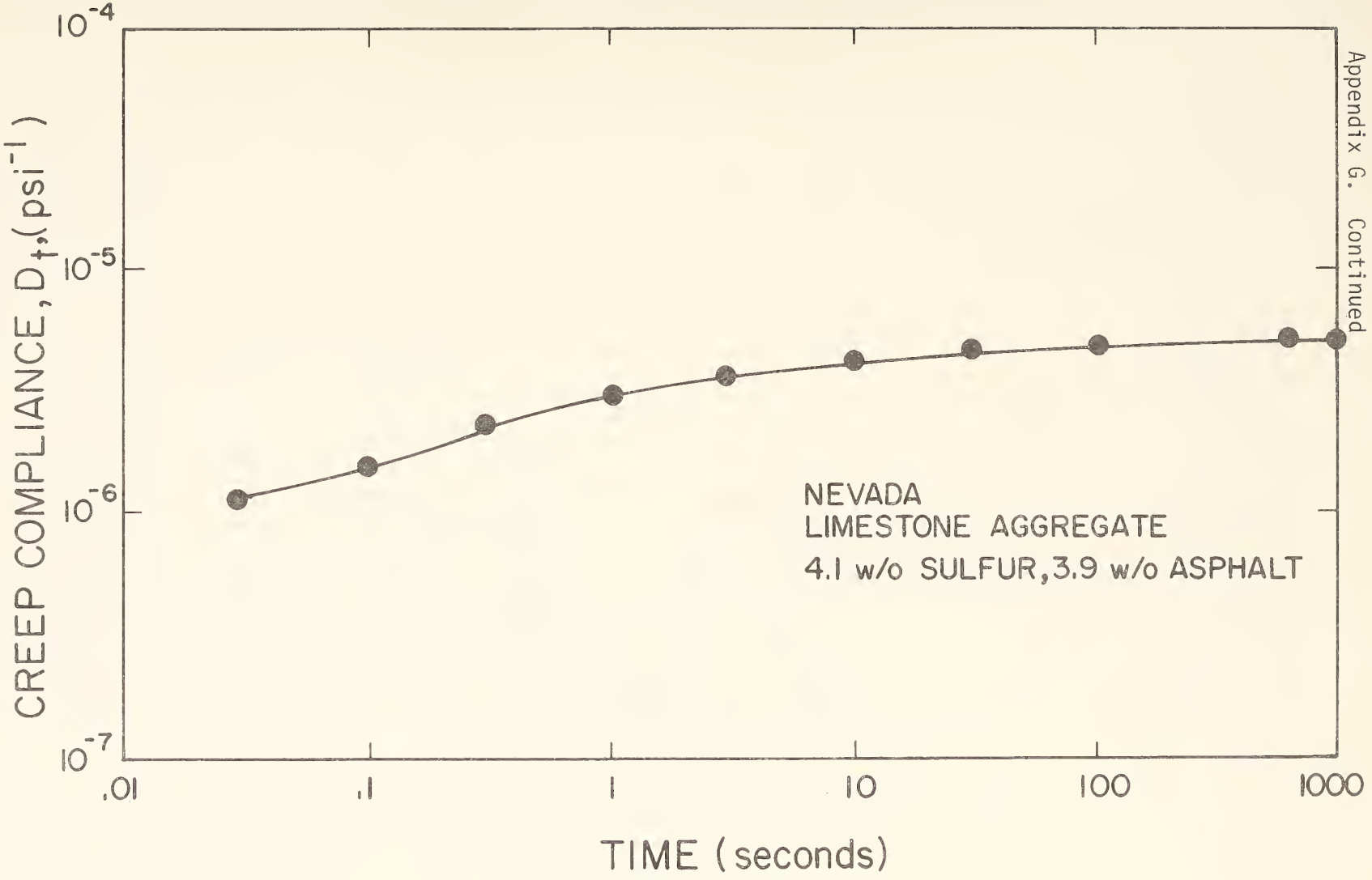

Fig. 118 COMPRESSIVE CREEP TEST RESULTS FOR NEVADA LIMESTONE AGGREGATE (4.1 w/o SULPHUR, 3.9 w/o ASPHALT)

1 psi = 6.894 kPa

Appendix H. Accumulated (Permanent) Strain Curves

Permanent strain parameters used in the Vesys IIM program are calculated from repetitive load uniaxial compression test results as follows:

$$\varepsilon_a = IN^S$$

$$\mu = \frac{IS}{\varepsilon_r}$$

$$\alpha = 1-S$$

where ε_a is accumulated axial strain

I is the intercept at 1 load repetition

S is the slope

ε_r is the resilient strain

μ is the parameter GNU

α is the parameter ALPHA

N is the number of repetitions

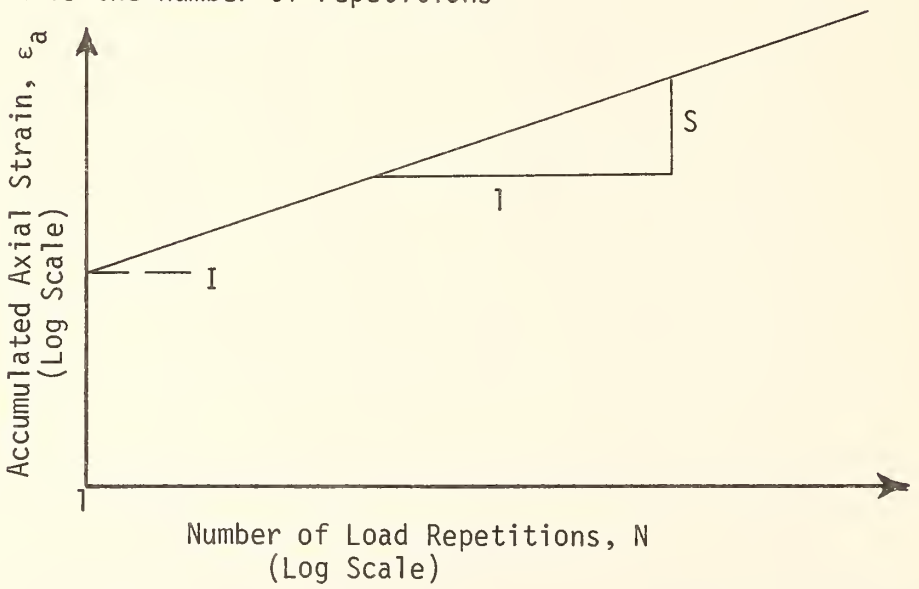

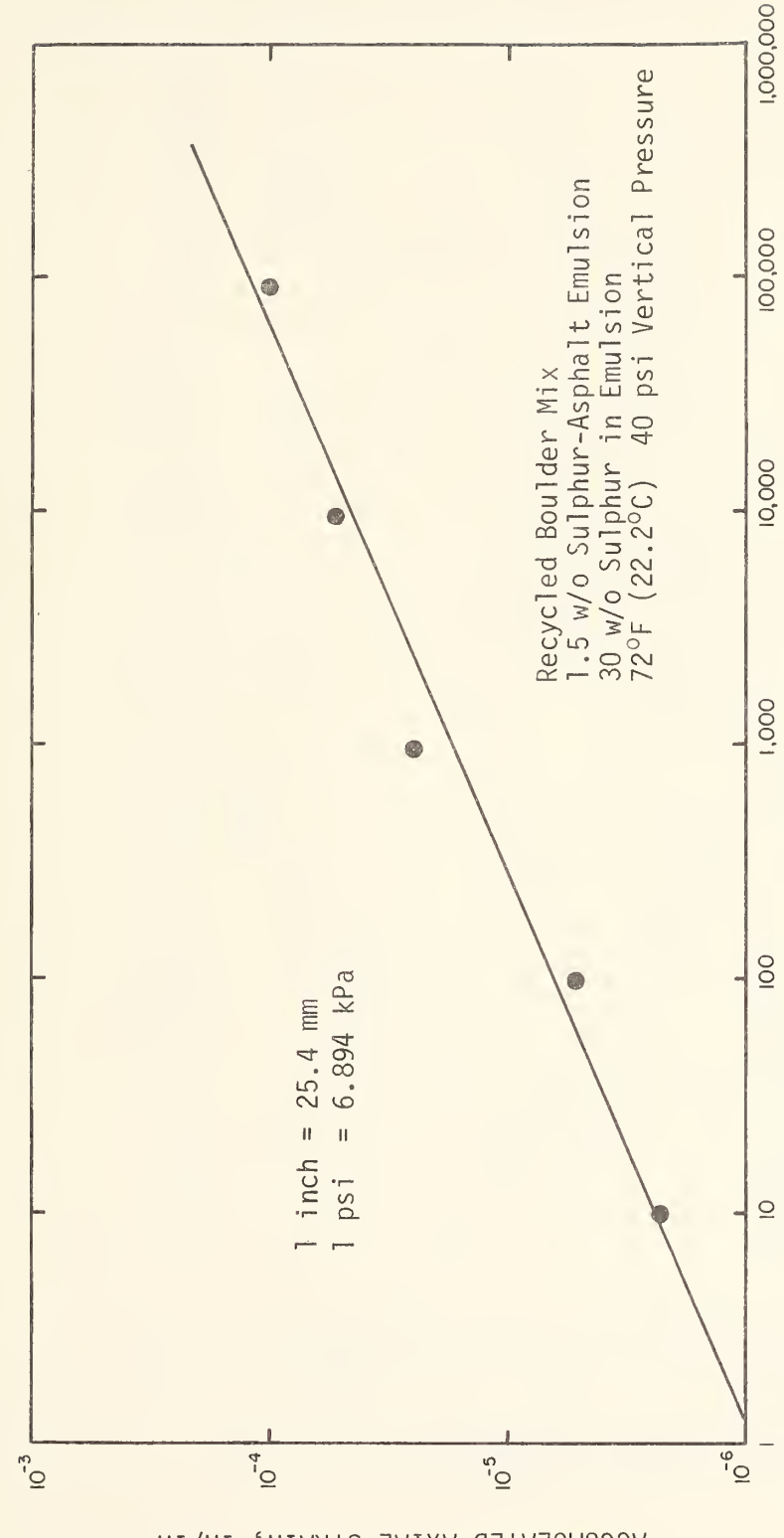

FIGURE 119 ACCUMULATED STRAIN RESULTS FROM COMPRESSIVE CREEP FOR 1/5 w/o SULPHUR-ASPHALT EMULSION (RECYCLED BOULDER MIX)

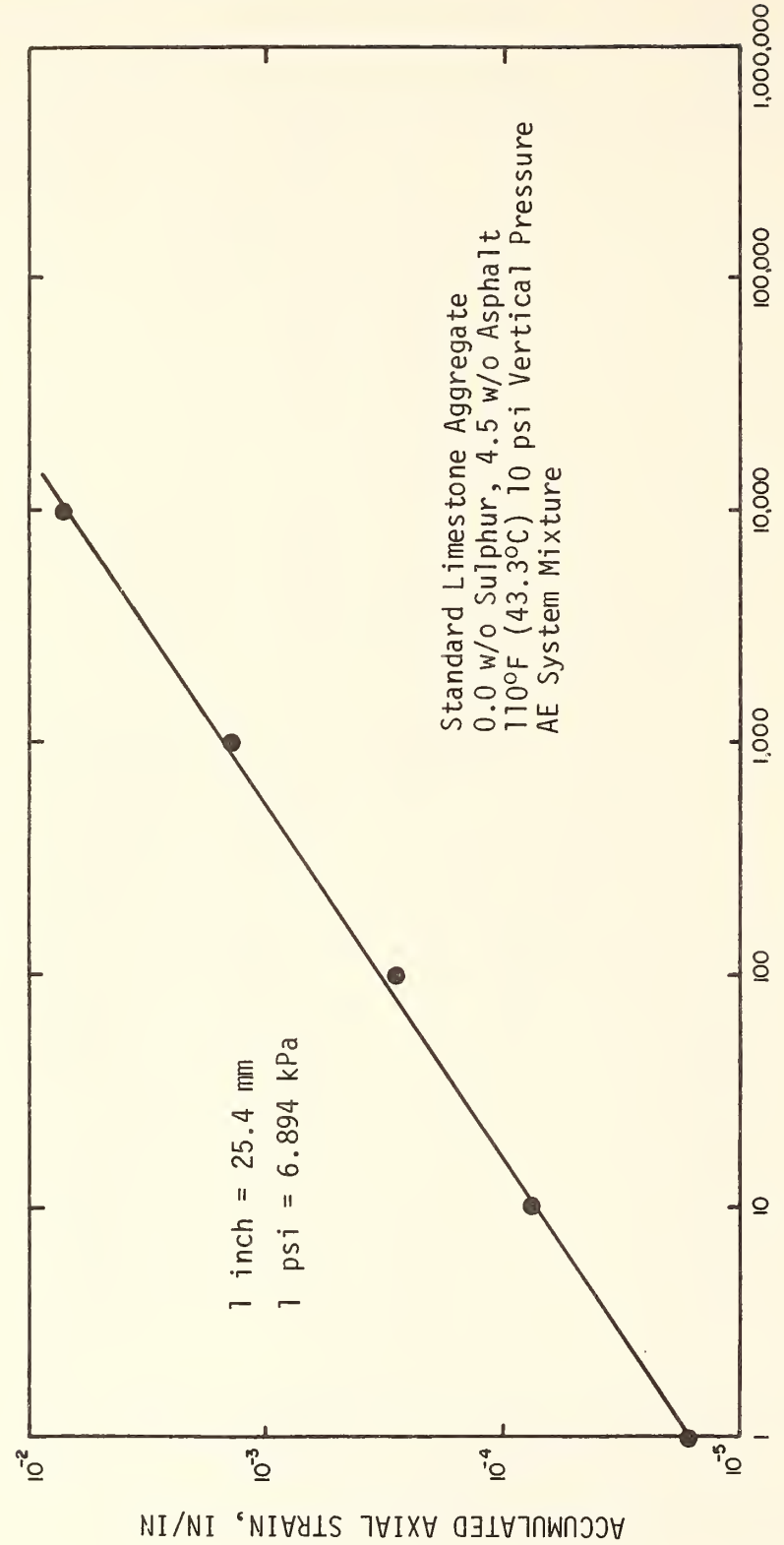

FIGURE 120 ACCUMULATED STRAIN RESULTS FROM COMPRESSIVE CREEP FOR LIMESTONE AGGREGATE AE (0.0 w/o SULPHUR, 4.5 w/o ASPHALT)

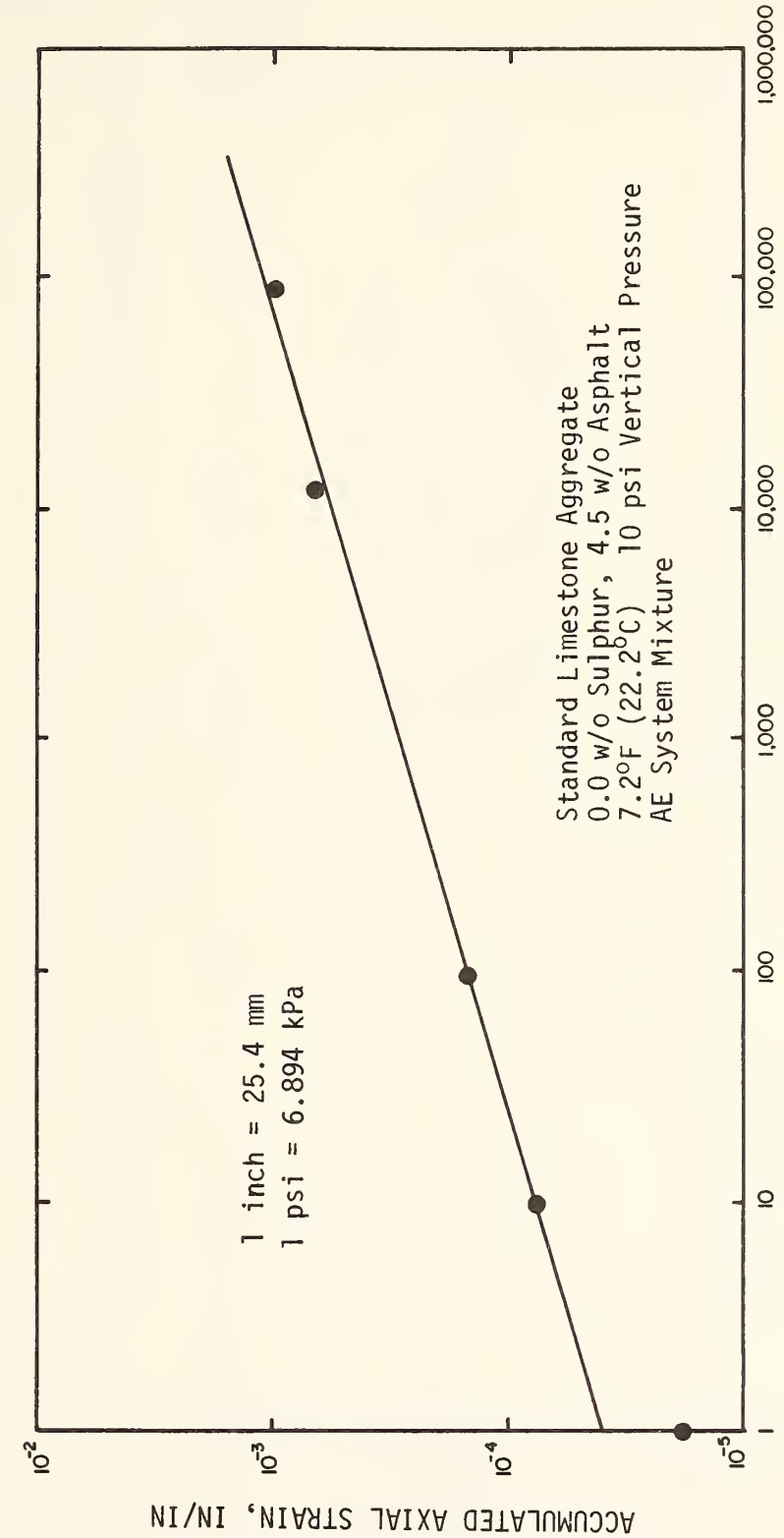

FIGURE 121 ACCUMULATED STRAIN RESULTS FROM COMPRESSIVE CREEP FOR LIMESTONE AGGREGATE AE (0.0 w/o SULPHUR, 4.5 w/o ASPHALT)

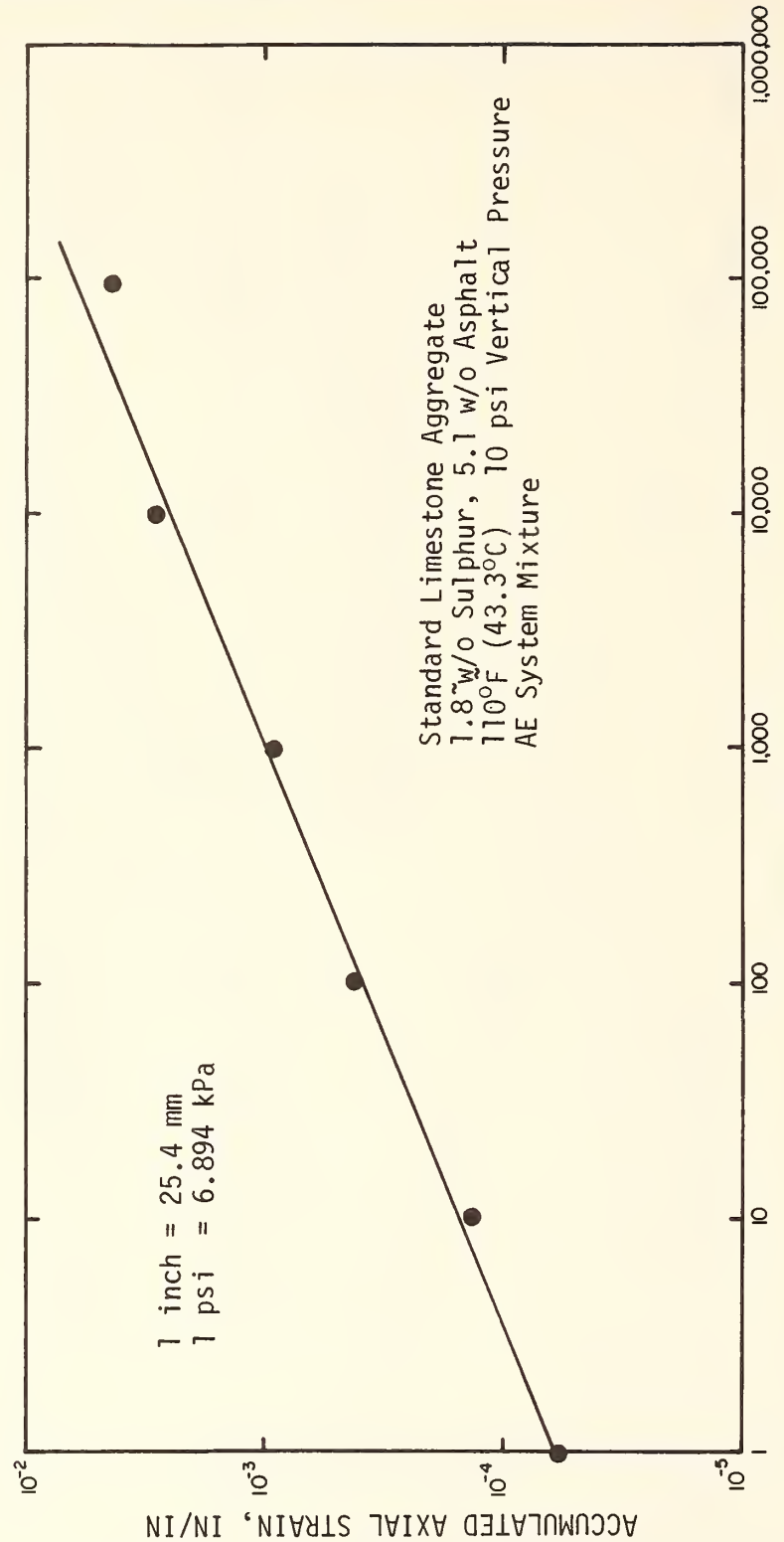

FIGURE 122 ACCUMULATED STRAIN RESULTS FROM COMPRESSIVE CREEP FOR LIMESTONE AGGREGATE AE (1.8 w/o SULPHUR, 5.1 w/o ASPHALT)

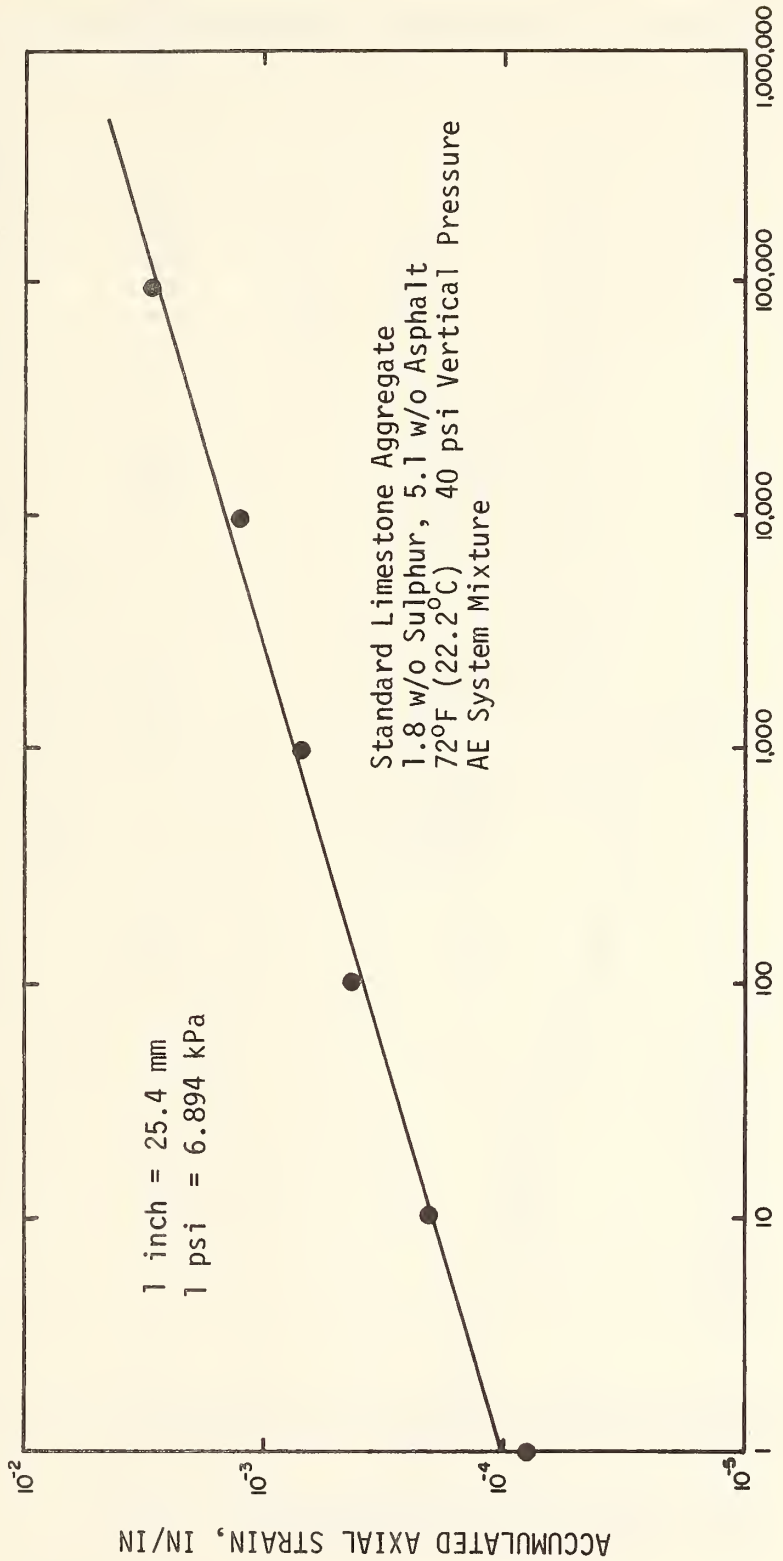

FIGURE 123 ACCUMULATED STRAIN RESULTS FROM COMPRESSIVE CREEP FOR LIMESTONE AGGREGATE AE (1.8 w/o SULPHUR, 5.1 w/o ASPHALT)

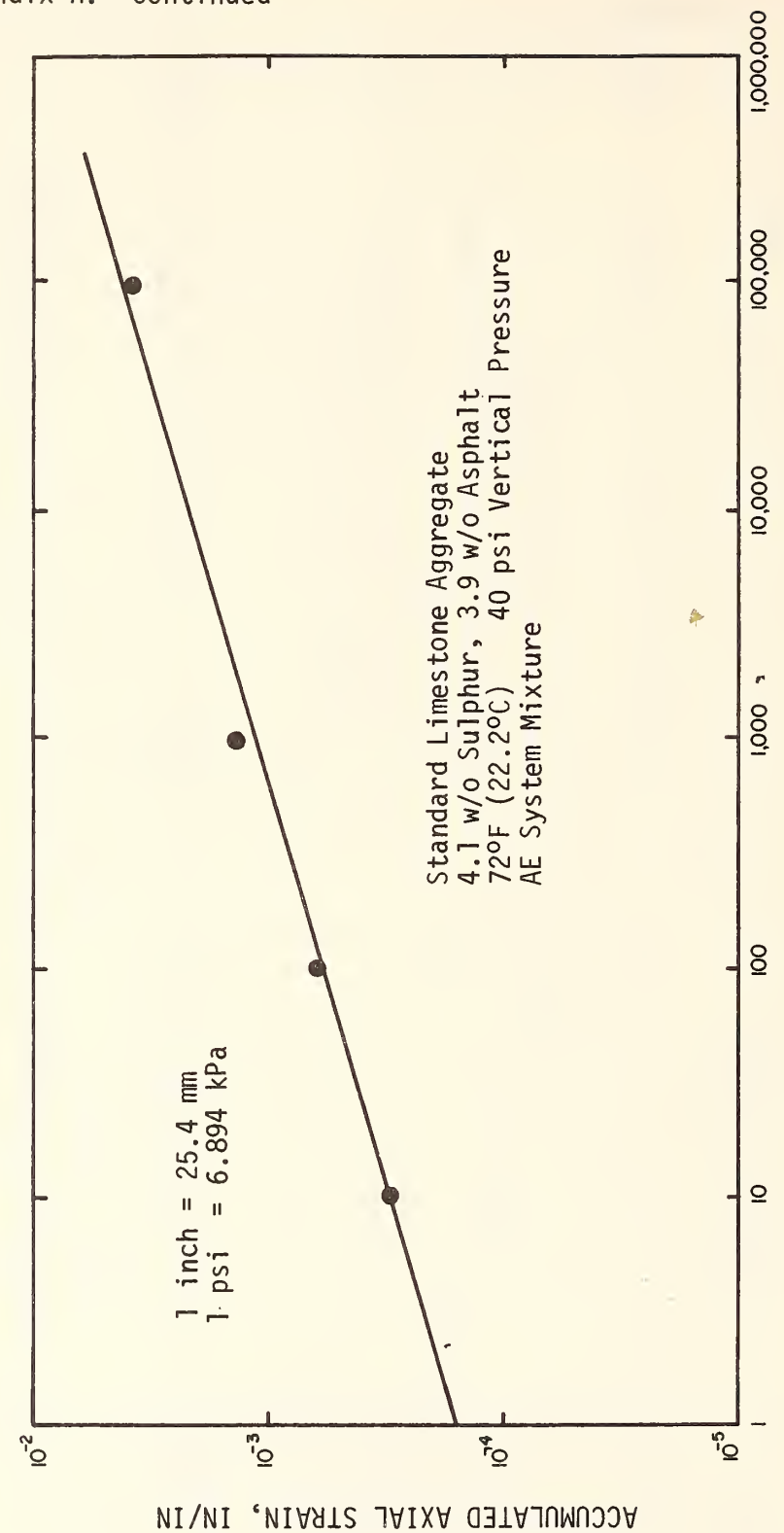

FIGURE 124 ACCUMULATED STRAIN RESULTS FROM COMPRESSIVE CREEP FOR LIMESTONE AGGREGATE AE (4.1 w/o SULPHUR, 3.9 w/o ASPHALT)

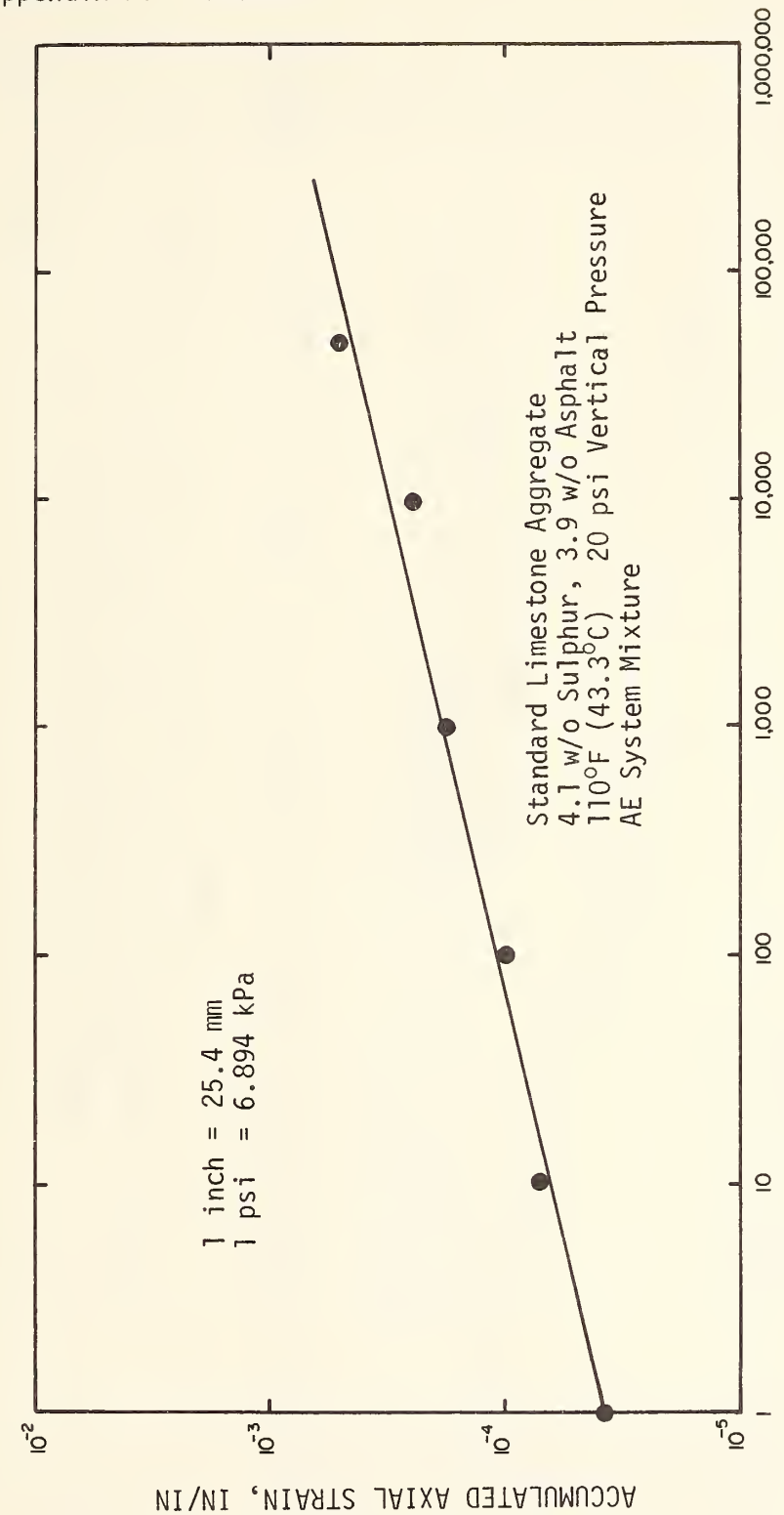

FIGURE 125 ACCUMULATED STRAIN RESULTS FROM COMPRESSIVE CREEP FOR LIMESTONE AGGREGATE AE (4.1 w/o SULPHUR, 3.9 w/o ASPHALT)

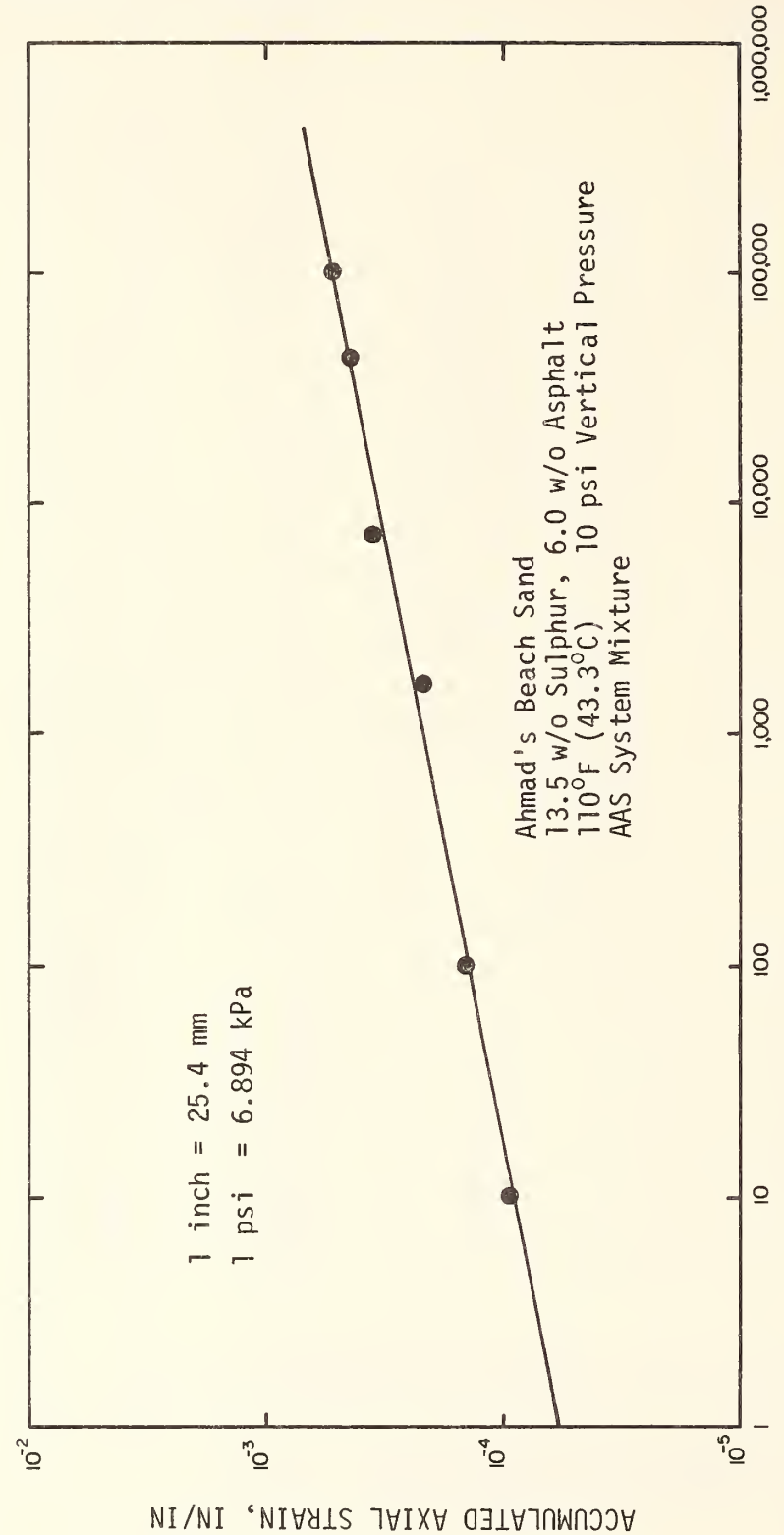

FIGURE 126 ACCUMULATED STRAIN RESULTS FROM COMPRESSIVE CREEP FOR BEACH SAND AAS (13.5 w/o SULPHUR, 6.0 w/o ASPHALT)

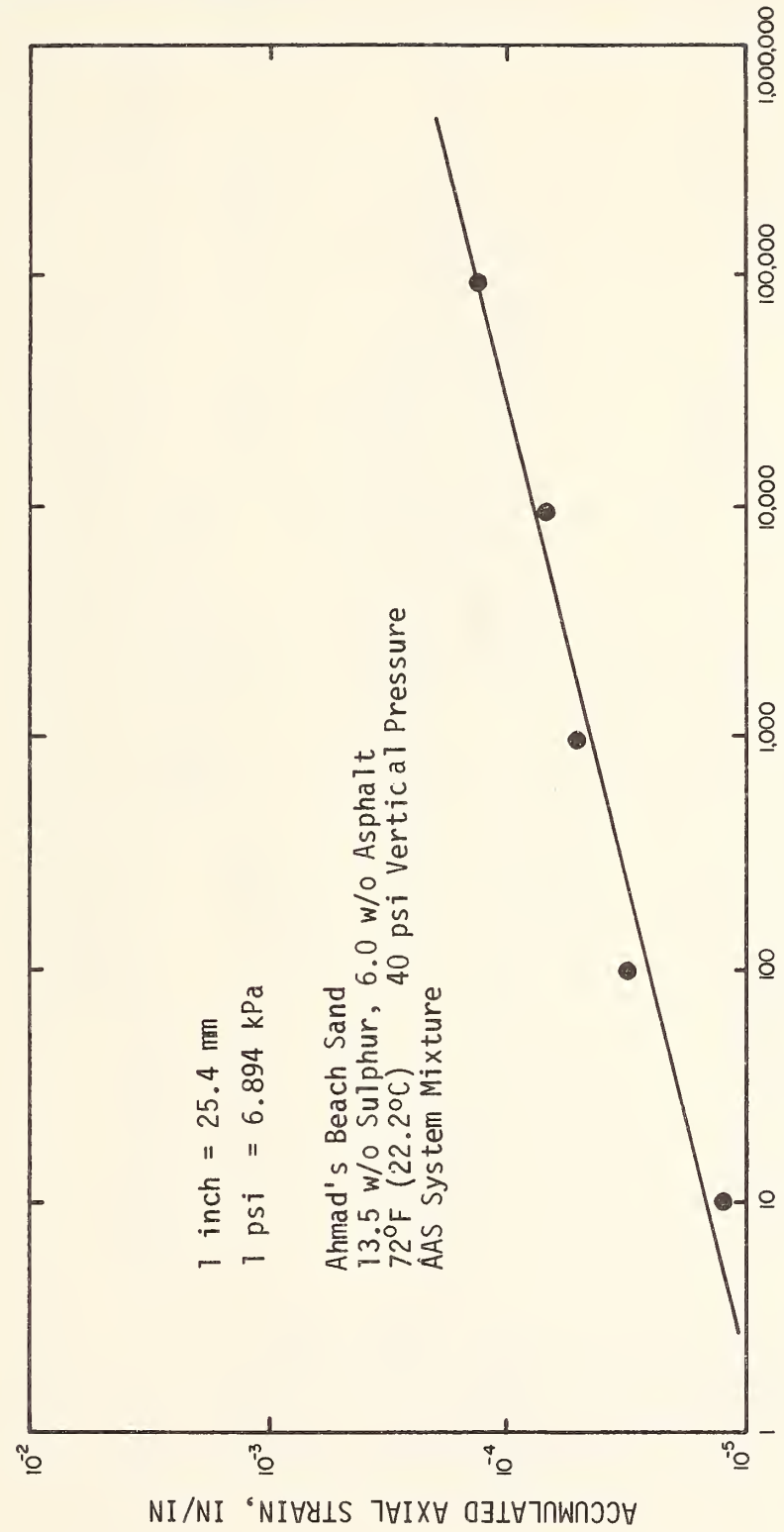

FIGURE 127 ACCUMULATED STRAIN RESULTS FROM COMPRESSIVE CREEP FOR BEACH SAND AAS (13.5 w/o SULPHUR, 6.0 w/o ASPHALT

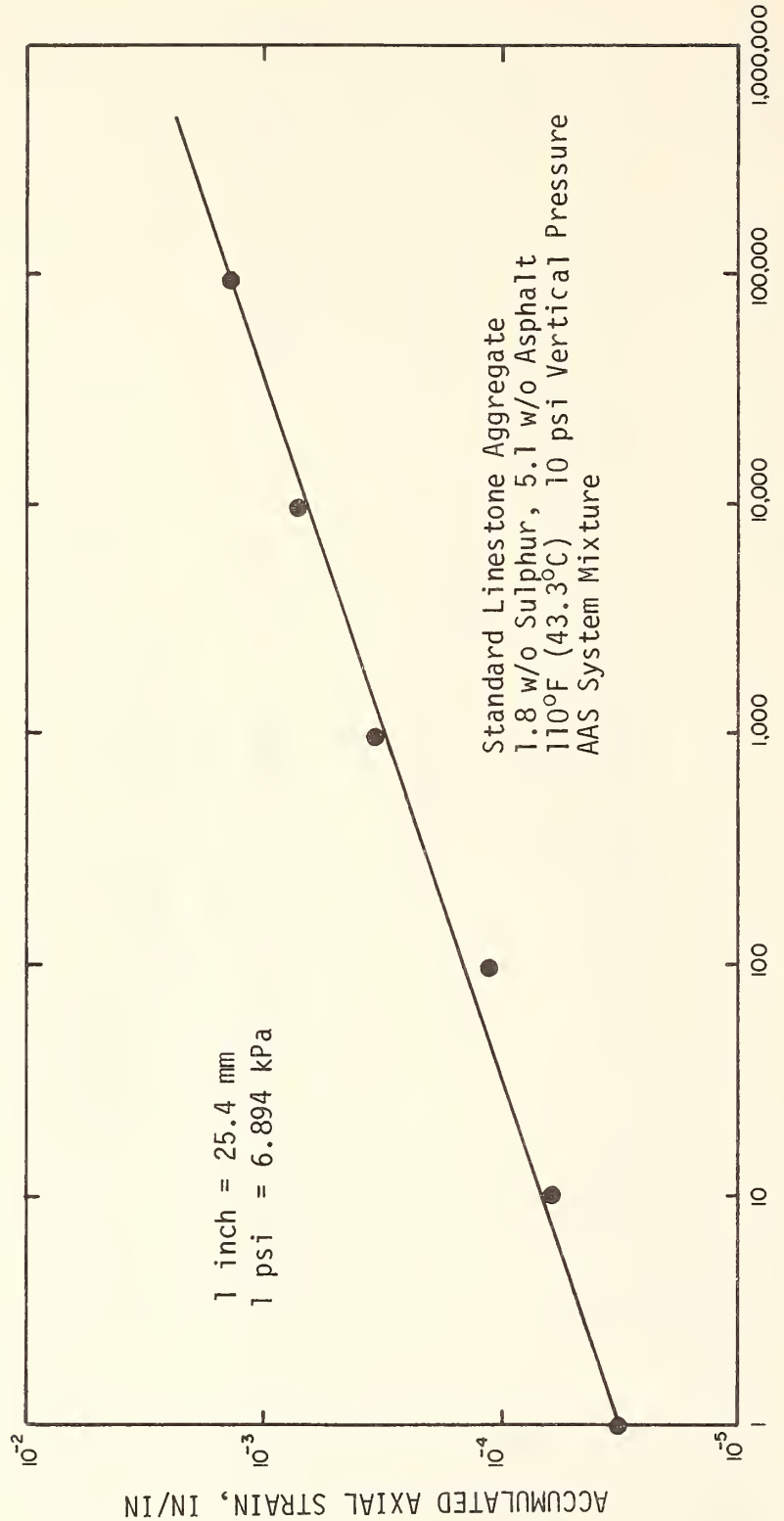

FIGURE 128 ACCUMULATED STRAIN RESULTS FROM COMPRESSIVE CREEP FOR LIMESTONE AGGREGATE AAS (1.8 w/o SULPHUR, 5.1 w/o ASPHALT)

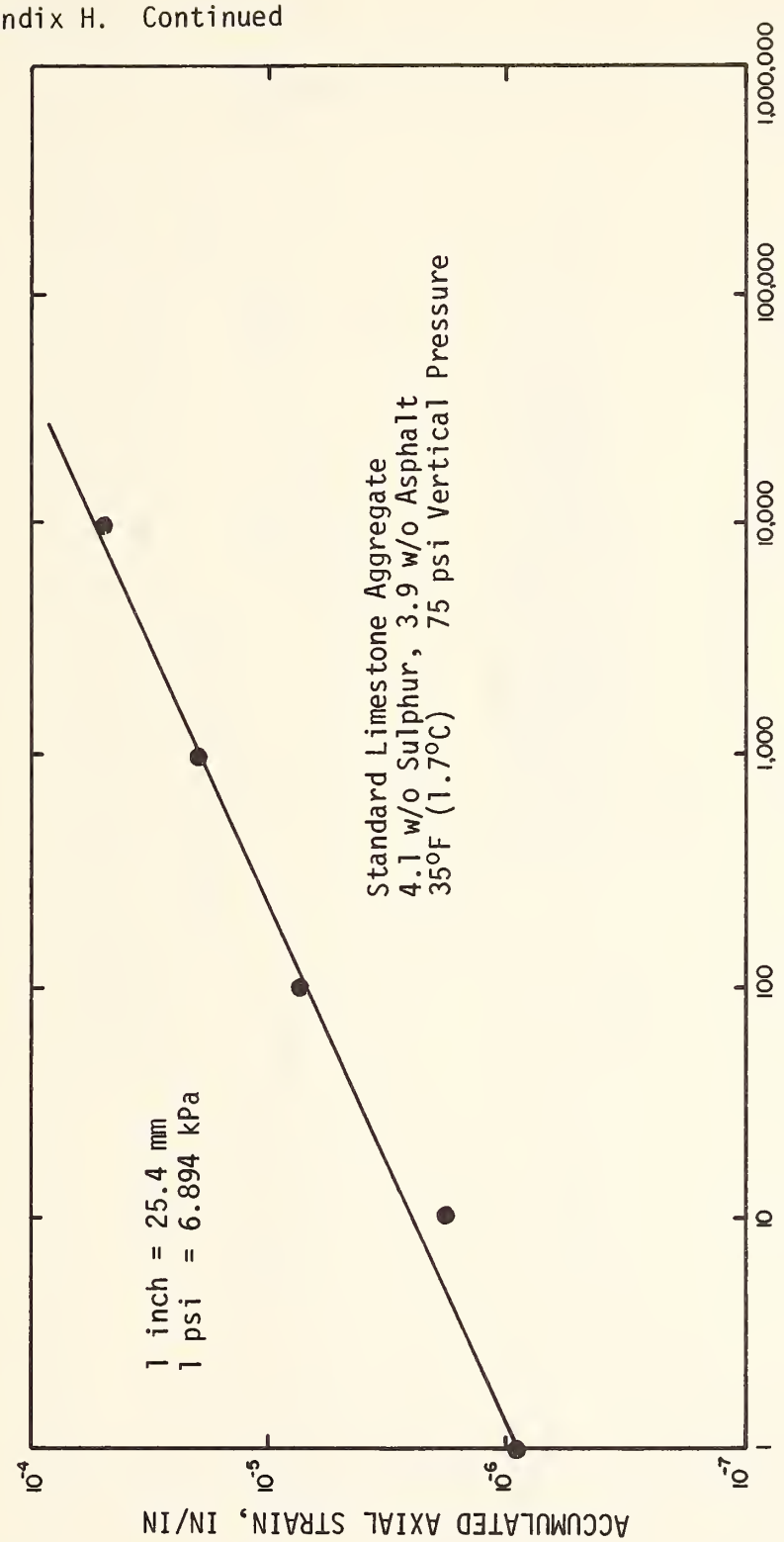

FIGURE 129 ACCUMULATED STRAIN RESULTS FROM COMPRESSIVE CREEP FOR LIMESTONE AGGREGATE AAS (4.1 w/o SULPHUR, 3.9 w/o ASPHALT)

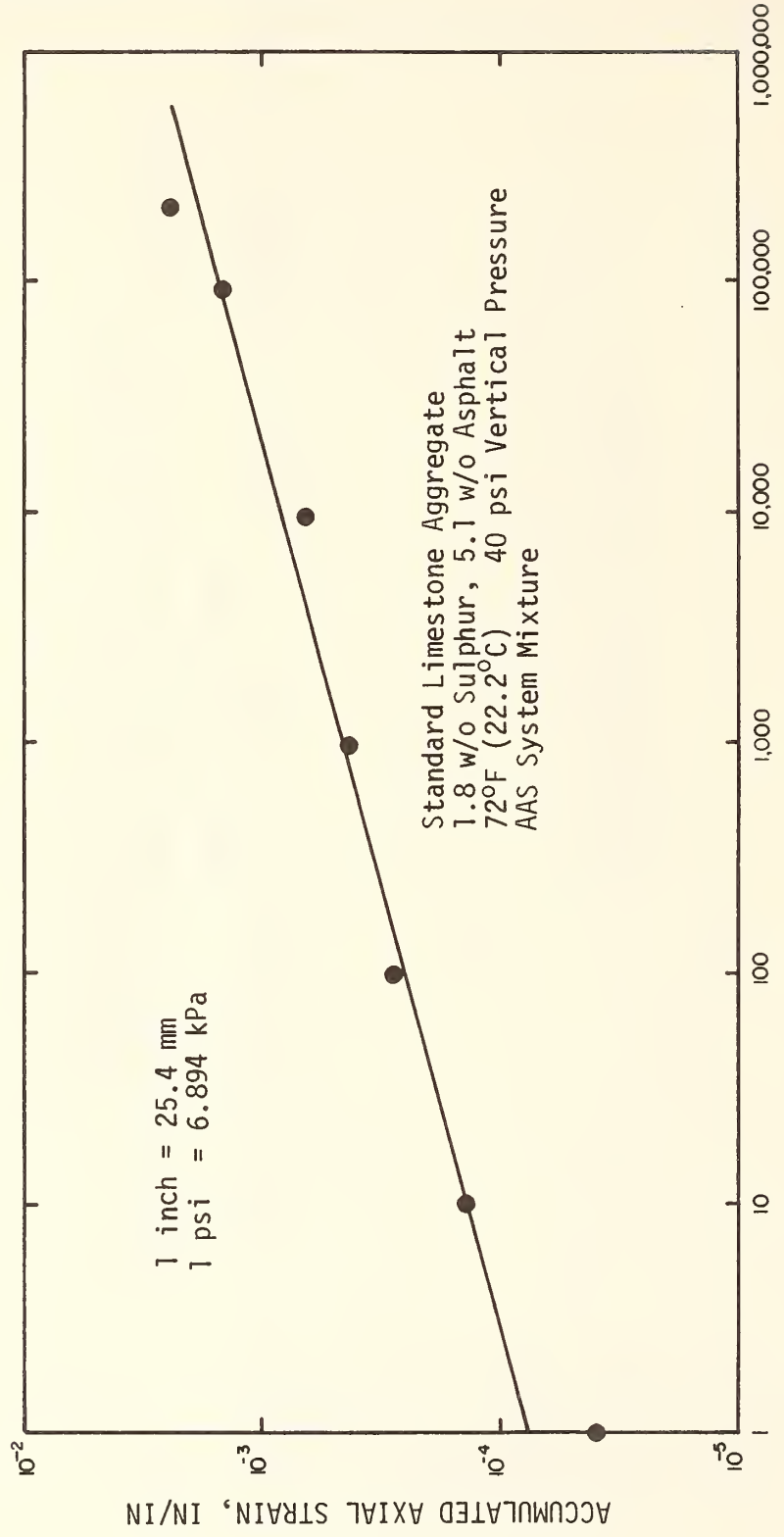

FIGURE 130 ACCUMULATED STRAIN RESULTS FROM COMPRESSIVE CREEP FOR LIMESTONE AGGREGATE AAS (1.8 w/o SULPHUR, 5.1 w/o ASPHALT)

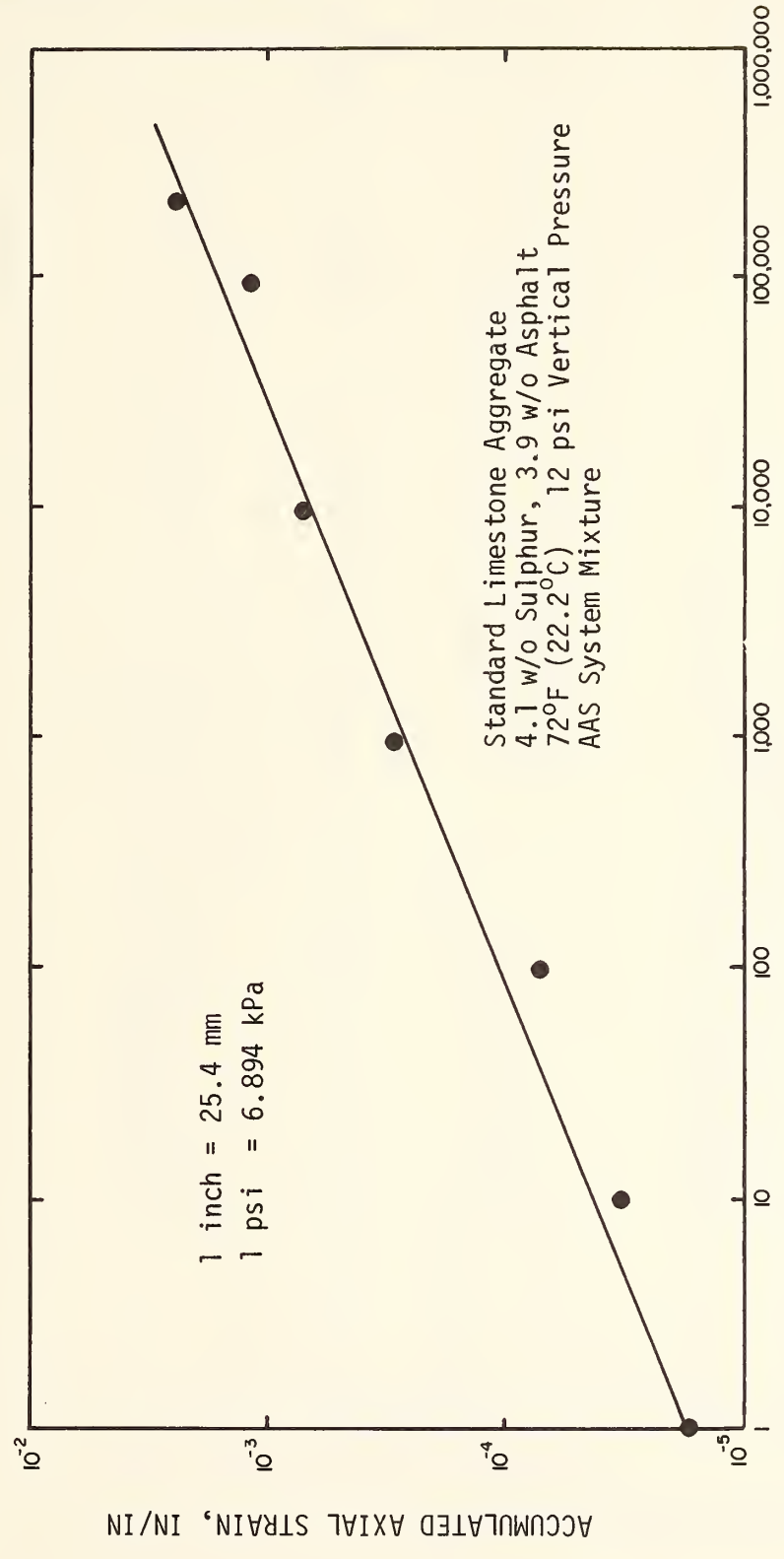

FIGURE 131 ACCUMULATED STRAIN RESULTS FROM COMPRESSIVE CREEP FOR LIMESTONE AGGREGATE AAS (4.1 w/o SULPHUR, 3.9 w/o ASPHALT)

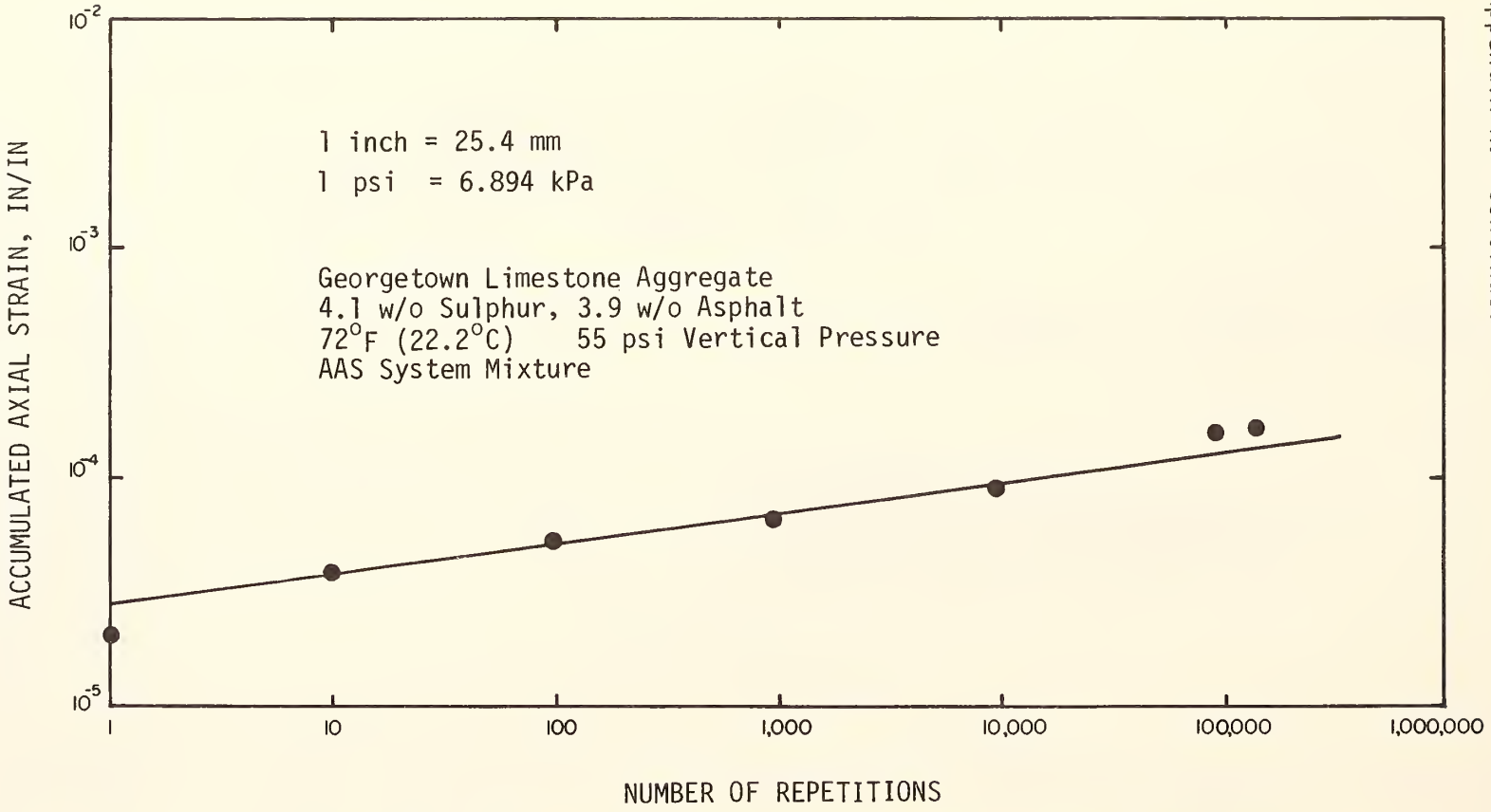

FIGURE 132 ACCUMULATED STRAIN RESULTS FROM COMPRESSIVE CREEP FOR GEORGETOWN LIMESTONE AGGREGATE AAS (4.1 w/o SULPHUR, 3.9 ASPHALT)

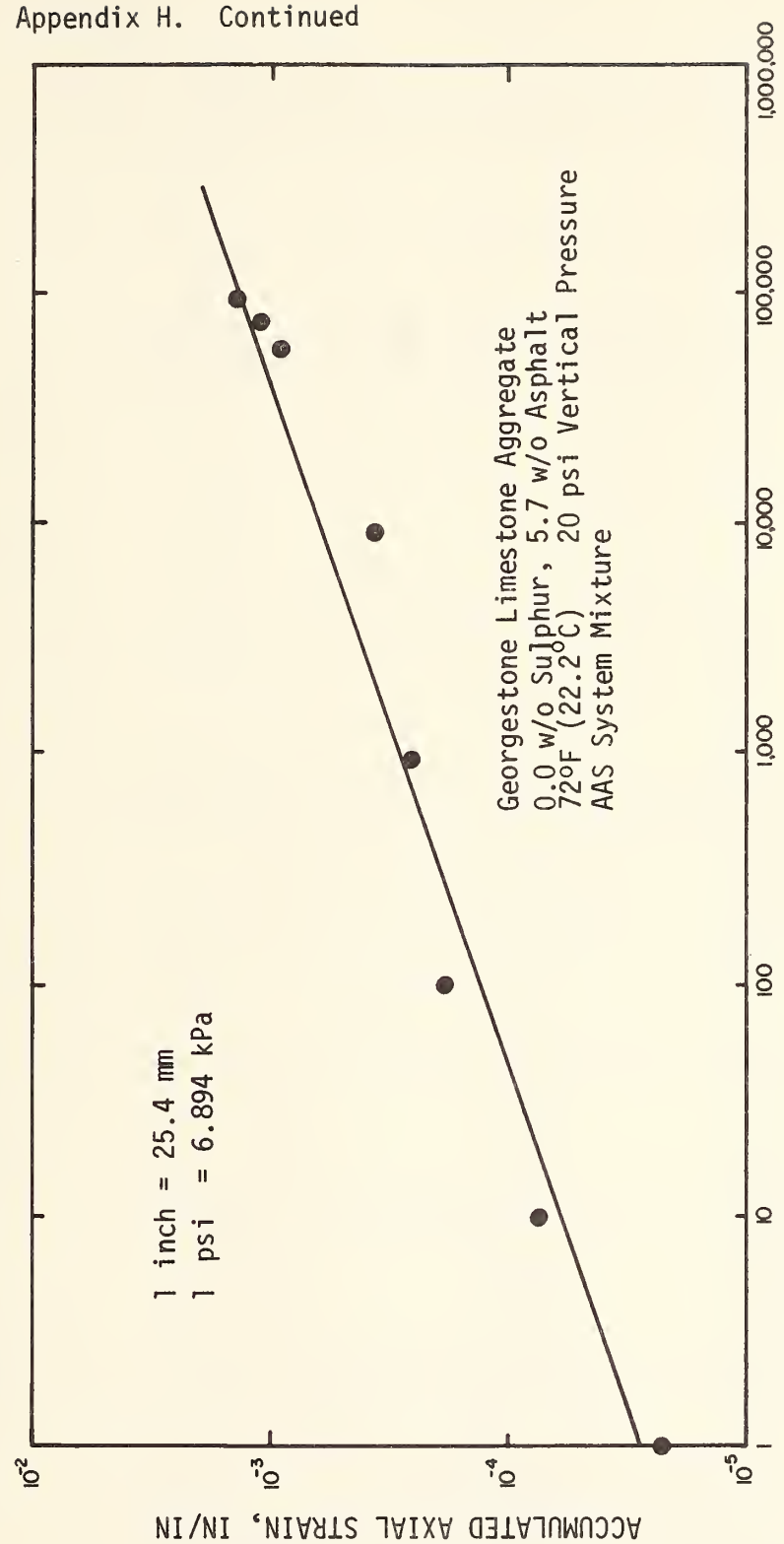

FIGURE 133 ACCUMULATED STRAIN RESULTS FROM COMPRESSIVE CREEP FOR GEORGETWON LIMESTONE AGGREGATE AAS (0.0 w/o SULPHUR, 5.7 w/o ASPHALT)

Appendix I. Results of Performance Prediction by VESYS IMM

TABLE 46 -- SUMMARY OF PERFORMANCE OF AC (0.0S/4.5A) SURFACE ON LIMESTONE BASE BY VESYS IIM SYSTEM

Climate	Layer Thickness		Time (Years)	Rut Depth (in)	Slope Variance ($x10^6$ Radians)	Log_{10} Cracking Index	Serviceability Index
	Surface	Base					
Cool (Hard Clay Subgrade)	4.00"	4.00"	4	0.0958	0.302	-1.73	3.98
			8	0.118	0.461	-1.39	3.88
			12	0.136	0.608	-1.17	3.80
			16	0.152	0.766	-0.979	3.73
			20	0.170	0.947	-0.805	3.65
Moderate (Medium Clay Subgrade	4.50"	4.00"	4	0.149	0.717	-1.75	3.74
			8	0.186	1.11	-1.41	3.58
			12	0.215	1.47	-1.19	3.44
			16	0.242	1.88	-1.00	3.31
			20	0.270	2.34	-0.824	3.17
Warm (Soft Clay Subgrade)	8.00"	10.00"	4	0.816	17.6	-0.633	0.89
			8	1.05	29.0	-0.290	-0.18
			12	1.23	40.2	-0.0647	-1.18
			16	1.41	52.8	0.123	-2.39
			20	1.60	67.9	0.297	-3.49

1 inch = 25.4 mm

Appendix I. Continued

TABLE 47 --SUMMARY OF PERFORMANCE OF AC (0.0S/4.5A) SURFACE ON SAS BASE BY VESYS IIM SYSTEM

Climate	Layer Thickness		Time (Years)	Rut Depth (in)	Slope Variance ($x10^6$ Radians)	Log_{10} Cracking Index	Serviceability Index
	Surface	Base					
Cool (Hard Clay Subgrade)	4.00"	4.00"	4	0.0719	0.320	-3.10	3.97
			8	0.0907	0.510	-2.76	3.86
			12	0.106	0.693	-2.54	3.78
			16	0.120	0.894	-2.34	3.70
			20	0.135	1.13	-2.18	3.60
Moderate (Medium Clay Subgrade	1.00"	4.75"	4	0.215	2.76	-1.30	3.14
			8	0.274	4.50	-0.961	2.81
			12	0.322	6.21	-0.736	2.55
			16	0.369	8.11	-0.548	2.32
			20	0.417	10.39	-0.374	2.08
Warm (Soft Clay Subgrade)	4.00"	4.75"	4	**			
			8				
			12				
			16				
			20				

**Compressive Radial Strain Calculated

1 inch = 25.4 mm

Appendix I. Continued

TABLE 48 -- SUMMARY OF PERFORMANCE OF AAS (4.1S/3.9A) SURFACE ON SAS BASE BY VESYS IIM SYSTEM (Severe Fatigue Shift Rule)

Climate	Layer Thickness		Time (Years)	Rut Depth (in)	Slope Variance ($x10^6$ Radians)	Log_{10} Cracking Index	Serviceability Index
	Surface	Base					
Cool			4				
(Hard Clay			8				
Subgrade)			12				
			16				
			20				
Moderate	2.00"	4.25"	4	0.227	1.29	-3.67	3.49
(Medium Clay			8	0.289	2.09	-3.33	3.29
Subgrade			12	0.339	2.87	-3.10	2.99
			16	0.387	3.74	-2.92	2.78
			20	0.437	4.78	-2.74	2.56
Warm			4				
(Soft Clay			8				
Subgrade)			12				
			16				
			20				

1 inch = 25.4 mm

Appendix I. Continued

TABLE 49 -- SUMMARY OF PERFORMANCE OF AAS (4.1S/3.9A) SURFACE ON LIMESTONE BASE BY VESYS IIM SYSTEM

Climate	Layer Thickness		Time (Years)	Rut Depth (in)	Slope Variance ($x10^6$ Radians)	Log_{10} Cracking Index	Serviceability Index
	Surface	Base					
Cool	3.00"	4.00"	4	0.0891	0.235	-3.31	4.02
(Hard Clay			8	0.106	0.334	-2.97	3.95
Subgrade)			12	0.119	0.422	-2.74	3.90
			16	0.131	0.511	-2.56	3.85
			20	0.144	0.611	-2.38	3.80
Moderate	3.75"	4.00"	4	0.122	0.422	-2.93	3.90
(Medium Clay			8	0.146	0.603	-2.59	3.80
Subgrade			12	0.164	0.764	-2.36	3.72
			16	0.181	0.930	-2.17	3.65
			20	0.198	1.11	-2.00	3.57
Warm	6.25"	4.00"	4	0.663	10.1	-2.48	1.66
(Soft Clay			8	0.833	16.0	-2.14	0.92
Subgrade)			12	0.968	21.5	-1.91	0.31
			16	1.10	27.6	-1.72	-0.30
			20	1.23	34.8	-1.55	-0.97

1 inch = 25.4 mm

Appendix I. Continued

TABLE 50 -- SUMMARY OF PERFORMANCE OF AAS (4.1S/3.9A) SURFACE ON SAS BASE BY VESYS IIM SYSTEM (Standard Fatigue Shift Rule)

Climate	Layer Thickness		Time (Years)	Rut Depth (in)	Slope Variance ($x10^6$ Radians)	Log_{10} Cracking Index	Serviceability Index
	Surface	Base					
Cool (Hard Clay Subgrade)	2.00"	4.00"	4	0.149	0.520	-6.17	3.84
			8	0.189	0.834	-5.83	3.68
			12	0.221	1.14	-5.60	3.54
			16	0.251	1.47	-5.42	3.41
			20	0.280	1.88	-5.24	3.27
Moderate (Medium Clay Subgrade	2.00"	4.00"	4	0.227	1.29	-5.34	3.49
			8	0.289	2.09	-5.00	3.21
			12	0.339	2.87	-4.77	2.99
			16	0.387	3.74	-4.59	2.78
			20	0.437	4.78	-4.41	2.57
Warm (Soft Clay Subgrade)	5.75"	4.00"	4	0.699	10.8	-3.14	1.53
			8	0.893	17.6	-2.79	0.68
			12	1.05	24.3	-2.57	-0.05
			16	1.20	31.8	-2.38	-0.79
			20	1.36	40.8	-2.21	-1.63

1 inch = 25.4 mm

Appendix I. Continued

TABLE 51 -- SUMMARY OF PERFORMANCE OF AE (1.8S/5.1A) SURFACE ON LIMESTONE BASE BY VESYS IIM SYSTEM

Climate	Layer Thickness		Time (Years)	Rut Depth (in)	Slope Variance ($x10^6$ Radians)	Log_{10} Cracking Index	Serviceability Index
	Surface	Base					
Cool (Hard Clay Subgrade)	3.00"	4.00"	4	0.14	0.55	5.60	3.51
			8	0.16	0.82	5.94	3.38
			12	0.19	1.05	6.17	3.28
			16	0.21	1.30	6.36	3.18
			20	0.23	1.59	6.53	3.08
Moderate (Medium Clay Subgrade	3.75"	4.00"	4	0.22	1.40	0.26	3.14
			8	0.27	2.08	0.61	2.92
			12	0.31	2.71	0.83	2.75
			16	0.34	3.37	1.02	2.59
			20	0.38	4.13	1.19	2.42
Warm (Soft Clay Subgrade)	6.25"	4.00"	4	1.29	45.2	0.31	-1.73
			8	1.63	72.7	0.66	-3.70
			12	1.91	99.5	0.88	-5.50
			16	2.17	129	1.07	-7.41
			20	2.45	164	1.24	-9.64

1 inch = 25.4 mm

Appendix I. Continued

TABLE 52 -- SUMMARY OF PERFORMANCE OF AE (1.8S/5.1A) SURFACE ON SAND-ASPHALT-SULPHUR BASE BY VESYS IIM SYSTEM

Climate	Layer Thickness		Time (Years)	Rut Depth (in)	Slope Variance ($x10^6$ Radians)	Log_{10} Cracking Index	Serviceability Index
	Surface	Base					
Cool (Hard Clay Subgrade)	1.00"	4.00"	4	**			
			8				
			12				
			16				
			20				
Moderate (Medium Clay Subgrade	1.00"	4.25"	4	**			
			8				
			12				
			16				
			20				
Warm (Soft Clay Subgrade)	5.75"	4.00"	4	**			
			8				
			12				
			16				
			20				

** Compressive Radial Strain Calculated

1 inch = 25.4 mm

Appendix I. Continued

TABLE 53 -- SUMMARY OF PERFORMANCE OF AE (4.1S/3.9A) SURFACE ON LIMESTONE BASE BY VESYS IIM SYSTEM

Climate	Layer Thickness		Time (Years)	Rut Depth (in)	Slope Variance ($x10^6$ Radians)	Log_{10} Cracking Index	Serviceability Index
	Surface	Base					
Cool (Hard Clay Subgrade)	7.00	4.50	4	0.08	0.18	1.51	3.74
			8	0.09	0.24	1.86	3.70
			12	0.10	0.30	2.08	3.66
			16	0.11	0.36	2.27	3.62
			20	0.12	0.42	2.44	3.58
Moderate (Medium Clay Subgrade	3.75"	4.00"	4	0.15	0.70	3.85	3.44
			8	0.19	1.01	4.20	3.30
			12	0.21	1.28	4.42	3.19
			16	0.23	1.56	4.61	3.09
			20	0.25	1.87	4.78	2.98
Warm (Soft Clay Subgrade)	5.75"	4.00"	4	0.90	20.4	1.51	0.23
			8	1.13	31.9	1.85	-0.84
			12	1.30	42.9	2.08	-1.76
			16	1.47	54.7	2.27	-2.69
			20	1.65	68.6	2.44	-3.74

1 inch = 25.4 mm

Appendix I. Continued

TABLE 54 -- SUMMARY OF PERFORMANCE OF AE (4.1S/3.9A) SURFACE ON SAND-ASPHALT-SULPHUR BASE BY VESYS IIM SYSTEM

Climate	Layer Thickness		Time (Years)	Rut Depth (in)	Slope Variance ($x10^6$ Radians)	Log_{10} Cracking Index	Serviceability Index
	Surface	Base					
Cool (Hard Clay Subgrade)	1.00"	7.00"	4	**			
			8				
			12				
			16				
			20				
Moderate (Medium Clay Subgrade	1.00"	4.25"	4	**			
			8				
			12				
			16				
			20				
Warm (Soft Clay Subgrade)	5.75"	4.00"	4	0.79	13.3	-1.44	1.18
			8	0.99	21.2	-1.10	0.25
			12	1.16	28.8	-0.88	-0.54
			16	1.31	37.2	-0.69	-1.35
			20	1.48	47.1	-0.51	-2.26

** Compressive Radial Strain Calculated

1 inch = 25.4 mm

Appendix I. Continued

TABLE 55 -- SUMMARY OF PERFORMANCE OF AES (1.8S/5.1A) SURFACE ON LIMESTONE BASE BY VESYS IIM SYSTEM

Climate	Layer Thickness		Time (Years)	Rut Depth (in)	Slope Variance ($x10^6$ Radians)	Log_{10} Cracking Index	Serviceability Index
	Surface	Base					
Cool (Hard Clay Subgrade)	8.25"	4.00"	4	0.41	4.46	2.14	2.33
			8	0.54	7.76	2.49	1.76
			12	0.65	11.2	2.71	1.29
			16	0.76	15.2	2.90	0.82
			20	0.88	20.1	3.07	0.31
Moderate (Medium Clay Subgrade	*		4				
			8				
			12				
			16				
			20				
Warm (Soft Clay Subgrade)	6.25"	4.00"	4	2.12	122	1.97	-7.01
			8	2.80	213	2.31	<-10.0
			12	3.37	308	2.54	<-10.0
			16	3.93	418	2.72	<-10.0
			20	4.53	555	2.90	<-10.0

*Texas FPS-BISTRO did not give a Feasible Design for this Climate

1 inch = 25.4 mm

Appendix I. Continued

TABLE 56 -- SUMMARY OF PERFORMANCE OF AES (1.8S/5.1A) SURFACE ON SAND-ASPHALT-SULPHUR BASE BY VESYS IIM SYSTEM

Climate	Layer Thickness		Time (Years)	Rut Depth (in)	Slope Variance ($x10^6$ Radians)	Log_{10} Cracking Index	Serviceability Index
	Surface	Base					
Cool (Hard Clay Subgrade)	1.50"	10.00"	4	**			
			8				
			12				
			16				
			20				
Moderate (Medium Clay Subgrade	*		4				
			8				
			12				
			16				
			20				
Warm (Soft Clay Subgrade)	5.75"	4.00"	4	1.56	53.5	-1.17	-2.76
			8	2.07	93.9	-0.83	-6.09
			12	2.49	136.0	-0.61	-9.40
			16	2.90	185.2	-0.42	<-10.0
			20	3.35	246.2	-0.25	<-10.0

*Texas FPS-BISTRO did not give a Feasible Design for this Climate

**Compressive Radial Strain Calculated

1 inch = 25.4 mm

Appendix I. Continued

TABLE 57 -- SUMMARY OF PERFORMANCE OF AES (4.1S/3.9A) SURFACE ON LIMESTONE BASE BY VESYS IIM SYSTEM

Climate	Layer Thickness		Time (Years)	Rut Depth (in)	Slope Variance ($x10^6$ Radians)	Log_{10} Cracking Index	Serviceability Index
	Surface	Base					
Cool (Hard Clay Subgrade)	*		4				
			8				
			12				
			16				
			20				
Moderate (Medium Clay Subgrade	*		4				
			8				
			12				
			16				
			20				
Warm (Soft Clay Subgrade)	*		4				
			8				
			12				
			16				
			20				

*Texas FPS-BISTRO did not give a Feasible Design for this Climate

1 inch = 25.4 mm

Appendix I. Continued

TABLE 58 -- SUMMARY OF PERFORMANCE OF AES (4.1S/3.9A) SURFACE ON SAS BASE BY VESYS IIM SYSTEM

Climate	Layer Thickness		Time (Years)	Rut Depth (in)	Slope Variance ($x10^6$ Radians)	Log_{10} Cracking Index	Serviceability Index
	Surface	Base					
Cool (Hard Clay Subgrade)	*		4				
			8				
			12				
			16				
			20				
Moderate (Medium Clay Subgrade	*		4				
			8				
			12				
			16				
			20				
Warm (Soft Clay Subgrade)	*		4				
			8				
			12				
			16				
			20				

*Texas FPS-BISTRO did not give a Feasible Design for this Climate

1 inch = 25.4 mm

Appendix I. Continued

TABLE 59 -- SUMMARY OF PERFORMANCE OF SULPHUR RECYCLED SURFACE ON LIMESTONE BASE BY VESYS IIM SYSTEM

Climate	Layer Thickness		Time (Years)	Rut Depth (in)	Slope Variance ($x10^6$ Radians)	Log_{10} Cracking Index	Serviceability Index
	Surface	Base					
Cool (Hard Clay Subgrade)	2.00"	4.00"	4	0.115	0.375	-0.251	3.93
			8	0.143	0.582	0.0912	3.50
			12	0.166	0.779	0.317	3.40
			16	0.187	0.992	0.505	3.30
			20	0.209	1.24	0.678	3.20
Moderate (Medium Clay Subgrade	4.00"	7.50"	4	0.138	0.451	-0.924	3.88
			8	0.176	0.729	-0.581	3.73
			12	0.206	1.00	-0.356	3.61
			16	0.235	1.30	-0.168	3.48
			20	0.265	1.66	0.00552	3.11
Warm (Soft Clay Subgrade)	*		4				
			8				
			12				
			16				
			20				

*Texas FPS-BISTRO did not give a Feasible Design for this Climate

1 inch = 25.4 mm

*U.S. GOVERNMENT PRINTING OFFICE: 1979 0-623-899/886

Appendix I. Continued

TABLE 60 -- SUMMARY OF PERFORMANCE OF SULPHUR RECYCLED SURFACE ON SAS BASE BY VESYS IIM SYSTEM

Climate	Layer Thickness		Time (Years)	Rut Depth (in)	Slope Variance ($x10^6$ Radians)	Log_{10} Cracking Index	Serviceability Index
	Surface	Base					
Cool	2.00"	4.00"	4	0.133	0.416	-3.21	3.90
(Hard Clay			8	0.171	0.692	-2.87	3.75
Subgrade)			12	0.202	0.967	-2.64	3.62
			16	0.232	1.28	-2.46	3.49
			20	0.264	1.65	-2.28	3.35
Moderate	2.00"	4.75"	4	0.199	1.07	-2.92	3.58
(Medium Clay			8	0.257	1.79	-2.58	3.32
Subgrade			12	0.305	2.52	-2.35	3.10
			16	0.351	3.35	-2.17	2.89
			20	0.401	4.35	-1.99	2.67
Warm	*		4				
(Soft Clay			8				
Subgrade)			12				
			16				
			20				

*Texas FPS-BISTRO did not give a Feasible Design for this Climate

1 inch = 25.4 mm

FEDERALLY COORDINATED PROGRAM OF HIGHWAY RESEARCH AND DEVELOPMENT (FCP)

The Offices of Research and Development of the Federal Highway Administration are responsible for a broad program of research with resources including its own staff, contract programs, and a Federal-Aid program which is conducted by or through the State highway departments and which also finances the National Cooperative Highway Research Program managed by the Transportation Research Board. The Federally Coordinated Program of Highway Research and Development (FCP) is a carefully selected group of projects aimed at urgent, national problems, which concentrates these resources on these problems to obtain timely solutions. Virtually all of the available funds and staff resources are a part of the FCP, together with as much of the Federal-aid research funds of the States and the NCHRP resources as the States agree to devote to these projects.*

FCP Category Descriptions

1. Improved Highway Design and Operation for Safety

Safety R&D addresses problems connected with the responsibilities of the Federal Highway Administration under the Highway Safety Act and includes investigation of appropriate design standards, roadside hardware, signing, and physical and scientific data for the formulation of improved safety regulations.

2. Reduction of Traffic Congestion and Improved Operational Efficiency

Traffic R&D is concerned with increasing the operational efficiency of existing highways by advancing technology, by improving designs for existing as well as new facilities, and by keeping the demand-capacity relationship in better balance through traffic management techniques such as bus and carpool preferential treatment, motorist information, and rerouting of traffic.

3. Environmental Considerations in Highway Design, Location, Construction, and Operation

Environmental R&D is directed toward identifying and evaluating highway elements which affect the quality of the human environment. The ultimate goals are reduction of adverse highway and traffic impacts, and protection and enhancement of the environment.

4. Improved Materials Utilization and Durability

Materials R&D is concerned with expanding the knowledge of materials properties and technology to fully utilize available naturally occurring materials, to develop extender or substitute materials for materials in short supply, and to devise procedures for converting industrial and other wastes into useful highway products. These activities are all directed toward the common goals of lowering the cost of highway construction and extending the period of maintenance-free operation.

5. Improved Design to Reduce Costs, Extend Life Expectancy, and Insure Structural Safety

Structural R&D is concerned with furthering the latest technological advances in structural designs, fabrication processes, and construction techniques, to provide safe, efficient highways at reasonable cost.

6. Prototype Development and Implementation of Research

This category is concerned with developing and transferring research and technology into practice, or, as it has been commonly identified, "technology transfer."

7. Improved Technology for Highway Maintenance

Maintenance R&D objectives include the development and application of new technology to improve management, to augment the utilization of resources, and to increase operational efficiency and safety in the maintenance of highway facilities.

---

* The complete 7-volume official statement of the FCP is available from the National Technical Information Service (NTIS), Springfield, Virginia 22161 (Order No. PB 242057, price $45 postpaid). Single copies of the introductory volume are obtainable without charge from Program Analysis (HRD-2), Offices of Research and Development, Federal Highway Administration, Washington, D.C. 20590.